Photoelectrochemical Characterization of Dye- Modified ZnO Hybrid Thin Films Prepared by Electrochemical Deposition

Dissertation
zur Erlangung des Doktorgrades
der Naturwissenschaften
(Dr. rer. nat.)

vorgelegt
dem Fachbereich 7
Institut für Angewandte Phyik
der Justus Liebig-Universität Gießen

von
Kazuteru Nonomura
aus Gifu

Mai 2006

Referees for the dissertation: Prof. Dr. D. Schlettwein
Prof. Dr. B. K. Meyer

Abstract

Dye- sensitized electrodeposited ZnO thin films were studied in their photoelectrochemical characteristics. Such electrodes can be applied for dye-sensitized solar cells. The main analysis techniques were wavelength- dependent photocurrent measurements to obtain the incident photon to current conversion efficiency (IPCE) of the films as well as time- and frequency- resolved measurements of the photocurrent (IMPS) and photovoltage (IMVS) to characterize in detail individual steps of photoelectrochemical reactions. The films were further analysed in their absorption spectrum, SEM, film thickness, dye content, porosity and surface area. 5,10,15,20-tetrakis-(4-sulfonatophenyl)porphyrin (TSTPPZn), 2,9,16,23-tetrasulfophthalocyanine (TSPcZn), Eosin Y and Coumarin 343 were used as sensitizer. Electrochemically induced deposition of ZnO from aqueous solutions can provide porous and crystalline ZnO at low temperature on a great number of conductive substrates. Sensitized ZnO can be prepared directly in one step if the sensitizers are dissolved in the deposition bath or in a multi- step procedure following deposition in the presence of specific structure-directing agents (SDA) that influence the morphology, orientation and porosity of ZnO. Films studied here were prepared in the presence of Eosin Y, Coumarin 343 or sodium dodecyl sulfate (SDS) as SDA.

Sensitized photocurrents were measured for all sensitizers studied here. Even more than one sensitizer could be used in one ZnO film to widen the spectral response. The interaction of two different sensitizers in the film further decreased the recombination of the generated electrons. Films prepared in one step generally showed only small efficiency because the sensitizers tended to aggregate and hindered the accessibility of ZnO pores. The photoelectrochemical efficiency of electrodeposited ZnO was clearly improved by removing the SDA from the surface after preparation and then adsorb the sensitizer in a separate step ("re-adsorption"). Eosin Y, e.g., is an efficient SDA to obtain a porous and highly crystalline ZnO and the efficiency of such re-ad TSPcZn / ZnO and re-ad TSTPPZn / ZnO have been improved considerably to IPCE values of 31 % (680 nm) and 15 % (420 nm). Intensity modulated analysis showed that the electron transit time of such efficient electrodes is approximately one order faster than the electron lifetime speaking for efficient harvesting of photogenerated electrons and widely suppressed recombination. A typical electron diffusion coefficient of about 1×10^{-5} $cm^2 s^{-1}$ at a photocurrent of 100 µA and a diffusion length above 5 µm, larger than the film thickness of 2-3 µm were found. The use of Coumarin 343 as SDA led to a rotation of the ZnO growth direction and thereby further improved the electron diffusion coefficient and also the diffusion length in ZnO. The results of the photoelectrochemical electrode kinetics confirm the good photoelectrochemical properties of these electrodeposited ZnO electrodes and show their perspective to be used as electrodes in dye- sensitized solar cells.

Zusammenfassung

In dieser Arbeit wurden farbstoffsensibilisierte elektrochemisch abgeschiedene Filme von ZnO in ihren photoelektrochemischen Eigenschaften charakterisiert. Solche Elektroden können in photoelektrochemischen Farbstoff- Solarzellen eingesetzt werden. Als wichtigste Charakterisierungsmethoden dienten spectral abhängige Photostrommessungen zur Bestimmung der externen Quantenausbeute (IPCE) sowie zeit- und frequenzaufgelöste Photostrom- (IMPS) und Photospannungsmessungen (IMVS), um einzelne Schritte der photoelektrochemischen Reaktionen im Detail zu charakterisieren. Die Filme wurden weiterhin mittels Absorptionsspektroskopie, Rasterelektronenmikroskopie sowie hinsichtlich Filmdicke, Farbstoffgehalt, Porosität und innerer Oberfläche untersucht. 5,10,15,20-Tetrakis-(4-Sulfonatophenyl)porphyrin (TSTPPZn), 2,9,16,23-Tetrasulfophthalocyanin (TSPcZn), EosinY und Cumarin 343 wurden als Sensibilisator eingesetzt. Die elektrochemisch induzierte Abscheidung aus wässrigen Lösungen kann poröses kristallines ZnO bei niedrigen Temperaturen und auf einer Vielzahl von leitfähigen Substraten bereitstellen. Sensibilisiertes ZnO kann entweder in einem Schritt präpariert werden, wenn die Sensibilisatoren im Abscheidebad gelöst sind oder in einem mehrschrittigen Prozess nachfolgend an eine Abscheidung in Gegenwart von spezifischen strukturdirigierenden Agenzien (SDA), die die Morphologie, Orientierung und Porosität des ZnO beeinflussen. Hier untersuchte Filme wurden in Gegenwart von Eosin Y, Cumarin 343 oder Natriumdodecylsulfat als SDA präpariert.
Für alle untersuchten Sensibilisatoren wurden sensibilisierte Photoströme gemessen. Auch mehr als ein Sensibilisator konnte in einem ZnO-Film eingesetzt werden, um die spektrale Empfindlichkeit zu verbreitern. Die Wechselwirkung zweier unterschiedlicher Sensibilisatoren verminderte weiterhin die Rekombination von generierten Elektronen. Filme, die in einem Schritt präpariert wurden, zeigten generell nur kleine Effizienz, da die Sensibilisatoren dann zur Aggregation neigten und die Zugänglichkeit von ZnO-Poren behinderten. Die photoelektrochemische Effizienz von elektrochemisch abgeschiedenem ZnO wurde klar verbessert , indem das SDA nach der Abscheidung von der Oberfäche entfernt und die Sensibilisatoren in einem separaten Schritt adsorbiert wurden ("Re-adsorption"). Eosin Y zum Beispiel ist ein efficientes SDA, um poröses hoch kristallines ZnO zu erhalten und die Effizienz solcher readsorbierter TSPcZn / ZnO und readsorbierter TSTPPZn / ZnO konnte auf Werte der IPCE von 31 % (680 nm) bzw. 15 % (420 nm) gesteigert werden. Die intensitätsmodulierten Messungen zeigten, dass die Übertragungszeit der Elektronen in solch effizienten Elektroden um etwa eine Größenordnung schneller ist als die mittlere Lebensdauer der Elektronen, was für ein effizientes Einsammeln der photogenerierten Elektronen bei weitgehend unterdrückter Rekombination spricht. Ein typischer Elektronendiffusionskoeffizient von etwa 1 x 10^{-5} cm^2 s^{-1} bei einem Photostrom von 100 µA und eine Diffusionslänge oberhalb 5 µm und damit größer als die Filmdicke von 2-3 µm wurden gefunden. Die Verwendung von Cumarin 343 als SDA führte zu einer Rotation der ZnO Wachstumsrichtung und einem dadurch weiter verbesserten Diffusionskoeffizienten und auch der Diffusionslänge für Elektronenin ZnO. Die Ergebnisse zur photoelektrochemischen Elektrodenkinetik bestätigen die guten guten photoelektrochemischen Eigenschaften dieser elektrochemisch abgeschiedenen ZnO Elektroden und zeigen ihre Perspektive für eine zukünftige Anwendung als Elektroden in farbstoffsensibilisierten Solarzellen.

Contents

1. Introduction

In 1960s, the concept of dye- sensitized solar cell was developed.[1] However, the parameters were not optimized for showing the high properties as photoelectrode. Many research was accomplished to push their properties for photoelectrodes; for example, finding a fact that the dyes shows the sensitization effect when those dyes are on the surface of a semiconductor,[2,3] dispersed particles were used to provide a sufficient interface,[4] and particulate photoelectrodes were employed.[5] Titanium dioxide, which is cheap, abundant, non-toxic, biocompatible and is widely used in health care products as well as in paints, was chosen among semiconductors.[6] Ruthenium complex sensitizer were introduced and found that the function of the carboxylate being the attachment by chemical adsorption of the chromophore onto the oxide substrate.[5,6] After those works, a photon to electron conversion efficiency of 7.1 % was achieved from a dye sensitized nanocrystalline solar cell.[7] The well-known sensitizer as N3,[Ru(dcbpyH2)2(NCS)2] (dcbpyH = 2,2'-bipyridyl-4,4'-dicarboxylic acid) was developed in 1993 and the efficiency reached over 10 %.[8] This achievement roused the people's interest to develop its potential further. A lot of researchers tried to find alternative materials for dye sensitized solar cells; semiconductor,[9-17] electrolytes,[15,18-22] and sensitizers.[11,14,23-33] As one of the example, Coumarin 343 (hereafter C343)[34] was adsorbed on the surface of TiO_2 and the efficiency of 7.4 % (13.5 mA cm^{-2} of short circuit photocurrent, I_{sc}, 0.716 V of open circuit photovoltage, V_{oc}, 0.77 of fill factor, FF under AM 1.5) has been reached. Generally, organic dyes like C343 are attractive sensitizers because of their several advantages. First, they have large extinction coefficient. Second, they have flexibility to modify their structure and hence to control the absorption spectrum. Third, they do not contain noble metals and it allows no concern to the resource limitation. By those advantages, many studies for dye-sensitized solar cells based on such metal-free organic dyes[11,14,36-40] and nature dyes[41-43] have been carried out. The alternative material to TiO_2 has been investigated intensively. Several kinds of metal oxide such as ZnO,[9,13,14,44] Fe_2O_3,[10] In_2O_3,[13,14] SnO_2,[11,13,14] CeO_2,[12] Nb_2O_5[13,14] and their combinations either as mixtures[15] or as core-shell structured composites[16,17] have proven their capability as the electrode candidate for dye- sensitized solar cells. Moreover, some researchers studied to use a solid p-type semiconductor instead of the redox electrolyte. Such as CuI or CuSCN or a hole-transporting solid, for example, an amorphous organic arylamine, were employed for the study.[36,45,46] The first report about the solid states cells is 1998 and the highest efficiency on this system is 3.8 %[47] so far. Beside solid system, the highest conversion efficiency, η of 11.18 % (I_{sc}; 17.73 mA cm^{-2}, V_{oc}; 846 mV, FF; 0.75) was achieved up to now by the combination of TiO_2 for semiconductor, I^-/I_3^- redox couple for electrolyte and $(Bu_4N)_2$[Ru(dcbpyH)$_2$(NCS)$_2$] (monoprotonated N719) for sensitizer.[48] The preferable properties of dye sensitized solar cells are their softness to the environment such as harmless, abundant and low temperature process. As one of the examples, the temperature of around 400 ℃is significantly low compared with the one required for other

kinds of solar cells. By those reasons, dye-sensitized solar cells have been discussed as one option for a next generation of solar cells.[49] Although the conversion efficiency of approximately 11 % has been achieved recently,[48] more improvement is demanded for the practical use.

Approximately 400 ℃ of sintering process is a feature of dye- sensitized solar cells, as described above. However, it is preferable if this temperature could be further reduced. One reason is simply that a lower temperature process is softer to the environment and another is that a low temperature process allows the choice of materials larger to non-heat-resistance materials like flexible, light-weight, and cheap polymers. Electrochemical deposition is one of the methods to cover such conditions since it is a low temperature process and highly crystalline thin films are available by this method. It was found that highly crystallized ZnO thin films can be obtained by the electrochemical deposition using the reduction of either nitrate[50,51] or oxygen.[52,53] The high qualities of crystallinity and high orientation were proven by its epitaxial electrochemical deposition on n-GaN single crystal substrate.[54] Later, new method was developed to prepare the dye modified ZnO films by electrochemical deposition in one-step by adding the dye into the deposition bath.[55,56] Many investigations for the preparation of dye / ZnO films by electrochemical deposition have been carried out so far with several kinds of dyes and crystalline ZnO thin films colored with the loaded dye were successfully obtained with dye molecules such as tetrasulfonated metallophthalocyanines,[57,58] Eosin Y,[59,60] (hereafter EY) tetrabromophenol blue,[61] riboflavin 5-phosphate,[62] and N3.[63,64]

One of the goals in this study is the enhancement of the efficiency in the red part of the visible light, in which the sufficient performance has not been shown. For this aim, 2,9,16,23-tetrasulfophthalocyaninatozinc (hereafter TSPcZn) is chosen since this dye has a high absorption coefficient in the red part of the visible light,[65,66] chemical stabilities[67] and good photoelectrochemical properties.[68] The preparation of TSPcZn / ZnO hybrid thin films by one-step electrochemical deposition method for the application to dye-sensitized solar cells and the understanding of the electron transport kinetics in such electrodes are aimed in this study. Moreover, by electrodepositing ZnO in the presence of two dyes such as TSPcZn and 5,10,15,20-tetrakis-(4-sulfonatophenyl)porphyrinatozinc (hereafter TSTPPZn), the fabrication of the panchromatic films and the influence of the two sensitizers in the film to their photoelectrochemical properties will be discussed.

Since the advantages of this method are one-step and low temperature process. These advantages can be utilized to prepare dye / ZnO hybrid thin films on non-heat-resistance material like conductive textile electrode. The applicability of the method to such material will be also tested.

Another goal in this study is the understanding of electron transport kinetics in dye / ZnO thin films. It was found during the study that the highly porous ZnO films were obtained by extracting EY molecules from the surface of the electrodeposited EY / ZnO.[55] The

sensitizer can be re-adsorbed on such porous ZnO film and the photoelectrochemical performance of such re-adsorbed dye / ZnO film (hereafter re-ad dye / ZnO film) has been improved significantly.[69] The structure of the electrodeposited ZnO films depends on the structure directing agents (SDA) such as EY, C343. Using the several ZnO thin films prepared in the presence of either EY or C343 or sodium dodecyl sulfate (SDS)[70] and having different structure, morphology and orientation due to the influence of SDA, re-ad TSPcZn / ZnO films are prepared mainly and the optimization of the photoelectrochemical performance and the understanding of the electron transport kinetics in such films are aimed.

To study their photoelectrochemical properties, the electrodes will be analyzed by the measurements such as photocurrent transient, intensity modulated spectroscopy (IMPS), intensity modulated photovoltage spectroscope (IMVS), photocurrent action spectrum (conversion efficiency for the incident monochromatic light) and solar cell efficiency (I-V characteristic). And moreover, the electrodes will be analyzed by absorption spectra of the films, the amount of dye and Zn in the films, SEM, AAS, and BET to see their physical properties.

2. Principals of the used model

2.1. Dye sensitized solar cells

The operating principle of dye-sensitized solar cells is described here and previous work related with porphyrins and phthalocyanines is summarized briefly in this section.

2.1.1. Basic of dye-sensitized solar cells

The dye sensitized solar cell was developed in 1960's originally. Following some innovations to achieve a high conversion efficiency, it has recently reached 11.18 % as described in introduction.[4 8] In Fig. 2.1, a schematic explanation of dye sensitized solar cells as the case of N3 / TiO_2 system is shown. The combination of nanocrystalline TiO_2 thin film, Ru complex dye as sensitizer, and iodine containing electrolyte shows the highest efficiency so far. Pt is commonly used as counter electrode.

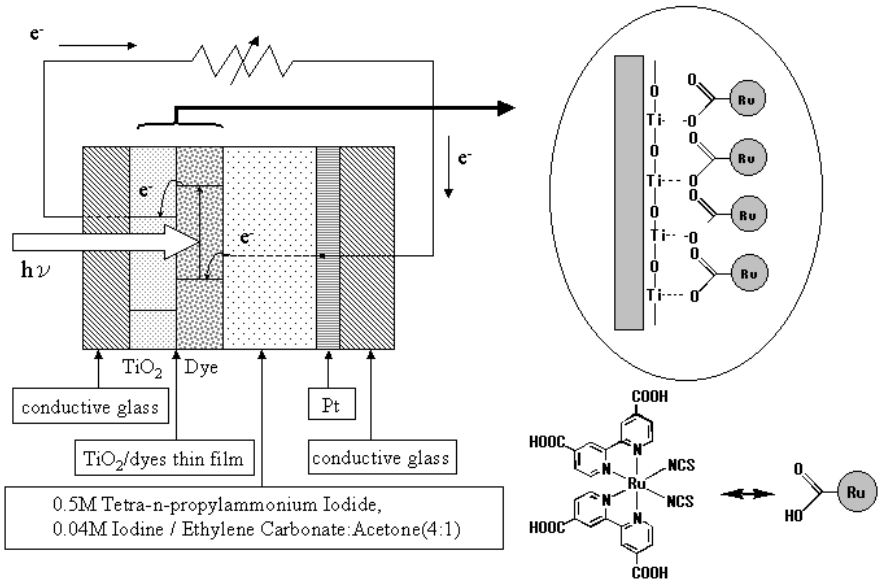

Fig. 2.1; Simple scheme of dye-sensitized solar cells

The cells operate as following; first, the dye adsorbed on the surface of nanocrystalline metal oxide semiconductor absorbs the photon, an electron is excited to the LUMO (lowest unoccupied molecular orbital) from the HOMO (highest occupied molecular orbital) in the dye, and such an electron is, second, injected to the conduction band of the semiconductor. Third, such an injected electron moves through the nanocrystalline semiconductor

network to the external circuit, fourth, the hole created after the excitation at the HOMO of the dye is recovered by an electron from the redox electrolyte. For working as solar cells in this system, it is important that the position of the LUMO is higher than the conduction band of the semiconductor and the position of the HOMO is lower then the position of the redox potential of the electrolyte.

A monolayer of dye is formed spontaneously through attachment via the carboxylic acid anchoring groups. The adsorption follows a Langmuir isotherm.[71] In the case of N3 / TiO_2 electrode, for example, the dye is attached via two of its four carboxylate groups. The carboxylate either bridges two adjacent rows of titanium ions through bidentate coordination or interacts with surface hydroxyl groups through hydrogen bonds. Generally, the optical transition of Ru complexes has metal-to-ligand charge-transfer (MLCT) character. The extinction of the dye involves the transfer of an electron from the metal to the π^* orbital of the ligand.

The characteristic features of this solar cell are the fast electron transportation process and the slow recombination process.

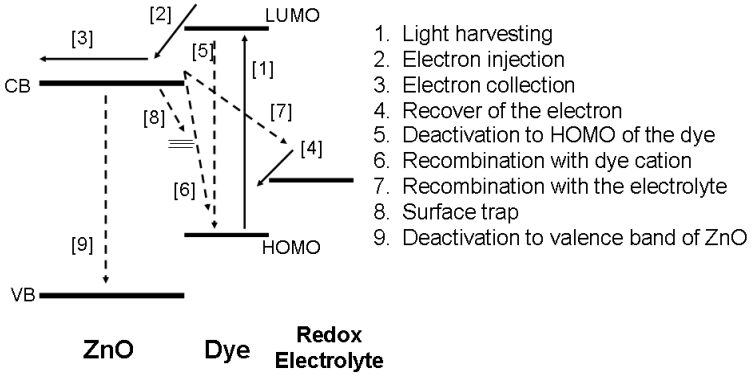

Fig. 2.2; A model of the electron transport and the recombination process in dye-sensitized solar cells. Ideal electron transfers are indicated in solid line and undesirable electron transfers are indicated in dashed line.

In Fig. 2.2, ideal and undesirable processes are shown. In the ideal case, an electron in a dye- modified metal oxide semiconductor electrode is collected at the external circuit without any disturbance. For such electron transfer, the electrode should fill the conditions of a good transport property in the semiconductor matrix (high electron collection efficiency) ([3] in Fig. 2.2), a fast recovery of the electron to the oxidized dye (an electron supply from the redox electrolyte) ([4]) and a good electron separation (charge injection from the sensitizer to the semiconductor) ([2]). Normally, the transportation of the electron through the semiconductor matrix is milli, micro second range.[71] The injection of electrons occurs on the picoseconds time scale.[72,73] And the reduction of the dye cation by I^- in the electrolyte occurs in a few to tens of microseconds, depending on the

concentration and species of cations.[74] The injection yield depends on the particle size and crystallinity of the metal oxide semiconductor[75] and the species and the concentration of the cations in the electrolyte.[76] The recovery of the electron at HOMO of the dye from redox electrolyte occurs in 10 ns range.[71] So it can be seen that overall process is limited by the electron transport in the semiconductor. Such gap of the times, however, gives a chance for the electrons to recombine before they reach the external circuit. An injected electron might recombine with the redox electrolyte [7], the oxidized dye [6], traps in the semiconductor [8] or the valence band of the semiconductor [9]. The recombination with the oxidized dyes takes tens of nanoseconds to a millisecond, depending on the density of electrons in the metal oxide semiconductor.[77] And the recombination with the redox electrolyte occurs in about 10 ms at a light intensity corresponding to illumination of the earth surface by the sun (conditions often referred to as "1sun").[71] This recombination process is almost negligible under short circuit conditions where the average transit time for the collection of electrons is shorter than the characteristic time constant for the back reaction.[78] To confirm such slow back reactions, the electron lifetime has been measured by various groups, showing that the lifetime scales between a few milliseconds to more than one second.[79-82]

The photovoltage of dye- sensitized solar cells can at most reach the difference of the energy between the conduction band of the semiconductor and the redox potential of the electrolyte. The photovoltage of real electrodes is less than this maximum value because the position of the Fermi level and the increased back reaction at an open circuit condition decreases the photovoltage. Many researchers are studying intensively to enhance the photovoltage.[49,71,78,81]

2.1.2.Preceding work based on porphyrins and phthalocyanines

In this study, 5,10,15,20-tetrakis(4-sulfonatophenyl)porphyrinatozinc (TSTPPZn) and 2.9.16.23-tetrasulfophthalocyaninatozinc(II) (TSPcZn) were chosen for sensitizers since such dyes have advantages of absorption coefficient, chemical stability and photoelectrochemical activity. For example, TSPcZn has an intense absorption of 1.6×10^5 l mol^{-1} cm^{-1} at 680 nm, it is approximately 11 times higher than the typical Ruthenium complex dye at the absorption maximum around 540 nm, and it is one of the highest absorption coefficients in longer wavelength.

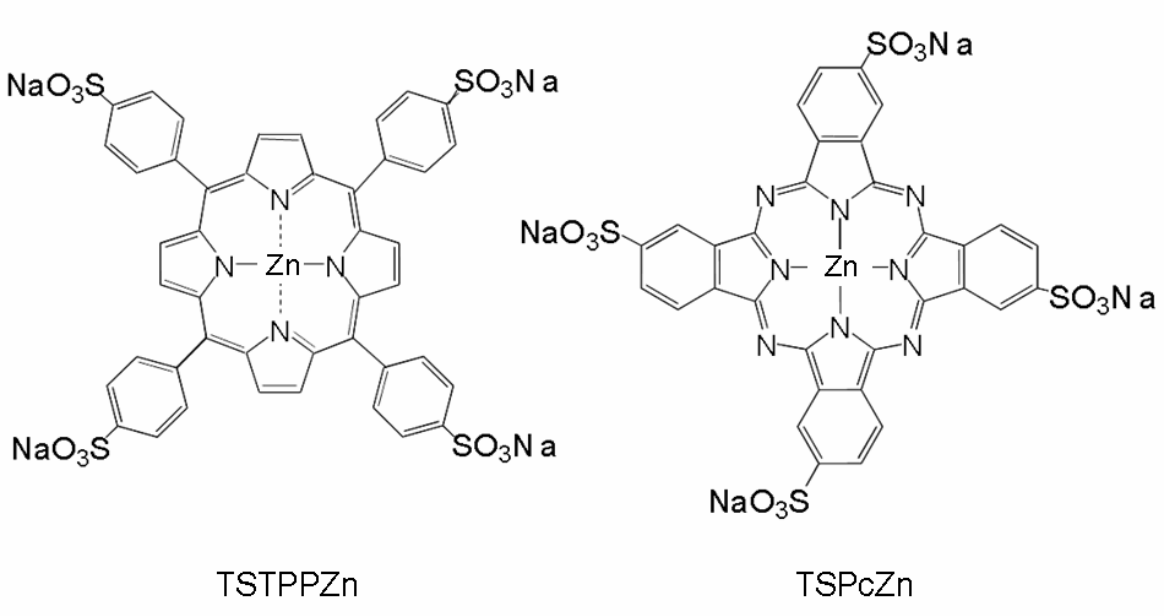

Fig. 2.3; Constitutional formula of TSTPPZn and TSPcZn

Other researchers have also investigated the photoelectrochemical performance of dye-sensitized solar cells with the choice of porphyrins and phthalocyanines as sensitizer. Phthalocyanines are attractive sensitizers since they absorb the photons in near-IR region efficiently and are known for their excellent stability. [83-99] The aggregation form of phthalocyanine molecules is the primary problem to decrease the high photoelectrochemical efficiency and avoiding the aggregation is the main subject when phthalocyanines are used as sensitizer for dye- sensitized solar cells. Yanagi et al.[89] have reported 0.35 % of IPCE (Incident Photon to Current conversion Efficiency) at 700 nm by adsorbing phthalocyanine on single crystal TiO_2. Shen et al.[27] have reported an improved IPCE of 4 % at 690 nm. Oekermann et al.[83] have reported a new method to prepare phthalocyanine- modified ZnO hybrid thin film by electrochemical deposition and 0.4 % of IPCE at 685 nm was obtained by using phthalocyanine. Nazeeruddin et al.[28] and Hagfeldt et al.[91] have adsorbed phthalocyanines to their optimized TiO_2 thin films and reported IPCE of 45 % at 700 nm and 24 % at 690 nm respectively.

As well as phthalocyanines, porphyrins have been also investigated by many researchers. And it has found that porphyrins have a high electron injection efficiency from the LUMO to the conduction band of the semiconductor.[29,100-107] Kalyanasundaram et al.[101] have reported the efficient charge injection from the excited state of Tetrakis(4-carboxyphenyl) porphyrinatozinc (TCPPZn) into the conduction band of TiO_2 and IPCE of 42 and 8 – 10 % at Soret- and Q- band of TCPPZn respectively. Dabestani et al.[104] have reported IPCE of 9.5 % at the Soret- band of TCPPZn. Boschloo et al.[29] also used TCPPZn as sensitizer for TiO_2 and have reported 40 and 10 – 16 % of IPCE at Soret- and Q- band of TCPPZn. Cherian et al.[101] have reported highest efficiency of 55 and 25 – 45 % of IPCE at the Soret- and Q- band respectively. This has been achieved by using deoxycholic acid as a co-adsorbate.

Some researchers have adsorbed both porphyrin and phthalocyanine to TiO_2,[108-111] as we are aiming in this study for electrodeposited ZnO thin films. Deng et al.[110,111] have reported that the photoelectrochemical efficiency at longer wavelengths has been improved by the effect of the doping with porphyrin to phthalocyanine / TiO_2 electrode. It seems that the porphyrin molecules affect to reduce the aggregation form of phthalocyanine and hence the photoelectrochemical efficiency was improved. Such preceding work gives us a positive sign for achieving panchromatic sensitization by using both porphyrin and phthalocyanine to utilize the wide range of the visible light.

2.2. Electrochemical deposition of ZnO

Fabrication of thin films such as metal chalcogenides and metal oxides by electrochemical deposition is attractive compared to other methods which require specific conditions such as vacuum, high temperature and so on. Its attractiveness is following; the economical benefit (equipment, maintenance), the harmless process to the environment, for example, low temperature process, and the flexibility for the size and the shape in the industrial applications.[53,60,112] And moreover, films which have transparency, crystallinity and adherence properties are available by electrochemical deposition method. A number of examples are found from publications for the electrodeposited metal oxide thin film such as CeO_2,[113] Fe_3O_4,[114] ZrO_2,[115] Cu_2O,[116] Bi_2O_3,[117] TiO_2[63,118] and ZnO.[119-121] ZnO is an attractive material due to its electronic, mechanical, and thermal properties. And ZnO is used in many applications such as chemical sensors, piezoelectric transducers, solar cells, light-emitting diode (LEDs) and blue laser diodes (LDs).[122-125] Since electrochemical deposition has such attractive properties and ZnO has quite similar characteristics with TiO_2 which is used commonly in dye- sensitized solar cells and has not established yet to prepare by electrochemical deposition with good characteristics, especially with high crystallinity, the electrodeposition of ZnO and the application to dye-sensitized solar cells have been chosen in this study. Several papers have been published on the cathodic deposition of ZnO.[50-53,119,120126-129]

To prepare ZnO films in this study, the reduction of either nitrate or oxygen was utilized. SEM image of the ZnO film prepared by using the reduction of oxygen is shown in Fig. 2.4 as one of the examples. The crystalline ZnO particles which have hexagonal shape are observed in the image.

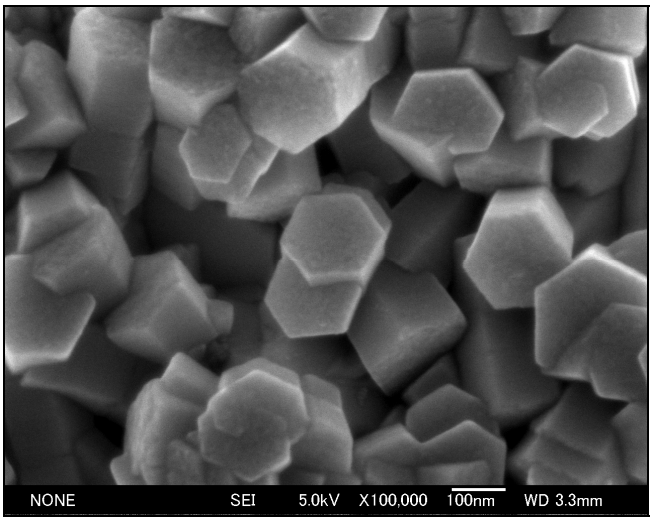

Fig. 2.4; SEM image of electrodeposited ZnO film precipitated by using the reduction of oxygen. SEM image was provide from collaboration partners in Gifu University

In the deposition using either nitrate or oxygen, the key reaction to precipitate ZnO is a generation of hydroxide ion at the cathode. The reactions for both cases are described in following;

$$NO_3^- + H_2O + 2e^- \rightarrow NO_2^- + 2OH^- \quad (E^0 = -0.240 \text{ V vs. SCE}) \qquad (2.1)$$

$$O_2 + 2H_2O + 4e^- \rightarrow 4OH^- \quad (E^0 = +0.16 \text{ V vs. SCE}) \qquad (2.2)$$

The created hydroxide ions are expected to react with Zn^{2+} and precipitate as zinc hydroxide. Following this reaction, zinc hydroxide is dehydrated to ZnO.[53,50]

$$Zn^{2+} + 2OH^- \rightarrow Zn(OH)_2 \rightarrow ZnO + H_2O \qquad (2.3)$$

The overall reaction for the precipitation of ZnO by using the reduction of either nitrate or oxygen is expressed in following;

$$Zn^{2+} + NO_3^- + 2e^- \rightarrow ZnO + NO_2^- \quad (E^0 = +0.246 \text{ V vs. SCE}) \qquad (2.4)$$

$$Zn^{2+} + \frac{1}{2}O_2 + 2e^- \rightarrow ZnO \quad (E^0 = +0.69 \text{ V vs. SCE}) \qquad (2.5)$$

The E^0 values were calculated from the standard reaction Gibbs energies (ΔG) derived from the Gibbs free energy of formation at 298 K (ΔG_f) of each chemical species in water from the literature.[130]

Interesting differences were found from these two methods that, for example, the ZnO deposited by using the reduction of nitrate has a random orientation, while the ZnO deposited by using the reduction of oxygen has a tendency to be self-oriented with the c-axis perpendicular to the substrate, and the reaction is limited by the kinetics of the reactions in the case of nitrate and by the mass transport in case of oxygen. [56,112,131] In the case of the oxygen reduction, the current reflects the concentration and mass transport of the oxygen to the electrode, sensitively. The control of the oxygen transportation appears as an important factor to control the growth of ZnO. Then, a rotating disk electrode (RDE) was used during the deposition.

By adding dye into the deposition bath, the fabrication of dye-modified ZnO thin films by electrochemical deposition in one-step has been achieved for both systems.[56,60] The presence of dye molecules in the deposition bath influences the deposition mechanism of the film significantly and its characteristics such as morphology, transparency, orientation and porosity. It was found that the current during the deposition by using the reduction of nitrate was decreased when dye molecules were added into the deposition bath, and the current was increased, on the other hand, in the deposition using the reduction of oxygen.[56,60] In the case of nitrate, Zn^{2+} ions adsorbed on either the substrate or the film are acting as a catalyst for the reduction of the nitrate and the current changes in proportion to the concentration of Zn^{2+} in the bath though "catalyst" is not true since Zn^{2+} ions are reacting to ZnO spontaneously.[131] When the dye is present in the deposition bath, it disturbs the adsorption of Zn^{2+} ions on the surface of the film and it appears as the decrease of the current since Zn^{2+} ions do not effect as catalyst if they could not be adsorbed. On the other hand, the current is increased in the case using the reduction of oxygen for the deposition due to the presence of the dye molecules in the bath.[56] It is caused since sensitizer molecules, e.g. Eosin Y, are working as catalyst for the reduction of oxygen. However, such an enhancement of the current can be observed only when Zn ions are present in the deposition bath. This shows the complexity of the reactions.

Regarding the application to dye sensitized solar cells, the preparation of dye-modified ZnO films by electrochemical deposition in one-step and at low temperature is one perfect method in the sense of its harmless character to the environment. However, such films show rather poor photoelectrochemical efficiencies up to now since the excess amount of dye molecules on the film fills the pores in the film and decreases the net porosity of the film.[58,63,64,83] Such situation opened up the idea to utilize the dyes as structure directing agents (SDA) since the dye influences significantly the morphology and porosity. The SDA can be removed following the deposition, and adsorbing the sensitizer on the surface of porous ZnO again achieves an ideal monolayer adsorption (thin layer with less aggregation form of sensitizer molecules) of the sensitizer on ZnO. Currently molecules such as Eosin Y,[69] Coumarin 343 and sodium dodecyl sulfate (SDS)[70] were found as an effective SDA and the photoelectrochemical efficiencies of the electrodeposited ZnO films

have been improved significantly.[6 9]

2.3. Absorption spectroscopy

In optics, the Lambert-Beer law, also known as Beer's law or Beer-Lambert-Bouguer law is a relationship that relates the absorption of light to the properties of the material through which the light is travelling. The simple image of this law is expressed in Fig. 2.5.

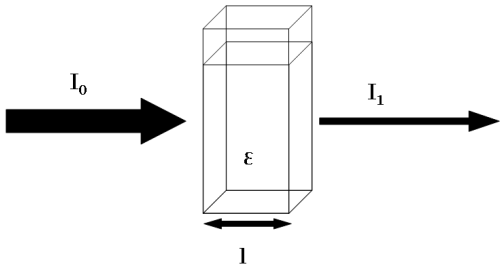

Fig. 2.5; Model of Lambert-Beer absorption of a beam of light as it travels through a cell of length l.

This law is expressed by;

$$A = \varepsilon cl = -\log \frac{I_1}{I_0} = -\log T \quad (2.6)$$

Here A is absorbance, I_0 is the intensity of the incident light, I_1 is the intensity after passing through the material, l (cm) is path length, c (mol l^{-1}) is the concentration of absorbing species in the material, ε (M^{-1} cm^{-1}) is molar extinction coefficient and T is transmittance.
This formula was used to check the concentration of the dye in the electrochemical deposition bath and the dye concentration in aqueous ammonia solution to calculate the dye content in the film.

The absorption coefficient α (cm^{-1}) is expressed by;

$$I_1 = I_0 \exp(-\alpha l) \quad (2.7)$$

the absorption coefficient in a solid material is interpreted that it is directly proportional to the concentration of the absorber in the solid and the molar extinction coefficient;

$$\alpha = \varepsilon c \ln 10 = 2.303\ \varepsilon c \quad (2.8)$$

The absorption coefficient α in the film was estimated by using this formula for the fitting to obtained the electron diffusion coefficient D_n ($cm^2\ s^{-1}$) in the analysis of IMPS and IMVS (see below). In this analysis, the concentration of the dye in the film was calculated from the amount of dye loaded and the film thickness. It should be mentioned, however, that the estimation of an absorption coefficient in this way is not precise enough because there is a scattering of light in the film. It means that the light might not continue to travel straight through the film due to the reflection. The influence of the light scattering and the light reflection can be seen in their transmission spectra. When the absorption coefficient in the film was estimated from transmission spectrum (transmission is obtained from the data measured in absorption spectroscopy), it is often the case that the absorption coefficient is higher than the one obtained from the dye concentration in the film. However, obtaining the absorption coefficients from the transmission spectra is not precise, either. The chosen method underestimates the amount of absorbed light because scattering and reflection will decrease the absorption in the cell, but using the transmission spectra would severely overestimate it since all light that is scattered or reflected would be assumed to be absorbed.

2.4. Action spectrum

One of the ways to analyze the efficiency of dye-sensitized solar cells is to measure the incident photon to current conversion efficiency (IPCE).[7] The wavelength dependent IPCE term can be expressed as a product of the quantum yield for charge injection (Φ_{inj}), the efficiency collecting electrons in the external circuit (η_c), and the fraction of radiant power absorbed by the material or light harvesting efficiency (LHE). It is expressed in the following formula.

$$IPCE = LHE \cdot \Phi_{inj} \cdot \eta_c \qquad (2.9)$$

While Φ_{inj} and η can be rationalized on the basis of kinetic parameters, LHE depends on the active surface area of the semiconductor and on the cross section for light absorption of the molecular. Practically, IPCE measurements are performed with monochromatic light and calculated as a ratio of the photocurrent (number of the electrons) and the photon flux (the number of photons). It is expressed by;

$$IPCE(\%) = \frac{1240 \times j_{photo}}{\lambda \times I_0} \times 100 \qquad (2.10)$$

Here, j_{photo} is photocurrent (mA cm^{-2}), λ is wavelength (nm) and I_0 is photon flux (mW cm^{-2}).

The quantum efficiency of the cell is expressed as absorbed photon to current conversion efficiency (APCE). This is the ratio of the photons which are absorbed by dyes and the electrons caused by the illumination. This is a better way to analyze the efficiency of the cell. However, there is a difficulty to estimate LHE (light harvesting efficiency) since the films have a light reflection and a light scattering in the cell. By those reasons, IPCE is often used to compare the efficiencies of the electrodes. Also, it is the technically relevant number since we can see how many photons are really converted.

2.5. Overall efficiency of the photovoltaic cell

The overall efficiency of solar cell, η, is calculated from;

$$\eta(\%) = \frac{I_{sc} \times V_{oc} \times ff}{I_0} \times 100 \qquad (2.11)$$

Here, I_{sc} is a short circuit photocurrent (mA cm^{-2}), V_{oc} is an open circuit photovoltage (V), ff is a fill factor and I_0 is a light intensity (mW cm^{-2}). The efficiencies reported till now are in the range of 7-11 %. It is strongly depending on the fill factor of the cells. Under an optimum current collection situation, minimizing ohmic losses caused by the resistance of the substrate, and in lower light intensities, fill factors of 0.8 have been obtained.[132]

2.6. Photocurrent transient

Time- resolved photocurrent measurements have turned out to be a valuable tool in studies of photoelectrochemical surface processes, especially surface recombination, at semiconductor surfaces,[133,134] in the case of molecular semiconductors,[135,136] and especially in the case of dye-sensitized oxide semiconductors.[83,137-139]

In this section, a model for time-resolved photocurrents in dye sensitized solar cells is shown.
Since dye- sensitized solar cells consisted of nanosize particles, their properties are unique compared to bulk materials. It can be expected that the electron transport in the films is dominated by the diffusion rather than by the migration (driven by electrical field). It is generally assumed that nanosize particles are too small to sustain the electric fields when

surrounded by excess ions of the electrolyte. It has been reported by several researchers that the electron injection in dye sensitized solar cells is ultrafast and it occurs in subpicosecond time scales.[72,140-146] As a result, the photocurrent transient response is expected to be dominated by electron transport through the particle network.

Södergren et al.[147] have considered generation, diffusion and back reaction of electrons with I_3^- ions in the dye sensitized nanocrystalline TiO_2. The time dependence of the electron density, $n(x,t)$ is given by;

$$\frac{\partial n(x,t)}{\partial t} = \Phi_{inj}\alpha I_0 e^{-\alpha x} + D_n \frac{\partial^2 n(x,t)}{\partial x^2} - \frac{n(x,t)-n_0}{\tau_n} \qquad (2.12)$$

Where D_n is the diffusion coefficient of electrons, n_0 is the electron density in the dark, τ_n is the lifetime of the electrons determined by back reaction with I_3^- ions in the electrolyte, α is the absorption coefficient of the electrode, I_0 is the incident photon flux and Φ_{inj} is the efficiency of electron injection.

The steady state solution of formula (2.12) is obtained by assuming that D and τ are constant and $\Phi_{inj} = 1$. Under these conditions, the photocurrent due to excess carriers is the independent of voltage, and the steady state photocurrent is given by

$$j_{ss} = \frac{qI_0\alpha L_n\left(-\sinh\left(\frac{d}{L}\right)\right) - \alpha L_n \exp(-\alpha d) + \alpha L_n \cosh\left(\frac{d}{L_n}\right)}{\left(\alpha^2 {L_n}^2 - 1\right)\cosh\left(\frac{d}{L_n}\right)} \qquad (2.13)$$

where q is the elementary charge, d is the film thickness and the electron diffusion length $L_n = (D_n\tau_n)^{1/2}$. It should be noted that the predicted photocurrent is independent of the voltage in this model. And the recombination process and the barrier to the electron extraction at the substrate are neglected. Those are unreasonable points in this model.

Cao et al.[148] have developed further to discuss the time dependent solutions of the generation and the collection for the case where the cell is illuminated from the substrate side. They assume that the electron transport occurs predominantly by diffusion at relatively low light intensities where the electric field is almost negligible. The expression derived for the response to a light step shows that the rise of the photocurrent is multi-exponential.

$$j_{photo}(t) = qD\frac{\partial n(x,t)}{dt} = j_{ss} - \sum_{k=0}^{\infty} C_k \frac{\pi}{2d}(2k+1)\exp\left[-\left(\frac{1}{\tau} + \frac{D\pi^2(2k+1)^2}{4d^2}\right)t\right] \qquad (2.14)$$

where C_k is given by

$$C_k = \frac{2qI_0\alpha {L_n}^2}{d\left(1-{L_n}^2\alpha^2\right)}\left(\frac{(-1)^{k+1}\alpha\exp(-\alpha d)+\frac{\pi}{2d}(2k+1)}{\frac{1}{{L_n}^2}+\frac{\pi^2(2k+1)^2}{4d^2}}+\frac{(-1)^k\alpha\exp(-\alpha d)-\frac{\pi(2k+1)}{2d}}{\alpha^2+\frac{\pi^2(2k+1)^2}{4d^2}}\right) \quad (2.15)$$

In this solution, the steady-state photocurrent is proportional to the light intensity. And this solution gives a nonexponential rise and a rise time independent of light intensity. It can be seen that I_0 is not in the exponential term. However, this simulation does not fit to the experimental results since the rise time of the photocurrent transient shows the dependency on the light intensity.

Then, they took notice that the diffusion coefficient represents the thermally activated transport of the electrons through the particle network. As example, the rise time of the photocurrent is varied by the characteristics (depth, concentration and so on) of the traps in the films and the resistance of the contact region between the film and the substrate. Taking these factors into account, they obtained the transportation formula by assuming that the effective diffusion coefficient is proportional to the electron concentration and the recombination losses are negligible.

$$\frac{\partial n(x,t)}{\partial t} = \Phi_{inj}\alpha I_0 e^{-\alpha x} + \frac{\partial\left(D_0\frac{n(x,t)}{n_0}\frac{\partial(n(x,t))}{\partial x}\right)}{\partial x} \quad (2.16)$$

where D_0 is the electron diffusivity in the dark. They defined the dimension less concentration n^*, dimensionless distance x^*, and dimensionless time t^*, as

$$n^* = \frac{n}{n_0}, x^* = \frac{x}{d}, t^* = \frac{D_0 t}{d^2}$$

Substituting these parameters into formula (2.16), they obtained,

$$n^*\left(\frac{\partial^2 n^*}{\partial {x^*}^2}\right)+\left(\frac{\partial n^*}{\partial x^*}\right)^2-\frac{\partial n^*}{\partial t^*}+\beta\exp(-\gamma x^*)=0 \quad (2.17)$$

where $\beta = I_0\alpha d^2/n_0 D_0$ and $\gamma = \alpha d$. The parameter γ expresses the absorbance of the film. And it can be seen that the term β is proportional to the light intensity.

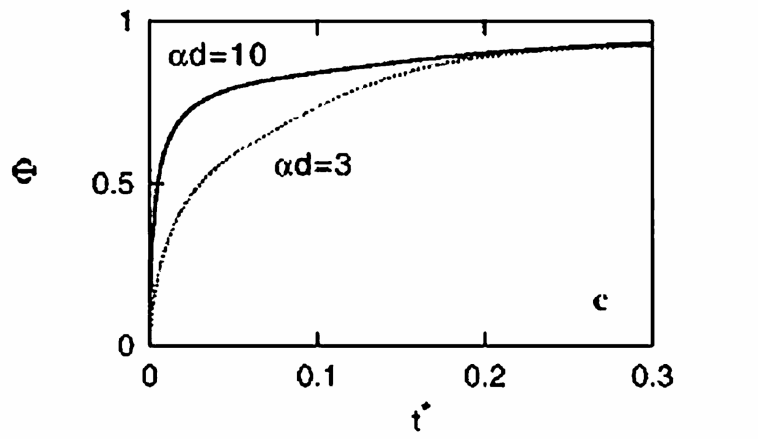

Fig. 2.6; Photocurrent transients calculated from formula 2.17 for $\alpha d = 10$ and $\alpha d = 3$. In the calculation, the value of 1000 and 300 respectively were used for β. And those are chosen to corresponding to the same light intensity. The abscissa is dimensionless time t* defined by $t^* = D_0 t / d^2$, and the ordinate is the quantum efficiency η. Recombination is neglected in the calculation $(\tau_0 \to \infty)$. (taken from ref. 1 4 8)

In Fig. 2.6, normalized transients predicted by formula (2.17) for different values of γ are shown. The calculated transients are comparable with the experimental photocurrent transients. The general features of the experimental transients are reproduced in the calculated plot. For the case with $\alpha d = 10$, it is corresponding to the strong absorption. And for the case which $\alpha d = 3$, it is corresponding to the weak absorption. Since a number of electrons will be generated close to the substrate if the film absorbs the photons relatively strong, the high concentration of electrons near the substrate appears as fast increasing of the photocurrent in the transient measurements. And in the case that the film absorbs the light weakly, rather homogenous generation profile of the electrons can be expected. Taking the electron transport in the nanoparticle matrix into account, it is clear that the photocurrent increases slowly.

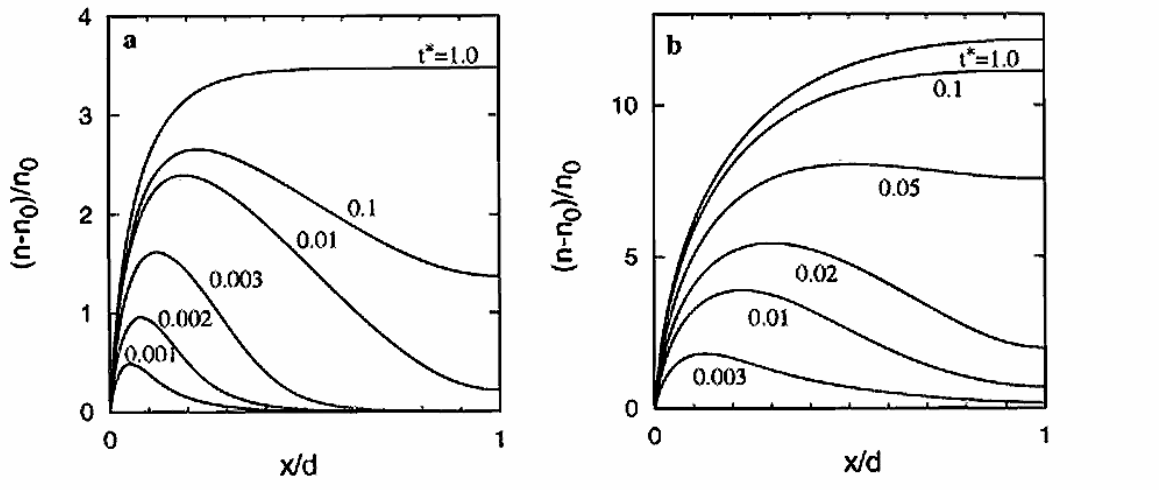

Fig. 2.7; Calculated spatial distribution of the electron concentration in the film obtained from formula 2.17 as a function of dimensionless time t^* for (a) $\alpha d = 10, \beta = 1000$ and (b) $\alpha d = 3, \beta = 300$. (taken from ref. 1 4 8)

In Fig. 2.7, electron concentration profiles as a function of time are shown. This is also calculated from formula (2.17) for the transients shown in Fig. 2.6. When the absorption of the film is strong as $\alpha d = 10$ (Fig. 2.7 a), a concentration peak will be built up in a short distance from the substrate and it appears as fast rise in the photocurrent transient. On the other hand, when the light absorption in the film is weak, the electron concentration in the outer part of the film builds up to the steady-state concentration profile (Fig. 2.7 b). In this weaker absorption case, the concentration peak is far away from the substrate, and the initial increase is much less visible. Those results show that the rising time of the photocurrent in the transient measurements are strongly related with the absorption of the photons in the film. It should be noted that the recombination process is neglected in this model. When the recombination process occurs in the device, it appears as the relaxation of the photocurrent after showing the overshoot as the illumination starts. And also it should be noted that the diffusion coefficient of the electrons and the electron lifetime in the electrode vary with the light intensity and hence the simulation of the photocurrent transients will be modified by those factors.

2.7. Intensity Modulated Photocurrent Spectroscopy (IMPS)

Intensity modulated photocurrent spectroscopy (IMPS) measures the complex ratio of the photocurrent flux to the incident light flux over many decades of frequency with either a frequency response analyzer or a lock-in amplifier. This measurement is useful to measure the transit time of the electrons from their absorption, the injection, traveling through the nanoparticulate semiconductor and finally detected as a current. Recombination processes in the device are observed by a phase shift between modulated light and photocurrent

detected by a response in the (+, +) quadrant of the complex plane plot. This is corresponding to the relaxation of the photocurrent shortly after the start of the illumination in photocurrent transient measurements. IMPS has been used before to study the electron transport in macroporous semiconductor electrodes,[134,149-151] electron-hole recombination processes, majority carrier injection at the bulk semiconductor / electrolyte interface,[152] and the kinetics of the electron tunneling between semiconductor quantum dots and a metal or redox system in solution,[153,154] and recently for dye- modified metal oxide semiconductors.[19,79,82,151,155-160]

In IMPS, a small-amplitude modulated light intensity δI_0 is superimposed to a steady-state light intensity I_0, giving a modulated photocurrent j_{photo} superimposed to the background steady-state photocurrent. The modulated photocurrent j_{photo} is measured at frequencies lower than the RC time constant of the electrochemical setup. The ratio of $j_{photo} / q\delta I_0$ is called the optoelectrical transfer function. Slow processes contributing to the total photocurrent will lead to a phase shift, $\theta(\omega)$ ($\omega = 2\pi f$, f is the modulation frequency), between δI_0 and j_{photo}, as is shown schematically in Fig. 2.8.

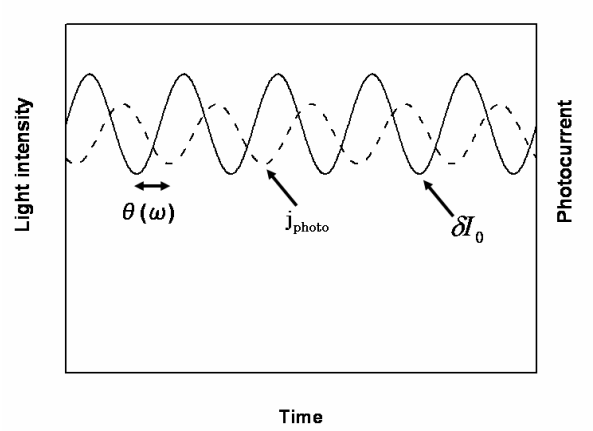

Fig. 2.8; The simple basic diagram of IMPS, the modulation of light intensity and the modulation of photocurrent. The photocurrent shows a phase shift relative to the light intensity. $\Phi(\omega)$ is modulated light intensity, $j(\omega)$ is modulated photocurrent, $\theta(\omega)$ is phase shift.

The transfer function, determined by the amplitude ratio and the phase shift, can be plotted in the complex plane (the imaginary component versus the real component) or in a Bode plot (the imaginary or the real component versus the frequency f) The frequency at which the imaginary part of the function shows a minimum is related to the average transit time of an electron through the device.[82,151]

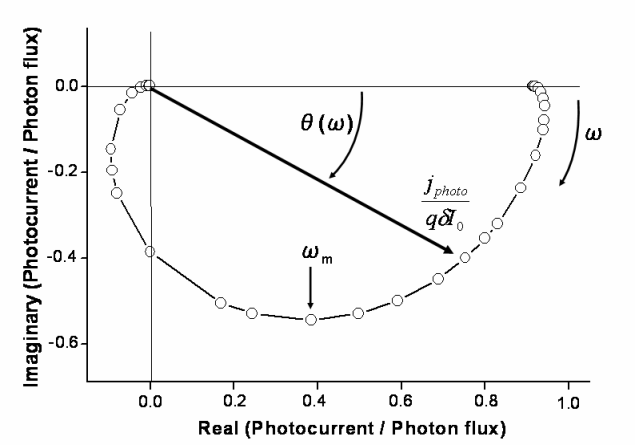

Fig. 2.9; Complex plane plot of the electron transport in dye / ZnO thin film. The optoelectrical transfer function j_{photo} / $q\delta I_0$, the phase shift $\theta(\omega)$ between the modulated light intensity and the photocurrent, and the typical frequency of the electron transfer process ω_m, are indicated in the figure.

In Fig. 2.9, a typical IMPS response for dye / ZnO thin film is shown in the complex plane with the frequency as a parameter. The shape of the IMPS is a flattened semicircle which is typical for nanocrystalline electrodes.[151] The plot indicates the lag of the photocurrent behind the illumination. When most electrons are collected efficiently, such lag is caused by the delay time associated with the electron transport from the injection site to the substrate. It implies the relatively longer electron lifetime in the electrode. If the electron lifetime was short, the photoelectrochemical response would be limited by this lifetime since most generated electrons are lost during their transit. The delay time associated with diffusion of electrons to the contact is roughly given by $t = d^2 / D_n$. However, the delay time depends on the site within the macroporous electrode and hence the distance from the collecting electrode. Therefore, the IMPS response is characterized by a distribution of delay times. This explains the flat shape of the IMPS response.

In the high frequency limit, the electron transfer is slower than the light modulation and both the real and the imaginary components are zero. When the frequency is decreased, the phase shift between the photon flux and the photocurrent decreases and one response appear on x- axis if the electrode has no recombination reaction. The frequency at the minimum of this distorted semicircles ω_m corresponds to the reciprocal of the average transit time of the photogenerated electrons through the dye / ZnO thin film. This transit time may depend on the steady-state illumination intensity because of a different level of trap filling. In the low-frequency limit, the function is real with a value close to one. It means that almost photogenerated electrons are collected at the back contact in the steady state. As described above, the responses in (+, +) quadrant in the complex plane mean the presence of recombination in the device. Such phenomena can be seen at bulk semiconductor electrodes. Rapid electron collection in the space charge region of bulk semiconductors at the frequencies used in IMPS gives no phase shift between the minority carrier flux and the illumination. The response in (+, +) quadrant arises from the contribution of majority carriers moving towards the surface to take part in recombination.

Since these carriers have the opposite sign to the minority carrier, the phase lag in the current associated with the kinetics of surface recombination appears shifted by -180°. In the prediction of IMPS response for nanocrystalline thin film electrodes, whole IMPS responses are expected to appear in (+, -) quadrant in the plot.[155] The responses in (-, -) quadrant are expected due to slow electron transport in the film[150] when the electrode is illuminated from electrolyte side and when the light penetration is not deep. The plot shown here was obtained by the illumination from the substrate side. Electrons are photogenerated rather near to the substrate. In such case, the responses in (-, -) quadrant are not expected principally.[151] The observed responses means that the electrode is effected by RC attenuation or that the distribution of the sensitizers is inhomogeneous in the film.[159] In most of the cases, these responses which are crossing the imaginary axis are caused by the RC attenuation.[82]

Modelling and fitting procedure to estimate the effective electron diffusion coefficients;

The collection of photo-injected electrons in dye- sensitized solar cells takes place by diffusion since the presence of the electrolyte in the porous film minimizes the electrical field in the electrode and it is negligible.[155] Reported values of the electron diffusion coefficient D_n at solar illumination intensities are < 10^{-4} cm^2 s^{-1}, which is more than two orders of magnitude lower than D_n for bulk metal oxide semiconductors such as anatase TiO_2.[156,161] It was also reported that D_n becomes smaller as the light intensity is decreased because of an increased trapping probability at a lower level of trap filling.[148, 155] And if it becomes smaller, the life time of electrons in the electrode will be the key issue for cell performance since the electrons should be collected in the external circuit before they recombine with the redox electrolyte. To investigate those factors, there is a model to estimate D_n from the intensity modulated photocurrent response.

In IMPS, it is assumed that the light scattering and any electric field in dye sensitized nanocrystalline solar cells are neguligible.
To express the injection, collection and back reaction of the electrons in dye- modified metal oxide semiconductor electrodes, the continuity equation (2.12) is used.
During this intensity modulated measurement, the sample is illuminated with modulated light (small ac component, 10 % or less of the dc component), which can be described by the periodic illumination function;

$$I(t) = I_0\left[1 + \left(\delta e^{i\omega t}\right)\right] \qquad (2.18)$$

Where $\omega = 2\pi f$ is the variable modulation frequency and δ is $\ll 1$. An electron transit time $\tau_D = 1/\omega_{\min} = 1/2\pi f_{\min}$, where f_{min} is the frequency of the minimum of the semicircle, can be defined, which gives an estimation of the average transit time of electrons. It is

comparable with the time taken for the electrons to travel halfway through the film, which is given by $d^2/4D_n$ where d is film thickness (exact calculations for illumination from the substrate side show that τ_D as defined here is between 1.3 and 1.5 times higher than $d^2/4D_n$ for $\alpha d < 5$).[82] Using τ_n from IMVS measurement (see below), the analytical solutions of the formula (2.12) derived by Dloczik et al.[155] can be used to fit the IMPS response and calculate the effective diffusion coefficient D_n of the electrons. The normalized solutions for the modulated photocurrent j_{photo} and therefore the IMPS response for illumination through the substrate side of films are

$$\frac{j_{photo}}{q\delta I_0} = \frac{\alpha}{\alpha+\gamma} \cdot \frac{e^{\gamma d} - e^{-\gamma d} + 2\alpha \dfrac{e^{-\alpha d} - e^{-\gamma d}}{\gamma - \alpha}}{e^{\gamma d} + e^{-\gamma d}} \cdot \Phi_{inj} \qquad (2.19)$$

And

$$\gamma = \left[\frac{1}{D_n \tau_n} + i\frac{\omega}{D_n} \right]^{1/2} \qquad (2.20)$$

Here, q is the elementary charge.
The effective diffusion coefficient takes into account the possible trapping and detrapping of electrons. In the case of only on trap level at a fixed trapping energy, it can be defined by

$$D_n = D_{cb}\frac{k_d}{k_t} \qquad (2.21)$$

Here, k_t and k_d are the first-order rate constants for trapping and detrapping, respectively, and D_{cb} is the diffusion coefficient of electrons in the conduction band.[159] In the case of TiO_2 films, it appears that electron traps are distributed exponentially in energy, giving rise to a characteristic intensity dependence of D_n, which arises from trap filling.[157,158] An important advantage of intensity modulated measurements such as IMPS and IMVS is that D_n as well as τ_n can be treated as a constant for a given dc light intensity, I_0.[155]
The experimentally measured IMPS response is effected by RC attenuation, especially toward higher frequencies. Therefore, (2.19) is multiplied with the complex attenuation function;

$$A(\omega) = \frac{1}{1 + i\omega RC} \qquad (2.22)$$

Here, R is the resistance, C is the capacitance of the electrode.[159] It has been found that

the factors of the resistance and the capacitance under short circuit conditions are due to the interface between the substrate (SnO_2) and the semiconductor (TiO_2 or ZnO), and the substrate (SnO_2) and the electrolyte. The capacitace is also related with the high surface area of the semiconductor. The typical value for those factors are from 10 to 20 Ω and 30 μF cm^{-2} respectively.[155] In this study, the resistance was assumed as 10 Ω in the fitting.

The photocurrent detected at the external circuit is the result of the competition between the electron diffusion and the electron recombination with the redox electrolyte. A quantity to decide the cell performance can be expressed as a diffusion length, L_n estimated from obtained τ_n and D_n.;

$$L_n = \sqrt{D_n \tau_n} \qquad (2.23)$$

In an efficient electrode, L_n should be larger than its film thickness. And the film thickness of a dye- sensitized solar cell should be thick enough to absorb most of the incident light. If L_n was not larger than the film thickness, a maximum (peak) will appear in the electron density profile in the film. And this maximum means that electrons generated beyond it diffuse away from the substrate and are lost by back reaction with the redox electrolyte. It follows that this part of the sensitized film does not contribute to the photocurrent at all although they absorb photons.

2.8. Intensity Modulated Photovoltage Spectroscopy (IMVS)

Intensity Modulated Photovoltage Spectroscopy (IMVS) measures the complex ratio of photovoltage to incident light flux over many decades of frequency. This measurement is closely related to IMPS. G. Schlichthörl et al. have considered dye- sensitized nanocrystalline n-type semiconductor electrodes and have discussed the relationship between the small amplitude- modulated photovoltage and the corresponding modulation of the number density of free and trapped electrons.[80,162] At open circuit condition, all excited electrons are injected into the conduction band of the semiconductor and such electrons must finally react at the semiconductor/electrolyte interface. Charge trapping, detrapping and recombination via the conduction band and surface states will determine the concentration of electrons in the electrode in the steady state.

Formula (2.12) is also used for the model of IMVS in dye- sensitized solar cells. The general boundary conditions are

$$D_n \left.\frac{\partial n}{\partial x}\right|_{x=0} = k_{ext}\, n_{x=0}; \left.\frac{\partial n}{\partial x}\right|_{x=d} = 0 \qquad (2.24)$$

For $\Phi_{inj} = 1$, the solution of formula (2.12) for small amplitude intensity modulation using the boundary conditions given in (2.24) takes the form;

$$n(x,t) = \left[Ae^{\gamma x} + B^{-\gamma x} + Ce^{-\alpha x}\right]e^{i\omega t} \qquad (2.25)$$

$$C = \frac{\alpha\delta\ I_0 / D}{\gamma^2 - \alpha^2} \qquad (2.26)$$

$$A = C\frac{\alpha e^{-\alpha d}\left(k_{ext} + \gamma D_n\right) - \gamma e^{-\gamma d}\left(k_{ext} + \alpha D_n\right)}{\gamma\left[k_{ext}\left(e^{\gamma d} + e^{-\gamma d}\right) + D_n\gamma\left(e^{\gamma d} - e^{-\gamma d}\right)\right]} \qquad (2.27)$$

$$B = -C\frac{\alpha e^{-\alpha d}\left(k_{ext} - \gamma D_n\right) + \gamma e^{\gamma d}\left(k_{ext} + \alpha D_n\right)}{\gamma\left[k_{ext}\left(e^{\gamma d} + e^{-\gamma d}\right) + D_n\gamma\left(e^{\gamma d} - e^{-\gamma d}\right)\right]} \qquad (2.28)$$

and

$$\gamma = \left(\frac{1}{D_n\tau_n} + i\frac{\omega}{D_n}\right)^{1/2} \qquad (2.29)$$

where k_{ext} is the rate constant for electron extraction at the substrate. The solution for open circuit conditions is obtained by setting $k_{ext} = 0$. Since the photovoltage depends on the position of the Fermi level in the semiconductor, the modulation of the incident photon flux will directly be related to the concentration of electrons in the conduction band of the semiconductor and hence the photovoltage. The IMVS response is a semicircle with a minimum located at $\omega_{min} = 2\pi f_{min} = 1/\tau_n$.

3. Experimental

3.1. Preparation of dye- modified ZnO electrodes

The details described here are about the procedures to prepare electrodeposited dye / ZnO hybrid thin films by using a rotating disk electrode (Radiometer EDI101, controller; Radiometer CTV101), in solutions containing dye, $ZnCl_2$ and dissolved oxygen. Also the procedure to prepare re-adsorbed dye / ZnO thin films (hereafter re-ad dye / ZnO thin film) is described. EY was mainly used as structure-directing agent (SDA) to prepare porous ZnO by electrochemical deposition. Then, the procedure written here is for the preparation of electrodeposited ZnO films in the presence of EY as SDA in the deposition bath.

Regarding the films prepared in the presence of C343 as SDA, the films were prepared by Mr. Hattori and MS. Sci. Komatsu (Gifu University, Japan). The preparation process in Gifu University is described briefly. In the study of those films, films were also prepared in the presence of EY for the comparison. To allow direct comparison, those films were also prepared in Gifu University.

Regarding the films prepared in the presence of sodium dodecyl sulfate (SDS) as SDA, the films were prepared by Dr. E. Michaelis (University of Bremen, Germany). The preparation process is briefly mentioned. She also prepared one-step dye / ZnO hybrid thin films for this study and the procedure for preparing those thin films by using the reduction of NO_3^- is written elsewhere in detail.[163]

3.1.1. Electrochemical deposition of Eosin Y / ZnO thin film

3.1.1.1. Preparation and cleaning of the substrate

F-doped SnO_2 conductive glass substrate (Asahi-Glas, Cond. 10 Ω / cm^2, transparent (> 85 % in visible region)) is cut as 25 mm x 25 mm.
Before the substrate is mounted to the substrate holder for the deposition, the substrate is cleaned ultrasonically in acetone, 2-propanol and distilled water for ten minutes each. The substrate is then etched in 45 % HNO_3 for 2 minutes and finally rinsed with distilled water.

3.1.1.2. Mounting of the substrate

The drawing of the substrate holder (workshop, University of Bremen) and the drawing of the electrode preparation are shown in Fig. 3.1. After the cleaning process of the SnO_2 conductive glass (substrate), the substrate is placed to the substrate holder. First (I in Fig. 3.1), the contact between the substrate and substrate holder is established by using conductive tape (Chomerics, Inc. tin-coated copper tape). To make the contact sure, silver paste (DOTITE, Fujikura Kasei) is put to the attachment side of the conductive tape and the tape is rubbed sufficiently. This process is introduced for all other corners of the substrate as well. (II in Fig. 3.1) Since silver paste is liquid material, it disturbs the bonding property of the tape on occasion. In such case (or any case), other pieces of tapes are recommended for fixing the tape which does the important role to establish the contact (Author used same kind of conductive tape for the fixing role.) A hole is made in insulating tape (Klarsicht-Klebeband 51mm, neoLab) by using a punch which has a diameter of 20 mm. Then, this insulating tape is attached over the substrate and substrate holder. (III in Fig. 3.1) The center of the hole in the insulating tape should be adjusted to the center of the substrate. The insulating tape is also rubbed sufficiently to make the gluing sure and to remove air bubbles which are enclosed by this tape. Removing air bubbles is an important process since such bubbles expand during the deposition due to the high temperature, which leads to separation of the insulating tape from the substrate holder. When the insulating tape is separated, it influences the bonding property of the conductive tape; it might lose or change the contact of the conductive tape and substrate. When it happens, strong influence can be expected to the growth of the thin film.

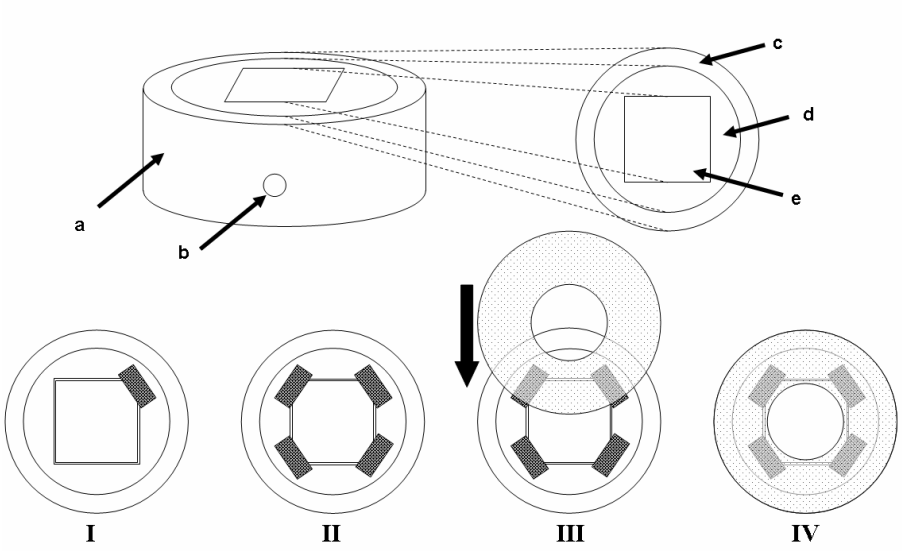

Fig. 3.1; Drawing of the substrate holder and the procedure to mount the SnO_2 substrate to the holder. a); outer part of the holder made of insulating polymer, b); the hole for the screw to fix the metal part, this hole is sealed by tape normally, c); outer part of the holder, d); stainless steel part of the holder, e); the part to install SnO_2 conductive glass (substrate), I, II, III, and IV is the order to prepare the electrode (detail is written in text)

3.1.1.3. Pre-treatment process before the deposition of the film

The electrolyte of 120 ml ultrapure H_2O containing 0.1 M KCl (Roth, ≥99 %) is filled into the electrochemical deposition cell (Glass- workshop, University of Bremen). The tube (Glass- workshop, University of Oldenburg) which supplies oxygen (99 %) into the deposition cell is put into the electrolyte and oxygen gas is allowed to flow at a rate of 200 ml / min. This condition is maintained approximately 10 minutes to let the electrolyte warm up to 70 ℃ and oxygen dissolve to saturation into the electrolyte. In this process, the cell is sealed as it is sealed during the deposition. The gas is exhausted from the exhaust attached to the oxygen tube (Glass- workshop, University of Oldenburg) (Fig. 3.2).

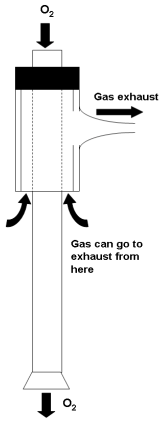

Fig. 3.2; The oxygen tube and the exhaust of the gas in electrochemical deposition cell

After this process, the substrate holder is placed in the electrochemical deposition cell as it is placed during the deposition. Then "pre-deposition electrolysis" should be performed before depositing an EY / ZnO thin film. A potentiostat (Jaissle IMP83) is used to give the bias to the electrode and the current is recorded by XY-recorder (Linseis LY199PL). A potential of -0.96 V vs. Ag/AgCl reference electrode (Radiometer, Red Rod, -40 mV vs.SCE), is applied to the electrode for at least 30 min and RDE is set to 500 rpm. (In this study, the potential for the deposition is mainly described with SCE.) Platinum is used as counter electrode. To protect the RDE from corrosion, nitrogen (99 %) is purged through the RDE with the rate of 400 ml / min. The oxygen tube was left in the electrolyte to make sure that sufficient amount of oxygen is supplied in the electrolyte. However it should be mentioned that any bubble of oxygen should not come to the surface of the conductive electrode. This process is necessary to activate the substrate since it was observed that the current increased during this process.[164] The current in this case is caused by the reduction of oxygen. Since it can be assumed that a sufficient amount of oxygen is in the electrolyte, the increase of the current is caused by the activation of the electrode.

3.1.1.4. Electrochemical deposition of the film

After the pre-deposition electrolysis, 5ml of high concentrated $ZnCl_2$ (FLUKA, >98 %) and EY (ALDRICH) are added to the electrolyte respectively. Then, the amount of the electrolyte is 130 ml after adding those solutions and the concentration of $ZnCl_2$ and EY is adjusted at 5 mM and 40 μM respectively. The counter electrode is replaced from platinum to Zn rod (Riedel-de Haën, 6 mm diameter, pure). The temperature of the electrolyte is 70 ℃. A scheme of the electrochemical deposition is shown in Fig. 3.3. The oxygen tube is taken from the electrolyte. However the top of the tube stays as close as possible to the surface of the electrolyte. The rate of oxygen and nitrogen is 200 ml / min and 400 ml / min respectively. It was noticed that the nitrogen used for the protection of RDE went into the deposition cell. The nitrogen comes out from the part between the rotating part and fixed part of RED, "e" in Fig. 3.3. And it was found that this nitrogen influences the current during the deposition. It means that it can change the concentration of the oxygen in the electrolyte. A piece of plastic sheet between the cap of the deposition cell and the substrate holder helps to prevent the invasion of nitrogen to the electrolyte although it does not solve this problem perfectly.

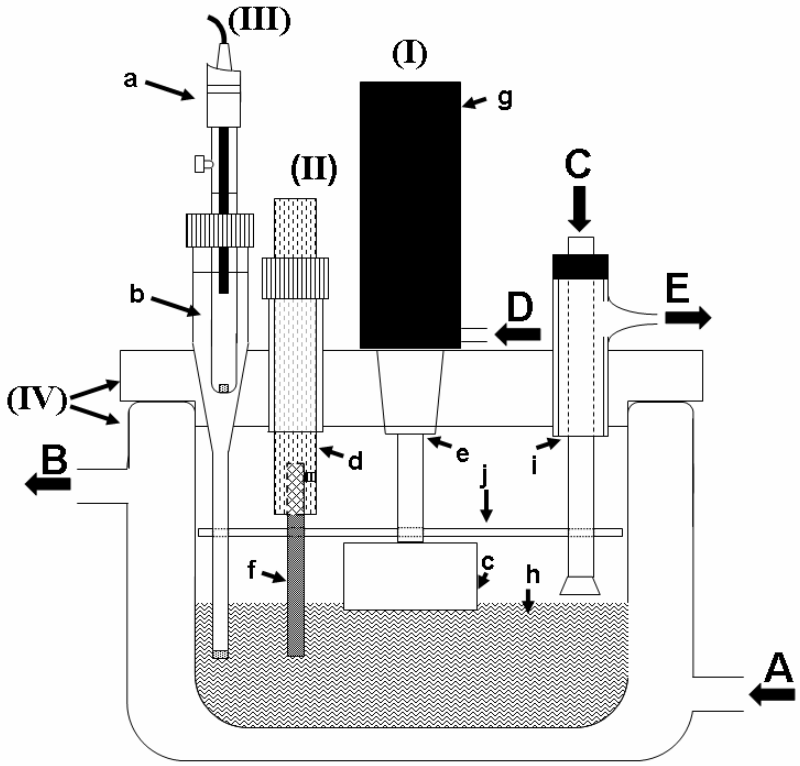

Fig. 3.3; Scheme of the electrochemical deposition cell, (I); Working electrode,(II); Counter electrode, (III); Reference electrode, (IV); the cell for electrochemical deposition with rotating disk electrode (University of Bremen), A); The entrance of water from thermostat, B); the exit of water to thermostat, C); the entrance for oxygen gas, D); the entrance for nitrogen gas, E); exhaust of gas, a); Red Rod reference electrode, b); saturated KCl aqueous solution, c); substrate holder, d); conductive Zn counter electrode holder made of copper (University of Oldenburg), e); the part from which the nitrogen gas comes out, f); Zn rod electrode, g); rotating disk electrode, h); electrolyte, i); the route which the gas go to exhaust, j); a piece of plastic sheet which has holes for each electrode and the oxygen tube

To obtain a 3 μm thick porous EY / ZnO thin film which is commonly used for the re-adsorption process, the deposition is carried out for 20 min at an applied potential of -1.0 V vs.SCE, the rate of RDE is 500 rpm.
When the deposition is completed, the SnO_2 conductive glass is taken out from the sample holder and rinsed by distilled water and dried by compressed air immediately.

3.1.2. The process of dye re-adsorption

A SDA / ZnO thin film (mainly EY / ZnO film for the re-adsorption process) is dipped into KOH aqueous solution (pH 10.5) for 24 hours to dissolve the SDA from the surface of ZnO. Before re-adsorbing a sensitizer to the surface of the ZnO film, the ZnO thin film is dried in an oven at 150 ℃ in air for 1 hour (conditions optimized by partner group at Gifu University). The purpose of this process is to remove the water adsorbed on the surface of ZnO and to activate the surface of ZnO.[164]

After this, the film is put into a sensitizer solution to adsorb the sensitizer on the surface of ZnO. The adsorption of a sensitizer is carried out at 80 ℃ for 1 hour.

3.1.3. Electrochemical deposition of Coumarin 343 / ZnO thin film

Those films were prepared in a similar experimental setup as described in 3.1.1 by Mr. Hattori in Gifu University, Japan. C343 / ZnO hybrid thin films were prepared by electrochemical deposition in the presence of Coumarin 343 (C343, laser grade, ACROS) in the deposition bath. The reduction of oxygen dissolved in the deposition bath was used for the precipitation of the ZnO on the SnO_2 conductive glass substrate. The concentration of C343 is 50 μM in the deposition bath. SCE and Zn wire was used as reference electrode and counter electrode respectively. The potential for the deposition is -0.9 V vs. SCE and the deposition time of 50 minutes to obtain 3 μm thick films. (30 minutes for 2 μm thick films) For comparison, ZnO films prepared in the presence of 45 μM EY in the deposition bath were prepared at -1.0 V vs. SCE for 15 minutes for 2 μm thick films and 20 minutes for 3 μm thick films.
The prepared films were also dipped into aqueous KOH overnight to remove C343 from the surface of the ZnO film.
Before a sensitizer is adsorbed on the surface of ZnO, the film is dried at 100 ℃ in air atmosphere for one hour. The sensitizer was adsorbed by dipping the film into an ethanolic solution of the sensitizer for one hour. The solution of the sensitizer was put on a hot plate set to 100 ℃.

3.1.4. Electrochemical deposition of SDS / ZnO thin film

These films were prepared by Dr. E. Michaelis in University of Bremen. A mixed aqueous solution of 5 mM $ZnCl_2$ (Aldrich) and 0.1 M KCl (Chimica) served as the bath for electrodeposition of the ZnO films. Sodium dodecyle sulfate (SDS) (ROTH) was added to the deposition solution to reach 600 μM. 100 ml of the deposition mixture were introduced into a round single-compartment cell, similar to the one of Fig. 3.3. The temperature of the bath was set to 70 ℃ with a thermostat, and a rotating disk electrode (Princeton Applied Research 636) was used at 500 rpm. Prior to the electrochemical deposition, oxygen gas was bubbled through the solution. Finally the upper part of the cell was flooded with oxygen to avoid the excessive foaming due to SDS. Pure Zn wire (Aldrich) was used as a counter electrode. A saturated calomel electrode (SCE) was used as a reference electrode, being bridged via a saturated KCl solution and kept at room temperature. Potentiostatic electrodeposition was performed at a potential of -1.0 V vs. SCE for 5 to 30 minutes. The potential and current were monitored by a Wenking POS 2 potentiostat (Bank). After deposition the films were rinsed with water and dried under air at room temperature. Detailed characteristics of such films were described elsewhere.[70]

For adsorbing a sensitizer on the surface of such films, the films were dipped into KOH aqueous solution (pH 10.5) for 50 hours. And then these films were dried at 110 ℃ for 1 hour. After dry treatment, films were dipped into the dye solution (concentration; 250 μM) for 1 hour.

3.2. Absorption spectroscopy

Absorption spectra were measured by using a Lambda 900 (PerkinElmer) at a scan speed at 300 nm / min (integration time; 0.16 s) and a slit of 1 nm. When the absorption spectrum of the film was measured, either air or SnO_2 conductive glass was introduced as reference.
For the absorption spectrum of solutions, ex. dye aqueous solutions, a quartz cell with an optical path length of 1 cm was used for the measurement. And an identical cell with pure solvent was introduced as reference.

3.3. Amount of dye loaded in the film

Dye / ZnO film was cut at 0.25 cm^2 (ex. multiply 5 mm by 5 mm). The sample is put into 5 ml of 7 N ammonia aqueous solution and dissolved completely. After the measurement of absorption spectrum of the solution, the amount of dye loaded (dye content) is calculated by use of the Lambert-Beer law and the extinction coefficient from the literature.
The dye concentration in the film was obtained by the calculation of the dye content and the film thickness.

3.4. Film thickness

The film thickness of the samples was measured by a stylus method by using an ALPHA-STEP Profiler (TENCOR INSTRUMENT).

3.5. Scanning Electron Microscopy

The SEM images of the films were observed by using Zeiss Digital scanning Microscope 940 controlled by Orion V6.22 software.

3.6. Atomic Absorption Spectroscopy

Zn^{2+} solutions (1, 2, and 3 ppm) of bidistilled water that was acidified with nitric acid were used as a calibration standard for the AAS measurements. The samples were cut into pieces of approximately 0.25 cm^2. The exact size was determined by weighing. Those samples were added to 50 ml of the acidified solution (pH; 2), so that the ZnO film was dissolved. The F-doped tin oxide does not dissolve under these conditions. The samples were stored in plastic jars because zinc is not adsorbed by this material. Each time, 100 µl of the solution were given to the suction nozzle of the spectrometer (Varian SpectrAA 30). The wavelength used by the spectrometer was the resonance frequency of zinc, 213.9 nm. The flame was generated by the combustion of acetylene with air, the ratio was 3.5 l min^{-1} air and 1.5 l min^{-1} acetylene. The resulting data was automatically compared with the calibration curve and the concentration in mg/l was calculated

3.7. BET measurement

In this kind of measurement, nitrogen is commonly used as an adsorptive for samples with surface areas of several tens of square meters. However, for materials with relatively low specific area as is very often the case for thin porous films, an adsorptive with lower saturated vapor pressure than the routinely used nitrogen such as krypton, should be used since it reduces the uncertainty associated with the equipment dead volume.[165,166] The surface area of the samples was measured by Jiri Rathousky (J. Heyrovsky Institute, Prague, Czech Republic). The surface area of the samples was determined from the adsorption isotherms of Kr at 77 K measured using an ASAP 2010 apparatus (Micromeritics). Prior to each adsorption measurement, samples were outgassed at 150 ℃ over night, this temperature being the upper limit of the stability of dyes used.

3.8. Photocurrent transient

The procedure and the setting for the measurement of photocurrent transients are described here. Moreover, the procedure to prepare the electrode is described in detail. When the electrode is dipped into the electrolyte for the measurements, a modification of the electrodes is necessary before the measurements. At first, the procedure for the modification is described. And later, the experimental procedure is described in detail.

When I_2 is one of the solutes, the samples were measured by using the photoelectrochemical cell showed in Fig. 3.8. In this case, the measurement only

illuminated from substrate side is possible since the electrolyte is colored. No special modification of the electrodes is needed to measure in this cell.
When I_2 is not in the electrolyte, the measurements with light incident from the surface side of the film are also possible. However, since the surface of the thin film has to have a contact with the electrolyte, the thin film is dipped into the electrolyte. When the electrode is dipped in the electrolyte for the measurements, the electrode should have a structure to hinder the contact between the electrolyte and the lead. And the lead should have tight contact with the sample. The preparation procedure of the electrode in such case is shown Fig. 3.4.

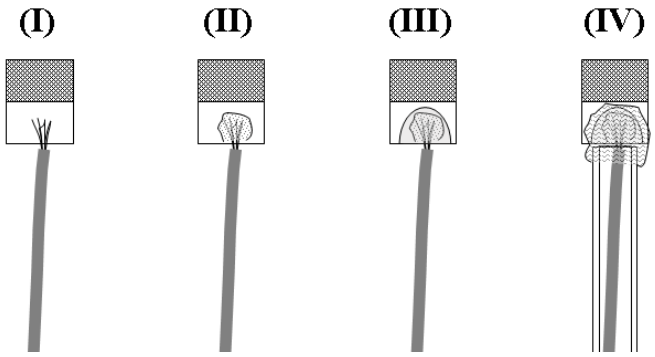

Fig. 3.4; Scheme of the procedure to prepare the electrode for photoelectrochemical measurement in the electrolyte. By preparing such electrodes, the measurement with the illumination to the surface side of the thin films becomes possible. (I) – (IV) is the order of preparing process. Detail is in text.

The preparation of the electrode is following; (I) put the lead on the conductive substrate, (II) put silver paste (DOTITE, Fujikura Kasei) on lead to have a tight contact (conductivity) between the conductive substrate and the lead and wait until the paste becomes dry (approximately 10 minutes), (III) put glue (Araldite, Nichiban Co. Ltd.) to fix the connection part between substrate and lead and wait until the glue becomes dry (it takes more than 30 minutes), (IV) install the glass tube around the lead and put silicone glue (1 component RTV KE45, Shin-Etsu Silicone) over the another glue (Araldite) and also put some silicone glue to fix the glass tube and glass substrate and wait until the silicone glue becomes dry (more than 6 hours). Silicone glue has nice endurance properties against organic solvent which is not the case for Araldite. However silicone glue is not sufficient to mechanically fix the silver paste and conductive glass substrate. This is the reason why two kinds of glues are necessary to prepare the electrode for photoelectrochemical measurement.

The photocurrent transients were measured in a conventional three-electrode arrangement with the deposited thin film as working electrode, a Pt counter electrode and a Ag/Ag^+ reference electrode with acetonitrile as internal solvent (=0.096 V vs. the ferrocene/ferricenium (FLUKA, >99 %) redox couple in acetonitrile). A mixture of

acetonitrile (ROTH, 99.9 %) -ethylene carbonate (FLUKA, >99 %) (1:4 by volume) was used as solvent for the electrolyte. The solute in the electrolyte was differed among 1) 0.5 M tetrabutylammonium iodide (TBAI, SIGMA, 99 %) and 0.05 M Iodine (I_2, SCHRARLAU, 99.8 %), or 2) 0.5 M KI (ROTH, >99.5 %)and 0.05 M I_2, or 3) 0.5 M TBAI, or 4) 0.5 M KI.

In Fig. 3.5, the photoelectrochemical cell used in the cases, for which no I_2 is used in the electrolyte and for which the films are illuminated from the surface side of the thin film, is shown. In the case which I_2 is in the electrolyte, another kind of photoelectrochemical cell is used. (shown in Fig. 3.8)

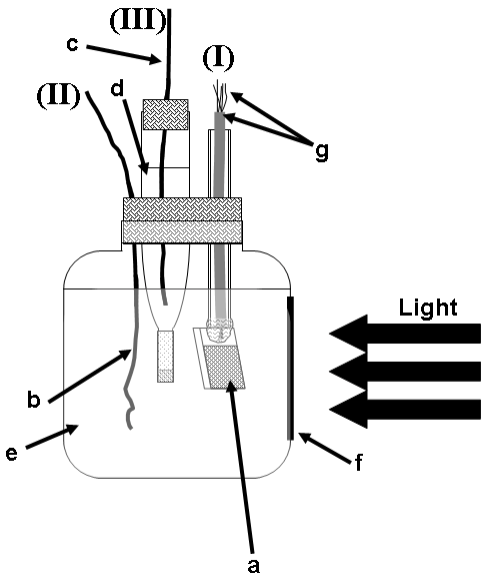

Fig. 3.5; The cell for the photoelectrochemical measurement in the case, for which no I_2 is used in the electrolyte and in which the measurements illuminated from the surface side of the thin film are carried out under illumination of the surface side. The meaning of the symbols are as follows; (I); working electrode, (II); counter electrode, (III); reference electrode, a); sample (dye / ZnO thin film), b); platinum wire, c); silver wire, d); reference electrolyte, e); electrolyte, f); quartz glass, g); lead, covered part and non-covered part.

For photocurrent transient measurements, an ORIEL 1000 W xenon arc lamp equipped with a water filter and a UV cut off filter (see Appendix 3) to restrict the illumination to the visible range (385 nm – 900 nm) of 200 mW cm^{-2} was used. The adjustment of the light intensity was carried out by using a Field master detector (COHERENT). And, in the practical adjustment, for example, the light intensity adjustment of visible light (385 nm – 900 nm), the wavelength setting of field master was set as 500 nm; all incoming photons are then treated at one wavelength and 500 nm is typical wavelength to calculate the photon flux of sun illumination. The illumination to the electrode was controlled by using a PRONTOR magnetic E/40 mechanical shutter, for which a controller box had been designed earlier[167], adjusting the time of illumination, typically 200 ms. The shutter needed about 15 ms to reach a completely open position (see Appendix 3) as measured

with a SIEMENS SFH 291 silicon-PIN-photodiode. As an alternative illumination source, LED (UV, white, blue, green, red) (equipment was constructed in University of Oldenburg, spectra are given in Appendix 4) were introduced, which showed much faster response of 20 μs to give the full illumination from the beginning of the illumination. The potential and the currents were measured with a JAISSLE Bi-Potentiostat-Galvanostat connected to a HAMEG HM 305 oscilloscope, which is triggered by a pulse generator connected to the shutter controller to start data acquisition some microseconds before the shutter was opened. The transients obtained by the oscilloscope were recorded by a personal computer using HAMEG SP91-2 software. A simple diagram of the equipment for the photocurrent transients is shown in Fig. 3.6.

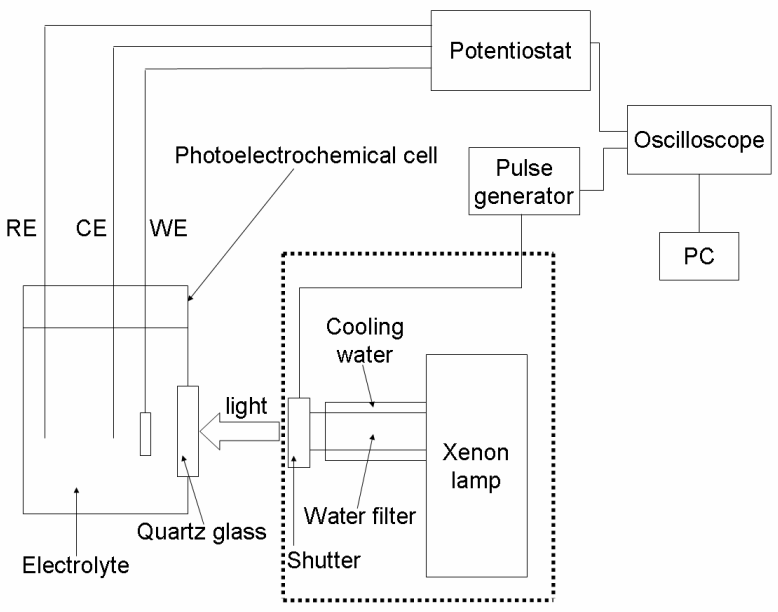

Fig. 3.6; Equipment for the photocurrent transient measurements. The part surrounded by dashed line can be replaced by LED.

When the composite films such as (TSPcZn+TSTPPZn) / ZnO were characterized, the photocurrent contribution from each dye was measured. To detect the photocurrent from TSPcZn, below 500 nm cutoff filter (L.O.T. 520FD22-50) was used. To detect the photocurrent from TSTPPZn, PcZn- coated glass (100 nm, prepared by Dipl. Chem. Christian Kelting) was used to cancel the photoactivity of TSPcZn. Spectra are given in Appendix 3.

To limit the measurement noise, the photoelectrochemical cell was placed in a Faraday cage, room light was excluded, and shielded cables were used where possible. It also helps to decrease or remove the noise in the current response to change the position of the cable, for example, trying to place the cable for the reference electrode away from other two cables. When the current was too low, the noise of 50 Hz can be caused by the power source. Since the potentiostat has an internal battery, a measurement after taking off the socket from the power source is still possible and it helps to decrease the noise further.

3.9. Intensity Modulated Photocurrent Spectroscopy (IMPS)

IMPS was also measured by a three electrode setup as described in the experimental of photocurrent transient section and also same electrolytes were used for the measurement. (Chapter 3.8) The modulation of the illumination was achieved by using LED and the modulation was generated by the function generate of a Lock-in amplifier (Model 7220, EG&G Instruments) and a potentiostat (IMP 83, Jaissle) to stabilize the signal and add a dc component to avoid negative voltage at the LED and/or to allow a non-zero bias signal. Aside from illumination by LED, bias white light of 100 mW cm^{-2} illuminated the electrode since it was found that the concentration of electrons in the conduction band of the semiconductor has a strong influence on the electron transport and recombination properties in the device.[7 8] This white light was supplied by using a halogen lamp (outer part (housing) of the lamp; 10 – 150 W Lamp Housing LSH102, L.O.T.-Oriel GmbH&co. KG, lamp; HLX64633, OSRAM), providing a more stable illumination than the xenon arc lamp. UV cutoff filter and distilled water were used to cut off the ultraviolet part and infrared part of the spectrum. A simple scheme of the equipment for IMPS is shown in Fig. 3.7. This setting is used for IMVS as well.

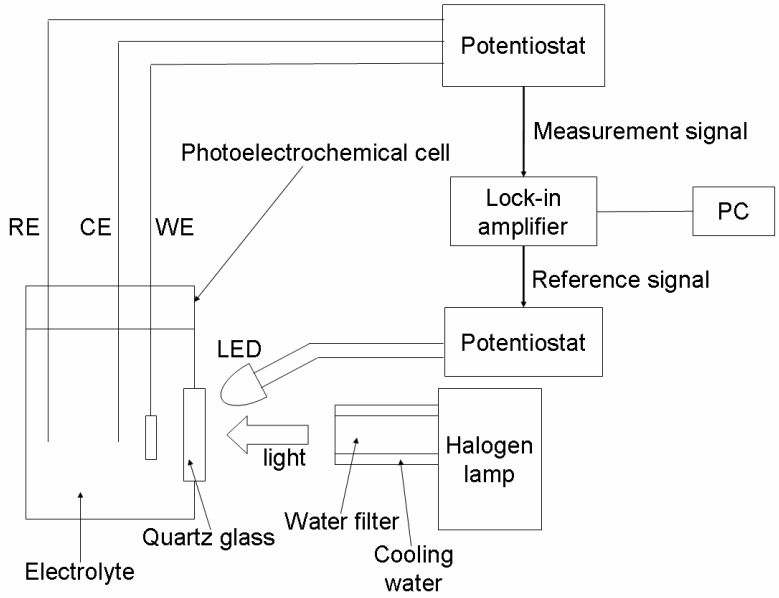

Fig. 3.7; The scheme of the equipments for IMPS and IMVS

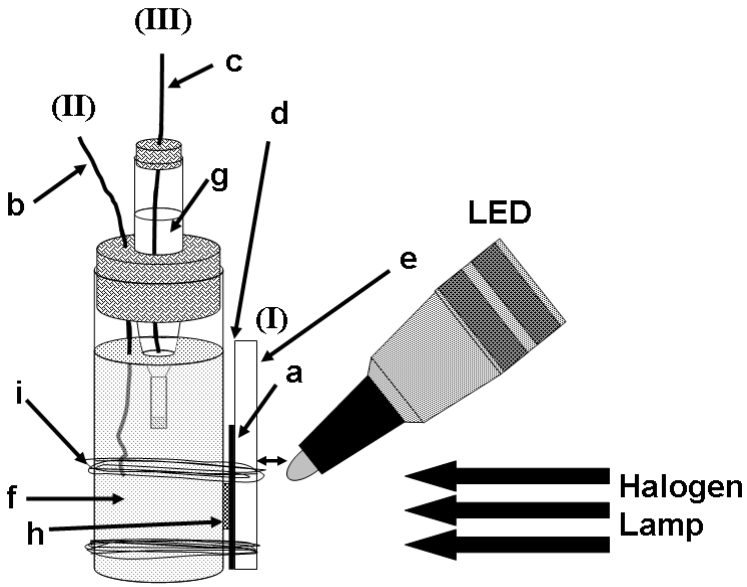

Fig. 3.8; The photoelectrochemical cell and the scheme of the positioning of equipment. The meaning of the symbols are following; (I); working electrode, (II); counter electrode, (III); reference electrode, a); dye / ZnO film, b); platinum wire, c); silver wire, d); conductive side of SnO_2 glass substrate and the contact is made by using alligator clip, e); glass side of the SnO_2 glass substrate, f); electrolyte, g); reference electrolyte, h); o-ring, i); rubber band. Some distance like 5 mm is necessary between sample and LED to install neutral density filter.

The diagram of the photoelectrochemical cell and the geometrical position of the equipments are shown in Fig. 3.8. The position of the LED was adjusted by measuring the current of a photodiode, which was recorded when the light intensity was measured initially. While the sample was introduced, the position which gave the highest photocurrent was searched. The position of the sample is adjusted by changing slightly the height, the angle and the horizontal position. The position of the LED and the position of the handle which fixes the basic position of the cell should not be changed. When the distance between the sample and the LED is changed, it can be expected that the photon flux was changed extensively.

The average number of photons from the LED was calculated by measuring the current at a photodiode, connected to an ampere meter. (see Appendix 6) The amplitude of the modulation was also measured by using a photodiode. A potential of -0.2 V was applied to the photodiode, and the wave form was recorded by a computer and the number of photons at the part of the illumination from the LED was calculated from the independent measurement of the average photon flux. Alternatively the modulation amplitude of the LED measured by photodiode was recorded by use of the Lock-in amplifier.

Before start of the measurement with a sample, “Auto Phase”, one of the functions in Lock-in amplifier, was introduced to correct the phase difference between the reference modulation and the response modulation of the LED signal measured at the photodiode. This phase difference is then automatically considered in the IMPS (and IMVS) measurements.

The measurement was carried out by changing the modulation of the photon flux from 0.2 Hz to 90000 Hz (see Appendix 8).

Typical settings for each LED and the photon flux is shown in Table 1.

Table 1; The settings used to drive the LED and the photon flux in intensity modulated measurements.

	bias voltage / V	current / mA	average photon flux / photons cm^{-2} s^{-1}	ac modulation voltage / mV	photon flux in ac modulation / photons cm^{-2} s^{-1}
red	1.85	8	2.82×10^{15} (= 4.7 µA at photodiode)	100	1.84×10^{15}
green	3.8	6	2.7×10^{15} (= 3.5 µA at photodiode)	200	6.51×10^{14}
blue	3.8	5	3.64×10^{15} (= 3.5µA at photodiode)	100	5.86×10^{14}

3.10. Intensity Modulated photoVoltage Spectroscopy (IMVS)

To measure IMVS, some changes are required in the setting for IMPS. The rest potential is measured during this measurement. So then, the output cable is connected to the voltage socket. Any potential should not be applied. The IMPS- software can be used. A setting of 1 V and 1 mA in the sensitivity gives the same values as shown on the Lock-in amplifier. In this case, the unit of the indicated voltage is “mV” which can be confirmed by checking the monitor of the Lock-in amplifier.

3.11. Measurements of electrode efficiency

I carried out this measurement in Gifu University by using a Bunko-Keiki CEP-2000 system. The photoelectrochemical cells shown in Fig. 3.5 and Fig. 3.8 were used. Photocurrent action spectra were obtained by measuring the photocurrent under monochromatic light illumination with a constant photon number (10^{16} photons cm^{-2} s^{-1}).

The photocurrent density at different potentials (IV- curve) under illumination with AM 1.5 simulated sun light (100 mW cm^{-2}) was also measured. The short- circuit photocurrent I_{sc}, the open- circuit photovoltage V_{oc}, and the fill factor FF (definition is written in chapter 2.5) were determined from the plot.

For some of the films, a sandwich cell was fabricated. The procedure to fabricate sandwich cells is shown in Fig. 3.9.

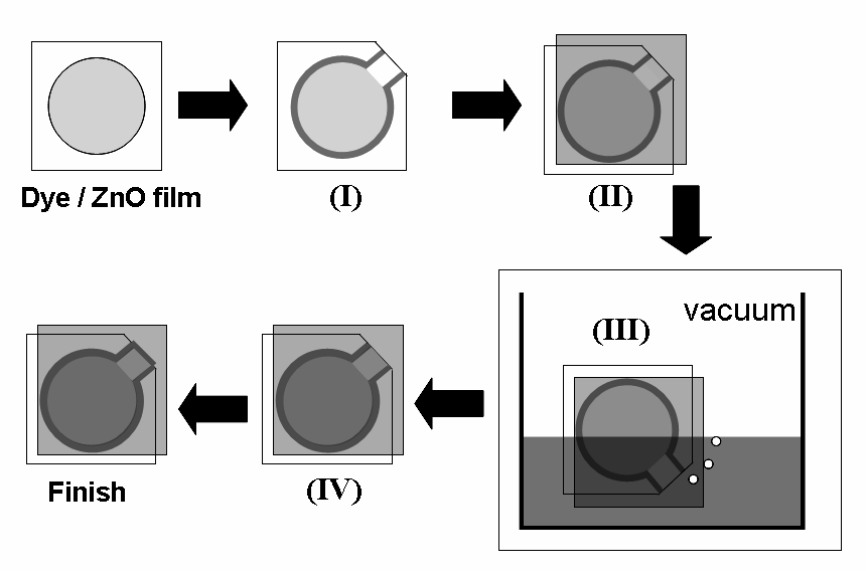

Fig. 3.9; The procedure to prepare a sandwich cell. (I); putting the sealant along the profile of the film, (II); attaching counter electrode with working electrode and treat with UV irradiation to crosslink the sealant, (III); put the cell into the electrolyte, evacuate the system slightly to remove air and the electrolyte is filled into the cell when the atmospheric pressure is established again, (IV); put additional sealant to seal the cell completely.

The size of the electrode was 3.14 cm^2 in this study when the sandwich cells were fabricated.

4. Electrochemical and photoelectrochemical characterization of one-step electrodeposited Dye / ZnO hybrid thin films

Dye modified ZnO thin films were prepared by one-step electrochemical deposition. The electrochemical and photoelectrochemical characterizations were carried out for these films and discussed in this chapter. Two subjects have been investigated, one is about the one-step electrodeposited (TSPcZn and/or TSTPPZn) / ZnO hybrid thin films. The photoelectrochemical properties have been investigated for those films. The fabrication and physical investigation of the films were studied by Dr. E. Michaelis in University of Bremen and their photoelectrochemical properties were studied in University of Oldenburg and University of Giessen by the author.

In another part of the chapter, the fabrication and the characterization of one-step electrodeposited EY / ZnO hybrid thin films on the textile electrode have been studied. This is a collaboration work with Dr. A. Neudeck (Chemical and Physical Research Thuringia-Vogtland Textile Research Institute). The conductive textile electrodes were supplied by Dr. Neudeck. And the film preparation and their characterization have been studied by author.

4.1. Characterization of one-step electrodeposited (TSPcZn and/or TSTPPZn) / ZnO hybrid thin film

Since the films can be prepared in one-step and low temperature of 70 ℃, there are big advantages for the electrochemical deposition method to prepare dye modified metal oxide semiconductors compared with other methods like sol-gel method. Many studies about electrodeposited dye / ZnO hybrid thin films have been carried out so far.[55-64] In this study, the enhancement of the photoelectrochemical performance of electrodeposited dye / ZnO films in the red part of the visible light and the fabrication of panchromatic films to utilize the whole visible light are aimed. And moreover, the understanding of the electron transport kinetics in such films by analyzing their photoelectrochemical properties is aimed. 5,10,15,20-tetrakis-(4-sulfonatophenyl)porphyrinatozinc (TSTPPZn) and 2,9,16,23-tetrasulfophthalocyaninatozinc (TSPcZn) were selected as sensitizer because those dyes have high absorption coefficient,[65,66] chemical stability[67] and good photoelectrochemical properties.[68] Especially, TSPcZn can enhance the efficiency in red part because of its high extinction coefficient in those wavelengths. In the beginning of the study, one-step electrodeposited TSPcZn / ZnO and TSTPPZn / ZnO hybrid thin films were prepared and analyzed. And it was tried to prepare and characterize the films prepared in the presence of both dyes in the deposition bath. A combination of TSPcZn and TSTPPZn leads the characterization easier since those have clearly different absorption spectrum

and their electronic and chemical structures are quite similar and the two sensitizers should be widely compatible in electrochemical deposition.

4.1.1. Structure and morphology

TSPcZn / ZnO, TSTPPZn / ZnO and (TSPcZn+TSTPPZn) / ZnO films were prepared by one-step electrochemical depositions from aqueous solutions containing $Zn(NO_3)_2$ as precursor for ZnO and the appropriate sensitizer. Already an observation by eye indicated uptake of TSPcZn by a blue color, uptake of TSTPPZn by a yellow color and uptake of both sensitizers from a mixture by a green color of the obtained electrodes. Spectroscopic analysis will be discussed in the next section. Simply such results indicate that the dye modified ZnO thin films can be deposited in the presence of more than one dye and the dyes adsorb to the ZnO.

Those films have the characteristic morphology since different kind of dyes were in the deposition bath and those dyes influence the growth of ZnO as reported earlier.[58,60,83] The morphology of the films were observed by SEM. (Fig. 4.1)

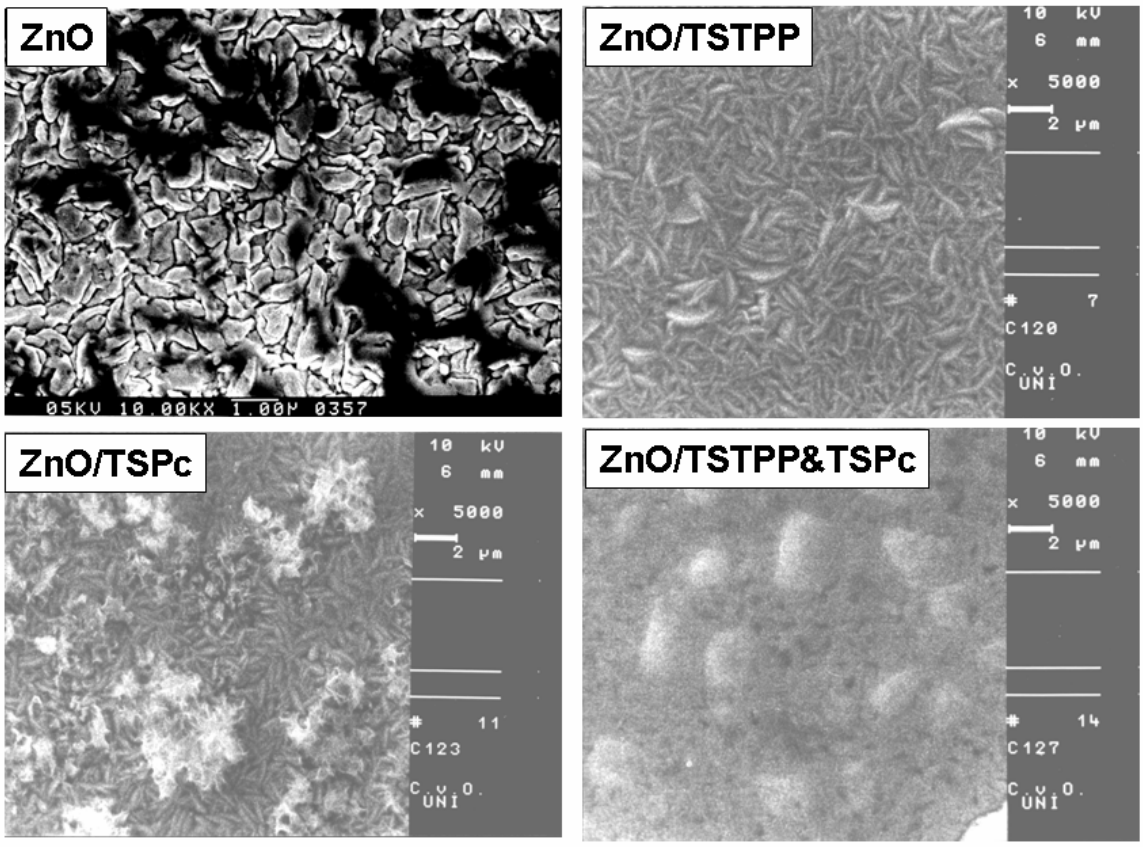

Fig. 4.1; SEM images of one-step electrodeposited dye / ZnO films on SnO_2 conductive substrate.

The morphology of ZnO film is relatively unique compared to the earlier report.[50] Some hundreds nanometre size of particles can be seen. Since ZnO films prepared by using the reduction of nitrate do not have a preferential orientation,[58] the hexagonal shape of the

ZnO could not been seen. Nevertheless, the high crystallinity of those films has been confirmed by XRD.[163]

The ordered ZnO particles can be seen from TSTPPZn / ZnO film. From the observation of a number of standing disklike crystals, 002 plain of ZnO seems to be perpendicular to the substrate from the image. Such structure of electrodeposited dye / ZnO hybrid thin films was also observed in earlier study.[58] The surface structure suggests that the sensitizer adsorb to 002 plane of the ZnO particles and hence the creation of ZnO tends to continuously takes place to the direction a, b-axis of ZnO.[58] This is a typical example that the mechanism and the creation of ZnO gets influence by the dyes present in the deposition bath. Similar phenomena can be expected from the surface structure of TSPcZn / ZnO film although the morphology of the film is not as clear as the one of TSTPPZn / ZnO film. From the image, it seems that another kind of precipitate forms on the film surface, as also observed earlier.[58] The shifts of the condition in the deposition bath such as the decrease of the dye concentration in the electrolyte and the different creation energy (conductivity) due to ZnO layer that has deposited in the early stage of the deposition, might influence the character of the electrodeposited ZnO.

Completely different morphology was observed for (TSPcZn+TSTPPZn) / ZnO hybrid thin film. The surface has a fine and a sponge-like structure and the grains are not distinguishable. The interaction of two dyes in the deposition bath influences significantly the growth of ZnO.

4.1.2. Photoelectrochemical characterization

Obtained films are investigated to see the photoelectrochemical properties as photoelectrodes. Since the photocurrents are generated from the adsorbed dyes,[60] their photoelectrochemical properties are compared in detail with their optical absorption profiles.

The absorption spectra of those films are shown in Fig. 4.2 (a). The absorption bands typical for porphyrins were detected for TSTPPZn adsorbed at ZnO. The bands were measured at around 425 nm (Soret- or B-band) and 550 / 600 nm (Q-band)[168,169] Only subtle shift and band broadening were observed for the TSTPPZn Soret band relative to solution spectra[170] speaking for a weak intermolecular coupling of the sensitizer molecules as also observed even in pure solid films of TSTPPZn.[170] For TSPcZn / ZnO, however, a clear broadening of the Q-band (650 / 680 nm) was observed speaking for the formation of strongly coupling dye aggregates.[101,170] From the solution that contained both TSPcZn and TSTPPZn sensitizers, both dyes were found to adsorb to the growing ZnO. Two different concentration of the dye molecules in the electrodeposition bath were used to either keep the overall dye concentration or the concentration of each dye constant when compared with the deposition of TSPcZn / ZnO or TSTPPZn / ZnO. The spectral characteristics in the porphyrin Soret range were quite comparable to TSTPPZn / ZnO whereas the uptake of TSPcZn was so little that even the weak porphyrin Q-bands dominated that part of the spectrum. In recently reported composite films with an increased content of TSPcZn in the deposition bath, however, it could clearly be seen that the TSPcZn aggregation was suppressed by the presence of TSTPPZn in the composite film,[170] so it can be assumed the less aggregation of TSPcZn in the present (TSPcZn+TSTPPZn) / ZnO films with an even smaller TSPcZn concentration. When the dye content of the (TSPcZn+TSTPPZn) / ZnO films was compared with that of either TSPcZn / ZnO or TSTPPZn / ZnO (Table 2) it was seen that the uptake of TSTPPZn is constant or slightly increased when both dyes were present whereas that of TSPcZn is significantly decreased.

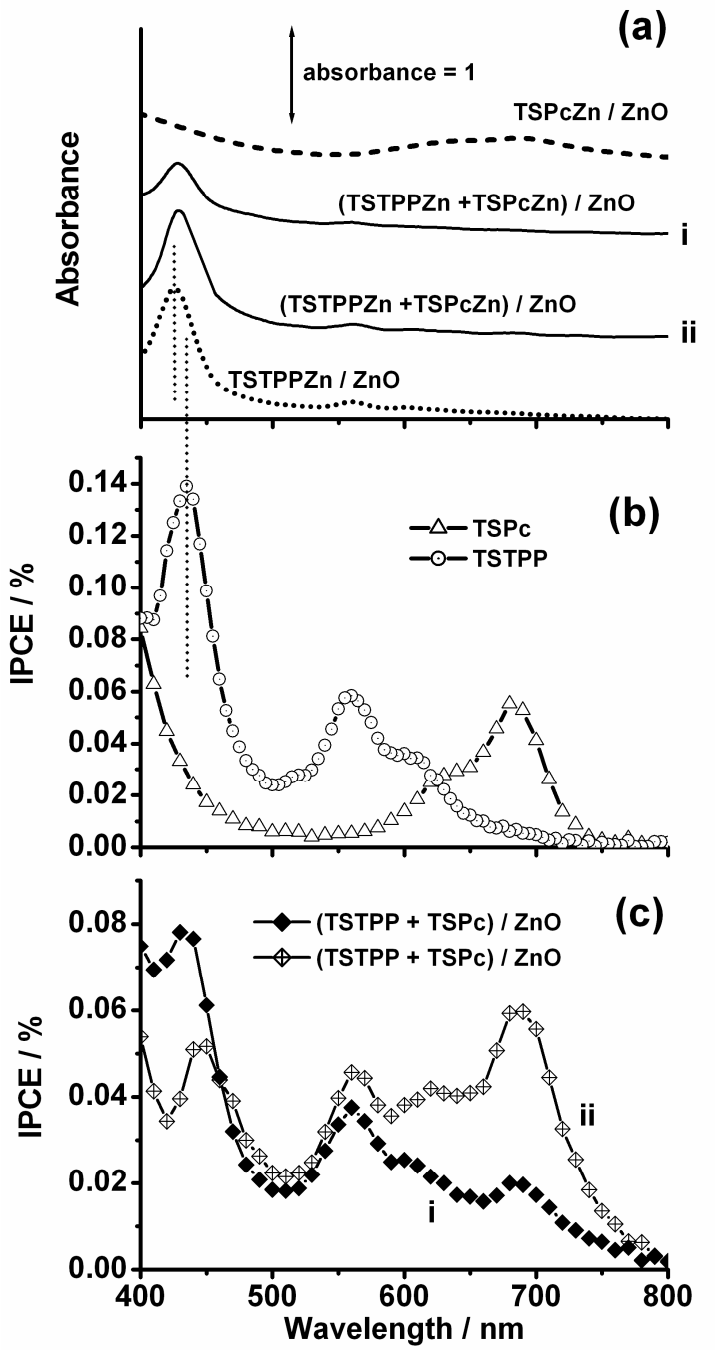

Fig. 4.2; Absorption spectra of TSTPPZn / ZnO (.....), TSPcZn / ZnO (-------) and (TSPcZn+TSTPPZn) / ZnO (——) electrodeposited in the presence of 25 μ M (i) or 50 μ M (ii) of each dye (a); photocurrent action spectra of TSPcZn / ZnO (--△--), TSTPPZn / ZnO (--○--) (b) and (TSPcZn+TSTPPZn) / ZnO electrodeposited in the presence of 25 μ M (I, --◆--) or 50 μ M (ii, --⊕--) of each dye (c).

In a comparison of the obtained dye concentrations in the films it was confirmed that the uptake of TSTPPZn during the electrodeposition was quite constant throughout the series whereas the uptake of TSPcZn was widely suppressed in the presence of TSTPPZn. A well-defined ratio of the two sensitizers was established. An increased concentration of both dyes in the deposition solution led to almost proportional increase of the adsorbed

sensitizers. Since also the average film thickness increased, the sensitizer concentration in the films was quite constant (Table 2) under both of these experimental conditions. Beyond the molecular absorption bands, light scattering in the films can be used as an indicator of crystal size. Films of TSTPPZn / ZnO and (TSPcZn+TSTPPZn) / ZnO had quite transparent appearance and also showed a lower background in the spectra when compared with TSPcZn / ZnO. This difference is caused by larger particulate domains in TSPcZn / ZnO when compared with TSTPPZn / ZnO or (TSPcZn+TSTPPZn) / ZnO as also revealed by atomic force microscopy.[170]

In Fig. 4.2(b), photocurrent action spectra are shown for these films prepared in one-step during the electrodeposition. It was confirmed that the photocurrent was caused by absorption in the adsorbed dyes and subsequent sensitization of ZnO. TSTPPZn / ZnO gave a conversion of IPCE = 0.14 % of the incident photons to an external current at 425 nm and 0.06 % at 560 nm. The photocurrent spectrum roughly follows the absorption spectrum of the film and both, Soret- and Q-regions contribute to the photocurrent. When looked at in more detail, however, it is seen that light absorbed in the Q-band of TSTPPZn (560 nm) contributed with a significantly higher quantum efficiency when compared with light absorbed in the B-band (425 nm). This is also evident from the normalized photocurrents listed for the different wavelengths in Table 2. A straightforward explanation for this observation considers the fact that the films were illuminated from the substrate side (glass / FTO side) but had contact to the electrolyte on the dye / ZnO side. Taking into account that films deposited in one-step show only a negligible accessible pore volume[166,171] and therefore allow access of the redox electrolyte mainly on the frontside of the electrode material, it becomes clear that light that penetrates deeply into the film and is absorbed close to the frontside will contribute most efficiently to the photocurrent generation. Since the extinction coefficient of the Q-band is clearly lower, an increased portion is absorbed close to the frontside leading to the observed higher quantum efficiency.

Table 2; Dye content, average film thickness, and dye concentration of the investigated films, and comparison of the observed photocurrents i_{ph} at an incident photon flux of 10^{16} s^{-1} cm^{-2} normalized for the given dye content to provide a rough measure of the sensitization efficiency (see text).

Electrode material	dye content / 10^{-9} mol cm^{-2}	film thickness / µm	dye concentration / 10^{-5} mol cm^{-3}	normalized i_{ph} (430 nm) / s^{-1}	normalized i_{ph} (560 nm) / s^{-1}	normalized i_{ph} (680 nm) / s^{-1}
one-step TSPcZn / ZnO	11.7	2.6	4.5			0.0007847
one-step TSTPPZn / ZnO	16.2	2.7	6.0	0.0014248	0.0005985	
one-step[i)] (TSPcZn+TSTPPZn)/ZnO	0.642 TSPcZn 13 TSTPPZn	2.2	0.29 6.0	0.0009747	0.0004692	0.0051731
one-step[ii)] (TSPcZn+TSTPPZn)/ZnO	1.37 TSPcZn 29.1 TSTPPZn	5.2	0.26 5.6	0.0002951	0.0002604	0.0072362

[i)] prepared in the presence of 25 µM of TSPcZn and 25 µM of TSTPPZn in the preparation solution

[ii)] prepared in the presence of 50 µM of TSPcZn and 50 µM of TSTPPZn in the preparation solution

This interpretation is supported by the fact that the Soret-band also does not contribute its IPCE peak at the wavelength of the absorption peak but shifted to longer wavelength of lower absorbance (optical filter effect), shown by the vertical lines in Fig. 4.2.
For TSPcZn / ZnO, on the other hand, the longer wavelength absorption at 680 nm dominated the contribution to the photocurrent leading to IPCE=0.05 %. This is well in line with earlier observation that this less aggregated absorption provides a clearly enhanced quantum efficiency because of a decreased probability of radiationless decay when compared with the aggregate absorption band at 650 nm.[83,139] The normalized photocurrent is similar to the one for TSTPPZn / ZnO (Table 2).
Films of (TSPcZn+TSTPPZn) / ZnO with both sensitizers adsorbed simultaneously during electrodeposition showed sensitized photocurrents with contributions from both, TSPcZn and TSTPPZn (Fig. 4.2 (C)). For (TSPcZn+TSTPPZn) / ZnO prepared from the solution with 25 µM (50 µM) of each dye, IPCE values of 0.08 % (0.05 %) in the TSTPPZn Soret region, 0.04 % (0.05 %) at 560 nm and 0.02 % (0.06 %) at 680 nm were detected, respectively. So the features of the individual sensitizers were also reflected in the composite films with both sensitizers adsorbed: the quantum efficiency for the Q-band absorption of the porphyrin was found considerably higher than that for its Soret-band and for the phthalocyanine the monomer absorption was considerably more efficient than the aggregate. A widely independent activity of the sensitizers also when both present in the films was thereby shown. Films deposited at the higher (50 µM) concentration in the deposition bath showed an increased contribution of TSPcZn relative to TSTPPZn in spite of a proportional increase of dye content for both sensitizers in the films. The considerably higher concentration of the sensitizer in the (TSPcZn+TSTPPZn) / ZnO films for TSTPPZn, when compared with TSPcZn, leads to a fast decay of light, which is strongly absorbed by TSTPPZn from the electrode backside to the electrolyte side. The contribution of the TSTPPZn Soret-band is therefore strongly suppressed and the IPCE maximum is shifted even further away from the absorption maximum as seen in Fig. 4.2 (a) and (c) and a minimum of IPCE develops at the absorption maximum (optical filtering effect). This was most obvious for the film of (TSPcZn+TSTPPZn) / ZnO with the higher dye content. Here, the contribution of TSPcZn represented the global maximum in the IPCE spectrum, due to its low concentration in the film and thereby deep penetration of the absorbed light towards the frontside of the electrode. This increased IPCE in the TSPcZn part of the spectrum is also reflected in a significantly increased normalized photocurrent (Table 2) in the (TSPcZn+TSTPPZn) / ZnO films when compared with TSPcZn / ZnO with its significantly higher sensitizer concentration. The normalized photocurrent of TSTPPZn showed a small decrease in the (TSPcZn+TSTPPZn) / ZnO films, in particular for the thicker (5.2 µm) film when compared with TSTPPZn / ZnO.

The concept of a panchromatic sensitization could be proven in these films deposited in one-step, however, at far too low efficiency to be of technical interest, with poor accessibility of pores as the main reason.[166,171] Time resolved photocurrent measurements were used to further elucidate the origin of such low efficiency (Fig. 4.3).

Films of TSTPPZn / ZnO clearly showed an overshoot upon opening of the shutter characteristic of a slow regeneration reaction[83,139] of the oxidized dye molecule following fast injection to ZnO, typically caused by poor accessibility of sensitizers by the redox electrolyte.

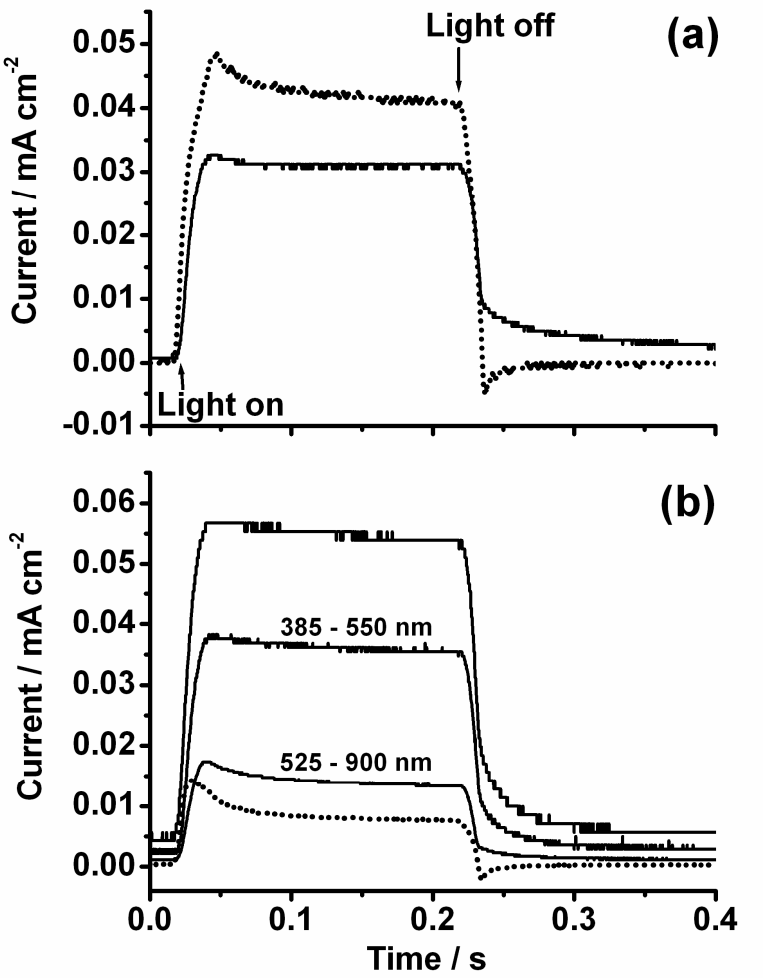

Fig. 4.3; Time-resolved photocurrent measured at one-step electrodeposited films of TSTPPZn / ZnO (·····) and TSPcZn / ZnO (——) (a) compared to (TSPcZn+TSTPPZn) / ZnO films deposited in the presence of 25 μ M (i, ·····) or 50 μ M (ii, ——) of each dye (b) under illumination with white light. For film ii also experiments with different wavelength ranges are shown as indicated at the curves.

Such a situation leads to increased recombination of charge carriers and hence a small photocurrent. Upon shutter closure, this recombination is directly observed in a small cathodic spike.[134] For TSPcZn / ZnO, the characteristics are similar but the initial overshoot was a little smaller and no cathodic spike was observed but rather a slow component in the decrease of the anodic photocurrent. The relaxation of electrons injected into the conduction band of ZnO into deep traps in the ZnO semiconductor material and their subsequent slow detrapping are the most reasonable explanation for the observed characteristics.[156,160] Also, the accessibility of TSPcZn / ZnO might be slightly improved relative to TSTPPZn / ZnO because of larger particulate domains in TSPcZn / ZnO detected in light scattering and AFM analysis,[170] but the trapping

reaction in ZnO might easily mask parts of the overshoot and recombination spike. The (TSPcZn+TSTPPZn) / ZnO films showed different transient behavior depending upon the deposition conditions, but not dependent upon the wavelength of illumination. The thinner film of lower dye content (i) showed clear overshoot of the photocurrent upon opening of the shutter and a clear cathodic spike upon its closure. Strong recombination currents are thereby indicated. The thicker film of higher dye content (ii), on the other hand, showed rather small recombination currents. Significantly better accessibility of the sensitizer molecules by the redox electrolyte is thereby proven for the film (ii). This observation was in good agreement with an increased porosity of the (TSPcZn+TSTPPZn) / ZnO[ii] that we concluded from the higher film thickness at comparable amount of ZnO in the films, measured by the charge passed into the film growth during the deposition. The film was investigated further under illumination with different parts of the visible spectrum (Fig. 4.3 (b)). Quite constant transient characteristics were observed when the film was illuminated either by Q- (385 – 550 nm) or Soret- (525 – 900 nm) part of the spectrum. So the different transients in Fig. 4.3 (a) were caused by different film morphology, but not by different photoelectrochemical kinetics when either TSPcZn or TSTPPZn were used as sensitizers. In the same matrix of a (TSPcZn+TSTPPZn) / ZnO film, both sensitizers follow quite constant kinetics. The panchromatic effect caused by such parallel working sensitizers observed already in Fig. 4.2 was thereby confirmed.

4.1.3. Summary

TSTPPZn/ ZnO and TSPcZn / ZnO hybrid thin films were prepared by electrochemical deposition in the presence of the dye in the electrolyte. The crystalline and coloured ZnO thin films were obtained. The absorption peak corresponding to the dye absorption in the solution was found by absorption spectrum. Those films worked as photoelectrode and it was found that the photocurrent was delivered by the photosensitization effect from the adsorbed dye molecules. The shape of action spectra measured for those films confirmed the photosensitization effect of the dye. By the photocurrent action spectrum for TSTPPZn / ZnO by the illumination from the substrate side, high IPCE was obtained for Q-band of TSTPPZn comparing with B-band of TSTPPZn. It was relatively high comparing with the ratio of absorbance between Q-band and B-band in the solution. It was caused by the different absorption coefficient at each band. And it indicates that the reaction with redox electrolyte to supply electron takes place at the surface of the film since the electrolyte can not come into the film due to the filled pores. TSPcZn / ZnO film also showed the photosensitized current. And it was found that the efficiency was clearly higher at its monomer state (680 nm) than aggregation state (640 nm) as it was reported earlier.[8 3] Photocurrent transient measurements showed the characteristic behavior for those films. TSTPPZn / ZnO film showed the overshoots at the beginning and the end of the illumination. It indicates the strong recombination after the injection of electrons to

ZnO. It was caused by slow regeneration reaction of the oxidized dyes following the injection to ZnO and this was strongly related with poor accessibility of the dyes. In the case of TSPcZn / ZnO film, the recombination reaction was not clearly observed in the photocurrent transient measurement. The aggregated dyes interact with the oxidized dyes and it appeared as the slow relaxation of the photocurrent after the cut off the illumination.

(TSPcZn+TSTPPZn) / ZnO hybrid thin film was also prepared by electrochemical deposition in the presence of TSTPPZn and TSPcZn in the electrolyte. The preferential adsorption of TSTPPZn was observed in composite film comparing with TSTPPZn / ZnO film. And the amount of TSTPPZn in the film was also enhanced by the presence of TSPcZn in the deposition bath. Such electrode also showed the sensitized photocurrent and that photocurrent was delivered by both adsorbed dyes. Although the IPCE values became smaller than the value obtained from the ZnO film which one dye was present, the quantum efficiency relative to the amount of dye molecules have been improved, especially for TSPcZn. By depositing the film with TSTPPZn, TSPcZn was spread effectively and it prevented the aggregation of TSPcZn in the film.[170] And moreover in the photocurrent transient measurement, it was found that the recombination at TSTPPZn dye molecules was reduced in such composite film. The photocurrent contribution from each dye was observed when the cut off filters were used for allowing only one dye excited in the composite film. It was found that the sum of the photocurrents contributed from each dye has a nice agreement with the photocurrent magnitude measured with visible light from 385 nm to 900 nm. It indicates that those two dyes do not disturb its photoelectrochemical activities each other and those dyes work as sensitizer at the same time in one film. Those results in this study promise the panchromatic sensitization and it was found that such films can utilize the wider range of spectrum to deliver the photocurrent.

4.2. Electrochemical deposition of dye / ZnO hybrid thin film on Au and conductive textile electrode

Since low temperature process is an advantage of the electrochemical deposition, ZnO can be prepared on a conductive plastic substrate which is normally not strong for high temperature. And since this method is soft process, ZnO can be prepared on a conductive textile electrode. There is a difficulty to coat a thin film of nanoparticulate metal oxide semiconductor on such electrodes by common methods like sol-gel. Thereby, electrochemical deposition provides a new pathway towards clothes with solar cells in the future.

This is a collaboration work with Dr. Andreas Neudeck (Textilforschungsinstitut Thüringe-Vogtland, Greiz). In his institute, he is able to prepare the conductive substrate which has textile structure. We try to deposit EY / ZnO hybrid thin films on Au coated textile electrode and characterize such electrodes. This is a first attempt to deposit dye modified ZnO on textile.

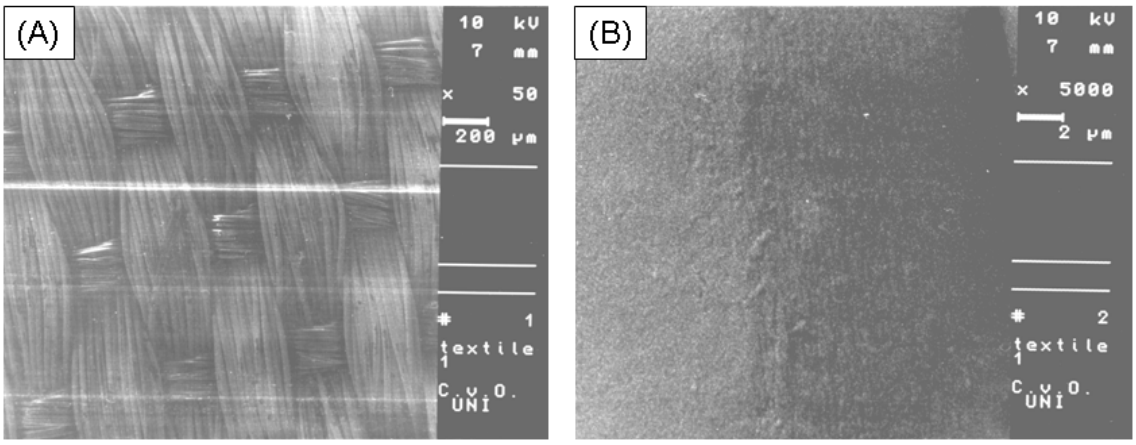

Fig. 4.4; SEM images of textile electrode

For this study, ZnO was prepared by using the reduction of nitrate. Generally, the ZnO deposited by using the reduction of oxygen is easier to control the growth of ZnO than by using the reduction of nitrate. The number of factors that change during the deposition is less in the case oxygen is used than nitrate is used. Only the mass transport of oxygen to the substrate is a critical point to control the growth of ZnO for the case of oxygen, whereas several factors are changing for the case of nitrate. RDE is normally used to control the oxygen mass transfer. However, there are some difficulties to mount a textile electrode and to establish a contact between RDE and textile. Therefore, ZnO were electrodeposited on textile electrodes by the use of $Zn(NO_3)_2$ containing solution. The films have been analyzed by the charge passed during the deposition, SEM, the amount of Zn in the film, the amount of dye loaded in the film, photocurrent transient.

4.2.1. Deposition of Eosin Y / ZnO film

Before EY / ZnO films were deposited on textile Au electrodes, the deposition of EY / ZnO films on Au electrodes was tested since the activity of Au is different from ITO. The total amount of charge during the deposition is shown in Table 3 for the film deposited at -0.9 V vs.SCE for 30 min. The growth of the film is strongly influenced by the substrate.

Table 3; The total amount of charge (mC cm^{-2}) during the deposition on different substrates. The films were deposited at -0.9 V vs.SCE for 30 min in the electrolyte contains 0.1 M $Zn(NO_3)_2$, 50 μM EY. Zn rod was used as counter electrode.

Substrate	ZnO	EY / ZnO
SnO_2	202.5	150
Au	840	510
Textile Au	8901.5	6347

After the electrochemical deposition of ZnO or EY / ZnO hybrid thin films, the deposition of the films were observed. Since SnO_2 is more transparent, the milky color of ZnO film could be observed clearly. However, the deposition of the film was not so clear since Au and Au textile electrode had shiny Au color. Some depositions were confirmed by observing at the edge part of the film; the milky color of the ZnO could be observed at the border between bare Au electrode and ZnO deposited Au electrode. In the case of EY / ZnO, the reddish color of EY was clearly observed from both Au and Au textile electrode.

During the deposition of ZnO, 202 and 840 mC cm^{-2} of charges through SnO_2 and Au conductive substrate respectively were passed. More than 3 times higher amount of charge was found for Au electrode. It is caused by the different activity between fluorine doped SnO_2 and Au electrode. Similar results were seen during the deposition of one-step EY / ZnO films. 150 and 510 mC cm^{-2} of charges through SnO_2 and Au conductive substrate respectively were passed. Smaller amount of charges comparing with the deposition ZnO is caused by the disturbance of the reaction by dyes in the deposition bath.[60] More than 10 times larger amount of charges were passed during the deposition in the case of textile electrode. It indicates the higher surface area of the electrode. The benefit of the electrochemical deposition can be seen that the electrochemical deposition can be applied to any shape of conductive electrode, even on textile, porous substrate, since film preparation is carried out in the soft process. In dye-sensitized solar cells, the porosity of the electrode gives the strong influence to its photoelectrochemical properties. The improvement of the dye-sensitized solar cells have been achieved by increasing the surface area simply.[60,71] The electrochemical deposition method can prepare thin layers of films on porous electrodes. The preparation of dye-modified ZnO thin films on textile electrodes confirms those benefits of the electrochemical deposition method.

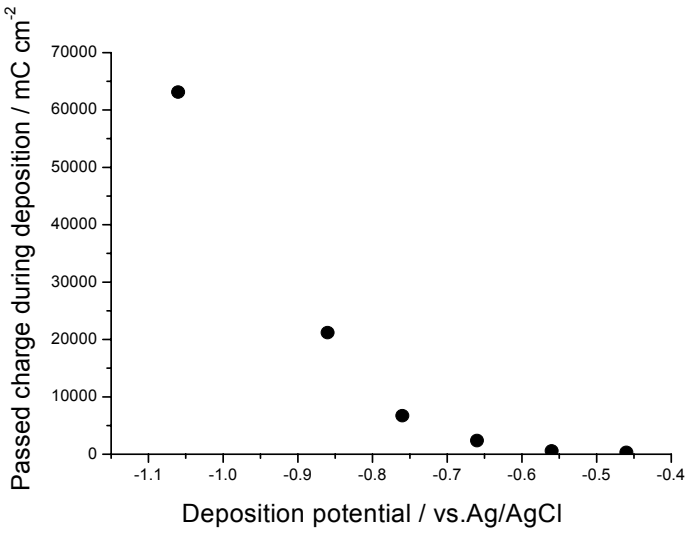

Fig. 4.5; The total amount of charge passed during the deposition at different potential

In Fig. 4.5, the total amount of charges passed through the electrode during the deposition at different potentials is shown. The amount of charges is significantly higher than in the preparation of EY / ZnO hybrid thin film on SnO_2 substrate as described above. The charges of about 350 and 63000 mC cm^{-2} were found after the deposition at -0.46 and -1.06 V vs. Ag/AgCl respectively. Approximately 180 time larger amount of charges were found during the deposition at negative potential. The higher activity of Au electrode reflects as the exponentially increased charges. However, it should be noted that degassing of oxygen from the deposition bath was not carried out before the deposition. At negative potential, there are four possibilities for the reaction; the reduction of 1, nitrate, 2, oxygen, 3, Eosin Y and 4, hydrogen. From these reactions, it is not clear how much reaction from oxygen, hydrogen and EY are contributing the current during the deposition. But concerning the concentration of nitrate, it can be assumed that the reaction of nitrate dominates the ZnO deposition.

The amount Zn atoms in the film was estimated by AAS measurement. (Fig. 4.6) 2.4 x 10^{-6} and 8.4 x 10^{-4} mol cm^{-2} of Zn atoms at the deposition potential of -0.46 and -1.06 V vs. Ag/AgCl respectively were detected from EY / ZnO textile electrode. The ratio of the difference has a nice agreement with the difference in the amount of charge. It was confirmed by this measurement that Zn atoms were on the textile electrode since it was not clear from the observation by eyes whether there was ZnO on the Au textile electrode due to its transparence property except for EY. The Faraday efficiency was calculated from the amount of Zn atoms comparing with the amount of charge passed during the deposition and more than 60 % of Faraday efficiency was found from all cases. However, it is not clear whether the amount of Zn atoms corresponds to the amount of ZnO molecules or not, since crystalline ZnO has not been proven by qualitative analysis like XRD. The deposition of ZnO on Au textile electrode can be assumed since those electrodes show the

properties to work as photoelectrode by generating the photocurrent (shown in section 4.2.3) although it still does not mean that all Zn atoms exist as ZnO on the film, there is a possibility to deposit as $Zn(OH)_2$ on the film.

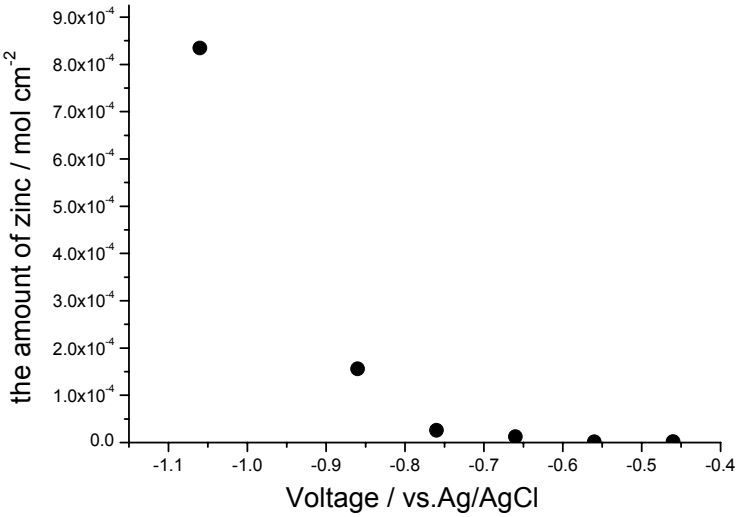

Fig. 4.6; The amount of Zn atoms in the film prepared at different potential

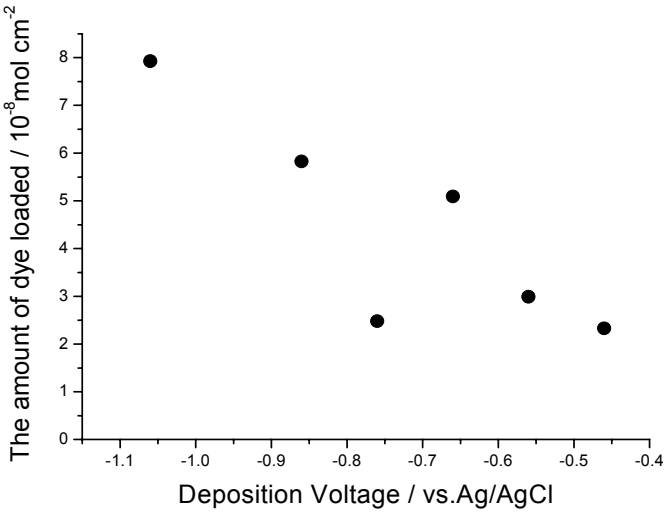

Fig. 4.7; The amount of dye loaded to the film prepared at different potential

The amount of dye on the film was estimated by measuring absorption spectroscopy of the NH_3 aqueous solution in which the film was dissolved. Rather high amount of dye molecules were found in the range of 10^{-8} mol cm^{-2} in all films. Surprisingly, there is no correlation between the amount of dye loaded and the amount of Zn atoms in the film. A relatively high concentration of EY was found in the film deposited at the positive potentials such as -0.46 and -0.56 V vs. Ag/AgCl.

Taking into account the molar ratio between the amount of Zn and amount of dye in the film, the molar ratio is 10000:1 and 100:1 in the film deposited at -1.06 and -0.46 V vs. Ag/AgCl respectively. In both case, it was found that relatively high amount of Zn was detected compared with the amount of dye loaded when the ratio of 1:1 was expected as ideal. In EY / ZnO hybrid thin films deposited at less than -0.9 V vs. SCE, it was reported that EY molecular produced a complex with Zn and precipitation of ZnO occur with the complex.[60] In this case, the deposition of the EY / ZnO hybrid thin film takes place with enclosing the EY molecular in the film. Simply, EY molecules are not on the surface of ZnO. On the other hand, if the potential is more negative than the redox potential of EY, EY molecular attaches after ZnO is created.[60] In this case, EY molecules stay at the surface of ZnO since the growth of ZnO continues from the site where EY has not adsorbed. From those previous works, it can be expected also for those textile electrodes that the dyes are in the film deposited at -0.46 V vs. Ag/AgCl and the dyes are on the surface of ZnO film prepared at -1.06 V vs.Ag/AgCl. It has been reported the positive shift of the redox potential of EY was caused by the existence of Zn^{2+} ions.[60] Such shift was observed in the concentration of Zn^{2+} larger than approximately 10^{-4} M in the electrolyte and the slope of the shift is approximately 64 mV / decade. This was measured with ITO. It can be expected that same phenomenon takes place with textile electrodes. Nevertheless, the deposition potentials of -0.46 and -1.06 V vs. Ag/AgCl are crossing the EY redox potential even if the shift of the EY redox potential for textile electrode is bigger than the case of ITO. Relatively higher amount of dye in the film prepared at positive deposition potential can be understood by the fact that ZnO precipitate following the formation of a complex by Zn^{2+} ions and EY molecules. On the other hand, relatively small amount of the dye in the film deposited at a negative potential can be understood by considering that the adsorption rate of EY is slower than the growth rate of ZnO particles. The higher activity of Au than SnO_2 leads the faster growth of ZnO. It can be seen from much bigger amount of the charge during the deposition. Then the creation of ZnO particles occurs mainly earlier than the adsorption of EY on the surface. Those different mechanisms of the deposition and different kinetics cause the different ratio of dye and Zn in the film significantly.

4.2.2. Morphology and structure

The morphology of an EY / ZnO hybrid thin film on an Au textile electrode was observed by SEM. The characteristic shapes of particles were observed.

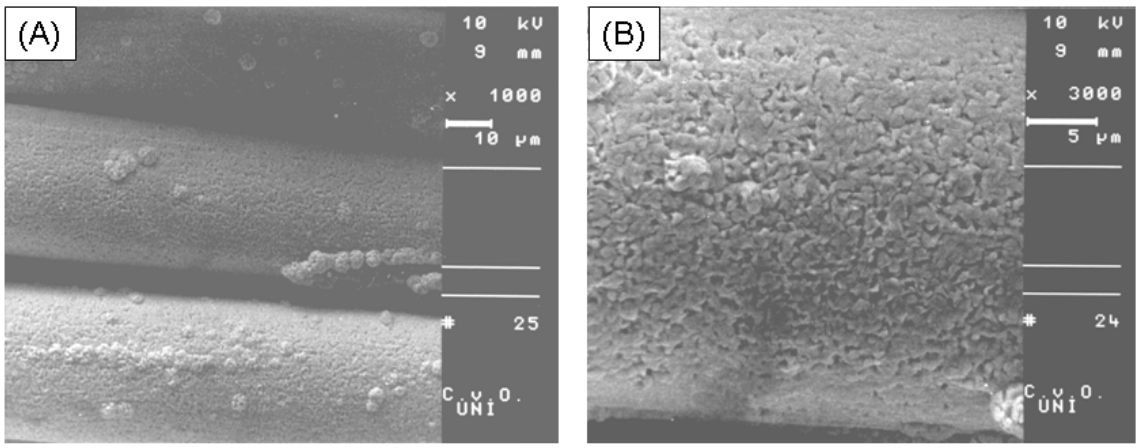

Fig. 4.8; SEM image of EY / ZnO hybrid thin film deposited on Au textile electrode at the potential of -0.76 V vs. Ag/AgCl for 60 minutes. The resolution of the image is (A) x 1000 and (B) x 3000.

The deposition on the textile electrode at -0.76 V vs. Ag/AgCl could be observed at Fig. 4.8. From Fig. 4.8 (A), the shape of textile is clearly seen. From the results of AAS and also the higher resolution image (B), it can be assumed that the film covers the all surface of the textile electrode rather homogeneously. At some points, further creation of the particles can be observed. All such particles have spherical shape. The three dimensional growth of ZnO particle can be seen from such particles.

Textile electrode has an advantage that the surface of the electrode is larger than the other electrodes due to the shape of the electrode. By depositing the film on such electrodes, an enhancement of the surface area can be expected. It is an important for dye-sensitized solar cells since an improvement of the surface area and an increase of the monomer adsorption of the sensitizer are the key issues to improve the photoelectrochemical efficiency.

From (B) in Fig. 4.8, a porous structure can be seen on a textile electrode. The specific shape of small particles is not observed from the image. It can be seen that those small particles connect each other and small pores can be observed part to part. Such pores remind of the high porosity of the electrode. This is an ideal outcome since the advantage of the electrochemical deposition, which is able to deposit the porous dye modified ZnO thin film, is achieved on the textile electrode. Its photoelectrochemical properties are discussed later in section 4.2.3.

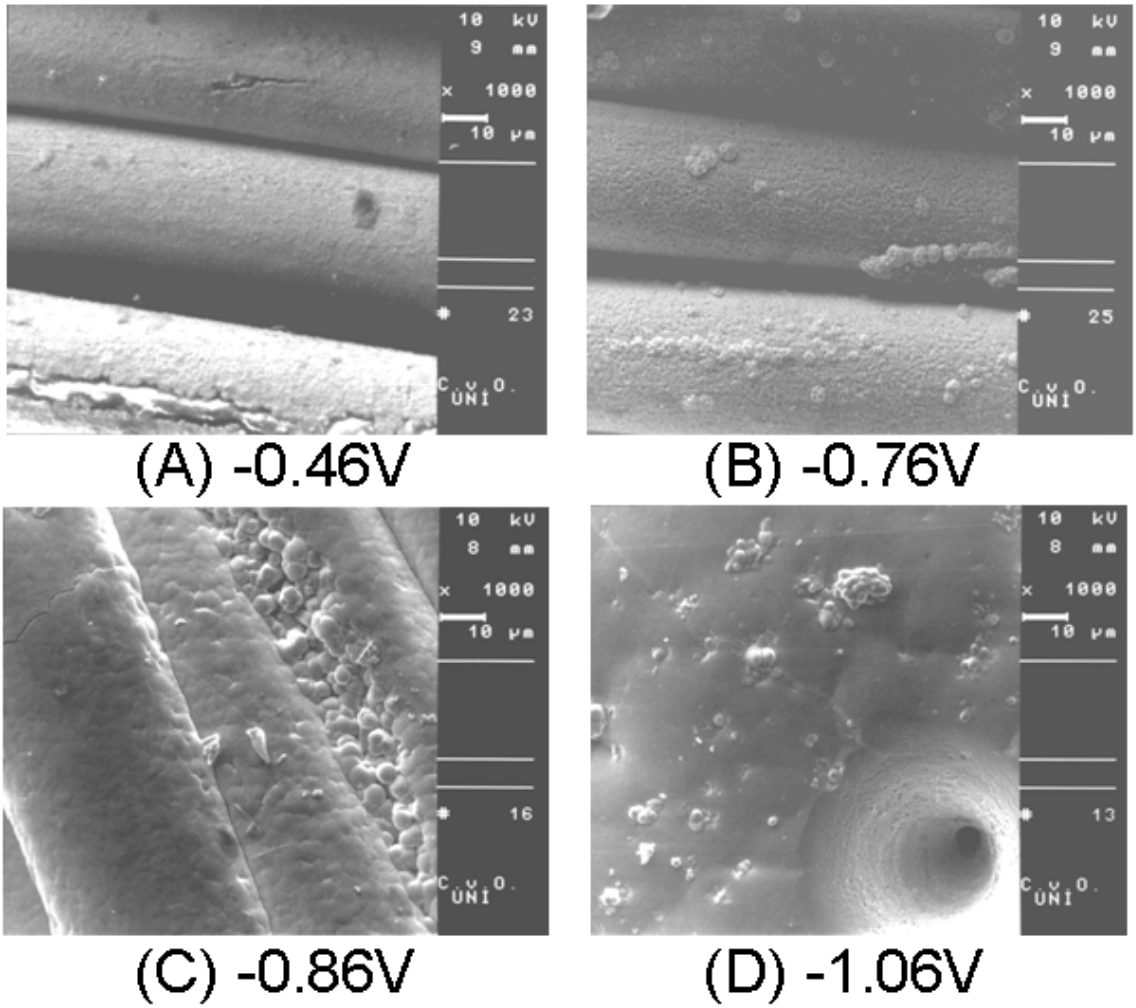

Fig. 4.9; SEM images of EY / ZnO hybrid thin film deposited on Au textile electrode at several deposition potential of (A) -0.46 V, (B) -0.76 V, (C) -0.86 V and (D) -1.06 V vs. Ag/AgCl for 60 minutes.

SEM images of the other EY / ZnO hybrid thin films prepared at different potentials on textile electrodes are shown in Fig. 4.9. In the film prepared at-0.46 V vs. Ag/AgCl ((A) in Fig. 4.9), the shape of the textile electrode and the space between the fibres are clearly seen. The deposition of the film is not clearly seen in the SEM image. Since Zn atoms were confirmed by AAS measurement, small and fine particles are deposited on the electrode. At part to part, the cracks are observed and the inside of the crack might be a bare textile electrode.

The porous structure was observed from the film deposited at -0.76 V vs.Ag/AgCl (Fig. 4.9 (B)). As described in Fig. 4.8, this is a kind of an ideal deposition for the application to dye-sensitized solar cells. However, the space between the fibers can be observed. Further deposition of the film with keeping the porous structure is necessary to achieve an even further increased surface area.

From the film prepared at -0.86 V vs. Ag/AgCl (Fig. 4.9 (C)), the textile electrode was fully covered after the deposition. Although the trace of the textile electrode can be distinguish from the image, the space between the fibers was filled by the deposition. The surface of the film seems rather flat. And the particles which have sphere shape are observed in

some part. Although the reason is not clear, the mechanism of the deposition seems not same in the whole film.

The trace of the textile electrode disappears after the deposition at -1.06 V vs. Ag/AgCl for 60 minutes (Fig. 4.9 (D)) since the film covered the surface of the electrode completely. The surface of the film is almost flat. Small particles on the surface of the film can be observed. It seems that further deposition is taking place from those parts. Surprisingly, a hole with the size of 10 μm was observed in the film. As mentioned above, it might happen that several reactions such as the reduction of nitrate, dye, hydrogen and oxygen might occur at negative deposition potential during the deposition. The hole is the fact that the reduction of hydrogen took place during the deposition and hydrogen was generated on the textile electrode. Such reaction does not happen in the case of SnO_2 conductive substrate. But it might happen with Au coated textile electrode since Au has higher activity. The SEM images of this film observed at several resolutions are shown in Fig. 4.10.

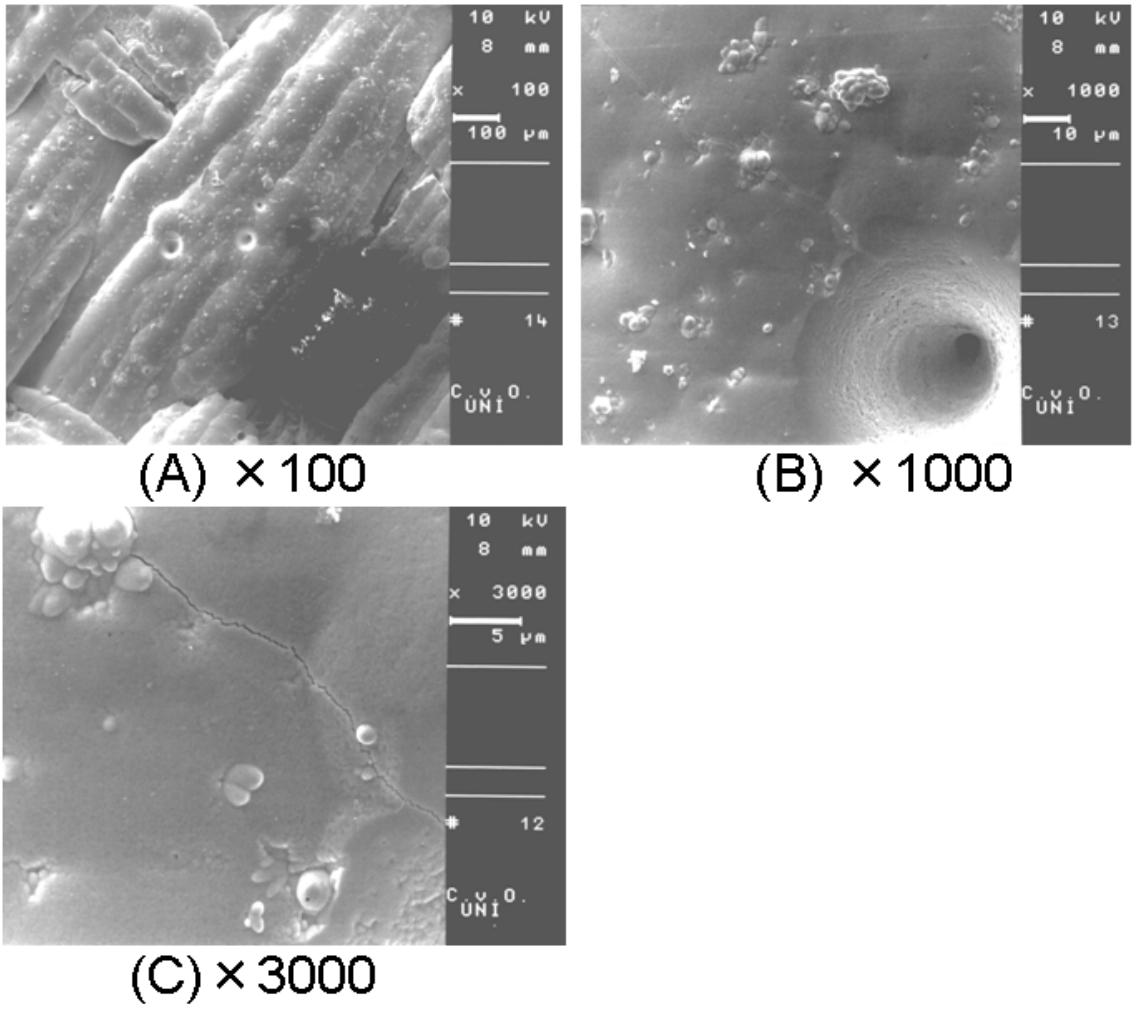

Fig. 4.10; SEM images of EY / ZnO hybrid thin film deposited on Au textile electrode at the potential of -1.06 V vs. Ag/AgCl for 60 minutes observed at different resolutions of (A) x 100, (B) x 1000 and (C) x 3000.

From Fig. 4.10 (A), the film was observed at low resolution of x 100. In such a low resolution, the trace of the textile electrode can be seen slightly. It is observed that the film covers the electrode fully. Some holes can be seen in this image and it indicates the gas creation at the Au textile electrode. The reaction to produce the gas at the electrode is competing with the other reactions, mainly with the deposition of ZnO. It can be expected that the reduction of nitrate which leads the creation of ZnO dominates the reaction at the electrode and at some parts the reduction of hydrogen can take place. The point, where the reduction of hydrogen occurs, continues the reaction and such points stays as it is during the deposition and be left as hole after the deposition.
Rather flat structure can be observed from high resolution image (Fig. 4.10 (C)). And each particle sticks strongly each other, a crack to break such connections is observed. When the creation of the gas does not occur, the continuous deposition can be expected from such places. Such homogenous structure, however, might decrease its photoelectrochemical properties since it does not seem to have large surface area. Generally it was found that one-step electrodeposited films fill their fine pores by adsorbed dyes.[6 9] Relatively small surface area can be expected form the image shown here.

The deposition on the textile electrode was confirmed by the analysis such as AAS and SEM. Characteristic structures were seen from the films prepared at different deposition potential and it seems that the deposition potential will influence strongly their porosity of the film, which influences also their photoelectrochemical properties. The photoelectrochemical properties of those films are studied in the next section.

4.2.3. Photoelectrochemical characterization

Photocurrent transient measurements have been carried out in ms range for EY / ZnO hybrid thin films electrodeposited on textile electrodes. Since the electrode has a textile structure consisted by fibers, the electrode must be illuminated from the surface side. The electrolyte containing KI in the mix solvent (ethylene carbonate : acetonitrile = 4 : 1 in volume) were used for the measurement since it was transparent. Measurements were carried out in a three electrode setup and Pt and Ag/Ag^+ were used as counter electrode and reference electrode respectively. The illumination source was a xenon lamp and its light intensity was adjusted to 200 mW cm^{-2} in visible region between 385 – 900 nm. In the measurements, it should be noted that 10 ms is necessary to open and close the mechanical shutter completely.

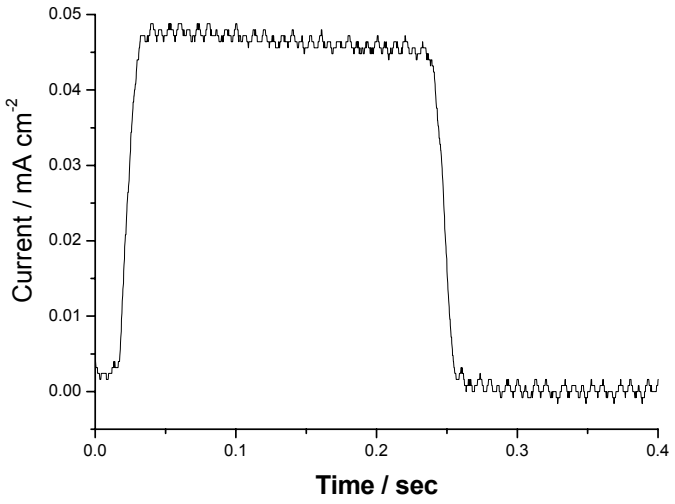

Fig. 4.11; Time-resolved photocurrent measured for EY / ZnO hybrid thin film deposited on an Au textile electrode at a potential of -0.76 V vs. Ag/AgCl for 60 minutes. A mixed solvent of ethylene carbonate : acetonitrile =4:1 (in volume) which contains 0.5M KI was used as an electrolyte.

Time-resolved photocurrent measured for EY / ZnO thin film deposited at -0.76 V vs. Ag/AgCl for 60 minutes on an Au coated textile electrode are shown in Fig. 4.11. The electrode shows the photocurrent response for the illumination, the current is increased quickly as the shutter opened. It is confirmed that this film works as a photoelectrode even if the film was prepared on the textile. The magnitude of the photocurrent was almost stable during the illumination for 200 ms. It indicates that no recombination is taking place in the device. The photocurrent of approximately 47 μA cm^{-2} is detected. This is a relatively high photocurrent in the study of one-step electrodeposited film although it is not high enough for the application to dye- sensitized solar cells. The reason of this high photocurrent are following; the high photochemical property of Eosin Y as reported before [60] and the relatively high surface area due to the textile structure comparing with conductive glass substrate. However, it should be mentioned that the electrode size of textile for the measurement might be underestimated since the electrode size was defined from its two dimensional size.

The surface morphology of this film is shown in Fig. 4.8. As mentioned above, the porous film was deposited on the textile electrode. Since no recombination evidence observed in the time-resolved photocurrent, it can be considered that such structure is one of the ideal as a photoelectrode. And moreover, considering the molar ratio of Zn atoms and dye in the film, it was found as approximately 1000:1. Such ratio can also be a reason for the ideal shape of the time resolved photocurrent.

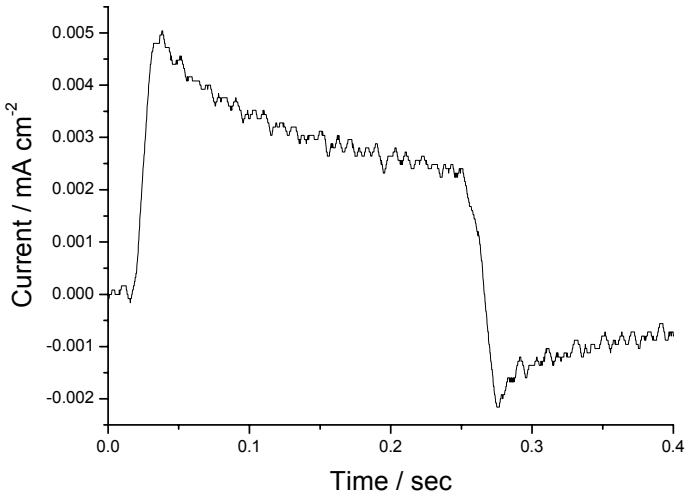

Fig. 4.12; Time-resolved photocurrent measured for EY / ZnO hybrid thin film deposited on Au textile electrode at a potential of -0.46 V vs. Ag/AgCl for 60 minutes. A mixed solvent of ethylene carbonate : acetonitrile =4:1 (in volume) which contains 0.5M KI was used as an electrolyte.

The film deposited at -0.46 V vs.Ag/AgCl for 60 minutes showed a characteristic shape of time- resolved photocurrent. (Fig. 4.12) An overshoot could be observed in the beginning and the end of the illumination and the relaxation of the photocurrent were observed during the illumination. Such shape of the time- resolved photocurrent was observed earlier.[64,83] After the absorption and excitation of electrons in sensitizer molecules and the injection of the electrons to the conduction band of the semiconductor, the oxidized sensitizer can not be supplied with an electron from the redox electrolyte since the oxidized sensitizers have only a poor contact with the redox electrolyte. Generally, the overshoot in the beginning can be understood by the electrons injected initial moment of the illumination and the relaxation is caused by decreasing number of the photoactive dyes in the film. Such oxidized dyes after the injection once stay as oxidized states during the illumination and those dyes require the electrons to recover from the oxidized condition. Since those dyes do not have a contact with the electrolyte, the electrons are taken from ZnO, such movement of the electrons is detected as an anodic peak at the end of the illumination, which was also observed in the Fig. 4.12. These phenomena might be related with the extra amount of dye loaded in the film. The molar ratio of Zn atoms and dye molecules are 100:1 in this film. Relatively high amount of dye molecules are in the film. And it can be expected that such extra amount of dye molecules fills the pores in the film. And also, since this film is prepared at more positive potential than the redox potential of EY, it can be expected that the dyes are enclosed in the film.[60] The photocurrents of 5 and 3 $\mu A\,cm^{-2}$ were detected at the peak and after the relaxation respectively. The enclosed dyes in the film and the rather flat structure of the films as observed in the SEM image (Fig. 4.9 (A)) can be the reason for the poor photoelectrochemical property.

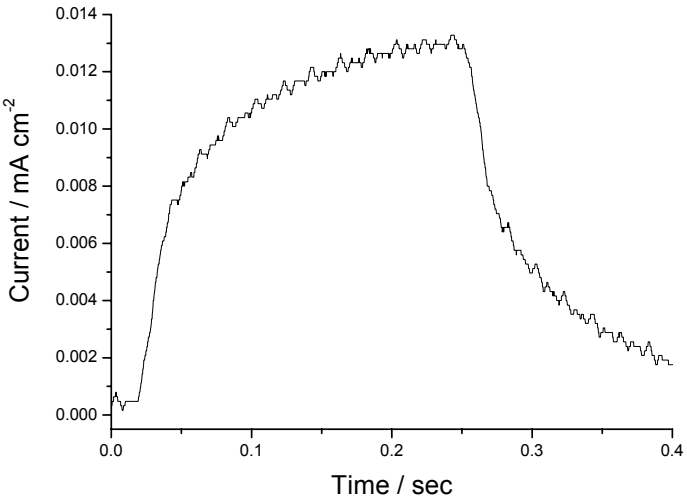

Fig. 4.13; Time-resolved photocurrent measured for EY / ZnO hybrid thin film deposited on an Au textile electrode at the potential of -1.06 V vs. Ag/AgCl for 60 minutes. A mixed solvent of ethylene carbonate : acetonitrile =4:1 (in volume) which contains 0.5M KI was used as an electrolyte.

The slow increase of the photocurrent was observed in the photocurrent transient measurements for the film prepared at -1.06 V vs. Ag/AgCl for 60 minutes. (Fig. 4.13) The textile electrode was almost covered after the deposition as shown in Fig. 4.10. Since this film was deposited at more negative potential than the redox potential of EY, it could be expected that the dyes were on the surface of the film. The photocurrent of 12 μA cm^{-2} was detected from the figure. The rather poor extent of the photocurrent is caused by the small number of the dyes adsorbed as monomer state on the surface of ZnO.[69] A slow increase of the photocurrent after the shutter open and the slow decrease of the photocurrent after the closer can be explained by the electron transport property of ZnO and the traps in ZnO film. The electron transport in electrodeposited ZnO films can be assumed fast enough as reported before.[60,64,83] Then, the slow response of the photocurrent is caused by time to fill the traps in the film. Since some kinds of the reactions take place during the deposition at such negative potential as mentioned above, it can be supposed that the film is deposited as the results of mixed reaction routes such as the reduction of oxygen, hydrogen and nitrate. It can be expected that the film has more traps than the one prepared by only the reduction of nitrate.

From the shape of the time- resolved photocurrent, no recombination was seen. It indicates the efficient photoelectrochemical activity of the device. However, aggregated dye molecules on the surface of the film depress the photoelectrochemical activity of the electrode. Such dyes do not contribute for the photocurrent although those dyes absorb the photons. Increasing of the amount of dye adsorbed as monomer states will be the key issue to increase the photoelectrochemical property.

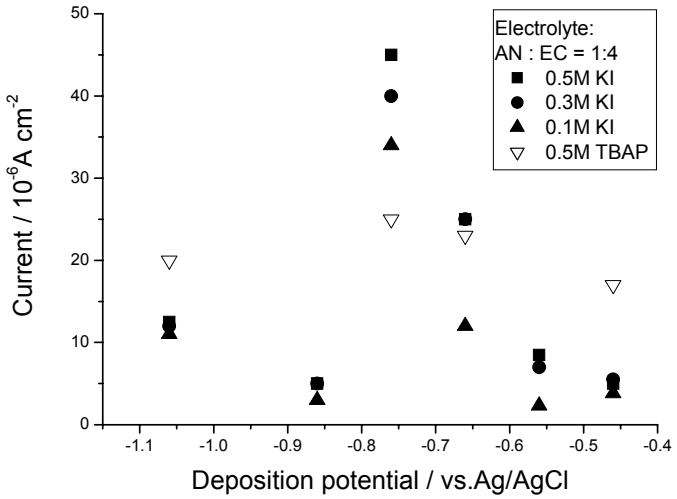

Fig. 4.14; The stable photocurrent values detected from the time-resolved photocurrents measured with different kinds and concentrations of solute in the electrolyte for EY / ZnO hybrid thin film deposited on an Au textile electrode.

The photocurrents were measured for the films prepared at several deposition potentials. And 0.5, 0.3, 0.1 M KI and 0.5 M TBAI were used for the electrolyte. (Fig. 4.14) It can be seen that the highest photocurrents have been achieved at the film prepared at -0.76 V vs. Ag/AgCl. At the other deposition potentials, the photocurrents are relatively low. The porosity of the film influences the photoelectrochemical property of the films. The film deposited at -0.76 V vs. Ag/AgCl has the most porous structure as observed in the SEM image and other films have a rather dense structure. By this reason, the photocurrent values is low in the film prepared at the negative potential more than -0.76 V vs. Ag/AgCl. At the potential less than -0.76 V vs. Ag/AgCl, the enclosed dye molecules do not contribute to the photocurrent and hence low photoelectrochemical properties. And those dyes cause the recombination and it is observed in the photocurrent transient measurement. The conditions of the dye in the film and the porosity are the key points to decide their photoelectrochemical properties.

When TBAI was used for the electrolyte, relatively larger photocurrents were detected except for the deposition potential of -0.76 V vs. Ag/AgCl. The bigger size of cation than potassium might influence the photoelectrochemical properties. The porous structure of the film prepared at -0.76 V vs. Ag/AgCl might not be facile for the big cation to enter. But the magnitude of the photocurrent at this deposition potential is still highest compared to the other potentials. It indicates the importance of the porosity for such devices even if solute is not suitable for its structure.

4.2.4. Summary

EY / ZnO hybrid thin films were prepared on Au coated textile electrodes. The films were deposited successfully on the textile electrode. The charge passed during the deposition was much higher than the case using SnO_2 substrate due to the high activity of Au. Such high activity shows the big difference by changing deposition potentials. The molar ratio of Zn atoms and dye molecules in the film changes about 2 orders by the deposition potential. The porous structure could be obtained by adjusting the deposition potential, dye concentration in the deposition bath and deposition time. In this study, the deposition potential of -0.76 V vs. Ag/AgCl was best condition to obtain the porous structure in the film, observed from SEM image.
Moreover, the deposition potential influences the position of the sensitizers. At positive potential, the sensitizers were enclosed in the film. It appeared as an overshoot in photocurrent transient measurements when the light was illuminated. On the other hand, the slow increase of the photocurrent was observed from the film prepared at a negative potential like -1.06 V vs. Ag/AgCl. It was caused by the traps in the film, the trap and detrap of the electrons during their transport through the film led to the slow increase and decrease of the photocurrent when the illumination started and ended respectively. Nevertheless, it was confirmed that EY / ZnO thin films on the conductive textile electrodes worked as photoelectrode.

This was the first challenge and the success to fabricate a dye modified ZnO on a textile electrode. The advantage of the electrochemical deposition was nicely utilized since it was not simple to prepare a nanocrystalline thin film on such textile electrode by a conventional way like sol-gel method. The improvement of its photoelectrochemical properties will be achieved by optimizing the preparation condition. This technique and achievement open the possibility to obtain the “solar cell cloth” in the future.

4.3. Conclusion for this chapter

TSPcZn / ZnO and TSTPPZn / ZnO films have been prepared by the electrochemical deposition successfully in one-step from a deposition bath in which the dye was present. Moreover, (TSPcZn+TSTPPZn) / ZnO films have been prepared by one-step electrochemical deposition method from mixed solutions. This result confirms that the electrochemical deposition is possible in the presence of more than one dye in the deposition bath. Since the sensitizers modify the growth mechanism of the ZnO, significant influences were found in their morphology. Dye uptake in ZnO pores beyond adsorbed sensitizers led to a small surface area and hence low photoelectrochemical efficiency. An overshoot in the photocurrent at the beginning of illumination was correlated with such low photocurrents. A cathodic spike caused by an opposite flow of electrons from the conduction band of ZnO to the oxidized dye was seen when the illumination was cut off. Correspondingly the strongest absorption bands led to an optical filtering effect since the electrodes were illuminated from the substrate side. The aggregation form of TSPcZn was decreased when the film was prepared in the presence of both TSPcZn and TSTPPZn. Although a significant change could not be seen in the photoelectrochemical efficiency, the increase of the monomer form leads to an enhancement of the quantum efficiency. Achieving the monomer adsorption of the sensitizer and increasing the contact between the sensitizer and the redox electrolyte are the key issues to improve the photoelectrochemical efficiencies of one-step electrodeposited films.

EY / ZnO was successfully deposited on Au- coated textile electrodes to utilize the versatility of electrochemical depositions. The deposition of ZnO depends on the potential for the deposition. It was found that such textile electrode also worked as photoelectrode although the magnitude of photocurrent was rather poor, approximately 20 $\mu A\ cm^{-2}$. The photoelectrochemical properties depended on the porosity of the film. When the film showed the higher photocurrent, the relatively porous structure of the film was observed from SEM image. Its low photoelectrochemical properties were strongly related with the results observed from the films deposited on SnO_2 substrate that the films has small surface area due to the extra amount of dye on the film and such low surface area lead to low accessibility of the redox electrolyte with the oxidized dyes in the film, then its photoelectrochemical properties was hindered.
It was proven by this study that the solar cells on textile could be possible. Further optimization such as, optimizing the preparation condition mainly to obtain a high porosity at optimized dye load is needed to further open up the possibility to introduce such solar cells. Electrochemical deposition is a promising method to prepare the device practically.

5. Electrochemical and photoelectrochemical characterization of re-adsorbed Dye / ZnO hybrid thin films

During the investigation, it was found that excess amount of dye adsorbed to the surface of ZnO during the electrochemical deposition in the presence of dye in the electrolyte and those dye molecules were the reason why the one-step electrodeposited dye / ZnO films showed rather poor photoelectrochemical properties.[58,64,83] It means that either many dye molecules do not have chemical bonding with ZnO, or they are not at the surface of the film. Such molecules fill the fine pores in the ZnO matrix and hence decrease the surface area of the film significantly and disturb their photoelectrochemical activities since the sensitizers, which are at the surface of ZnO and deliver the sensitized photocurrents, can not have an access with the electrolyte which is important to recover the oxidized dyes after the injection of excited electrons.[171] However, it was found that such excess amount of dye molecules could be removed from the surface of ZnO by dipping the film into aqueous KOH (pH 10.5) since they were on the surface of ZnO. And sensitizer can be "re-adsorbed" after the extraction of the dyes. It brings the monolayer adsorption of the sensitizer on the surface of the ZnO and it leads to a nice contact for photoactive sensitizers with both the ZnO and the redox electrolyte. Such situation is ideal for dye-sensitized solar cells, and such re-ad films show much better photoelectrochemical performance than the one-step electrodeposited films.[69] Although this re-adsorption method is not one-step process, the temperature demanded during the preparation is still less than 150 ℃, which is much lower than the 400 ℃ required in the sol-gel method.[8,47]

Historically, this re-adsorption method was found during the analysis whether the dyes are on the surface of the ZnO or in the ZnO. When the dyes are on the surface of the film, the dye can be removed from the surface by dipping it into a soft alkaline solution for several hours. Since electrodeposited dye / ZnO films had a porous, highly crystalline structure, and enough amount of dye content in the film to achieve close to 100 % of light harvesting efficiency,[55,58,59,60] the reason was not clear why those films showed rather poor photoelectrochemical properties. One of the reasons can be that the dyes are enclosed in the film during the deposition, so it does not allow the access of the redox electrolyte. Then, accessibility test was carried out. And it was found for one-step electrodeposited EY / ZnO thin films that the films prepared at more negative potential than the redox potential of Eosin Y did not contain dye molecules in the film, but EY could be removed completely by a treatment in soft alkaline. It means all dyes adsorbed on the surface of the ZnO during the deposition. On the other hand, the films, prepared at more positive potential than the redox potential of EY, contain the dye molecules in the film, so dyes can not be removed by dipping the film into alkaline solution. This is strongly related with the mechanism of the deposition; how the dye molecules attach to the film during the deposition, either attaching after the creation of ZnO particles or attaching first with Zn

ions; forming complex and precipitate as ZnO. First case can be seen when film was deposited at more negative potential than the redox potential of EY. Latter case can be seen when the films are deposited at more positive potential.[60]
And the excess amount of dye in the films was found by calculating both the molar and volume ratio of ZnO particles and dye molecules. The porosity of the film can be estimated approximately from the amount of Zn in the film and the film thickness. And a suitable amount of dye adsorbed to the surface of ZnO can also be estimated by letting the dye adsorb to ZnO powder and measure the amount of dye. From such information, it was found that the excess amount of dye molecules were on the surface of ZnO.[60]
After the optimization of the film preparation, Eosin Y / ZnO films deposited at -1.0 V vs.SCE for 20 minutes, for instance, give highly crystalline porous ZnO thin films. Besides EY, the modification of the structure, the morphology and the orientation of ZnO films has been observed also when C343[194] and SDS[70] are present in the deposition bath. Such films can be used as a matrix to allow an adsorption of a variety of sensitizers to the surface of the film.[69]

In this chapter, several kinds of sensitizers, mainly TSPcZn and TSTPPZn, were re-adsorbed on such ZnO films and their photoelectrochemical properties have been investigated. EY, C343, SDS were used as SDA in this chapter. The factors to improve the photoelectrochemical performance, especially in the red part of the visible light, and the influences of different film structure have been studied to understand the electron transport kinetics in such films.

5.1. Basic investigation of films prepared by the re-adsorption method

A lot of results have been reported for the electrochemical deposition in the presence of EY in the electrolyte.[55,56,60] The constitutional formula of EY is shown in Fig. 5.1.

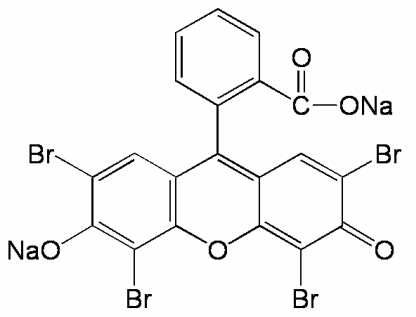

Fig. 5.1; The constitutional formula of Eosin Y

It was reported that EY / ZnO films had a porous, highly crystalline and single crystal structure.[56] In this section, re-ad dye(sensitizer) / ZnO films were prepared and EY was

used as SDA to modify the surface structure of the ZnO. The properties of such films were measured after adsorbing the sensitizer. Moreover, the practical details of film preparation were also discussed.

5.1.1. Preparation of Eosin Y / ZnO film

The reproducibility of the sample preparation is one of the most important points in the study. Electrochemical deposition of dye / ZnO films by utilizing the reduction of nitrate has a serious problem in reproducibility. And it is difficult to control since there are too many factors changing during the deposition, e.g. concentration of Zn ions. On the other hand, the deposition by utilizing the reduction of oxygen has better features to prepare the film with a nicer reproducibility since many factors are able to control to be constant. However a reproducibility problem occurs in this also because of the different oxygen concentration in the electrolyte for each deposition, existence of gas oxygen, different concentration and total amount of the dye in the electrolyte, the condition of the substrate's surface and the contact between the SnO_2 glass and the substrate holder. The reproducibility could be improved by minimize the change of such factors. Typical examples are shown here. And the preparation of another film in the same electrolyte after a deposition was also studied and its possibility was discussed.

5.1.1.1. Pre-deposition electrolysis and deposition of Eosin Y / ZnO films

When an EY / ZnO hybrid thin film is electrodeposited, the increase of the current in the initial stage of the deposition is observed in a current-time curve. It does not only mean the surface area of the substrate is increased three- dimensionally due to the creation of ZnO particles on the substrate. If this was the only factor, the current would decrease after a short while, corresponding to the time that the ZnO particles cover the whole substrate. It was found that the increase of the current was also caused by the fact that the activity of the SnO_2 conductive substrate was increasing by the applied potential.[164] To obtain the films with a nice reproducibility, the condition of the substrate should be prepared identically. Before starting the electrochemical deposition of EY / ZnO hybrid thin film, the "pre-deposition electrolysis" should be introduced to activate the surface of the SnO_2 conductive glass substrate, and it leads to increase the number of the seeds of ZnO particles on the substrate in the initial stage of the film precipitation.[164]

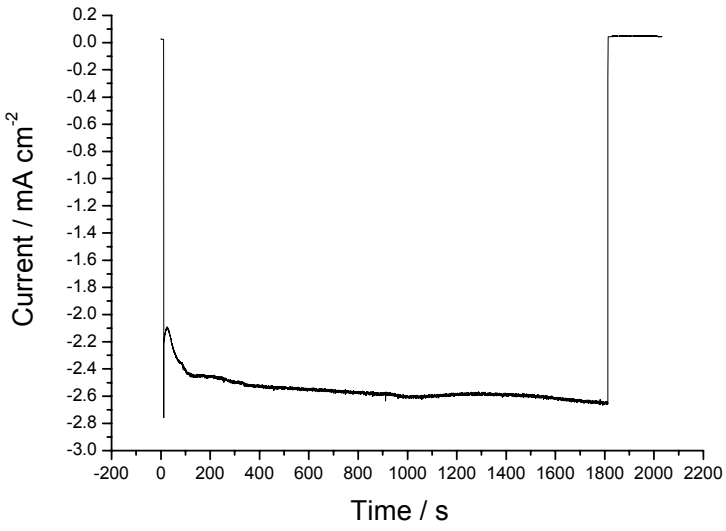

Fig. 5.2; The current-time curve during the pre-deposition electrolysis. The potential of -1.0 V vs. SCE was applied to the electrode for 30 minutes in the solution of 0.1 M KCl with the bubbling of oxygen in the bath. Pt electrode was used as counter electrode. A rotating disk electrode was set at 500 rpm. The flow rate of oxygen and nitrogen was 200 and 400 ml / min. respectively.

The current-time curve during the pre-deposition electrolysis is shown in Fig. 5.2. The current of 2.6 mA cm^{-2} was reached at the end. The current is caused by reduction of the oxygen bubbled in the deposition bath. The Zn rod electrode must not be used for pre-deposition electrolysis because the precipitation of ZnO starts if Zn ions are present in the deposition bath. For pre-deposition electrolysis, a Pt electrode was used as counter electrode. The increase of the current was observed at the beginning of the electrolysis, which indicates the activation of the substrate. The increased activity of the substrate and also the increased number of the active site in the substrate leads the increase of the current. The number of the seed of ZnO particles is increased by increasing the number of active site in the substrate.[164]

Close attention should be also paid for the preparation process of working electrodes. The contact between the substrate and the sample holder must be established tightly. The same holds for the insulating tape. When the contact was not well established, intense noises might be observed in the current-time curve; it is caused by the unstable contact between the sample holder and the SnO_2 substrate. When the insulating tape was not well attached, the current would increase as time goes; it is caused by the increase of the substrate's surface area as result of that the insulating tape peeled off. Those factors disturb the reproducibility of the film deposition. It should be noted that the oxygen bubbling is carried out in the deposition bath during the pre-deposition electrolysis process. To activate the substrate, it seems to be necessary to contain a high concentration of oxygen in the deposition bath since the evidence of the activation can be seen only when the oxygen is supplied into the deposition bath sufficiently. And the magnitude of the current depends strongly on the concentration of oxygen in the deposition bath. For the

deposition of EY / ZnO hybrid thin films, on the other hand, the gas tube of the oxygen should be out from the deposition bath to avoid the gas oxygen in the bath. (The detail is written later.) But for the pre-deposition electrolysis process, this does not matter. Therefore the gas tube should be in the bath during the activation to keep a high concentration of oxygen in the bath.

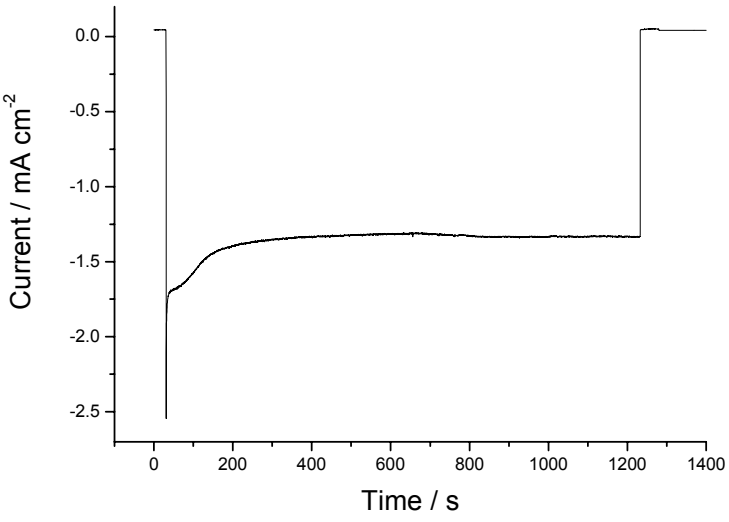

Fig. 5.3; The current-time curve during the deposition of EY / ZnO hybrid thin film. The film was prepared at -1.0 V vs. SCE for 20 minutes in the solution containing 5 mM $ZnCl_2$, 0.1 M KCl and 50 μM EY with allowing to flow oxygen into the deposition cell. Zn rod was used as counter electrode. A rotating disk electrode was set at 500 rpm. The flow rate of oxygen and nitrogen was 200 and 400 ml / min. respectively.

After the activation of the substrate, the process is stepped to the deposition of EY / ZnO hybrid thin film. The high concentrated $ZnCl_2$ and EY solutions are added to the deposition bath. The concentration of Zn^{2+} and EY in the bath is adjusted to 5 mM and 50 μM respectively. Pt counter electrode is replaced with a Zn rod electrode. And the oxygen tube is removed from the deposition bath and set close to the water surface. During these processes, the SnO_2 substrate stays in the deposition bath to keep the activated condition. Following those procedures, the deposition of EY / ZnO hybrid thin film can be started.

The position of the oxygen is one of the most important points for the deposition. To obtain porous ZnO (EY as SDA) films, it is known that there should be no gas oxygen under these conditions.[164] A porous structure of ZnO is obtained when EY molecules are reduced condition.[56] And if EY molecules are reduced state, a transparent film can be obtained after the deposition since the EY molecules are reduced state (colorless). Such reduced dyes are slowly oxidized by exposing the film in air atmosphere and the film finally get the color approximately in 24 hours.[60] However, Oxygen bubbles in the solution can oxidize the EY molecules which are on the surface of ZnO even during the deposition. In this case,

the film has the reddish color of EY even just after the deposition. When EY molecules are oxidized during the deposition due to the gas oxygen, the film shows the features as it was seen in the films prepared at more positive deposition potentials than the redox potential of EY even if the deposition potential is more negative than the redox potential of EY. In such films, the EY molecules are enclosed in the film and those dyes can not be removed by dipping into aqueous KOH (pH: 10.5). Therefore, the oxygen tube must be out from the deposition bath, but should be placed as close as possible to the water surface to keep the concentration.

The current-time curve during the electrochemical deposition of EY / ZnO hybrid thin films is shown in Fig. 5.3. The current of 1.4 mA cm^{-2} was detected during the deposition. Higher current of 1.7 mA cm^{-2} was seen in the beginning of the deposition. This relatively higher current was caused by the higher concentration of oxygen at the electrode surface. The concentration of the oxygen at the electrode surface can be expected to be higher in the beginning of the deposition. To utilize the activated substrate and to increase the number of ZnO seeds in the beginning of the deposition, it is required to start the deposition at the highest achievable concentration of oxygen in the bath. Once ZnO particles are created on the substrate, continuous growth can be expected. The decrease of the current can be seen as the result of that the time passed after removing the oxygen gas tube from the bath and some unavoidable intermixing with N_2 for purging the electrode. Finally, the current becomes a stable value, it indicates the stable supply of the dissolved oxygen to the surface of the substrate.

The reproducibility of the film preparation was optimized in this way. But nevertheless, further improvement especially for obtaining a stable and high concentration of oxygen in the deposition bath will lead to increased reproducibility.

5.1.1.2. Aging of the solution by film preparation

Effective use of the material is also an important factor. In such case too, the electrochemical deposition is ideal since the deposition of the film can be repeated in the electrolyte. In this section, repeating of the deposition after finishing the first deposition was tried and discussed in the function of the consumption of the dye in the electrolyte. The films were electrodeposited at -1.0 V vs.SCE for 20 minutes in the presence of 41 µM Eosin Y, 5 mM $ZnCl_2$ and 0.1 M KCl. In these measurements, the amount of the electrolyte was adjusted to 100 ml.

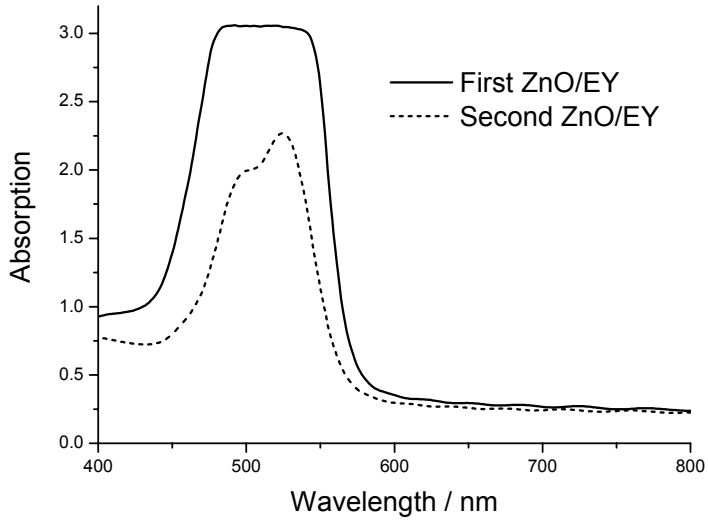

Fig. 5.4; Absorption spectrum of the films prepared in the same electrolyte in series.

The absorption spectra of the films are shown in Fig. 5.4. The different magnitude of the absorption was seen. The absorption of EY is clearly detected from the second EY / ZnO film, whereas it is not clear from the first film because of a too high absorption. The different dye contents of 1.12×10^{-7} and 0.37×10^{-7} mol / cm^2 for the first and the second film show the corresponding result to the absorption spectra of the films. These results indicate that the condition of the deposition is not the same between the first and the second film. It could be caused by different concentrations of the compounds in the electrolyte. The concentration of Zn in the electrolyte can be assumed as almost constant since a Zn rod was used as counter electrode and it supplied Zn ions proportion to the current flowing at working electrode. However it has a small increase after the deposition (from 4.8 mM to 5.8 mM).[172] It may happen since the faraday efficiency of the ZnO deposition is not unity. So, more Zn ions are supplied to the electrolyte than were consumed.

The total charge during the second deposition was 1676.1 mC, whereas it was 1711.9 mC for the first deposition. In the deposition using the reduction of oxygen, the current during the deposition is principally dominated by the reduction of oxygen. Then the similar charge amount for the first and the second deposition is not surprising. And this result indicates that the concentration of oxygen in the electrolyte is almost constant.

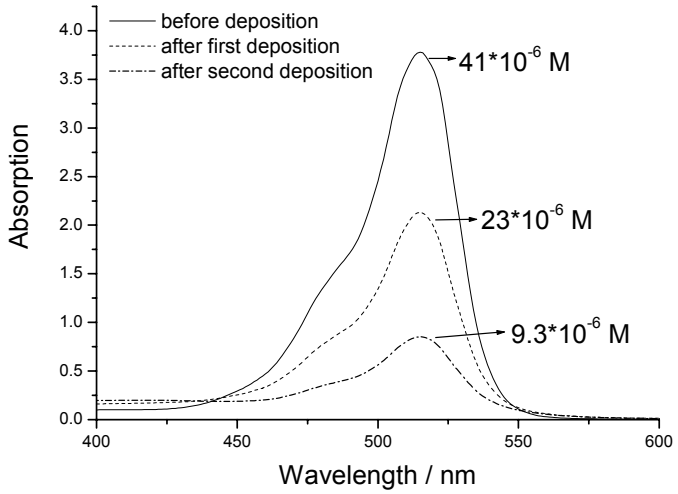

Fig. 5.5; The absorption spectra of the electrolyte before and after the deposition.

The large change of the EY concentration in the electrolyte can be seen from Fig. 5.5. Approximately 50 % of EY molecules were consumed during the deposition. Considering the amount of dye loaded during the deposition, the extra amount of EY molecules were consumed during the deposition. Since it was observed by eyes that the Zn counter electrode became red after the deposition, it means that EY molecules adsorb to the Zn counter electrode during the deposition. The extra consumption of EY molecules after the deposition can be understood from the adsorption of the EY to the counter electrode. The tendency of the dye consumption is summarized in Fig. 5.6.

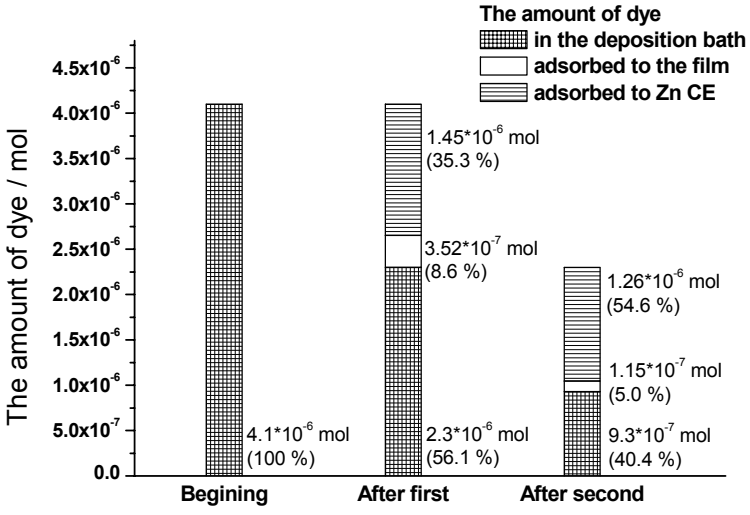

Fig. 5.6; Summary of the Eosin Y consumption during the deposition. The dye concentration in the bath and the amount of dye loaded in the film were obtained by measuring absorption spectroscopy of the electrolyte and the solution which the film was dissolved. The amount of dye adsorbed to the counter electrode was estimated by subtracting the amount of dye in the solution and the film from the total amount of the dye.

From Fig. 5.6, it was found that the consumption of EY in the film was less than 10 % in the total consumption of the dye during the deposition. Since it is such small number, it is principally possible to repeat the deposition in the same electrolyte for saving the material. However, a rather high proportion of EY molecules in the electrolyte was consumed at the Zn counter electrode. The high loss lies beyond the reasonably adsorbed amount. Some oxidative decomposition must occur. Such high consumption of EY at the counter electrode changed the concentration of EY in the electrolyte which leaded to the different film growth. To obtain highly porous ZnO films, 40 μM of EY is known as an ideal concentration.[60] It was observed that the second film does not have better IPCE than the first film. (see Chapter 5.1.1.3) The EY concentration of 23 μM is not suitable to deposit the porous ZnO film. It was often seen that EY molecules adsorbed to the second films did not dissolve in aqueous KOH (pH 10.5). (In the first film, it may also happen if gas oxygen was in the electrolyte. In this series of study, the EY molecules on the first film were dissolved in aqueous KOH successfully, so the reason of inaccessibility of the dye with aqueous KOH was not because of gas oxygen in the electrolyte.)
The significant change of the concentration even during the deposition will influence to the film growth naturally. The dye concentration in the electrolyte should be a constant to control the film growth.

Surprisingly, the EY consumption at the counter electrode during the second deposition was found in a similar range as during the first deposition. The reaction at the counter electrode is assumed as the dissolution of Zn electrode itself. So, then it is unclear why EY adsorbed to the counter electrode during the deposition. Since the dye should not have a relation with the reaction at the counter electrode, the dye adsorption can be caused by a chemical adsorption. So, in such case, the dye consumption at a counter electrode is strongly related with the size of the electrode. In this study, a rather big Zn rod was used. But it will be better to use small Zn counter electrode to keep the EY concentration and to save EY molecules in the electrolyte. And also it is important to use the same size of the counter electrode to keep the reproducibility of the film preparation.

5.1.1.3. Morphology and action spectra of EY / ZnO films

The SEM images and the results of action spectra are shown in this section to see the difference of the properties of the films prepared from the same electrolyte in series. Since the concentration of the deposition bath changed significantly after a deposition, such difference of the dye concentration can be expected to appear as a different morphology and a photoelectrochemical efficiency.

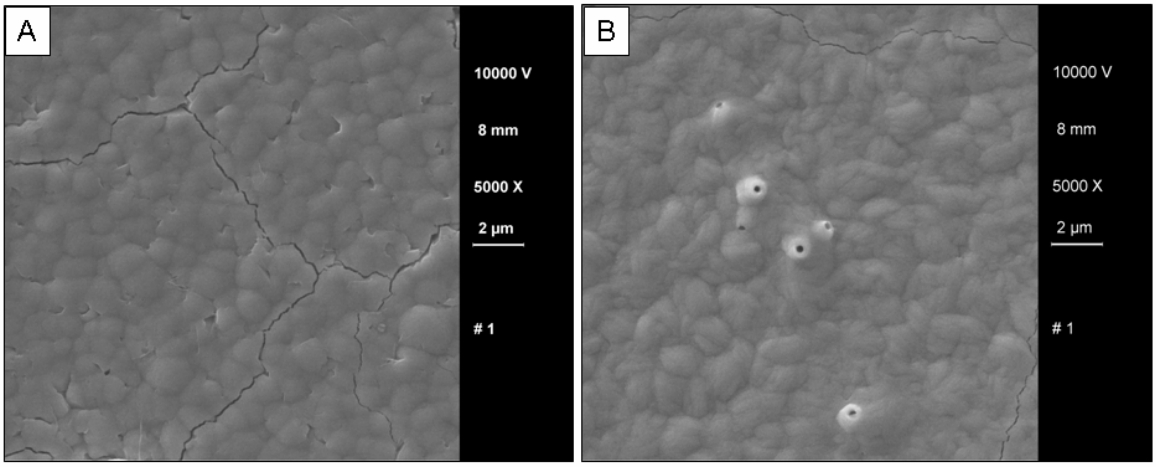

Fig. 5.7; SEM images of one-step electrochemical deposited EY / ZnO hybrid thin films prepared from the same solution; (A) first film and (B) second film.

The SEM images of the EY / ZnO films prepared from the same solution in series are shown in Fig. 5.7. A rather rugged surface was observed from both films. The particles were not clearly distinguishable and the films seemed to construct many grains. And moreover the cracks were observed in places. It can be expected that distinguishable particles were caused by the existence of the EY molecules on the film and then the shape of the particles will be clear after removing the dye from their surface as shown later in Fig. 5.9. The surface area of such films can be assumed in the range of 1 to 10 cm^2 / cm^2 since the pores are filled by the excess amount of dyes adsorbed on the film.[171] The cracks might be created in the process to dry following that the film was taken out from the electrolyte after the deposition.

The clear difference was not observed between those two films; Fig. 5.7 (A) and (B). However there are some points which are different slightly; for second film (Fig. 5.7 (B)) the size of the grains are slightly bigger than the other, some holes are also observed, and the extent of the cracks becomes smaller. The slightly bigger size of grains is assumed to be caused by the less concentration of EY in the deposition bath. The influence of the less concentration will appear as less porosity of the film.[60] The different size of particles and less porosity of the film might lead to the strong binding among the particles and to the less cracks in the film. The difference in the SEM images was seen slightly, but not clearly.

The influence of such different films to their photoelectrochemical properties are the more important issue to see the validity of repeating the deposition in the same electrolyte. To see the difference of those films in photoelectrochemical properties, the photocurrent action spectra was measured for those films and the spectra are shown in Fig. 5.8.

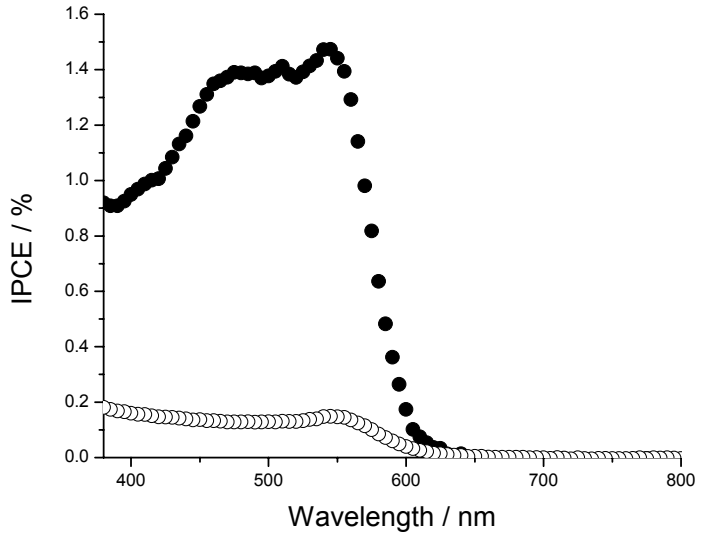

Fig. 5.8; Action spectra of one-step electrochemical deposited EY / ZnO hybrid thin films prepared from the same solution; first film (●) and second film (○).

Sensitization photocurrents were confirmed from the action spectra. The IPCE values of 1.5 and 0.15 % at 540 nm were detected from the films prepared at first and at second respectively. The relatively low magnitude of IPCE is caused by the small surface area due to the excess amount of adsorbed dye molecules which fill the pores in the ZnO matrix[69, 171] and the low injection efficiency from the LUMO of the dye to the conduction band of ZnO.[82] The difference of the IPCE magnitude in the films studied here might be caused by the difference structure of the film. In both films, it has been studied that the films had the excess amounts of dye on the film. However, it has been also found that the film prepared in the presence of 40 (or 50) μM of EY in the deposition bath had a porous structure. And another film had a relatively less porous structure. This difference appears as the result of different efficiency in the action spectrum.

The films prepared in the same electrolyte in series showed the different character, especially in action spectrum. Taking the continuous produce of the electrode account, it is important to establish the almost identical condition for the second condition. As mentioned above (section 5.1.1.2), it will be important to depress the consumption of the dye at the Zn rod counter electrode.

5.1.1.4. Summary

The preparation process is the most important to obtain highly porous films, effective photoelectrodes for the application to solar cells. However, the electrochemical deposition method is so sensitive that the reproducibility of the film preparation appears as a problem. It was found that the surface condition of the substrate, the concentration of the

oxygen in the deposition bath and the state of the oxygen in the deposition bath give a significant influence to the film growth. Careful attention must be paid to establish identical conditions for those factors in the film fabrication process.

On the other hand, the influence of the dye concentration in the deposition bath to the film morphology is not so obvious comparing with other factors mentioned above. Continuous preparation of films without abandoning the electrolyte is attractive when considering the smaller influence to the environment and saved costs in the sense to save the consumption of the materials.
The repeating of the deposition in the same electrolyte is possible. However there is a problem, the decrease of dye concentration; it is changing significantly because of the counter electrode, and such decrease leads to a poor porosity of the film. And such a poor porosity reflects to the decreased efficiency in the photoelectrochemical measurements. This problem would perhaps already be solved by using small Zn counter electrode.

The films prepared in the way described here are developed to the “re-adsorption” method, since one-step electrodeposited EY / ZnO thin films have a high porosity under the dye layer. Sensitizers are “re-adsorbed” on such porous films and its photoelectrochemical properties are studied in the following sections.

5.1.2. Preparation and characterization of re-ad EY / ZnO (EY as SDA) films

The preparation and the characterization of re-ad EY / ZnO (EY as SDA) films have been carried out in this section. Moreover, the validity and the reason of the enhancement of the photoelectrochemical properties by introducing the re-adsorption method were considered. The difference between one-step electrodeposited EY / ZnO films and re-ad EY / ZnO (EY as SDA) films were studied by measuring absorption spectrum, BET, photocurrent action spectrum of the films. The films are electrodeposited at -1.0 V vs. SCE for 20 minutes. The detail process of the preparation is written in the experimental section (section 3.1).

5.1.2.1. Structure and morphology

The relatively poor photoelectrochemical efficiency of one-step electrodeposited dye / ZnO is caused by the excess amount of dye molecules in porous ZnO, which leads to a small surface area caused by the dyes filling the pores in the film.[171] By removing such dyes from the surface, the surface are of ZnO are increased significantly.[69] The change of the morphology can be observed from the SEM images (Fig. 5.9) taken before and after the KOH treatment to extract the dyes from the surface of the film.

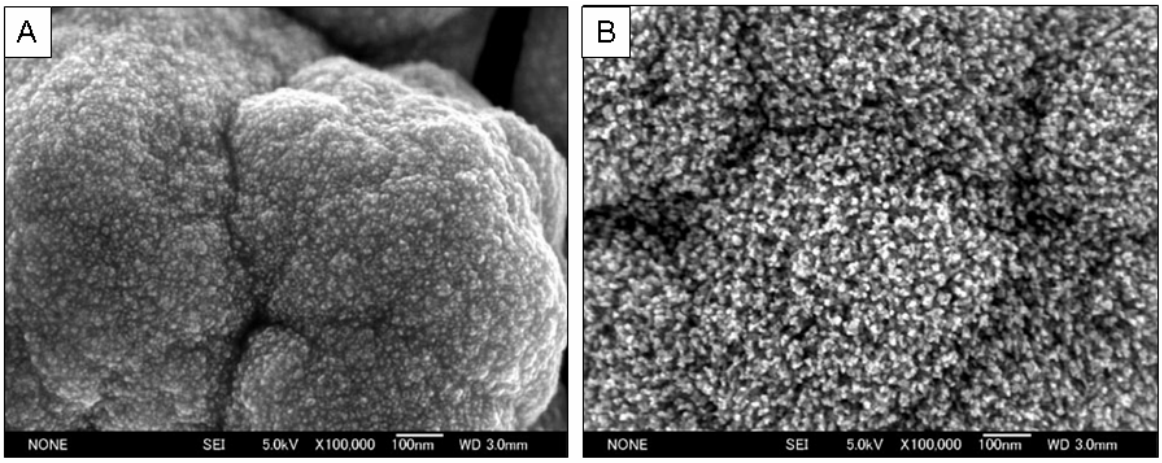

Fig. 5.9; SEM images of one-step electrodeposited EY / ZnO hybrid thin film (A) and ZnO film (B) after extracting EY from ZnO surface in aqueous KOH. The data was provided by Prof. T. Yoshida, Gifu University.

The structure of one-step electrodeposited EY / ZnO hybrid thin films (prepared in Gifu University) is shown in Fig. 5.9(A). Round and fine particles were observed. A high porosity of the film can be expected from the image. The diameter of the particles is approximately in the range of some nanometres to ten nanometres. This is contrast to the hexagonal shape obtained in ZnO deposited without SDA (Fig. 2.4).
From Fig. 5.9(B), an even finer morphology was seen in the film which was dipped into the

aqueous KOH (pH: 10.5). It could be seen from a cross section image of the film (shown in Fig. 5.40 (A), (B), (C)) that those particles had morphology like a rod and the rods were standing independently without an intimate contact to other rods. This is one of the favorable features of the electrochemical deposition method since the electrical contact of ZnO from the bottom (substrate) to the top of the rod (electrolyte) is provided and this is an ideal morphology for the application to dye-sensitized solar cells due to the large surface area. It was found by BET measurements that the surface area of the films was increased at least 150 times (average : 400 cm^2 / cm^2, max : 700 cm^2 / cm^2, up to now[173]) after KOH treatment.[171] The surface area of the film is increased by exposing the pores by extracting the SDA molecules from the surface. The filled pores could be observed in Fig. 5.9(A).

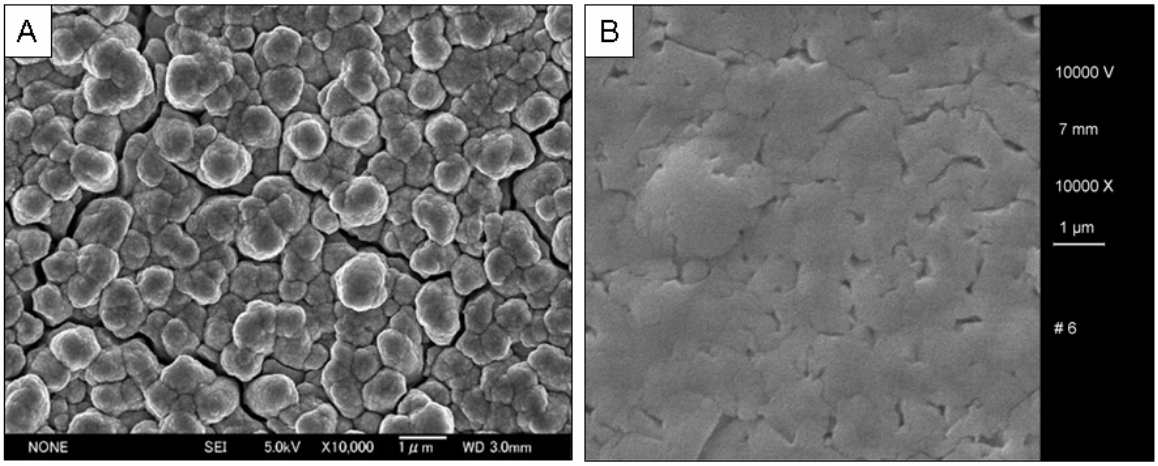

Fig. 5.10; SEM images of one-step electrodeposited EY / ZnO hybrid films prepared in Gifu (A) and in Giessen (B). Image (A) is provided from Gifu University.

As a reference, the SEM images of EY / ZnO hybrid thin films prepared in Gifu (Fig. 5.10 (A)) and prepared in Giessen (Fig. 5.10 (B)) are shown in the same resolution. Rather distinguishable grains are observed from the film prepared in Gifu. On the other hand, the grains are not clear in the film prepared in Giessen. As it was shown above, the film prepared in Gifu has a fine structure constructed from nano-rods in each grain. Although the film has not observed at the high resolution of x 100000, it can be assumed that the film prepared in Giessen has also been a fine structure in each grain since the extraction of the SDA was possible and an increased surface area was obtained.

The reason of the different morphology is strongly related with the matter of reproducibility. The following factors might be different; the water, the substrate, the chemicals, the concentration of solute, the oxygen concentration, the net potential applied to the working electrode, and the change of the dye concentration during the deposition. It can be assumed that the difference of the water is negligible. The substrate, the chemicals and the concentration of the solute in the electrolyte must be adjusted to be identical. Using the chemical from the same provider will be the best solution for this. The fine tuning of the concentration is, of course, important since it was found by Zhang et al. that

the number ratio of the ions which reach the SnO_2 substrate is an important factor for the film creation.[174] The change of the oxygen and dye concentration should be considered. Keeping a high concentration of oxygen and avoiding gas bubbles in the bath are required. The change of the dye concentration during the deposition due to the consumption (see section 5.1.1.2) should be minimized. A simple solution for this problem is the use of an increased electrolyte volume. When the total amount of the ions in the electrolyte is huge, the consumption of the ions at the electrode will become relatively small. An optimized setup would separate the counter electrode by a semipermeable membrane through which the SDA can not pass. The net potential applied to the working electrode is related to the preparation of the electrode with the substrate holder. The tight contact between the substrate and the holder must be established as it was mentioned above.
Those things indicate the high sensitivity of the electrochemical deposition method. It leads to further possibilities for more unique characters and properties of electrodeposited films.

5.1.2.2. Absorption spectrum

EY was adsorbed (re-adsorbed) on the surface of the porous ZnO electrodeposited in the presence of EY as SDA in the deposition bath and following the extraction of EY. After the re-adsorption of EY, a red film was obtained again. Absorption spectrum of such re-ad EY / ZnO was measured and compared with one-step electrodeposited EY / ZnO. The spectra are shown in Fig. 5.11.

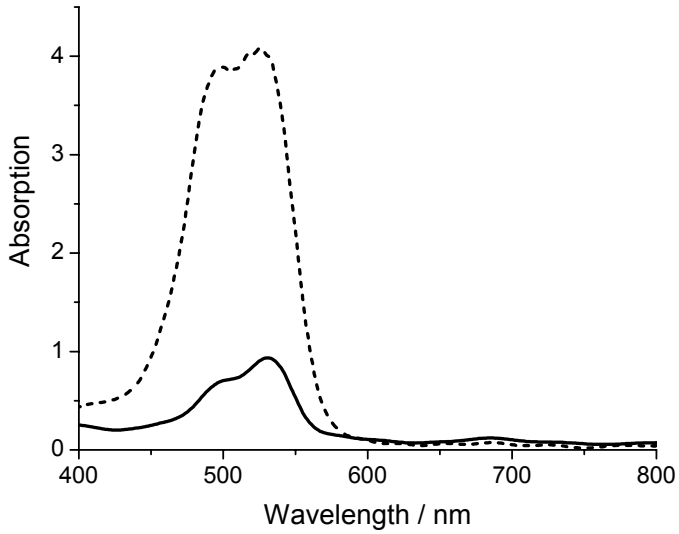

Fig. 5.11; Absorption spectra of one-step electrodeposited EY / ZnO (dashed line) and re-ad EY / ZnO (EY as SDA) (solid line)

Clearly different absorbance is observed between one-step electrodeposited EY / ZnO film

(dashed line in Fig. 5.11.) and re-ad EY / ZnO (solid line in Fig. 5.11.). The amount of dye loaded was measured and it was 1.07×10^{-7} and 1.24×10^{-8} mol cm^{-2} for the one-step EY / ZnO and the re-ad EY / ZnO respectively. This supports the results concluded before that an excess amount of EY molecules is on the surface of one-step EY / ZnO and it can be expected that the pores in the film were filled by this excess amount of EY molecules. For re-adsorbed films, it can be assumed that EY molecules are mostly adsorbed in a monolayer.[6 9] Such a expectation was also confirmed by BET measurements. While one-step EY / ZnO films have approximately 1 or 2 cm^2 / cm^2 of surface area, re-ad EY / ZnO films have 127 cm^2 / cm^2 which is almost the same value measured for ZnO films after extracting the SDA.[1 7 1]

5.1.2.3. Photoelectrochemical efficiency (Action spectrum)

A photocurrent action spectrum of re-ad EY / ZnO was measured to study its photoelectrochemical efficiency and compared with one-step EY / ZnO. The spectra are shown in Fig. 5.12.

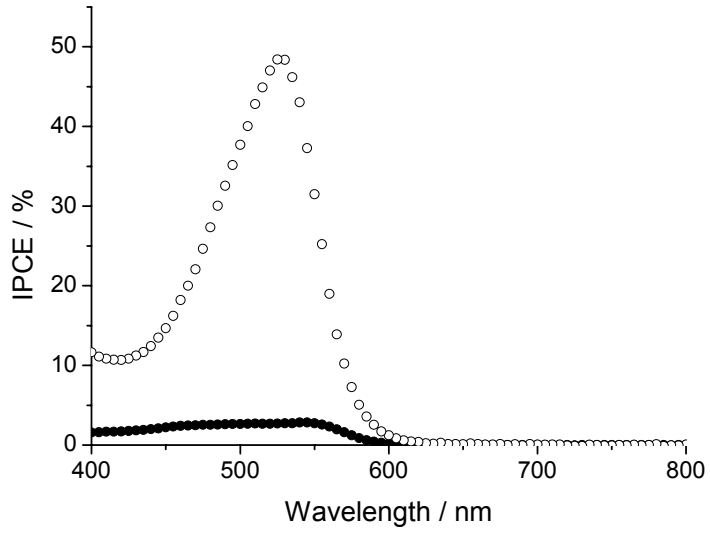

Fig. 5.12; Photocurrent action spectra of one-step electrodeposited EY / ZnO (●) and re-ad EY / ZnO (EY as SDA) (○) measured at -0.2 V vs. Ag/Ag^+ in the mixed solution of ethylene carbonate and acetonitrile (4:1 in vol.) containing 0.5 M TBAI and 0.05 M I_2. The electrodes were illuminated from the substrate side.

Much higher IPCE value of 48 % at 525 nm was detected from re-ad EY / ZnO, while the one from one-step EY / ZnO film is 2.8 %. The advantage of the re-adsorption method is clearly indicated from this result. And it is also seen that the key factor to obtain effective electrodes for dye sensitized solar cells is the porosity of the film. Comparing with one-step films, the re-ad films have a bigger surface area though the amount of dye loaded is

smaller. An attention for the further improvement should be paid for increasing the surface area of the electrodes.

Although much improved, 48 % of IPCE is not sufficient for technical applications. Since IPCE consists of the product of the light harvesting efficiency, the injection efficiency and the collection efficiency, at least one of them is reducing the efficiency of the electrode. Regarding to the light harvesting efficiency, it should be noted that approximately 10 % of the incident photos are missing since the light are reflect at the glass substrate. Assuming an identical extinction coefficient of the sensitizers in the film with the one in solution, the light harvesting efficiency can be estimated from the sensitizer content in the films. Such calculation has been carried out for the re-ad film and the light harvesting efficiency was estimated as 92.7 %. Take the reflection into account, about 83.4 % of incident photons are expected to be absorbed at the film. It indicates that other about 45 % of IPCE is missing by other factors, either by the injection efficiency or the collection efficiency. It was found by measurements using modulated light intensity (details in section 5.3) that the films studied here had high electron collection efficiency confirmed by the results of longer diffusion lengths than the film thickness, and the injection efficiency was in the range of 10 to 60 %. It can be expected that the injection efficiency depends on the condition of the dye on the film; whether the dye is attaching to ZnO or not, and how strong the dye attach to ZnO. And also this low injection efficiency indicates that the monomer adsorption of the dye molecules might not be achieved perfectly.

For a reference, other sensitizers were also re-adsorbed to ZnO (EY as SDA) and their photocurrent action spectra were measured.
5, 10, 15, 20-Tetrakis-(4-carboxyphenyl)-porphyrin-Pd (II) (hereafter TCTPPPd) and 5, 10, 15, 20-Tetrakis-(4-carboxyphenyl)-porphyrin-Pt (II) (hereafter TCTPPPt) were used as sensitizer here. The constitutional formulas of those sensitizers are show in Fig. 5.13. The re-adsorption of TSTPPZn, TSPcZn and both of them on ZnO and the properties of such electrodes will be discussed in detail in the next section, Coumarin 343 as sensitizer to such films is discussed in section 5.3.2.

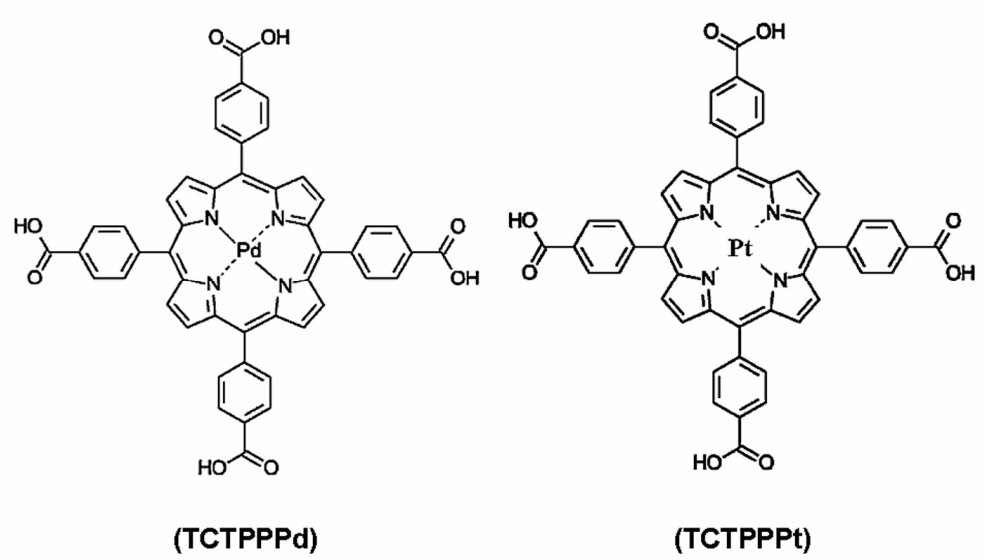

Fig. 5.13; Constitutional formula of 5,10,15,20-Tetrakis-(4-carboxyphenyl)-porphyrin-Pd-(II) (TCTPPPd) and (B) 5,10,15,20-Tetrakis-(4-carboxyphenyl)-porphyrin-Pt(II) (TCTPPPt)

Porphyrins are one of the preferable sensitizers because of their high absorption coefficient and good photoelectrochemical properties.[103] The carboxylic acid will work to anchor the sensitizer on the surface of ZnO.

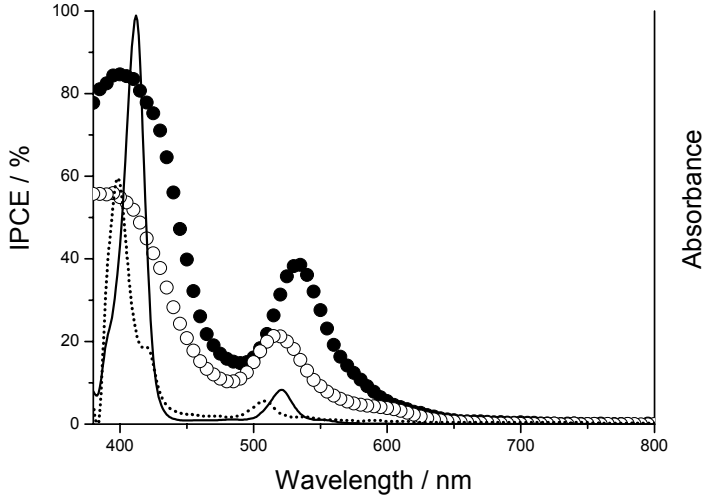

Fig. 5.14; Photocurrent action spectra measured for re-ad TCTPPPd / ZnO (EY as SDA) film (●, left axis) and re-ad TCTPPPt / ZnO (EY as SDA) film (○, left axis). And absorption spectra of the dye solution are also shown; TPP-Pc (solid line, right axis) and TCTPPPt (dashed line, right axis)

The photocurrent action spectra measured for re-ad TCTPPPd / ZnO (EY as SDA) film and re-ad TCTPPPt / ZnO (EY as SDA) film are shown in Fig. 5.14. From re-ad TCTPPPd / ZnO film, the IPCE values of 85 % at 400 nm and 35 % at 535 nm were found. And from re-ad TCTPPPt / ZnO film, 56 % at 395 nm and 21 % at 520 nm are found. Taking the reflection and the scattering of the incident light into account, the highest

IPCE is reached in re-ad TCTPPPd / ZnO film. These examples show that a variety of sensitizers can be “re-adsorbed” to ZnO prepared with EY as SDA. A combination of sensitizers adsorbed in parallel may then lead to an optimized panchromatic sensitization.

5.1.2.4. Summary

Re-ad EY / ZnO (EY as SDA) films were prepared by introducing the re-adsorption method and their properties were investigated. The photoelectrochemical efficiency of the electrodes has been enhanced significantly. The IPCE (incident photon to current conversion efficiency) was increased from 2.8 % (one-step electrodeposited film) to 48 %. The amount of dye loaded in the films, however, was decreased about 10 times. It was found by BET measurements that the surface area of re-ad EY / ZnO (EY as SDA) films was increased more than 150 times. The amount of dye molecules adsorbed to the film during the deposition was too high and those dyes clogged the fine pores in the film. Following the extraction of the dye from the surface of the film, it was found that the ZnO prepared in the presence of EY had a porous structure as seen from SEM images. Re-adsorbing a sensitizer on such porous ZnO as a monomer, an enhancement of the photocurrent has been achieved. From these results, it was seen how important it is for dye- sensitized solar cells to achieve monolayer adsorption of the sensitizer on the surface and to establish a good contact between the sensitizer and the redox electrolyte.

5.1.3. Characterization of re-ad (TSPcZn and/or TSTPPZn) / ZnO (EY as SDA) films

The enhancement of the photoelectrochemical efficiencies has been achieved by using re-adsorption method. One of the benefits in this method is that any sensitizer can be adsorbed on the porous ZnO following the extraction of EY used as SDA.

In this section, TSPcZn was used as sensitizer to improve the photoelectrochemical efficiency in the red part of the visible light and this is one of the main goals in this study. The understanding of the electron transport kinetics in such re-ad films and the optimization of their photoelectrochemical efficiencies have been carried out in this section.

As things turned out, two kinds of ZnO film were prepared in the presence of EY as SDA although those films were prepared in identical conditions. One was porous ZnO film, EY could be removed completely from the film. Another was non-porous ZnO film, some EY molecules were enclosed in ZnO matrix and those could not be removed perfectly. Such factors are strongly related with surface area of the film and hence their photoelectrochemical properties.

TSPcZn and/or TSTPPZn were adsorbed on porous ZnO films and their photoelectrochemical properties of those re-ad films were studied in section 5.1.3.1. And moreover, the effect of a panchromatic sensitization to their photoelectrochemical efficiencies was studied.

The EY molecules enclosed in ZnO matrix showed the different electron transport kinetics compared to the sensitizers which was adsorbed on non-porous ZnO films. The origin of such results and their photoelectrochemical properties were studied in section 5.1.3.2.

In section 5.1.3.3, the optimization of the photoelectrochemical efficiency for re-ad TSPcZn / ZnO films was carried out. To understand the properties further, the optimized film was studied by measuring photocurrent action spectrum in different condition such as different applied potential to the electrode and different electrolyte. The complete sandwich cell was fabricated and the photoelectrochemical efficiency was studied.

5.1.3.1. Characterization of porous re-ad (TSPcZn and/or TSTPPZn) / ZnO (EY as SDA) films

TSPcZn and TSTPPZn were adsorbed on ZnO films prepared in the presence of EY as SDA. It can be expected that the re-adsorption method overcomes the problem of poor accessibility of the sensitizers with the redox electrolyte in one-step films.[6 9] Utilizing the red part of the visible light by using TSPcZn as sensitizer and the panchromatic sensitization by adsorbing TSPcZn and TSTPPZn simultaneously were aimed at this section. The photoelectrochemical properties were studied in detail by photocurrent action spectra and photocurrent transient measurements. The results were also compared with

one-step TSPcZn / ZnO, TSTPPZn / ZnO and (TSPcZn+TSTPPZn) / ZnO films.

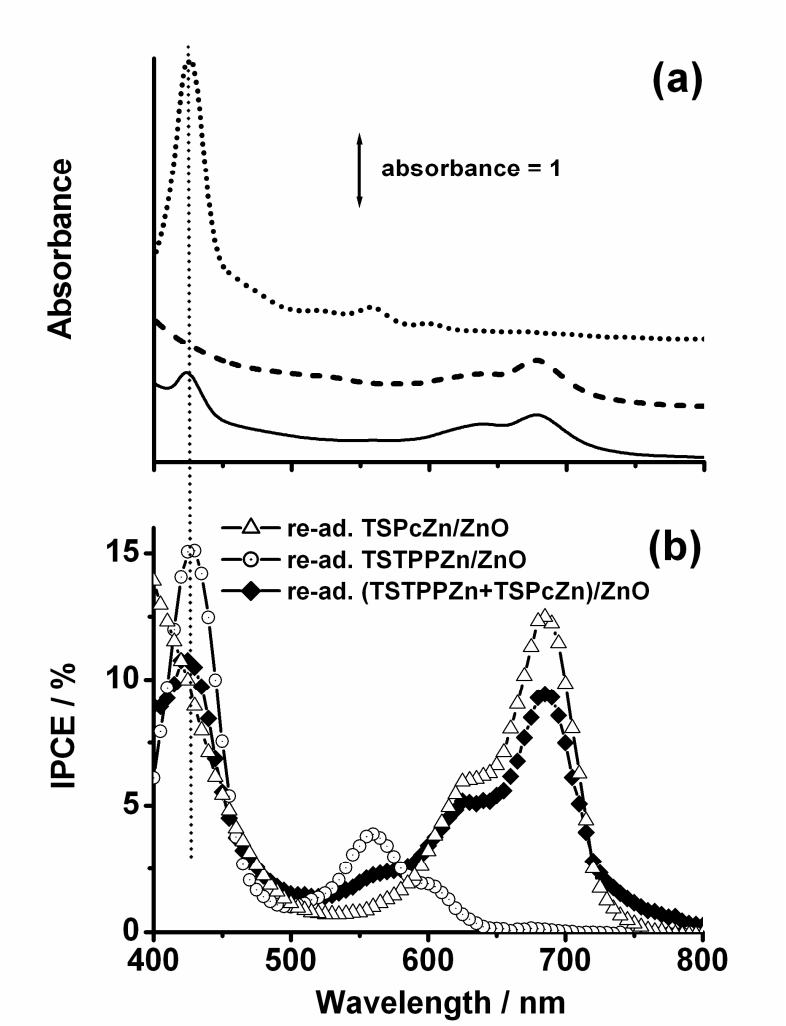

Fig. 5.15; Absorption spectrum of re-ad TSTPPZn / ZnO (·····), re-ad TSPcZn / ZnO (-------) and re-ad (TSTPPZn + TSPcZn) / ZnO (——) prepared by the re-adsorption method (a) and the photocurrent action spectra (b) of the same films as indicated in the figure.

The obtained coloured films showed the absorption in the specific wavelengths which correspond to the absorption band of the sensitizers in the solution (Fig. 5.15 (a)). Similar results were observed in one-step films in Fig. 4.2 (a). The information about dye content, film thickness and dye concentration are shown in Table 4. Those values are in similar ranges compared to the one-step electrodeposited films. (see Table 2) For one-step (TSPcZn+TSTPPZn) / ZnO films, the dye concentration was clearly low for TSPcZn compared to the one of TSTPPZn. On the other hand, for the re-ad films with both sensitizers present TSTPPZn was found to adsorb at clearly increased yield relative to TSTPPZn. Such films generally showed a significantly increased surface area. [166,171] Consequently, also the photocurrents for these electrodes of re-ad TSPcZn / ZnO, re-ad TSTPPZn / ZnO and re-ad (TSPcZn+TSTPPZn) / ZnO were significantly higher under otherwise identical conditions (Fig. 5.15 (b)). External efficiencies (IPCE) of up to

15 % were reached, a range significantly closer to technical applicability than those obtained by the one-step films. From re-ad TSPcZn / ZnO, 12.5 % of IPCE at 680 nm was obtained. It was 0.06 % in the case of one-step TSPcZn / ZnO. 15.1 % was obtained at 425 nm from re-ad TSTPPZn / ZnO instead of 0.14 % from the one-step film. 9.4 % and 10.8 % at 680 nm and 425 nm from re-ad (TSPcZn+TSTPPZn) / ZnO also were clearly improved compared with 0.02 % and 0.08 % from one-step (TSPcZn+TSTPPZn) / ZnO. The absorption bands of the sensitizers were reproduced in the photocurrent spectra. In particular, no optical filtering effects were observed, speaking for highly accessible pores in these materials. Also, it was shown in these experiments that more than one dye can be adsorbed also in the re-adsorption method and that each dye contributes to the photocurrent in its specific wavelength region. As it was observed in one-step films, the TSTPPZn Q-band showed higher quantum efficiency than the Soret band but the effect is by far not as significant as described above for the films prepared in one-step where even a shift of the IPCE maximum relative to the absorbance maximum was measured. Although differences in the efficiency of light absorbed either in the Soret- or Q-band of porphyrin sensitizers in porous electrodes were observed earlier,[29,101] a clear explanation is still missing. In general illumination through the back electrode was used. When conduction in the porous oxide was limiting, the Soret band was found to be more efficient because of a reaction zone closer to the back contact.[29] Also, a lower efficiency of charge injection of the excited state from Soret excitation was assumed.[101,107] On the other hand, an excited state lifetime in the 100 fs – 10 ps time range was measured.[175] For porphyrins on TiO_2 recombination half life of 4 ms was reported.[176] In our experiments, we found an increased quantum efficiency for the Q- relative to the Soret band. Because of the fast reported injection times and because both Q- and Soret excitation should lead to an electron in the same LUMO orbital,[168,169] the recombination was appeared in time-resolved photocurrent caused by either a slower regeneration reaction with the electrolyte or faster recombination reaction with electrons from the ZnO conduction band. The hole of the excited state following Soret excitation is left in a lower energy level[168,169] when compared to Q-band excitation and hence a faster recombination reaction with electrons from the ZnO conduction band appears most reasonable. Quite independent photoelectrochemical activity leading even to a different direction of the observed photocurrent was observed following absorption either in the Q- or Soret-band.[177] Different quantum efficiencies of the Soret vs. Q-band absorption in photoelectrochemical reactions had also been observed in semiconducting films of differently substituted porphyrins with almost identical absorbance in the Q- and Soret region, cases for which a different penetration depth would not apply.[177]

In re-ad (TSPcZn+TSTPPZn) / ZnO, we could observe clear panchromatic sensitization indicating that both sensitizers were acting simultaneously (Fig. 5.15), as it was also observed in one-step films. The contribution of the TSTPPZn sensitizer was rather little. This was caused by small dye content in the films as it can be seen in Fig. 5.15 and Table 4. An almost identical dye concentration was reached for TSPcZn and TSTPPZn from

parallel adsorption of the two sensitizers. In the re-ad films with both sensitizers present, the amount and concentration of adsorbed TSTPPZn were found smaller than in re-ad TSTPPZn / ZnO, whereas the amount and concentration of TSPcZn were quite constant. It is in strong contrast to the observations during one-step depositions (Table 3). An active role of the dye as structure directing agent in the redox chemistry in the electrodeposition step was thereby confirmed as opposed to the pure chemical adsorption steps involving quite identical sulfonic acid anchoring groups. Excellent values of the normalized photocurrent (Table 4) were reached corresponding to the attractive IPCE value (Fig. 5.15 (b)). This goal was reached for re-ad electrodes with the individual sensitizers, and at quite constant level also for the films with both sensitizers present. TSTPPZn even showed a slightly increased normalized photocurrent in the film with both sensitizers present whereas the normalized photocurrent of TSPcZn was decreased. This is directly inversely correlated with the respective dye concentration in the films (Table 4). The lower TSTPPZn concentration in the film with both sensitizers led to higher quantum efficiency and hence increased normalized photocurrent, whereas the higher concentration of TSPcZn led to decreased values of quantum efficiency and normalized photocurrent. Low dye concentrations favoured efficient sensitization reactions whereas high dye concentrations led to a smaller absorption probability and increased probability of dye-dye interactions and hence radiationless decay reactions of the excited states.

Table 4; Dye content, average film thickness, and dye concentration of the investigated films, and comparison of the observed photocurrents i_{ph} at an incident photon flux of 10^{16} s^{-1} cm^{-2} normalized for the given dye content to provide a rough measure of the sensitization efficiency. The values in parentheses are those from one-step films.

Electrode material	dye content / 10^{-9} mol cm^{-2}	film thickness / µm	dye concentration / 10^{-5} mol cm^{-3}	normalized i_{ph} (430 nm) / s^{-1}	normalized i_{ph} (560 nm) / s^{-1}	normalized i_{ph} (680 nm) / s^{-1}
re-ad TSPcZn / ZnO	2.38	3.0	0.79			0.8744309 (0.0007847)
re-ad TSTPPZn / ZnO	17.4	2.5	6.9	0.1453607 (0.0014248)	0.037274 (0.0005985)	
re-ad (TSPcZn+TSTPPZn)/ZnO	4.30 TSPcZn 5.43 TSTPPZn	3.0	1.4 1.8	0.3290574 (0.0002951)	0.068625 (0.0002604)	0.3758654 (0.0072362)

The higher photocurrents observed for the re-ad films were also reflected in significantly different electrode kinetics. No overshoots were detected in photocurrent transient measurements at the re-ad electrodes, which would be indicative of recombination reactions of the charge carriers. This is shown in Fig. 5.16 for electrodes of re-ad TSPcZn / ZnO and re-ad TSTPPZn / ZnO.

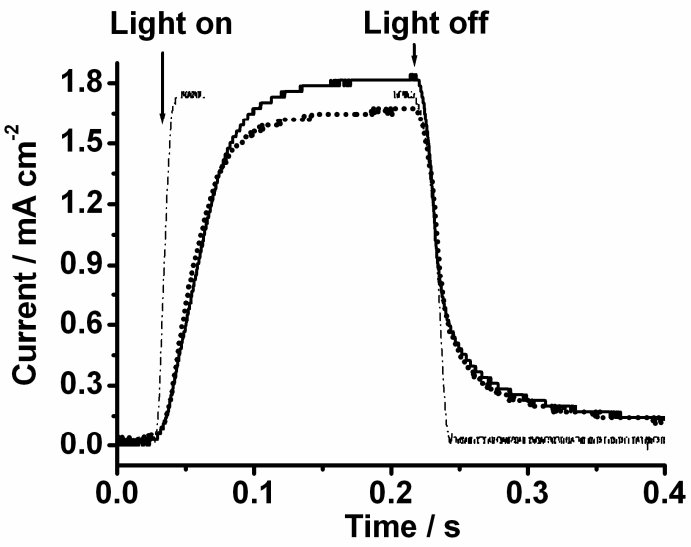

Fig. 5.16; Time-resolved photocurrent measured at re-ad TSPcZn / ZnO (·····) and re-ad TSTPPZn / ZnO (——) under illumination with white light. The opening and closing profile of the shutter measured by the response of a Si photodiode are also shown as thin broken lines, normalized to provide a good comparison to the observed photocurrents.

When opening the shutter, the photocurrent increased monotonously at a significantly slower rate than the shutter opening and also slower than for the one-step films in Fig. 4.3. Since larger photocurrents were obtained compared with one-step films and since no recombination was observed in these re-ad films, the conduction in the porous ZnO network could be analyzed in detail. It was reported earlier for nanoparticulate TiO_2 electrodes that electron trap levels are present in these materials, that they can be subsequently filled by injected electrons and that therefore the trapping probability was lower at higher electron concentration in the films.[156] A similar conclusion was also drawn from intensity- modulated experiments at re-ad ZnO electrodes.[160] We here present photocurrent transients in which this effect is directly observed in the delayed response of the photocurrent relative to the opening profile of the shutter for sensitized ZnO electrodes prepared by the re-adsorption method. (Fig. 5.16) Following closure of the shutter, the observed photocurrent again showed a corresponding delay, caused by continued detrapping of electrons and their collection at the back electrode even after the injection of electrons into ZnO had stopped. The photocurrent transients under white light illumination were found at very comparable level for re-ad TSPcZn / ZnO and re-ad TSTPPZn / ZnO.

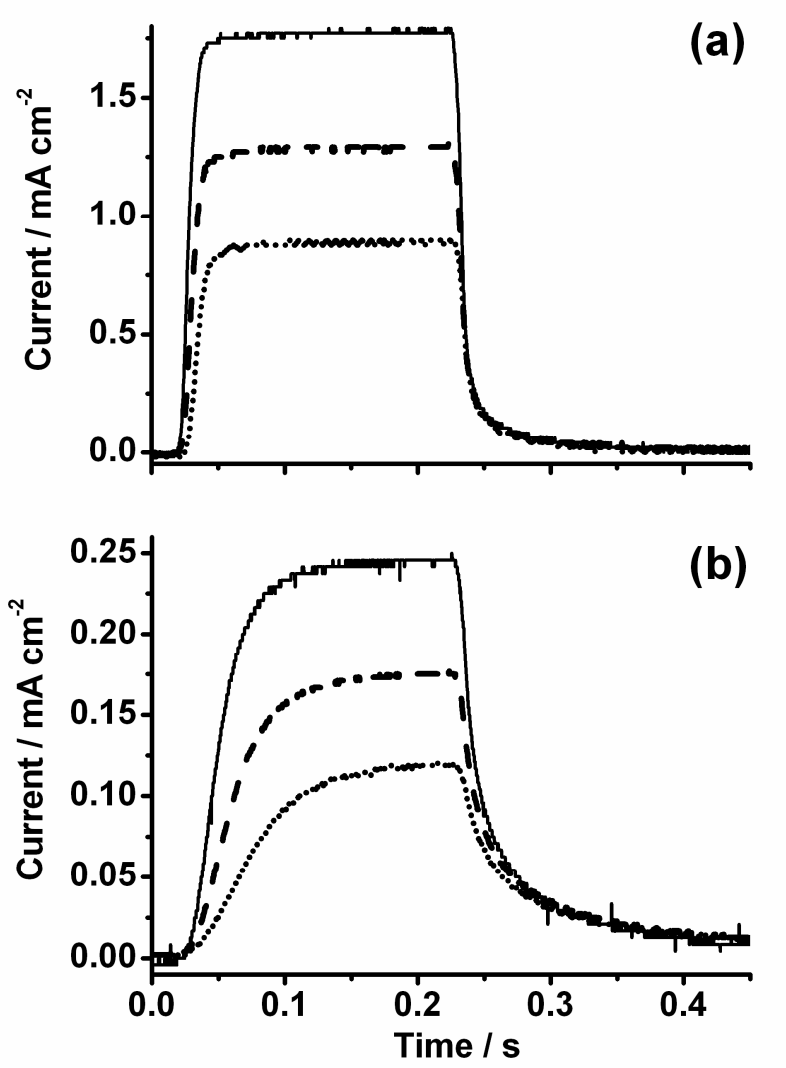

Fig. 5.17; Time-resolved photocurrent measured at re-ad (TSTPPZn + TSPcZn) / ZnO under different light intensities of 200 mW cm^{-2} (a) or 20 mW cm^{-2} (b) white light and in different wavelength ranges of 385-550 nm (·····), 525-900 nm (-------) or the full spectrum (——).

In the time- resolved photocurrent transient measurements at (TSPcZn+TSTPPZn) / ZnO of Fig. 5.17, fast increase and decrease of the photocurrents were observed in the range of shutter opening and closing times. This speaks for efficient sensitization and a considerably lower electron trap concentration in this film compared to those of Fig. 5.16. When the light intensity was decreased by 90 %, however, quite comparable characteristics were obtained in Fig. 5.17(b) as it was observed in Fig. 5.16. This is well in line with the understanding that a lower injection rate of electrons would lead a longer time to fill a given concentration of electron traps. For both light intensities, the contribution in the Q-band range was found clearly increased relative to that from the Soret- contribution when compared with one-step films (shown in Fig. 4.3 (b)), caused by a considerably higher contribution of TSPcZn in the re-ad films (Table 4).

As summary, TSPcZn and TSTPPZn were used as sensitizers in films prepared by the

re-adsorption method. Re-ad TSPcZn / ZnO, re-ad TSTPPZn / ZnO and re-ad (TSPcZn+TSTPPZn) / ZnO were prepared successfully and the absorption of the light by those films corresponded to the absorption of the dyes in solution. It was confirmed that those films work as photoelectrodes better than one-step films. The problems of the poor pore accessibility in one-step films could be overcome by use of the re-adsorption method. The efficiency could be increased more than 100 times comparing with the one-step films. Contrary to one-step films, the photocurrent increased slowly, which was explained by the filling of traps in ZnO. Whereas uptake of TSPcZn was hindered during the one-step electrodeposition when TSTPPZn was present as competitor, this was found for TSTPPZn during re-adsorption to ZnO. Although TSTPPZn adsorbed more efficiently than TSPcZn when individually present, its uptake was decreased in the presence of TSPcZn. The presently reported progress in the IPCE at ZnO sensitized by readily available metal complexes like TSPcZn and TSTPPZn is seen as an important step towards technically applicable electrodes, and the complex characteristics of sensitizer uptake and its correlation to photoelectrochemical characteristics are seen as tools for further optimization.

5.1.3.2. Characterization of non-porous re-ad TSPcZn / ZnO (EY as SDA) films

In the previous section, re-ad dye / ZnO films were prepared and their photoelectrochemical properties were discussed. The surface area of those films is approximately 400 cm^2 / cm^2 and such large surface area allows the monolayer adsorption of the sensitizer on ZnO and hence the high light harvesting efficiency of the film, leading to high photoelectrochemical performance. On the other hand, some of EY / ZnO films do not allow the extraction of the dye completely from their surface since some EY molecules are enclosed in ZnO particles. Nevertheless, even in such nonporous films, some EY molecules can be removed from their surface and it allows introducing re-adsorption method. Re-ad dye / ZnO (EY as SDA) films are also available for such nonporous films although the reddish color from EY can still be seen. In this section, TSPcZn was used as sensitizer for such films and their photoelectrochemical properties are discussed. The photoelectrochemical measurements were carried out in a three electrode setup. Pt wire and Ag/Ag^+ electrodes were used as counter electrode and reference electrode respectively. The electrolyte contains 0.5 M KI in the mixed solvent of ethylene carbonate and acetonitrile (4:1 in volume).

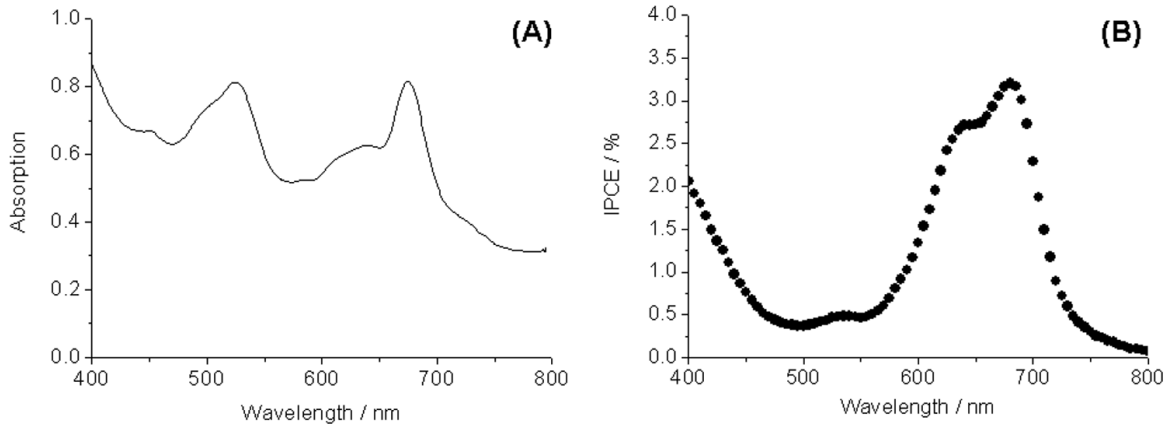

Fig. 5.18; Absorption spectrum (A) and action spectrum (B) of nonporous re-ad TSPcZn / ZnO (EY as SDA)

The absorption spectrum of the film and the action spectrum was measured for such a film and it is shown in Fig. 5.18. In the absorption spectrum (Fig. 5.18 A), the peaks were detected at 525 nm and 680 nm which were corresponding to the absorption from EY and TSPcZn respectively. Since this spectrum was measured after completing the re-adsorption process with TSPcZn, it indicates that some EY molecules were still in the film after the KOH treatment. Such enclosed states reflected clearly to the action spectrum. In action spectrum, the IPCE at 525 nm and 680 nm were 0.47 % and 3.20 % respectively. The photocurrent contribution from TSPcZn is higher than that from EY although the extent of the absorption is almost similar. These results indicate clearly an ideal condition for the effective electrodes that the sensitizer must be on the surface of the film and must have contact with the redox electrolyte.

It is interesting to note that some photocurrent is generated from such enclosed EY molecules. One of the reasons is that some of the EY might be still on the surface of ZnO. But it is hard to suppose after staying in KOH solution for 24 hours. To investigate more details about this photocurrent contribution from EY, time-resolved photocurrents were measured by LEDs.

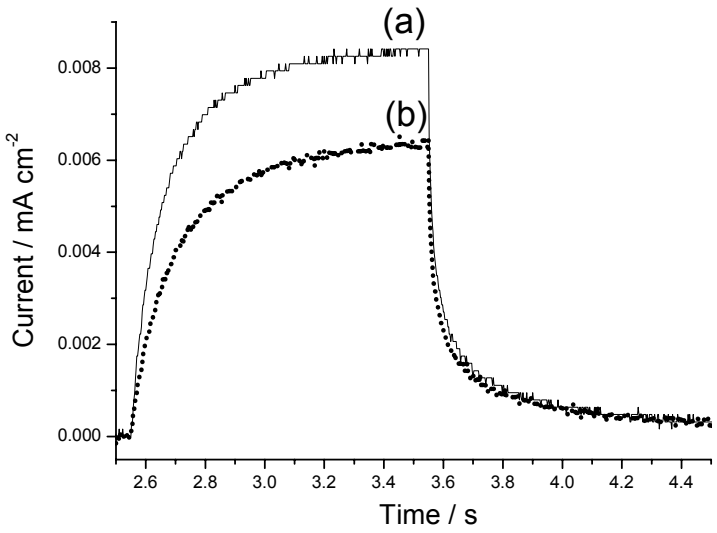

Fig. 5.19; Time-resolved photocurrent measured for a nonporous re-ad TSPcZn / ZnO (EY as SDA). White LED was used as light source and light is illuminated from the electrolyte side (solid line, (a)) or the substrate side (dashed line, (b)).

For the starting point of the investigation, time-resolved photocurrents were measured with white LED. (Fig. 5.19) Characteristic shapes of the photocurrent transients were obtained. The photocurrents detected by the illumination from the electrolyte side and the substrate side were 8.4 and 6.4 μA cm^{-2} respectively. A slow increase of the photocurrents was observed. It is a typical shape of time- resolved photocurrents in dye sensitized solar cells.[148] These slow increases can be interpreted by the existence of the trap states in ZnO matrices and the electron transport by diffusion, not a drift by an electric field.[147, 148, 151, 155]

A higher photocurrent by the illumination from the electrolyte side was observed. It can be expected that the photocurrent is higher when the electrode is illuminated from the substrate side if the sensitizers are near to the substrate and have a contact with the redox electrolyte. When the absorption and the excitation occur near to the substrate, the generated electrons are collected efficiently since the probability of the recombination is smaller due to the short path way compared to the case when the excitation occurs at the surface of the film. Take these considerations into account, the higher photocurrent by the illumination from the electrolyte side implies either that the sensitizers which are close to the substrate do not have a contact with the redox electrolyte, or some disturbance of the illumination like a filter before the active sensitizers, for example a strong scattering from FTO / ZnO side. Since EY molecules are enclosed in the films studied here, the detected photocurrents are the mixture of the photocurrents generated from both EY and TSPcZn. And it is clear due to the preparation process that the EY molecules are enclosed in the film and the TSPcZn molecules are on the surface of the ZnO. If the observed photocurrent was delivered mainly from the EY, it can be understood that the lower photocurrent by the illumination from the substrate side is due to the less contact between the sensitizers and

the redox electrolyte. However, it is still not clear how the EY molecules enclosed by ZnO can contribute to the photoelectrochemical activities. To investigate more details about these questions, the photocurrent transients were measured with a green LED and a red LED to excite either EY or TSPcZn only. In the measurements, an UV LED was also used to see the photocurrent from ZnO and its response for the illumination. The results of the measurements are shown in Fig. 5.20.

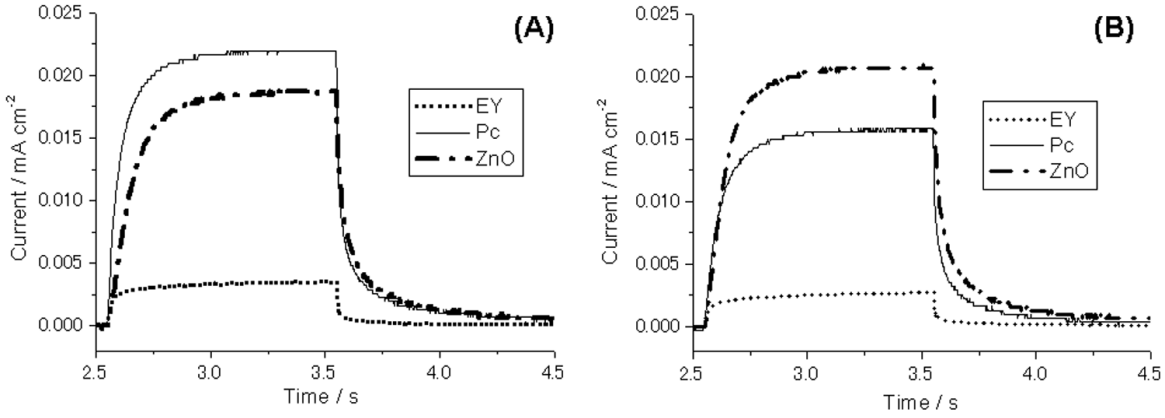

Fig. 5.20; Time-resolved photocurrents measured for a nonporous re-ad TSPcZn / ZnO (EY as SDA) film illuminated from (A) the electrolyte side and (B) the substrate side. For sensitizing EY, TSPcZn and ZnO, green LED, red LED and UV LED were used respectively.

When the UV LED was used for the excitation of ZnO, a higher photocurrent was detected when the light was illuminated from the substrate side. As described above, the short path way and the higher collection efficiency of the excited electrons appears as a higher photocurrent.

When the red LED was used to sensitize TSPcZn, a higher photocurrent of 23.8 mA cm^{-2} by the illumination from the electrolyte side was detected compared to that (15.9 mA cm^{-2}) by the illumination from the substrate side as it was also seen in the measurements using the white LED. Since the illumination of ZnO showed a good accessibility of the pores with the redox electrolyte also near the substrate and since TSPcZn could be adsorbed at the electrode surface, only a disturbance by the scattering from the substrate side remains as a valid explanation. It can therefore further be assumed that TSPcZn was adsorbed at higher concentration near the electrolyte when compare with the substrate side.

The relatively smaller photocurrents were detected by the sensitization of EY. Interestingly, the photocurrent is also higher under the illumination from the electrolyte side. It seems that a small portion of EY molecules are still on the surface of the ZnO and those dye molecules are much more effective than the enclosed one. When the light is illuminated from the electrolyte side, the active EY molecules can absorb the photons significantly and consequently the higher photocurrent can be detected.

In the plot, it can be found that the increasing rates of the photocurrent were different by sensitizers. In Fig. 5.20 (A), it can be seen that the current from TSPcZn rises faster than ZnO. Moreover, it can be seen that the current rise from EY is almost similar compared to

the others although the magnitude of the current is smaller. It is surprising since the slow rise of the photocurrent transients are commonly interpreted to occur by the time to fill the traps in the semiconductors.[156] And the time to fill the traps is dependent on the photocurrent density. If the photocurrent is lower, it can be expected that the longer time will be required. On the other hand, if the distance of the path way to the external circuit was shorter for the electrons generated by EY compared to the electrons generated by TSPcZn, the number of traps would be less. So there are at least two factors which may change the rate of the photocurrent increase.

Avoid the influence of different trapping probabilities simply because of a different electron concentration in ZnO, the magnitude of the photocurrents was adjusted to the similar range by adjusting the light intensity and the time to reach the steady-states photocurrent was compared. The results are shown in Fig. 5.21.

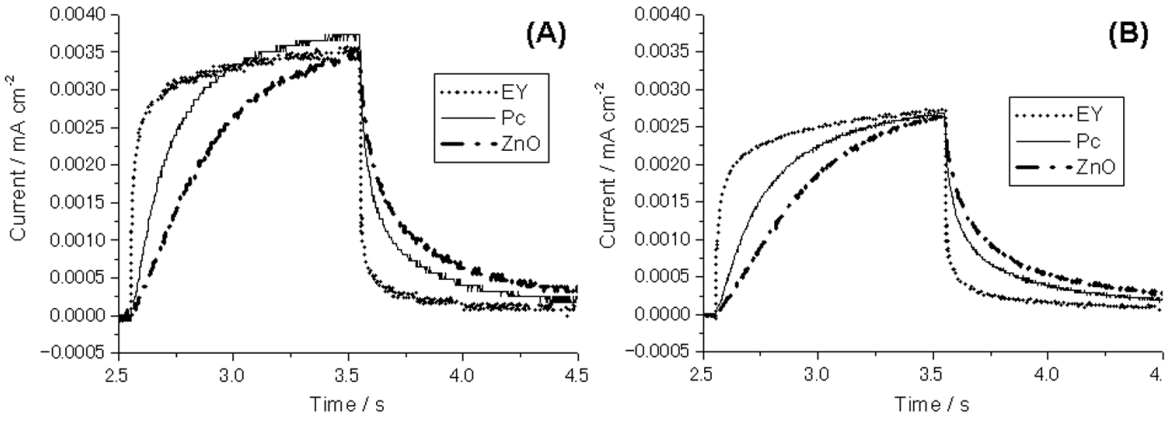

Fig. 5.21; Time-resolved photocurrents measured at the identical magnitude of photocurrent for a nonporous re-ad TSPcZn / ZnO (EY as SDA) film illuminated from (A) the electrolyte side and (B) the substrate side. The photocurrent is adjusted by tuning the light intensity. For sensitizing EY, TSPcZn and ZnO, green LED, red LED and UV LED were used respectively.

In the measurements shown in Fig. 5.21, the photocurrents were adjusted at the steady-states photocurrent. The measurements were carried out with the illumination time of 1 second to see clearly the different increasing rate of the photocurrent although it can be seen that more than 1 second of time is necessary to reach the steady states. It can be seen from both plots (Fig. 5.21 (A) and (B)) that the rise of the photocurrent delivered from EY is clearly faster than the others and the photocurrent from ZnO is slowest. When the photocurrent is observed by the illumination of the UV LED, the holes and the electrons are generated in ZnO by the band gap excitation. Then, the photocurrent transient responses are related with the kinetics of both the electron and the hole transfer. And moreover, the holes might create additional paths for the electrons to be transferred to the electrolyte. There are some factors to retard the transient response of the photocurrent from ZnO.

Comparing the transient response of EY and TSPcZn, it is clearly seen that the photocurrent from EY rise more rapidly than the photocurrent from TSPcZn. Similarly,

the faster decrease of the photocurrent delivered from EY is observed. Since the photocurrents are adjusted to similar magnitude, it can be assumed that the electron density in the conduction band of ZnO is also in the same range. Then, the fast increase of the photocurrent from EY indicates the shorter path way to the substrate. However, the fast increase of the photocurrent from EY is also observed in the illumination from the substrate side. Since these EY molecules were not possible to remove by dipping the film into aqueous KOH, it is clear that these dyes are enclosed in the film. However it is unclear how far from the substrate these EY molecule can be. Nevertheless, it can be expected that the positions of the electron generation are not far between EY on the illumination from electrolyte side (EY in Fig. 5.21(A)) and TSPcZn on the illumination from the substrate side (TSPcZn in Fig. 5.21(B)). Therefore, it is obvious that the photocurrent from EY is faster than TSPcZn. An interesting point in this measurement is that the light intensity is adjusted to control the electron density in the conduction band of ZnO. Much more photons are illuminated to EY compared to TSPcZn. It was reported by Oekermann et al. that the electron injection efficiency from the LUMO of EY to the conduction band of ZnO is low in one-step electrodeposited EY / ZnO hybrid films.[82] It is obscure how the EY molecules, which absorbed the photons and do not inject the electrons to ZnO, effect for the transient response of the photocurrent. As one of the suggestions, those dyes affect to decrease the trap density level in ZnO matrix and therefore it appears as the fast increase of the photocurrent. If it is true, such influence could be seen when both dyes are illuminated at the same time by using a white LED. The increasing rate of the photocurrents are compared by plotting on semilogarithmic plots and shown in Fig. 5.22.

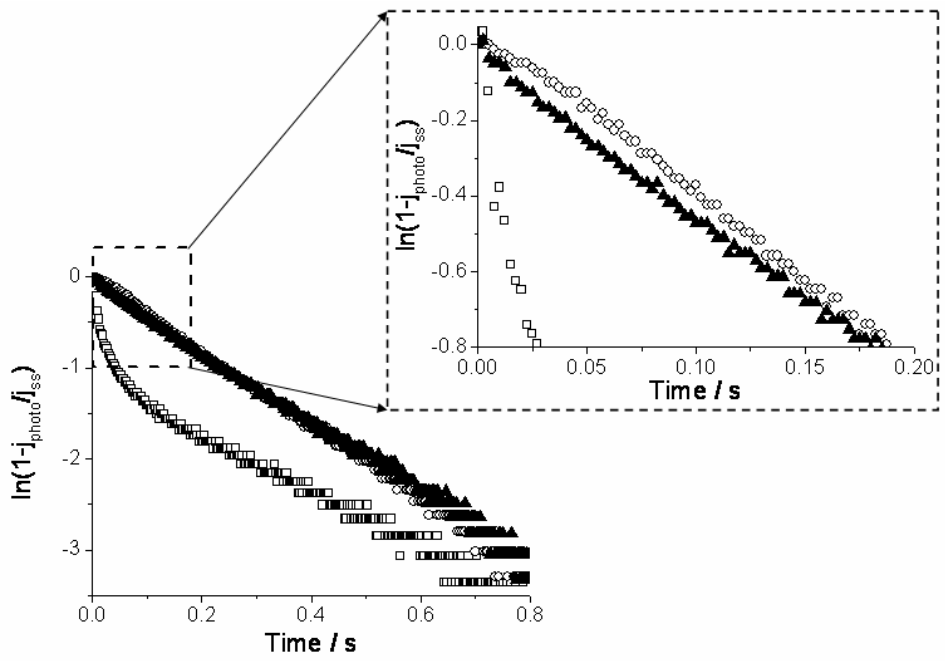

Fig. 5.22; Semilogarithmic plot of photocurrent transients under illumination from the red LED (sensitization of TSPcZn, ○), the green LED (sensitization of EY, □) and the white LED (sensitization of both dyes, ▲). Photocurrent is adjusted to be same magnitude.

The plots shown in Fig. 5.22 are developed from the photocurrent transient results measured by the illumination from the substrate side. In such plot, a simple exponential rise would yield a straight line from which the time constant of the transient could be determined.[148] Almost a straight line was obtained from the photocurrent transients from TSPcZn (○). It indicates that the photocurrent rise exponentially. On the other hand, a nonlinear line was obtained from the photocurrent transients from EY (□). A steep decline is seen in 100 ms and the decline becomes relatively easy as well as the other lines. Such different declines imply that the increasing rate of the photocurrent transients is characterized by a fast component and a slow component; it can be seen by the two almost liner parts in the plots. However, it can be seen that the time constant in the fast component is not only one; the decline shows a continuous change by time although the change is small. Cao et al. have interpreted this rapid increase by the product of the absorption coefficient and the distance from the substrate.[148] Since the film was illuminated from the substrate side, the shorter distance for EY from the substrate can be assumed. However, the results with the same tendency were obtained when the film was illuminated from the electrolyte side (not shown). Therefore, the factor of the distance from the substrate can be ignored. The results suggest that the fast increase of the photocurrent from the EY is caused by the higher net absorption coefficient. It means that the EY molecules are only in a narrow part of the film with a high concentration. When those dye molecules are excited, the high concentration peak in the electron concentration profile can be expected and hence it appears also as a peak (rapid rise) in the photocurrent transient as modelled in Fig. 2.7. And the TSPcZn molecules, in contrast, adsorb on the surface of ZnO homogeneously and widely. In such case, the electron density in the film increases rather homogeneously and there is no peak in the electron density profile.
Compared to the photocurrent delivered from TSPcZn, the photocurrent from EY is much smaller although EY absorb the photons as well as TSPcZn. If EY molecules, which absorb the photons but do not contribute to the sensitization photocurrent, were one of the factors to give the fast increase of the photocurrent, such influence might be seen when both sensitizers were illuminated. However the decline in the plot obtained by the illumination by the white LED (▲) is almost identical to the one of the TSPcZn. A slightly faster increase of the photocurrent can be seen when both dyes were excited. It should be considered that TSPcZn dominates the photocurrent quantitatively compared to EY and when the light intensity is decreased the increasing rate of the photocurrents is also decreased. Taking these considerations and the use of the white LED for the sensitizations of both dyes into account, the light intensity for each sensitizer is smaller compared with the cases using the green LED or the red LED. Therefore, the slightly steeper decline of both dyes (▲) might indicate the influence of the EY molecules.

As summary of this section, photoelectrochemical characterizations of nonporous re-ad TSPcZn / ZnO (EY as SDA) were studied to see the influence of the enclosed dye molecules and to understand in more detail the role of relative location of sensitizers in the ZnO. Although similar amount of dye contents can be expected from the absorption

spectrum, the clearly different conversion efficiencies were observed between EY and TSPcZn. The importance of the position of the sensitizers was indicated; the sensitizer must be on the surface of the semiconductor and must have contact with the redox electrolyte. However, the increase rate of the photocurrent from EY was much faster than TSPcZn. Consequently, a fast increase is caused by the strong net absorption coefficient rather than a shorter path way to the substrate. Still some points such as how the enclosed EY molecules recover from the oxidized form and how nonactive EY molecules are behaving after the photon absorption in the film, remains as a question.

5.1.3.3. Characterization and optimization of the photoelectrochemical efficiency for re-ad TSPcZn / ZnO (EY as SDA) films

It becomes clear by the investigations up to now that the high surface area of the ZnO films and the monolayer adsorption of the sensitizers are the key issues to obtain the efficient photoelectrode for dye sensitized solar cells. In this section, several re-ad TSPcZn / ZnO (EY as SDA) films are prepared to characterize and optimize the photoelectrochemical efficiency. An optimized electrode will be studied at different applied potential and for different compositions of the electrolyte. A sandwich cell with re-ad TSPcZn / ZnO will also be fabricated for the first time. The measurements were carried out in a three electrode setup. Pt wire and Ag/Ag^+ electrode were used as counter electrode and reference electrode respectively. The solvent for the measurement is mixture of ethylene carbonate and acetonitrile (4:1 in volume).

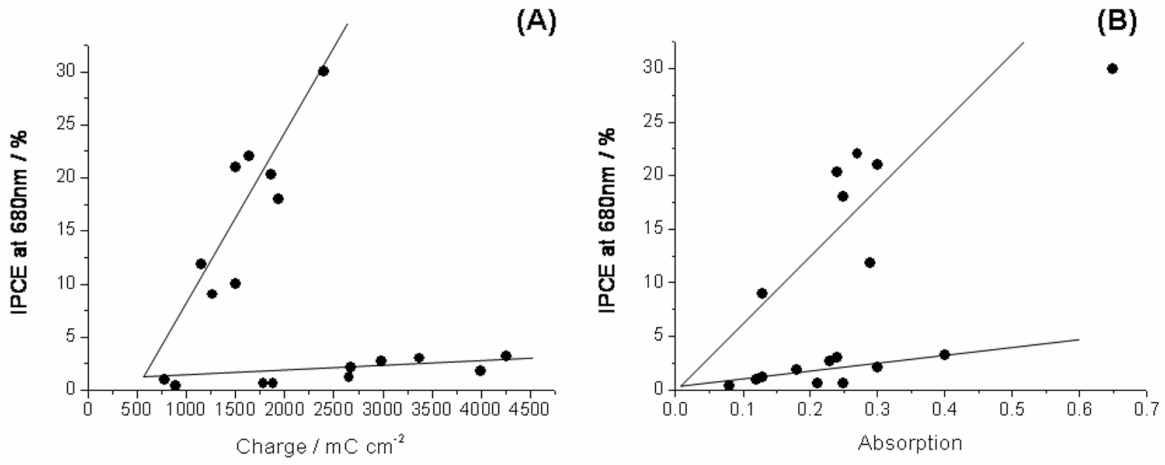

Fig. 5.23; IPCE measured at 680 nm for re-ad TSPcZn / ZnO (EY as SDA) films as the function of (A) the charge passed during the deposition and (B) the absorbance at 680 nm. The absorbance is estimated from a transmission spectrum of the film and by subtracting an estimate of the light scattering.

From Fig. 5.23(A), there seems a tendency that there are two kinds of films. One seems to have the high porosity since it can be seen from the fact that the IPCE value at 680 nm increase rather rapidly as the charge passed during the deposition increases and the dye

extraction for those films in aqueous KOH following the film preparation was done successfully. On the other hand, another seems to have the dense structure since the increase of IPCE value is smaller than the other kind of films, nevertheless IPCE value at 680 nm still tends to increase as the charge increases. And for those films, the EY molecules as SDA were not removed completely in KOH solution and the red color of EY could be seen after the extraction process. Such different porosities appear as different conversion efficiencies. Up to now, the highest IPCE of approximately 30 % has been achieved in re-ad TSPcZn / ZnO (EY as SDA) films. The high porosity of the film and a monolayer adsorption of the dye on the surface of ZnO are the key issues to improve the efficiency further. The IPCE at 680 nm is also compared with the light absorption at 680 nm and it is shown in Fig. 5.23 (B). The absorption is estimated from the transmission spectrum of the film and by subtracting an estimate of the light scattering. As it can be seen from the plot, 30 % IPCE is achieved from the film which has the high absorption of more than 0.6. It can be expected that achieving higher absorption leads to higher conversion efficiency. Considering the light harvesting efficiency from the absorption at the film, the quantum efficiency of the film can be estimated as 40 %. This is a comparable value with the values obtained in TiO_2 electrode.[28] And since the electrodeposited films do not need any heat treatment, a similar magnitude of IPCE already implies an advantage of the electrochemical deposition method. The reason why the quantum efficiency is not 100 % has not been understood clearly. It might indicate an aggregation form of TSPcZn molecules on the surface of ZnO and such aggregated dye molecules might hinder both, good contact to ZnO and to the redox electrolyte. The first would increase the amount of non-radiative decay of the excited state, the second would lead to increased back transfer of electrons from the conduction band of ZnO to the oxidized sensitizer molecule left after the charge injection. And furthermore, several factors such as electron collection efficiency, electron transport efficiency in ZnO, the recombination with the redox electrolyte and the injection efficiency should be considered and the detailed investigations are carried out in chapter 5.3.

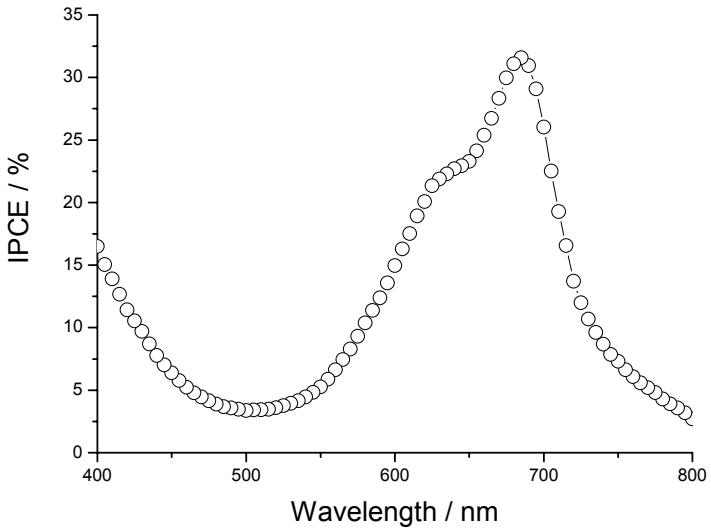

Fig. 5.24; Photocurrent action spectrum measured for TSPcZn / ZnO (EY as SDA) at -0.2 V vs. Ag/Ag^+ in the mixture of ethylene carbonate and acetonitrile (4:1 in volume) containing 0.5 M tetrabutylammonium iodide (TBAI) and 0.05 M I_2. The size of the electrode is 0.096 cm^2.

The action spectrum of the most efficient re-ad TSPcZn / ZnO (EY as SDA) in this study is shown in Fig. 5.24. The highest IPCE of 31 % at 680 nm has been achieved. And 2.3 mA cm^{-2} of photocurrent is detected in the current-voltage characteristics measured at a short circuit condition.(Fig. 5.26 (B)) This film was prepared at -1.1 V vs. SCE for 30 minutes in the presence of 50 μM Eosin Y. From the figure, the sensitization current from the monomer form of TSPcZn is seen. The aggregation form of TSPcZn also showed the sensitization photocurrent. However, it appeared as a shoulder in the spectrum, it indicates the less efficiency compared with the monomer form as reported earlier.[83] As discussed above, the efficient film was obtained when the film had a porous structure and a monomer adsorption of the sensitizer on ZnO. The EY molecules were extracted successfully after the film deposition indicating the porous character of the film. Any sensitization photocurrent from EY can not be seen in the spectrum. The sensitization photocurrent at around 500 nm seen in the spectrum is the sum of the contribution from both Q-band and Soret band.

Achieving high efficiency at longer wavelength is attractive and required in dye sensitized solar cells to utilize the whole visible light region. In this study, the promising properties of phthalocyanine dyes are optimized to serve this purpose. Although further improvement in the efficiency is necessary, the high conversion efficiency at 680 nm has been confirmed in this study. However, this result was obtained by measuring the efficiency under simulated short circuit conditions with an applied potential by using a reference electrode and using the small size electrode (0.096 cm^2). A complete sandwich cell was fabricated with re-ad TSPcZn / ZnO (EY as SDA) of rather large size (3.14 cm^2), although the sandwich cell was not fabricated with the same film shown here. The result

is discussed later.

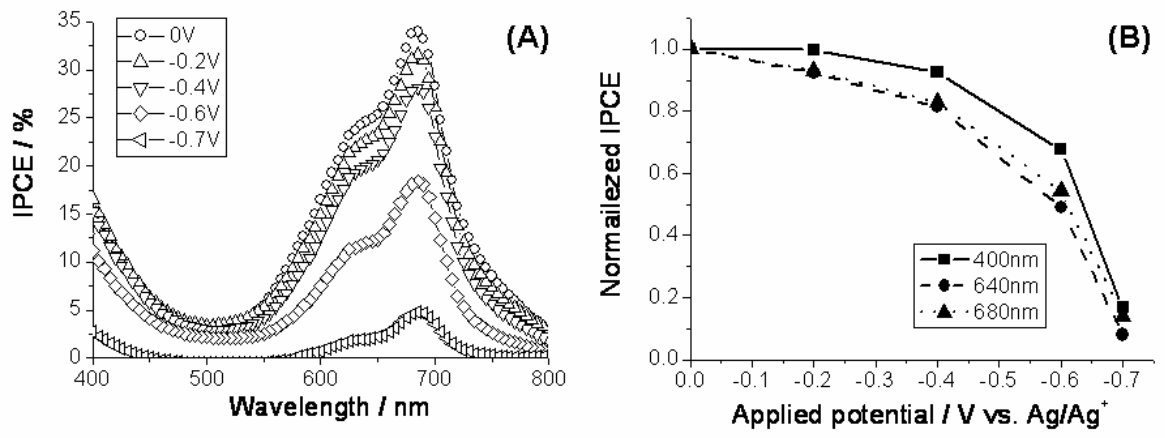

Fig. 5.25; (A) Photocurrent action spectra measured for TSPcZn / ZnO (EY as SDA) at different applied potentials of 0 V (○), -0.2 V (△), -0.4 V (▽), -0.6 V (◇), -0.7 V (◁) vs. Ag/Ag^+, (B) IPCEs as a function of electrical bias applied to the electrode for the illumination at 400 nm (—■—), 640 nm (- -●- -), 680 nm (···▲···) normalized to unity for a potential of 0 V.

The film which was obtained following the optimization was investigated further by measuring the photocurrent action spectrum at different potential. (Fig. 5.25 (A)) The efficiency of the electrode decreased as the applied potential shifts to negative. When -0.7 V vs. Ag/Ag^+ was applied to the electrode, the efficiencies were close to zero, which agreed with the results reported earlier.[139] The IPCEs are normalized to see the influence of different wavelengths of 400, 640 and 680 nm which is corresponding to the Soret band, the aggregation peak of Q-band and the monomer peak of Q-band respectively. (Fig. 5.25 (B)) The efficiency decreases more clearly in the Q-band region. It can be assumed that the electron transport in the ZnO matrix is identical at any excitation wavelength. The different decrease of the efficiencies, therefore, could be caused by either the decrease of the injection efficiency or the increase of the recombination from the electrons injected into the conduction band of ZnO to either the redox electrolyte or to the oxidized sensitizer. It should be noted that the possibility of the photocurrent contribution from ZnO at 400 nm is ignored in this consideration. Tachibana et al.[178] reported in their study about the anodic photocurrent loss in Ru-complex dye / TiO_2 films that the electron injection efficiency is independent of an excitation wavelength upon the applied potential. And moreover it was also reported that the electron injection rate at close to the Fermi level is sufficiently fast compared to the electron transport in the semiconductors.[179] Therefore it can be expected that the decrease of the efficiency is caused by the acceleration of the recombination rather than the injection efficiency. Since it can be assumed that the ground state of Q-band is higher than Soret band, the probability which the recombination takes place from the electrons injected into the conduction band of ZnO to the ground state of Q-band might be higher than Soret band. An interesting point in Fig. 5.25(B) is that the difference of the efficiencies between the monomer form (680 nm) and the aggregation form (640 nm) of Q-band becomes bigger as

the applied potential becomes more negative. Since, it can be expected that the aggregated TSPcZn molecules have poor contact with ZnO, such a different situation might cause the different efficiency.

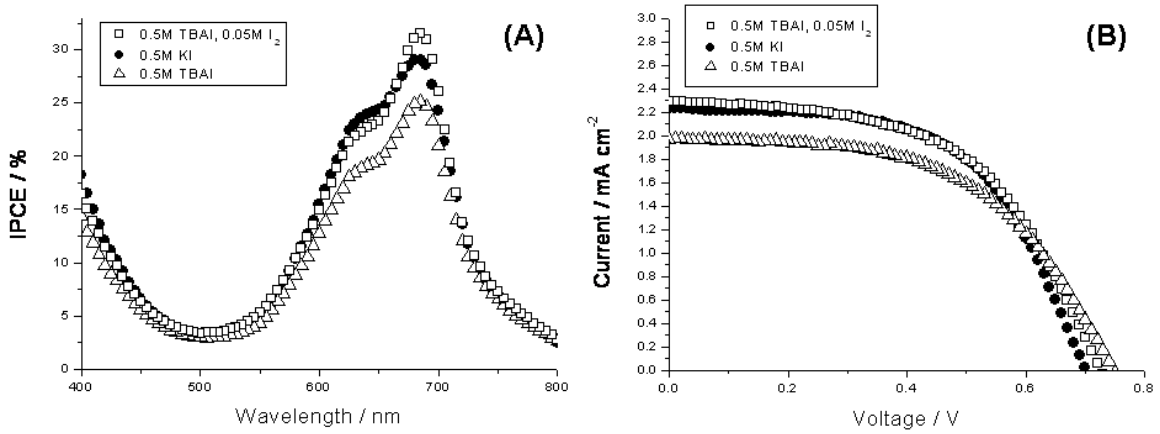

Fig. 5.26; (A) Photocurrent action spectra and (B) photocurrent – voltage characteristics measured for re-ad TSPcZn / ZnO (EY as SDA) in the different solute of (□) 0.5 M TBAI and 0.05 M I2, (●) 0.5 M KI and (△) 0.5 M TBAI. The measurements are carried out in a three electrode setup. The action spectrum is measured at -0.2 V vs. Ag/Ag^+.

The composite of the electrolyte is one of the important factors to decide the cell efficiency. Three kinds of electrolytes are tested to see the influence on the photoelectrochemical efficiency. The used electrolytes are following;

1) 0.5 M tetrabutylammonium iodide (TBAI) and 0.05 M I_2,
2) 0.5 M KI
3) 0.5 M TBAI.

In the electrolyte 1 and 3, it is confirmed that the adsorbed dye molecules on ZnO do not dissolve to the electrolyte. However some dissolution was observed after the measurement in electrolyte 2. The photocurrent action spectrum and current-voltage characteristic were measured for re-ad TSPcZn / ZnO (EY as SDA) (Fig. 5.26). The IPCE of 31 % from the electrolyte 1, 29 % from the electrolyte 2 and 25 % from the electrolyte 3 were detected at 680 nm. From all cases, rather high sensitization efficiencies were detected. The discussion about the different efficiencies is written later. The shapes of the spectra, the ratio of the photocurrent contribution in dye monomer (680 nm) and aggregation form (640 nm), are slightly different by the electrolyte. By normalizing the IPCE, the normalized IPCE at 640 nm are obtained as 0.72, 0.82 and 0.76 from the electrolyte 1, 2 and 3 respectively. The relatively low normalized IPCE from the electrolyte 1 comparing with the electrolyte 3 is because of the iodine. It was reported that the existence of I^{3-} at high concentration in the electrolyte increases the probability to recombine with the electrons injected to the conduction band of semiconductor.[180] However, the highest IPCE at 680 nm is obtained from the electrolyte 1 and relatively lower efficiency is found

at 640 nm. It means that the recombination occurs in a higher probability with the aggregation form of TSPcZn. Actually it is better to contain I_3^- at a proper concentration in the electrolyte, it is because I_3^- ions have to diffuse to the counter electrode to cycle the system.[180]

Taking the difference efficiencies between the electrolyte 2 and 3, the simple difference is the size of cation. It was reported by Liu et al.[181] that the largest short circuit photocurrent and the smallest open circuit photovoltage were found in the electrolyte containing Li^+ compared with other kinds of cation such as Na^+, K^+, Rb^+ and Cs^+. The adsorption of cation on the surface of the semiconductor leads to a potential drop in the Helmholtz layer. And such potential drop depends on the cation and it increased as the radius of the cation decreases. This potential drop leads to a positive shift of the conduction band in the semiconductor.[181,182] And when the position of the conduction band shifted to positive, the driving force of the electron injection from the excited dye to the conduction band of the semiconductor is increased and appears as a higher photocurrent.[183] It agrees with the results shown in Fig. 5.26 (A) and (B). A higher IPCE at 680 nm was obtained in the electrolyte 2 than in the electrolyte 3. And also a higher photovoltage was obtained in the electrolyte 3 (-0.75 V vs. Ag/Ag^+) than in the electrolyte 2 (-0.7 V vs. Ag/Ag^+). Since TBA^+ has clearly bigger radius than K^+, it can be expected that the conduction band of ZnO in 0.5 M KI shifts positive compared to the case of 0.5 M TBAI. It explains well the higher photocurrent and the smaller photovoltage in the electrolyte 2 compared with the electrolyte 3. Beside this, it was found that the normalized IPCE at 640 nm is higher in the electrolyte 2 than the electrolyte 3. It is interpreted that the adsorption of K^+ on the surface of ZnO decreases the probability of the recombination between I_3^- and the injected electrons to ZnO due to the less contact of those species, or that the efficiency at 640 nm is increased due to the positive shift of the conduction band of ZnO.

By adding I_2 to the electrolyte 3 (corresponding to the electrolyte 1), the enhancement of the photocurrent was achieved and the photovoltage was still in similar magnitude. The electrolyte has a significant influence on the photoelectrochemical properties. Since the presently used electrolytes are optimized for TiO_2 electrodes, the tuning of the electrolyte for ZnO represents an important issue for an optimized use of dye / ZnO electrodes and these electrodes prepared by electrochemical deposition.

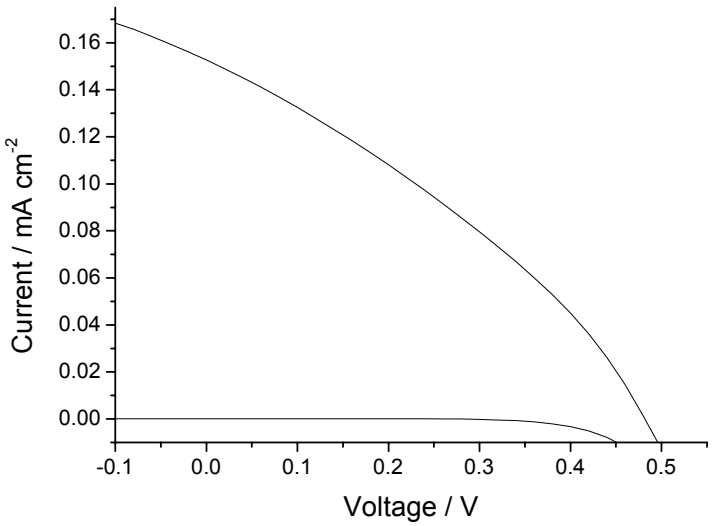

Fig. 5.27; Photocurent – voltage characteristics of re-ad TSPcZn / ZnO (EY as SDA) prepared as a sandwich cell. It is measured under AM 1.5 sun using 3.14 cm^2 size electrode. 0.5 M TBAI, 0.05 M I_2 in mix solution of ethylene carbonate : acetonitrile = 4:1 in volume is used as electrolyte. Pt coated glass is used as counter electrode.

As one of the challenges, a complete sandwich cell was fabricated for the first time with Pt coated glass as a counter electrode and re-ad TSPcZn / ZnO (EY as SDA) film although the measured film is not the same film which reached 31 % of IPCE at 680 nm. And even the photoelectrochemical measurements under the potential control condition have not been carried out for the film used for the sandwich cell since the sandwich cell was fabricated by using the whole part of the film (3.14 cm^2).

The current-voltage characteristics are shown in Fig. 5.27. A short circuit photocurrent of 0.15 mA cm^{-2}, an open circuit photovoltage of 0.48 V, a fill factor of 0.33, and a conversion efficiency of 0.024 % were obtained. For a control purpose, an action spectrum was measured for this sandwich cell and only 1.7 % of IPCE at 680 nm was obtained. The chosen film has a photocurrent at short circuit more than 10 times lower than the optimized film shown in Fig. 5.24. A photovoltage of 0.5 V agrees with the value obtained in Fig. 5.26(B) when the potential of the counter electrode of +0.2 V vs. Ag/Ag^+ reference electrode is considered. A clear difference can be seen in the fill factor compared to the current-voltage characteristics shown in Fig. 5.26 (B). In the sandwich cell, several resistances such as the resistance of the substrate, ZnO, electrolyte and Pt counter electrode contribute to the fill factor. It can be assumed that the low fill factor of 0.33 is mainly caused by a bigger size of the electrode which increases the resistance in ZnO and SnO_2 conductive substrate because the electrolyte and Pt counter electrode used in this study are commonly used in the study of dye- sensitized solar cells for which significantly higher efficiencies are reported.

For the fabrication of sandwich cells, it seems to have several technical issues to change the cell resistance. Further trial for the construction and the investigation to reduce the

resistance will improve the efficiency of the device.

5.1.3.4. Summary

The photoelectrochemical properties of re-ad TSPcZn / ZnO (EY as SDA) films have been investigated in this section. The photoelectrochemical efficiency of the electrodes depends strongly on the structure of ZnO. The states of oxygen in the deposition bath affect significantly the position of EY in the film. EY molecules are on the surface of the film when the oxygen is dissolved in the electrolyte (porous ZnO), whereas EY are enclosed in the film when the oxygen gas bubbles are in the electrolyte (non-porous ZnO). Such structure difference directly correlates with the surface area of the films and hence their photoelectrochemical efficiencies. The improvement of the photoelectrochemical efficiency in the red part of the visible light was achieved by adsorbing TSPcZn on porous ZnO. TSTPPZn can be adsorbed simultaneously with TSPcZn and the panchromatic sensitization was achieved by both dyes present in the film.
The response of time- resolved photocurrent shows the significantly different characteristics compared to that of one-step electrodeposited films although the observed responses for re-ad films are the common characteristics in the study of dye- sensitized solar cells, e.g. Ru-complex dye / TiO_2.[156] The slow increase of the photocurrents in photocurrent transients indicate the existence of the traps in the films and hence the time is necessary to fill those traps as the illumination opens. No spike in the beginning and the closure of the illumination, which was observed in one-step films, implies any recombination reaction in the electrode.

TSPcZn was also adsorbed on ZnO from which SDA (EY) could not be extracted completely in aqueous KOH. The relatively poor photoelectrochemical efficiency was obtained compared with the re-ad TSPcZn / ZnO (porous) films. The absorption from EY molecules enclosed in ZnO matrix is clearly seen from the absorption spectroscopy and the absorbance is almost corresponding to the one of TSPcZn. Some EY molecules still generate photocurrent although the efficiency is significantly smaller than the one of TSPcZn. A slow increase of the photocurrent was observed in time- resolved photocurrents as it was observed in other re-ad films. Interestingly, much faster electron transport was observed from the photocurrent generated by EY. This is caused by a shorter path way to the substrate and the high absorption coefficient in the narrow part of the film. This analysis might contribute to further optimization of the dye / ZnO films by a decreased path way of the charge transfer in ZnO or a further improved charge transport in the ZnO matrix (see below).

It becomes clear that the electrodes which have high photoelectrochemical performance have a high porosity and EY molecules are not in the film after the extraction process. In an optimization of the ZnO matrix material obtained by the deposition in the presence of

EY, 31 % of IPCE could be reached at 680 nm from re-ad TSPcZn / ZnO. An increase of the surface area and establishment of the monolayer absorption of the sensitizer can further improve the light harvesting efficiency. Optimization of the redox electrolyte, especially for dye / ZnO electrodes, will improve the efficiency of cells.

As one of the goals in this study, the enhancement of the photoelectrochemical efficiency in the red part of the visible light has been achieved. The efficiency of the film prepared by the electrochemical deposition method reached the equivalent level reported earlier for Pc / TiO_2 electrodes.[9 1] However, due to the low light harvesting efficiency, the illumination in the red part is still not fully utilized. Further improvement is expected by optimizing the several factors such as the electrolyte and the condition to adsorb the sensitizers.

5.2. Samples with optimized interface area using SDS as SDA

The enhancement of the photoelectrochemical efficiency by introducing the re-adsorption method opened the idea to use other kind of SDA for obtaining more porous ZnO thin films. In this sense, SDA need not to be dyes although dye molecules are easier to see whether those molecules are removed completely or not before the sensitizers are re-adsorbed. It was reported recently that the electrochemical synthesis of nanostructured ZnO films from $Zn(NO_3)_2$ solution utilizing the self-assembly of surfactant molecules like sodium laurlsulfate, also named sodium dodecyl sulfate (hereafter SDS)[70] (Fig. 5.28) or cetyltrimethylammonium bromide (CTAB) at the solid-liquid interfaces could be performed.[184] There, they show that the positively charged CTAB headgroups can not strongly coordinate to zinc species, and therefore CTAB has no influence on the morphology of the ZnO films. If SDS is added, however, each ZnO particle is composed of a lamellar nanostructure.[70]

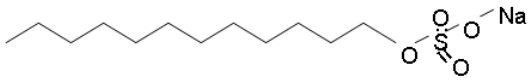

sodium dodecyl sulfate (SDS)
Mw = 288.37

Fig. 5.28; Constitutional formula of SDS

This is a collaboration work with Dr. E. Michaelis (University of Bremen). ZnO thin films were prepared by the electrochemical deposition in the presence of SDS. SDS was extracted following the film preparation by dipping the film into aqueous KOH (pH:10.5) for 50 hours and dried at 110 ℃ in air atmosphere for 1 hour. Following the dry treatment, re-ad dye / ZnO thin films were prepared by adsorbing the sensitizer by dipping into the dye solution for 1 hour.

The electrochemical characterizations were carried out in detail elsewhere.[70,163] The photoelectrochemical characterization has been investigated in this section by the measurements such as photocurrent transient measurements and light intensity modulated measurements. The dyes such as EY, TSPcZn and TSTPPZn are used as sensitizer.

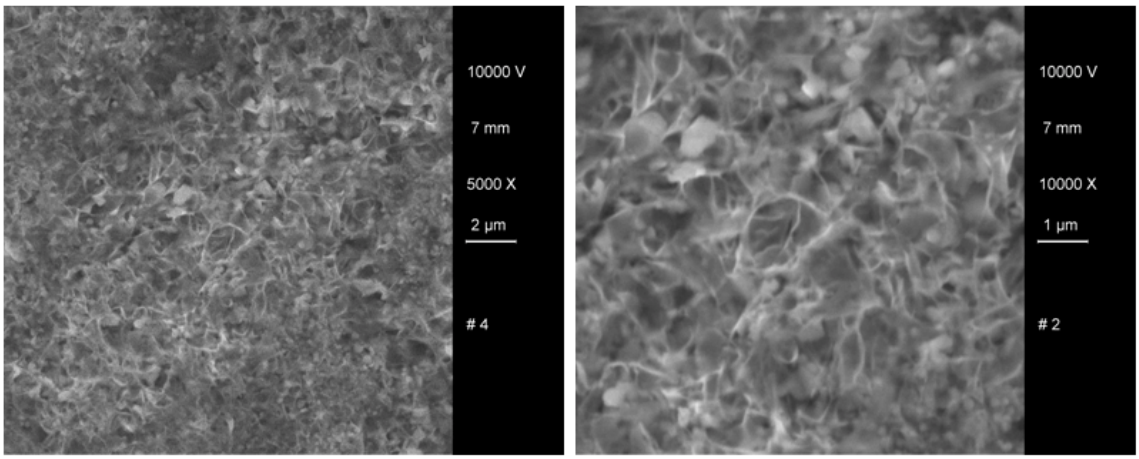

Fig. 5.29; SEM images of electrodeposited ZnO film prepared in the presence of 400 µM SDS as structure directing agents. The images were supplied from Dr. E. Michaelis.

The films were prepared successfully and the films have clearly different features such as the colour, thickness, morphology and porosity. A rather high current of more than 2 mA cm^{-2} was detected during the deposition.[70] It is higher than the case of ZnO deposited in the presence of Eosin Y. When EY is present in the deposition bath, as information, the average current during the deposition is about 1.4 mA cm^{-2}. Although it is not clear so far, the deposition in the presence of SDS enhances the kinetics of the film growth and it can be seen that SDS is working as a catalyst during the position. A clear white colour and a rather strong light scattering were seen. The crystalline character of ZnO was confirmed by XRD and it was found that such films did not have a preferential orientation like the films grown in the presence of EY. Thicker films of 6 µm were obtained after a deposition of 20 minutes when compared with the electrodeposited ZnO films in the presence of other SDA.[60,64,69] And rather high roughness factors of about 200 cm^2 / cm^2 were detected for as-deposited ZnO (SDS as SDA) from BET measurements. A relatively higher surface area of ZnO (SDS as SDA) can be seen from the rough surface of the film. It was found from AFM (not shown) that there are about 2 µm differences of the height in the film.[70] The rough surface of the film can be observed also in the SEM images shown in Fig. 5.29.[70]

Those features indicate a chance to perform good photoelectrochemical properties for the application to dye sensitized solar cells since an increased surface area was stated earlier as an important optimization criterion. The photoelectrochemical analyses for such optimized films are discussed in the following sections.

5.2.1. Characterization of re-ad EY / ZnO (SDS as SDA) films

EY was adsorbed as sensitizer on ZnO prepared in the presence of SDS as SDA. The absorption spectrum shown in Fig. 5.30 was measured for re-ad EY / ZnO (SDS as SDA).

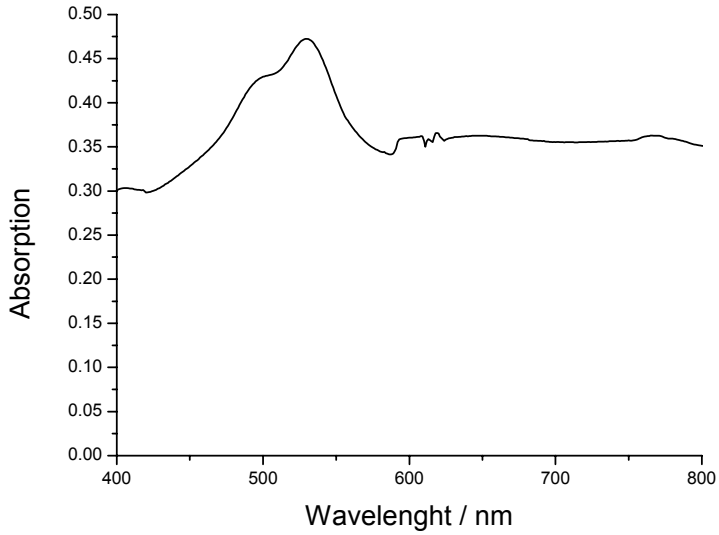

Fig. 5.30; Absorption spectrum of re-ad EY / ZnO (SDS as SDA). ZnO was electrodeposited at -1.0 V vs. SCE for 30 min in the presence of 600 µM SDS in the deposition bath.

The absorption peak at 530 nm corresponding to the absorption spectrum of EY was observed. As it was seen by eye observation, a rather strong light scattering can easily be seen, for example, from the absorbance at 800 nm where there is no absorbance from both EY and ZnO. It is also related to the larger film thickness of 10 µm compared with ZnO with EY as SDA (3 µm by 20 minutes deposition). By the BET analysis, it was found that the surface area of ZnO (SDS as SDA) following the extraction of SDS is 559 cm^2 / cm^2.[173] As average, the surface area is larger in the films with SDS as SDA (200 - 600 cm^2 / cm^2) compared to the films with EY as SDA (100 - 400 cm^2 / cm^2).[173] It indicates the effectiveness of SDS as the function of SDA. Because of this increased surface area, the ZnO films prepared in the presence of SDS have a chance to perform better photoelectrochemical performance. As a result of such increased surface area, the EY content could be increased from 1.24 x 10^{-8} mol cm^{-2} in the case of ZnO (EY as SDA) to 5.50 x 10^{-8} mol cm^{-2} for the case of ZnO (SDS as SDA). Assuming the monolayer adsorption of EY on the surface of the film, it allows to expect the higher light harvesting efficiency which should improve the photoelectrochemical performance if the charge transport and recombination kinetics in ZnO are maintained at the good level of ZnO (EY as SDA).

Photocurrent transient measurements have been carried out for re-ad EY / ZnO (SDS as SDA) films and the results are shown in Fig. 5.31.

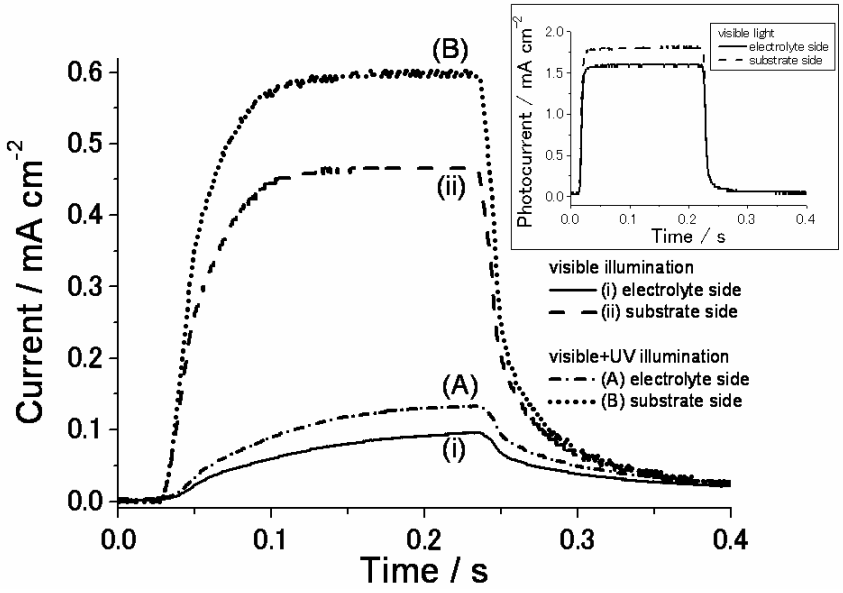

Fig. 5.31; Time-resolved photocurrents measured at -0.2 V vs. Ag/Ag^+ for re-ad EY / ZnO (SDS as SDA) in the electrolyte of 0.5 M KI in a mixed solution of ethylene carbonate : acetonitrile = 4 : 1 in volume. The film was prepared at -1.0 V vs. SCE for 30 min in the presence of 600 μM SDS, 5 mM $ZnCl_2$ and 0.1 M KCl. The SDS was dissolved from the film in aqueous KOH. The light intensity was 200 and 250 mW cm^{-2} for visible light (i and ii) and white light (visible + UV) (A and B) respectively. The electrode was illuminated from the substrate side (ii and B) and the electrolyte side (i and A). The inset shows time-resolved photocurrents of a re-ad EY / ZnO (EY as SDA) film under the same experimental conditions.

By the illumination with the visible light, the photocurrents of 0.096 and 0.46 mA cm^{-2} were detected by illumination from the electrolyte side and the substrate side respectively. Higher photocurrents of 0.13 and0.6 mA cm^{-2} were detected by the (visible+UV) illumination. A rather large difference was seen in the magnitude of photocurrents by the different side of the illumination. It is strongly related with the large light scattering and the large film thickness. Injected electrons have to be transported from the sensitizer location to the substrate electrode. This path is longer for sensitizer molecules near to the electrolyte side of the film. This increases the possibility to be trapped in the ZnO matrix and to recombine with either the oxidized sensitizers or the redox electrolyte, although no evidence of the recombination was observed from the shape of the time- resolved photocurrents. The shapes of the transients are similar to those observed in Ru-dye / TiO_2 films[156,185] and in re-ad dye / ZnO (EY as SDA) films. However, the times to reach the steady state photocurrents are relatively long, especially for the electrolyte side illumination, when compared to the one of re-ad EY / ZnO (EY as SDA) film shown in inset. Many traps in the ZnO matrix can be expected.

As one of the key issues in this section, it is important that the magnitude of the photocurrents from the film prepared in the presence of SDS as SDA is smaller than those for films prepared in the presence of EY as SDA, although both the surface area and the dye content are larger for the film with SDS as SDA. The results indicate that other factors such as electron transport, electron injection efficiency, and condition of the

binding between the sensitizer molecules and the semiconductor, affect to their photoelectrochemical efficiencies.
In the next section, the photoelectrochemical characterization is reported when TSPcZn and/or TSTPPZn are used as sensitizers for such ZnO films prepared in the presence of SDS as SDA.

5.2.2. Characterization of dye- modified ZnO (SDS as SDA) films with TSPcZn and/or TSTPPZn as sensitizer

TSPcZn and/or TSTPPZn were adsorbed on the ZnO films electrodeposited in the presence of SDS as SDA. The extraction of SDS molecules was carried out by dipping the film into aqueous KOH (pH: 10.5) for 50 hours. Following the dry treatment at 110 ℃ for one hour, the electrodes were dipped into 250 μM of dye aqueous solutions for one hour to adsorb the sensitizers.
Coloured films were obtained after the adsorption of the sensitizers. The films have a turbid appearance because of the strong light scattering. (As information, the films supplied for the study in this section showed at least over 90 % of absorption at 800 nm. The absorption peaks corresponding to those of sensitizers in solutions were not detectable in the absorption spectra of the film. The adsorption of the sensitizers was confirmed by photocurrent action spectra (see below) and by absorption spectra of the solution measured following dissolution of the film to aqueous NH_3.) Photoelectrochemical measurements were carried out by a three electrode setup in the mixed solvent of ethylene carbonate and acetonitrile (4 : 1 in volume) containing 0.5 M TBAI and 0.05 M I_2. Pt and Ag/Ag^+ electrodes were used as counter electrode and reference electrode respectively. The xenon lamp was used as light source and the light intensity of the visible light illumination (385 – 900 nm) was 200 mW cm^{-2}. Due to the color of the electrolyte, the measurements were carried out only by the illumination from the substrate side.

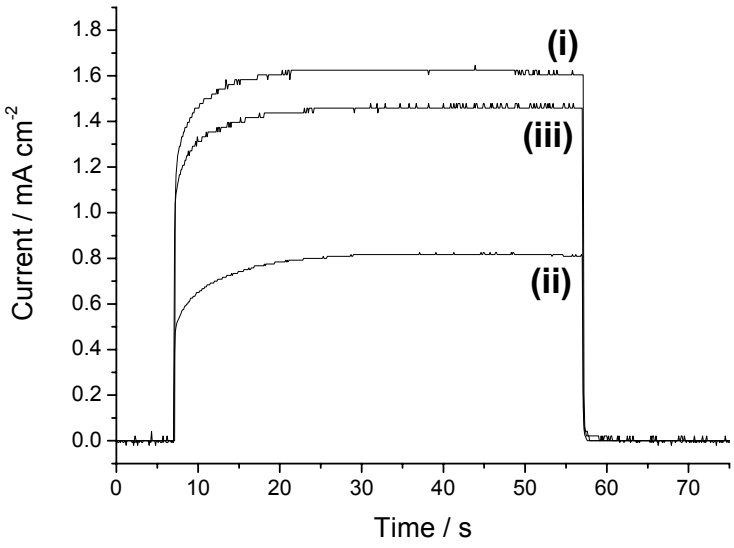

Fig. 5.32; Time-resolved photocurrents measured for re-ad TSPcZn / ZnO(SDS as SDA) (i), re-ad TSTPPZn / ZnO(SDS as SDA) (ii) and re-ad (TSTPPZn + TSPcZn) / ZnO(SDS as SDA) (iii) under illumination with the visible light. Aqueous KOH had been used for the dissolution of SDS following the deposition.

Time- resolved photocurrents were measured for those films and sensitized photocurrents were observed. (Fig. 5.32) Photocurrents of 1.63, 0.82 and 1.46 mA cm^{-2} were detected from re-ad TSPcZn / ZnO (SDS as SDA) (i), re-ad TSTPPZn / ZnO (SDS as SDA) (ii) and re-ad (TSPcZn+TSTPPZn) / ZnO (SDS as SDA) (iii), respectively when KOH was used for the dissolution of SDS. From the shape of the transients, a good contact of the sensitizers to the redox electrolyte can be expected. One of the characteristics in the films prepared in the presence of SDS as SDA is the relatively slow increase of the photocurrent compared with the films with EY as SDA (Fig. 5.16). It took approximately 14, 22 and 16 seconds for the film (i),(ii) and (iii) respectively to reach a steady-state photocurrent. A rather large number of traps in ZnO can be expected from such slow electron transport kinetics. It can be expected that the density of the traps are related with SDS molecules since it is not sure that SDS was fully extracted from the surface of the film. (see below) Moreover, the strong light scattering in the films and the relatively large thickness also affect the electron generation profile in the film and hence the electron transport in ZnO to reach a steady-state.[148]

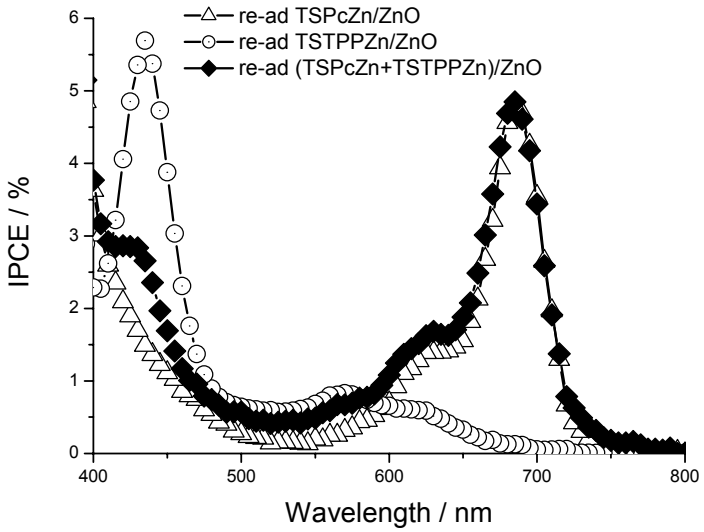

Fig. 5.33; The photocurrent action spectra of re-ad TSTPPZn / ZnO (—△—), re-ad TSPcZn / ZnO (—⊙—) and re-ad (TSTPPZn + TSPcZn) / ZnO (—◆—) prepared by the re-adsorption method with SDS as SDA. Aqueous KOH was used for the extraction of SDS following the deposition.

The photocurrent action spectrum was measured for those films (Fig. 5.33) and it confirms that the photocurrents were caused by dye- sensitization. 4.8 % (12.5 % obtained from the film with EY as SDA) of IPCE at 680 nm from re-ad TSPcZn / ZnO (SDS as SDA) was obtained. 5.7 % (15.1 %) was obtained at 425 nm from re-ad TSTPPZn / ZnO (SDS as SDA), and 4.8 % (9.4 %) and 2.8 % (10.8 %) at 680 nm and 425 nm from re-ad (TSPcZn+TSTPPZn) / ZnO (SDS as SDA) were obtained. Other information such as the amount of dye loaded and the film thickness are shown in Table 5.

A large film thickness is one of the features of the films prepared in the presence of SDS as SDA. However, the dye concentrations are similar or even smaller compared to the films with EY as SDA. Small dye concentrations are caused by the relatively small amount of dye content in the film compared to their large film thickness. Considering the fact that the films with SDS as SDA have an approximately 1.5 times larger surface area than the films with EY as SDA, it is obvious that the adsorption of the dye molecules is not efficient. As one of the reasons, it was found by ATR-IR measurements that SDS had not been dissolved completely from the films in aqueous KOH.[163] SDS molecules might disturb the adsorption of sensitizers and therefore the dye content became small. Nevertheless, it can be seen that a larger amount of TSPcZn molecules adsorbed to the surface of the films compared with TSTPPZn and an opposite tendency was seen in the case of EY as SDA. The dye content for TSPcZn in re-ad (TSPcZn+TSTPPZn) / ZnO (SDS as SDA) was increased by adsorbing together with TSTPPZn as it was also observed in the films with EY as SDA. TSTPPZn supports the adsorption of TSPcZn to ZnO which is preferable to improve the light absorption in the red part of the visible light. The concentrations of TSPcZn in the films are, however, slightly smaller than those for films with EY as SDA. It means that just TSTPPZn molecules do not adsorb to the surface of the film efficiently.

The reason is unclear. Further investigation is necessary to understand the surface condition of the films which were modified by SDS during the electrochemical deposition.

Table 5; Dye content, average film thickness, and dye concentration of the investigated films with SDS as SDA, and comparison of the observed photocurrents i_{ph} at an incident photon flux of 10^{16} s^{-1} cm^{-2} normalized for the given dye content to provide a rough measure of the sensitization efficiency. The values in parenthesis are those from the films with EY as SDA. Note that the deposition time for the films was 30 minutes for the films with SDS as SDA and 20 minutes for the films with EY as SDA.

Electrode material	dye content / 10^{-9} mol cm^{-2}	film thickness / μm	dye concentration / 10^{-5} mol cm^{-3}	normalized i_{ph} (430 nm) / s^{-1}	normalized i_{ph} (560 nm) / s^{-1}	normalized i_{ph} (680 nm) / s^{-1}
re-ad TSPcZn / ZnO	6.4	9.4	0.681			0.11244
	(2.4)	(3.0)	(0.79)			(0.8744309)
re-ad TSTPPZn / ZnO	3.9	8.9	0.438	0.2424	0.0354	
	(17.4)	(2.5)	(6.9)	(0.1453607)	(0.037274)	
re-ad	9.7(4.3) TSPcZn	9.1	1.066(1.4)	0.2141	0.0509	0.0830
(TSPcZn+TSTPPZn)/ZnO	2.2(5.4) TSTPPZn	(3.0)	0.242(1.8)	(0.3290574)	(0.068625)	(0.3758654)

By using SDS as SDA, it is clear that the photoelectrochemical efficiency of the electrodes got large improvements as well as the case of EY as SDA when compared with one-step films. However, the efficiencies were generally lower than those of films with EY as SDA. Normalized photocurrents also show the characteristic results compared with the films with EY as SDA. (Table 5) The efficiencies of TSPcZn in re-ad TSPcZn / ZnO (SDS as SDA) and re-ad (TSPcZn+TSTPPZn) / ZnO are relatively smaller compared to those obtained from the films with EY as SDA. For TSTPPZn, the efficiencies are almost comparable to the film with EY as SDA. Again, relatively higher efficiencies were obtained in the Q-band of TSTPPZn compared to the Soret- band when the ratio of the absorbance in the solution is considered. For re-ad TSTPPZn / ZnO (SDS as SDA), a relatively larger difference of the efficiencies between Q- and Soret- band were obtained when compared with other results.

The decrease of the efficiencies for TSPcZn is due to the increase of the amount of sensitizer molecules and the decrease of the number of the generated electrons. And it should be noted that the total amount of dye molecules were larger than the one of the films with EY as SDA. Such results indicate the less photoelectrochemical activity of TSPcZn on ZnO with SDS as SDA. The interaction between TSPcZn and SDS increased the dye content in the film. However, such interaction might also lead to the aggregation of TSPcZn or different states of binding to ZnO which lead to less injection efficiency. Moreover, the larger surface area relative to the adsorbed sensitizers might lead to an open space for the injected electrons to recombine with the redox electrolyte. The normalized efficiencies for TSTPPZn indicate the similar photoelectrochemical activities in the films with both EY and SDS as SDA. By increasing the dye content in the film, the improvements of the photoelectrochemical efficiencies can be expected. A rather large

ratio of the efficiencies between the Q- band and the Soret- band in re-ad TSTPPZn / ZnO (SDS as SDA) are caused by the strong light scattering of the film. From the transmission spectra of the films (not shown), it was seen that almost no light can go through the film because of the light scattering and the reflection. It can be expected that the electron generation profiles in the ZnO matrix would be similar for any wavelength even if the absorption coefficient should be different. Therefore, the efficiencies show the rather corresponding ratio with the one in the solution. For re-ad (TSPcZn+TSTPPZn) / ZnO, the dye content for TSPcZn was enhanced by adsorbing together with TSTPPZn. However, such increased portion does not reflect to the photoelectrochemical efficiency as it was observed also in the film with EY as SDA. The further interactions with TSTPPZn, not only with SDS, decrease the photoelectrochemical efficiency of TSPcZn.
The considerations with normalized photocurrents suggest the interaction of TSPcZn with SDS to lead the decrease of its photoelectrochemical performance and the necessity to decrease such interaction; complete extraction of SDS from the film. For TSTPPZn, the further optimization of the adsorption of TSTPPZn is necessary to improve the photoelectrochemical properties.

As mentioned above, it was found by ATR-IR measurement that aqueous KOH treatment was not sufficient to completely dissolve SDS molecules from the film, and later it was found that ethanol was more efficient to extract SDS molecules. The roughness factor was measured for as-deposited film, the film after the aqueous KOH treatment and the film after the ethanol treatment by BET measurements and was found to 154, 241 and 1183 respectively.[163] The surface area of the films was increased dramatically by the dissolution with ethanol. It means that a rather large amount of SDS molecules stayed in the film when dipped into KOH. Such SDS molecules can be one of the reasons for the smaller photoelectrochemical efficiencies compared with the films with EY as SDA. A hard point, generally, for the surfactant like SDS is that the molecules do not have colour, then it is difficult to judge the progress of the dissolution process. Ethanol was found better for the dissolution process, but still it does not mean that ethanol can remove all SDS molecules from the surface of the film. A SDA like Eosin Y is more convenient since the colour of the film gives information about the progress of the dissolution.

A re-ad TSPcZn / ZnO (SDS as SDA) film was prepared with ethanol for the dissolution. And the photoelectrochemical performance of the film has been analyzed. The SDS was dissolved by the dissolution with ethanol for 48 hours and TSPcZn was adsorbed on the film by dipping the film in hot 250 μM TSPcZn aqueous solution for one hour.
The film thickness of the film is 6.5 μm after 30 minutes deposition and the dye content is 3.4×10^{-9} mol cm^{-2} and therefore the dye concentration in the film is 0.52×10^{-5} mol cm^{-3}. Comparing with the one shown in Table 5, the dye concentration in the films is even less than for the one with aqueous KOH used for the dissolution, although the surface area of the film has been significantly increased. Such results imply the answer of an increased

adsorption of TSPcZn relative to TSTPPZn (Table 5), the chemical interaction between SDS and TSPcZn might increase the adsorption of TSPcZn.

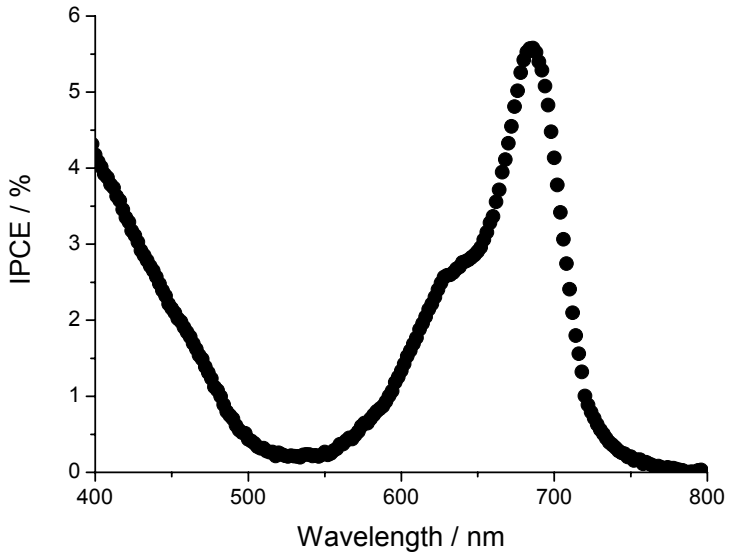

Fig. 5.34; The photocurrent action spectra of re-ad TSTPPZn / ZnO prepared by the re-adsorption method with SDS as SDA. Ethanol was used for the dissolution of SDS following the deposition.

The action spectrum of the film is shown in Fig. 5.34. The electrode shows a sensitized photocurrent at the wavelength corresponding to the absorption peak of TSPcZn in the solution. 5.6 % of IPCE was found at 680 nm. It is slightly higher than 4.8 % obtained from re-ad TSPcZn / ZnO (SDS as SDA, KOH for the dissolution). Take the larger surface area of the film into account, however, the efficiencies suggest the no influence of the surface area to the photoelectrochemical performance. A normalized efficiency of 0.27 was obtained from the number of sensitizer molecules and the number of generated electrons, compared to 0.11 following SDA- dissolution with KOH and 0.87 for EY as SDA. The larger efficiency than the film with KOH for the dissolution is due to a higher value of IPCE (more generated electrons) and a smaller amount of dye content (less sensitizer molecules). However, this IPCE value is still smaller than the one obtained from the film with EY as SDA. Although the larger surface area did not support to improve the efficiency in the case of SDS since the dye concentration in the film did not increase by using ethanol, the results suggest that the electrode can generate more electrons efficiently by decreasing the number of SDS molecules from its surface. SDS molecules clearly play some roles in the film for the absorption of the sensitizers and for the photoelectrochemical performance. For the photoelectrochemical performance, further optimization to extract SDS molecules completely from the surface of the film and then to increase the dye content in the film are necessary to improve the efficiency.

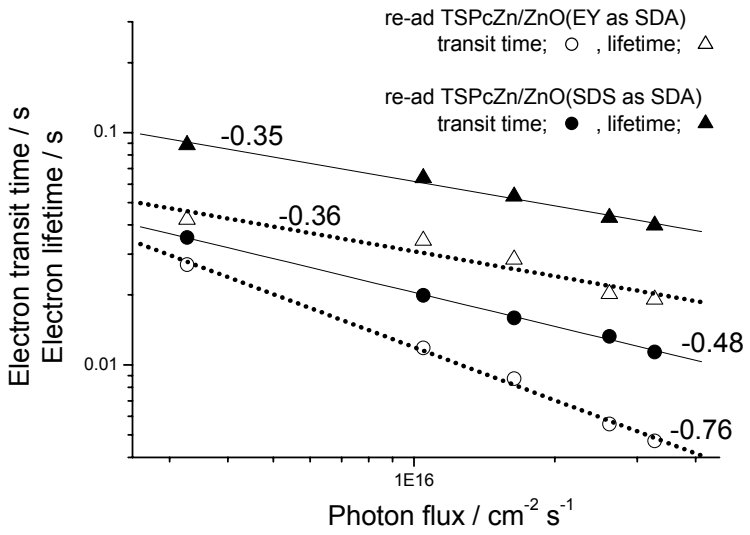

Fig. 5.35; Electron transit times τ_D and lifetimes τ_n for re-ad TSPcZn / ZnO (EY as SDA) film (τ_D = ○, τ_n = △) and re-ad TSPcZn / ZnO (SDS as SDA) film (τ_D = ●, τ_n = ▲) at different bias light intensities. The electron transit time was measured at -0.2 V vs. Ag/Ag^+. The numbers described on the figure are the slope of the line. Note these measurements still contain the early technical problem of the equipment. (Appendix 9)

The electron transit time and the electron lifetime were estimated for re-ad TSPcZn / ZnO (either EY or SDS as SDA) films by measuring IMPS (Intensity Modulated Photocurrent Spectroscopy) and IMVS (Intensity Modulated Photovoltage Spectroscopy). The obtained times are plotted in double logarithmic plot in Fig. 5.35. The details about the measurements are described in chapter 2.7 and 5.3. It should be noted that the results shown here have been carried out without an additional white- light (bias illumination), therefore the values of both the electron transit time and the electron lifetime are larger than the values obtained with an additional bias illumination since the electron density in the conduction band of ZnO is smaller when the light intensity is weak, and it should also be noted that those values were obtained when there was a technical problem in intensity modulated measurements at small frequencies. The explanation about the technical problem is described in Appendix 9. By this problem, the obtained data may have some tolerances in the values. Nevertheless, since shorter times play a decisive role here and since measurements have been carried out under the same conditions for these films, the results are valid to compare these two electrodes.

Electron transit time and lifetime obtained for both electrodes are approximately 1 order smaller than the values obtained for colloidal ZnO films.[82] It indicates that the electron transport properties for both electrodeposited films are relatively better than other films prepared in a conventional method like sol-gel. However, the efficiencies in the photocurrent action spectrum of these films are still smaller than 20 %. T. Oekermann et al. reported that a relatively smaller efficiency of one-step electrodeposited EY / ZnO hybrid thin films is caused by the low electron injection efficiency from the excited state of

EY to the conduction band of the ZnO.[82] This may also hold for the films studied here since these films have good efficient electron transport properties and hence good collection efficiency. The light harvesting efficiency is expected to decrease the photoelectrochemical efficiencies since it is around 50 % or less so far. However, the relatively low values of IPCE can not be caused only by low light harvesting efficiency. Therefore, the electron injection efficiency is left as a factor to determine the photoelectrochemical performance of these films.

The obtained values indicate a slower electron transport and a longer electron lifetime in the film with SDS as SDA. Such slow electron transport can be explained by the larger film thickness.

Slopes of -0.76 and -0.48 are found for the light intensity dependence of the electron transit time for the film with EY and SDS as SDA respectively. A faster transit time with a stronger light intensity is explained by higher trap occupancy. The deep traps are filled more completely at higher light intensity and electron trapping and detrapping involves shallower levels. Therefore the electron transit time becomes faster. The value of -0.76 is similar extent obtained in the previous studies for nanoporous dye-sensitized TiO_2 films and one-step electrodeposited EY / ZnO films.[79,82,148,156] The smaller slope of -0.48 for the film with SDS as SDA indicates a smaller influence of light intensity for the electron transport property. It might imply a smaller number of deep traps in the film with SDS as SDA.

The intensity dependence of the electron lifetime is caused by the influence of the surface state energy on the rate of interfacial electron transfer to the redox electrolyte.[80]

The difference of the transit time and the lifetime is similar for both films. The electron transport is approximately 4 times faster than their lifetime in the electrode. From such results, it can be expected that the electrons are collected efficiently at the external circuit. And it can be assumed that the yields of electron collection are similar for the films with EY or SDS as SDA since the difference of the time constants is in the similar range.

5.2.3. Summary

Sodium dodecyl sulfate (SDS) was used as SDA for the deposition of ZnO. Sensitizers were adsorbed to ZnO following the extraction of SDS. The photoelectrochemical characterizations for those films were carried out by the measurements such as photocurrent transients, action spectrum and intensity modulated measurements. By electrodepositing ZnO in the presence of SDS, the ZnO films which have the large surface area of about 600 cm^2 / cm^2 (max: 1183 cm^2 / cm^2 with ethanol for the dissolution process) were obtained. Such surface area is larger than the one obtained from the films with EY as SDA. And also the relatively large film thickness of about 9 μm was obtained after 30 minutes of deposition.

The prepared re-ad dye / ZnO (SDS as SDA) films showed much better photoelectrochemical performance compared to the one-step electrodeposited dye / ZnO

films. The validity of the re-adsorption method with the films prepared in the presence of SDS as SDA was confirmed. However, the photoelectrochemical performances of these films were not better than the films prepared in the presence of EY as SDA although the surface area became larger by introducing SDS. The interactions between SDS molecules and sensitizers might affect their performance. It was found that TSPcZn readily adsorbed to the film whereas TSTPPZn did not adsorb efficiently. However, the higher amount of TSPcZn molecules did not show up in the photoelectrochemical efficiencies. The normalized efficiency of TSPcZn decreased. The normalized efficiency for TSTPPZn was in a similar range as the one obtained from the films with EY as SDA. The optimizations such as reducing the interaction with SDS and increasing the number of active sensitizers, are required for those films.

It was found that ethanol was better to use for the dissolution of SDS from the surface of the films and the surface area was increased further by using ethanol. TSPcZn was adsorbed easily on film following the ethanol treatment. However, it did not help to increase the dye concentration in the film. Nevertheless, the efficiency of such film was increased slightly. The optimization is necessary to increase the dye concentration in the film to improve the photoelectrochemical performance.

By intensity modulated measurements, relatively longer electron transit time and longer electron lifetime than the one obtained from the films with EY as SDA were obtained. The difference of such time constants was in the similar range with the one obtained from the films with EY as SDA. Then, it can be concluded that the slower electron transport is due to the larger film thickness. The electron collection to the external circuit can be assumed to a similar extent.

The large surface area of the semiconductor is the key for the efficient electrodes in dye-sensitized solar cells. The goal to increase the surface area of electrodeposited films was achieved by using SDS as SDA. However, there were some factors to suppress the dye adsorption to the film and hence decrease the photoelectrochemical performance. The quantitative analyse for the extraction of SDS molecules from the films are necessary, and the optimization for the dye adsorption will help to improve its photoelectrochemical performance.

5.3. Characterization and optimization of electron transport in the ZnO matrix by use of Coumarin 343 as SDA

C343 is well known as a sensitizer.[34,35] Since it does not need any metal atom in the molecule and the broad light absorption in the visible region following the modification of the molecular design to reform the sharp absorption bands, it is an attractive sensitizer for practical use of dye-sensitized solar cells. The constitutional formula of C343 is shown in Fig. 5.36.

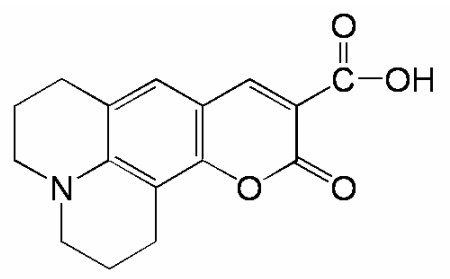

Fig. 5.36; Constitutional formula of C343

Many investigations with this sensitizer have been carried out so far. [26,34,35,186-193] And it was found that it had an efficient injection efficiency of the electrons from the excited state to the conduction band of the semiconductors. The electron injection property in the system with C343 was studied before and 20 - 200 fs of the electron injection time from C343 to the conduction band of TiO_2 has been reported.[188,189] The highest efficiency with this sensitizer was reported by Hara et al. recently and the efficiency is I_{sc}: 13.5 mA cm^{-2}, V_{oc}: 0.71 V, ff: 0.77 and η: 7.4 %.[35] This is a comparable efficiency with the one of Ru complex dye. A further enhancement can be expected by improving the molecular design to increase the light harvesting efficiency at longer wavelength. By those facts, the coumarin dye is a candidate dye in Ru complex dye's place because the Ru complex dye is a rare and expensive compound.

The electrochemical deposition of dye / ZnO films was tested in the presence of C343 by colleagues in Gifu University.[194] As in the case of EY, the electrochemical deposition of C343 / ZnO hybrid films is also possible in one-step and at a low temperature of 70 ℃. And these work as photoactive electrodes. But their efficiency is rather poor as it was seen for other one-step electrodeposited films due to the excess amount of dye loaded.[171] It was found that C343 is also a nice SDA to produce a porous structure of ZnO. Films prepared with C343 were applicable to the re-adsorption method.[194] As a unique difference, it was observed here that the 002 plain of ZnO is deposited perpendicular to the substrate.[194] This is in contrast to the ZnO films with EY as SDA (ZnO (EY as SDA)). For ZnO (EY as SDA) films, its 002 plain is parallel to the substrate.

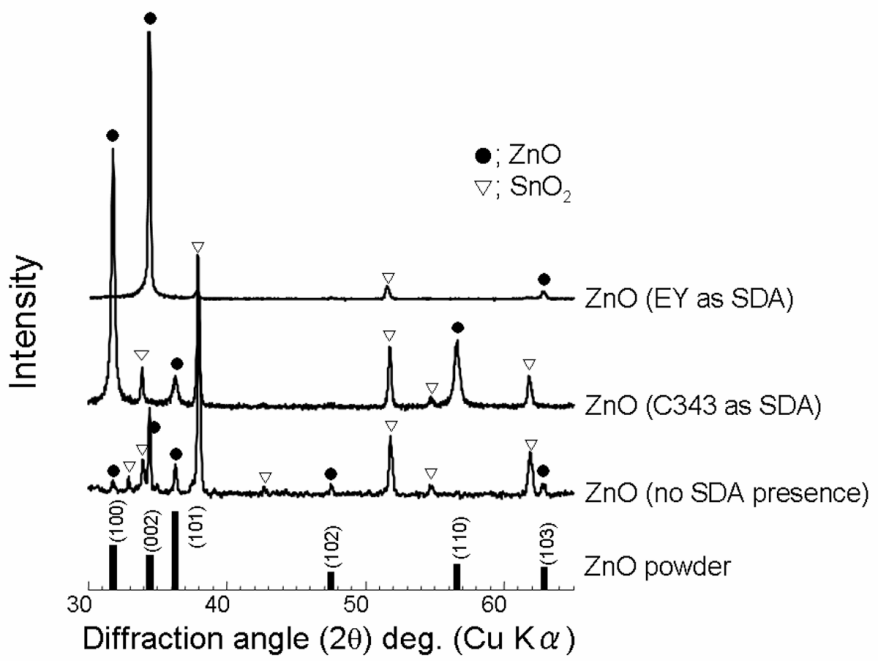

Fig. 5.37; XRD of ZnO films prepared without SDA and with SDA, Eosin Y or Coumarin 343

The XRD analysis shows such different orientations. (Fig. 5.38) XRD measurements were carried out in Gifu University and the ZnO powder standard data was referred from ZnO JCPDS 36-1451. Clear diffraction peaks were observed for all films, indicating that electrodeposited films are highly crystalline. ZnO films electrodeposited by using the reduction of oxygen has some preference for growth with a 002 orientation (002 plain of ZnO is parallel to the surface of the substrate) and a clear hexagonal shape of ZnO was observed by SEM (Fig. 2.4). In the films electrodeposited in the presence of EY, the 002 orientation of ZnO film is clearly increased since the 101 is not observed at all although the most intense peak in the powder spectrum. However, the hexagonal shape of ZnO is not seen as it was observed in SEM images (Fig. 5.40) since EY molecules influence the growth of the film by their adsorption to the surface of ZnO and porous structures were created. (see chapter 5.1.2)

The image of the different orientation of the ZnO unit cell is shown in Fig. 5.38.

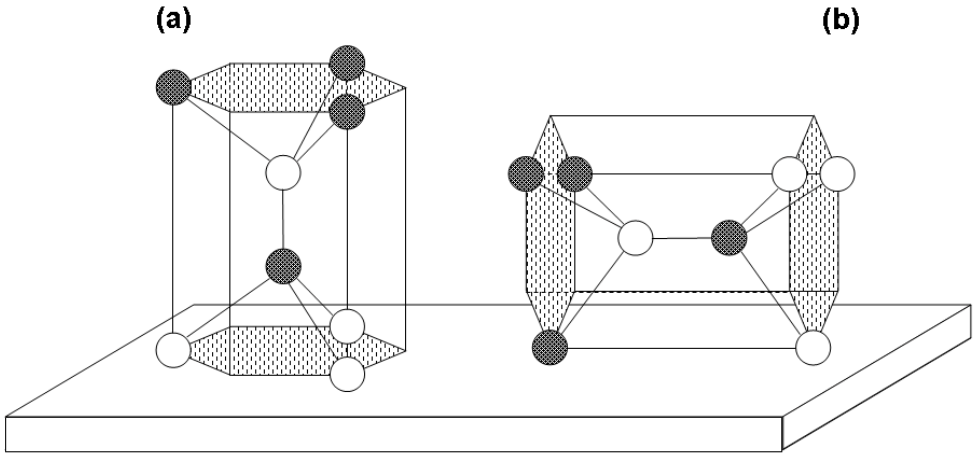

Fig. 5.38; The image of the ZnO unit cells, 002 plain of ZnO is (a) parallel to the substrate, (b) perpendicular to the substrate. The black and white spheres indicate the Zn or O atom.

It can be expected that such different orientations might influence the photoelectrochemical properties by the following reasons such as the different pathways for the electrons in ZnO, the number of atoms which the electrons move through, and the order of atoms to pass. And moreover, the different orientation of the film means that the plain which the dyes adsorb is also different since it can be assumed that the dye molecules will adsorb on the side which is perpendicular to the surface of the SnO_2 substrate. It can be assumed that the dye molecules do not adsorb to the side which is parallel to the substrate since the continuous growth of ZnO occurs to the direction perpendicular to the substrate. In earlier time, the difference of the mobility for a single crystal ZnO at different orientations was studied by several researchers.[195,196] The mobility is slightly higher when the 002 plain of ZnO is perpendicular to the substrate. However such difference was not studied for nanocrystalline metal oxides so far and hence for the dye- sensitized solar cells. There are difficulties to prepare such oriented film with nanocrystalline particles by conventional methods.

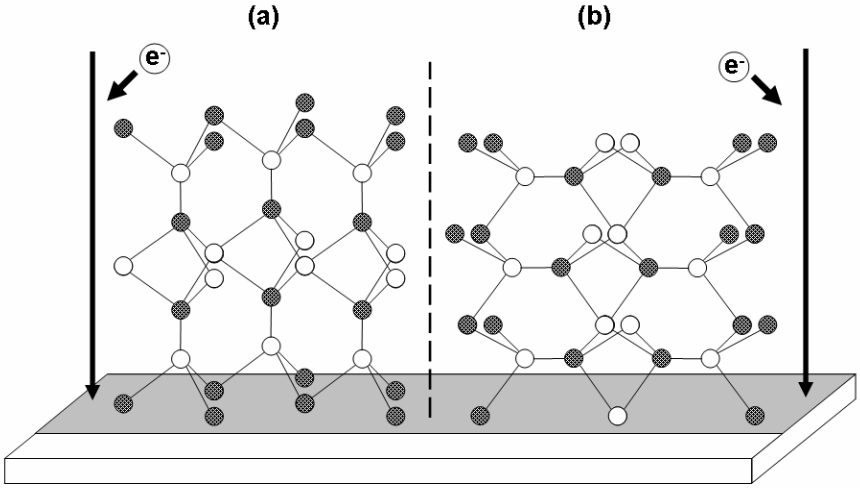

Fig. 5.39; Structural illustration of ZnO films which have different orientations; (a) 002 plain is parallel, (b) 002 plain is perpendicular to the substrate. The black and white spheres indicate the Zn or O atom.

In Fig. 5.39, the diagram of the film structure is shown. Taking into account when an electron moves from the surface of the film to the back contact and assuming that the electron moves straightly, it can be expected that the electron moves through an atom to the other atom in the case (a), whereas the electron moves though one kind of atoms, either Zn or O in the case (b). Simply moving through one kind of atoms is supposed to provide a smoother movement of the electrons.
S. Haque et al. reported recently that the optimum performance requires the avoidance of any "kinetic redundancy".[197] The electron injection from the LUMO of the sensitizer to the conduction band of the semiconductor occurs in the range of subpicosecond to tens of picoseconds.[140-146,179198-200] On the other hand, the electron transport in dye-sensitized solar cells is a trap limited diffusion process, it is much slower than the injection kinetics.[138,185,201-206] One of the approaches to solve this is making the charge separation dynamics slower; just fast enough to achieve a high yield of charge separation.[197] Another approach is making the electron transport in the oxide faster to minimize the kinetic redundancy. To optimize the device, both approaches will be required. The later approach can be achieved by optimizing the trap density, the crystallinity of oxides and the diffusion coefficient (diffusion length). Electrochemical deposition of ZnO in the presence of other kinds of SDA and different orientation of ZnO may change such factors.

The influences of such different orientations to the photoelectrochemical properties have been studied in this section and to understand the general electron transport mechanisms in electrodeposited dye / ZnO films. The films were investigated by measuring photocurrent transient, IMPS and IMVS. The effective diffusion coefficient and the diffusion length of such films were calculated from the IMPS result and the lifetimes obtained from IMVS. This is a collaboration work with Gifu University. Re-ad dye / ZnO films and bare ZnO films electrodeposited with different SDA were prepared in Gifu University and their photoelectrochemical properties were analyzed in University of Giessen. The films were studied mainly by using EY and C343 as sensitizer. In the later part of the section, the films were studied also by using TSPcZn as sensitizer.

5.3.1. Comparison of bare ZnO (Eosin Y or C343 as SDA) films

For the beginning of the study, bare ZnO films prepared in the presence of either EY or C343 were characterized. Such films were analyzed by SEM, BET, photocurrent transient and IMPS. By investigating without sensitizers, ZnO films were compared directly.

5.3.1.1. Morphology and structure

The SEM images of the ZnO with EY as SDA and the ZnO with C343 as SDA are shown in Fig. 5.40.

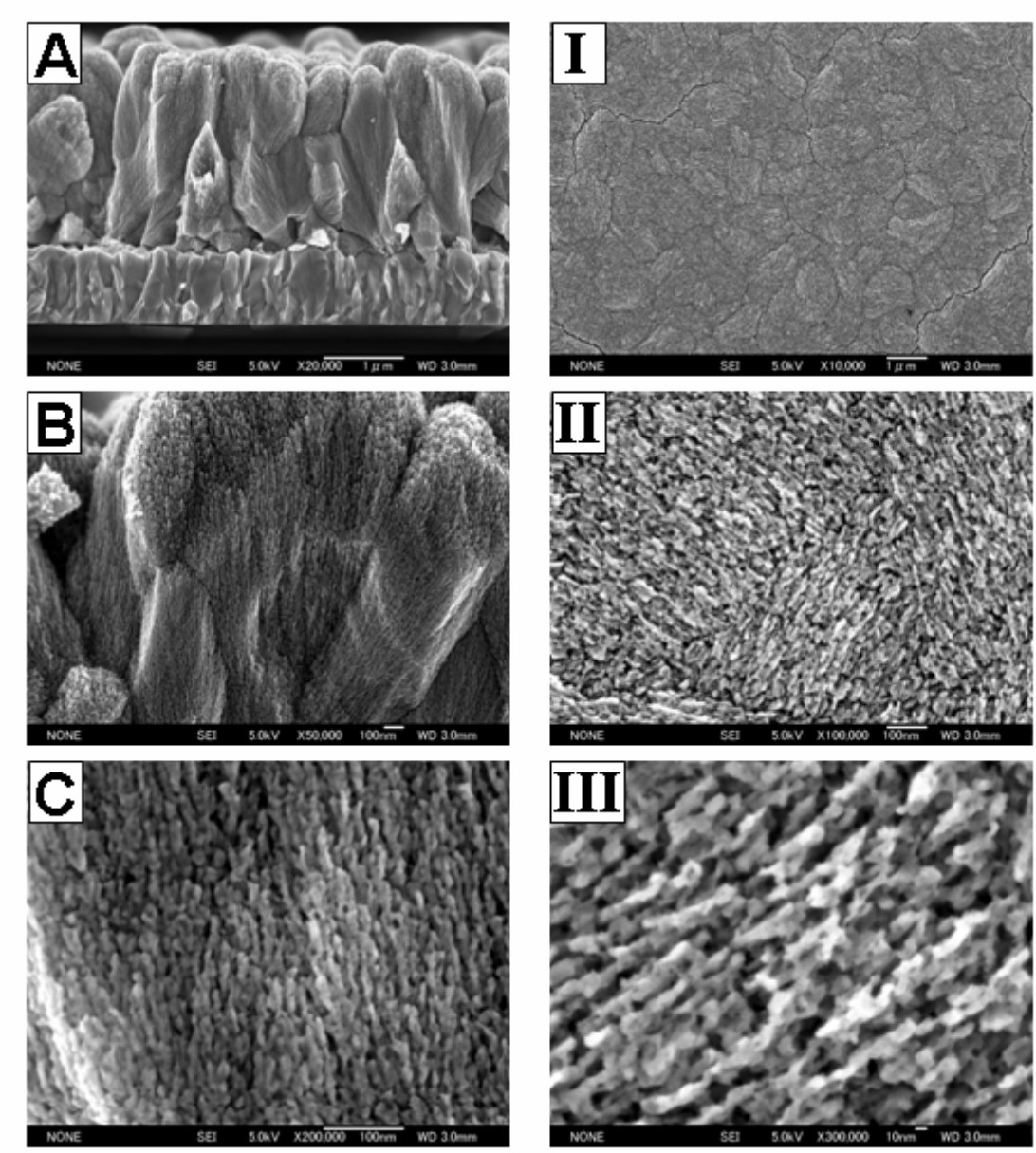

Fig. 5.40; SEM images of the ZnO films (provided by T. Yoshida, Gifu University). (A, B, C); cross section images of the ZnO with EY as SDA, (I, II, III); surface images of the ZnO with C343 as SDA. The magnitude of the image is following; (A) x 20000, (B) x 50000, (C) x 200000, (I) x 10000, (II) 100000, (III) x 300000.

The cross section images are shown for the ZnO with EY as SDA and the surface images are shown for the ZnO with C343 as SDA at a different magnitude. Since the results of XRD show that the 002 plain of the ZnO with EY as SDA is parallel to the substrate and that of the ZnO with C343 as SDA is perpendicular to the substrate, these images are showing the same plain of ZnO. At high magnitude of the film with EY as SDA (C), large numbers of small rods can be observed. It clearly indicates the high porosity of the electrodeposited ZnO prepared in the presence of EY. And it can be assumed that those rods reach to the substrate since those are prepared electrochemically. Such features of electrodeposited films can be expected as an ideal structure for the application like dye-sensitized solar cells.

A porous structure was observed also in the films with C343 as SDA. By the same reason with the films with EY as SDA, it can be assumed that those small particles reach to the substrate continuously. Surprisingly, similar structures were observed both in a film with EY as SDA and a film with C343 as SDA although one was a cross section image and another was a surface image. Because of different orientations, the plain shown in the SEM images indicates the 100 or 101 plain for both films.

These SEM images indicate that the structures of ZnO are strongly effected by SDA and also that the dye adsorption to the ZnO takes place to the side which is perpendicular to the substrate during the deposition. The precipitation of ZnO takes place at the side which is parallel to the substrate.

5.3.1.2. Photocurrent transient and IMPS

Photocurrent transient and IMPS were measured for ZnO films prepared in the presence of either EY or C343 and those SDA molecules were extracted by dipping the film into an aqueous KOH (pH:10.5). The photocurrent transient measurement is useful to see the non steady-state photocurrent response for the illumination. In this study, the measurements were carried out in the ms range. 0.5 M TBAI and 0.05 M I_2 in a mixed solvent of ethylene carbonate / acetonitrile (4:1 by volume) was used as electrolyte. An UV-LED was used for light source and the electrodes were illuminated from the substrate side for 50 ms. Pt and Ag/Ag^+ were used as counter electrode and reference electrode respectively. The potential of -0.2 V vs. Ag/Ag^+ was applied to the electrode during the measurement.

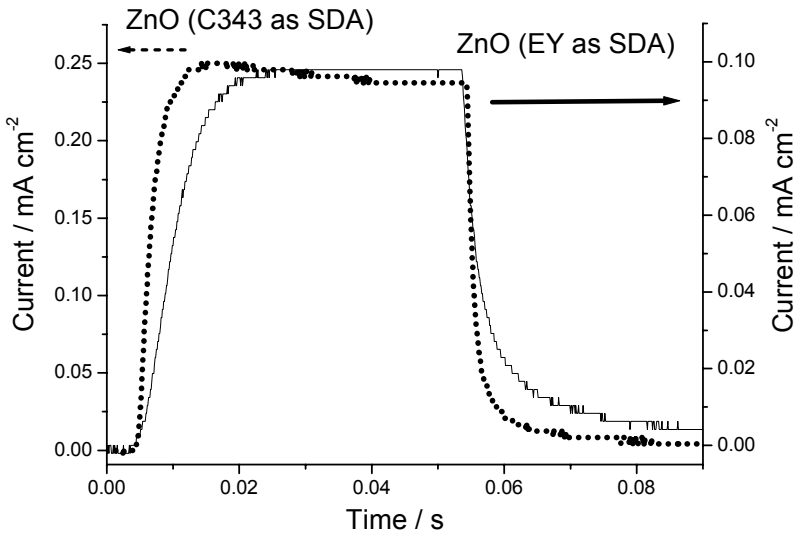

Fig. 5.41; Time-resolved photocurrents measured for ZnO films which have different orientation.

The results of photocurrent transients are shown in Fig. 5.41. The stable photocurrent of 0.225 and 0.009 mA cm^{-2} were obtained from a ZnO with EY as SDA and a ZnO with C343 as SDA respectively. It takes about 30 ms or less to reach the steady- state photocurrents for both films. Such times are necessary for filling the traps in the ZnO matrix. Although the magnitude of the photocurrent was not same; the photocurrent measured for the film with C343 as SDA was higher than the film with EY as SDA, a clearly faster response for the illumination was observed from the film with C343 as SDA (dotted line in Fig. 5.41). And also the faster decrease of the photocurrent was observed when the illumination was cut off. Those results suggest the faster electron transport property in ZnO with C343 as SDA or less number of traps in ZnO with C343 as SDA. In both cases, it shows that films with C343 as SDA have nicer photoelectrochemical properties.

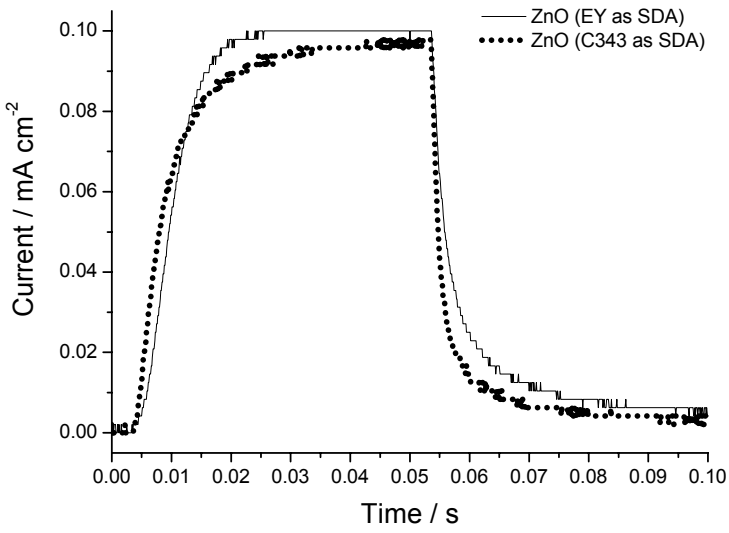

Fig. 5.42; Time-resolved photocurrents measured for ZnO films which have different orientations. Photocurrents were adjusted to the similar magnitude by changing the light intensity.

However, when the photocurrent is higher, it can be expected that the concentration of the electrons in the conduction band is also higher than the other. In such case, the traps in ZnO matrix can be filled quickly by a higher number of electrons in the conduction band. It makes these different characteristic films harder to compare. Then time-resolved photocurrents were measured at a similar magnitude of the photocurrent. The photocurrents were adjusted by adjusting the light intensity. The result of such time-resolved photocurrents is shown in Fig. 5.42.

Even when the photocurrents were adjusted to the similar magnitude, it was seen from the plots that the response of the film with C343 as SDA was faster than that of the film with EY as SDA. And when the illumination was cut off, a faster decrease of the photocurrent was observed for the film with C343 as SDA than for the film with EY as SDA, clearly speaking for either faster electron transport or less number of traps in the film.

To see the difference of the electron transport properties of those films in more detail, IMPS measurements were carried out to obtain the electron transit time in such ZnO films by using an UV-LED. The result is shown in Fig. 5.43. It should be noted that these measurements were carried out with the previous setting (see Appendix 9) and without a bias illumination. The results below 10 Hz were removed.

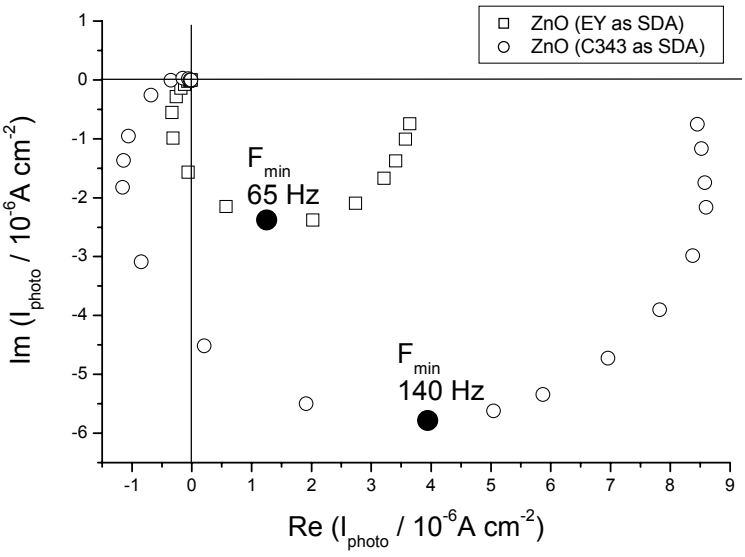

Fig. 5.43; IMPS plots of a ZnO with EY as SDA and a ZnO with C343 as SDA measured by using an UV-LED from the substrate side. 0.5 M TBAI and 0.05 M I_2 in a mixed solvent of ethylene carbonate / acetonitrile (4:1 by volume) was used as electrolyte. Note that these measurements were carried out with the previous setting without a bias illumination. (See Appendix 9)

Rather flat shapes of IMPS responses were obtained for both films. 65 and 140 Hz of f_{min} values were found from the ZnO with EY as SDA and the ZnO with C343 as SDA respectively. Since the average electron transit time can be calculated from the value, $f_{min,}$ by using the formula; $\tau_D = 1/(2 \cdot \pi \cdot f_{min})$, the transit times of the electrons for those films are found at 2.4 x 10^{-3} s and 1.1 x 10^{-3} s for the ZnO with EY as SDA and the ZnO with C343 as SDA, respectively. The larger photocurrent and the faster response for the ZnO with C343 as SDA were clearly confirmed by these IMPS data.

Such improved electron transport in porous semiconductor electrodes has become an important for the further optimization of dye- sensitized solar cells.[78,207,208] Generally, the injection time of the electron from LUMO to the conduction band of the semiconductor is much faster than the electron transit time in the nanocrystalline semiconductor matrix.[200] And it leads to a higher concentration of the electrons in the conduction band and the probability for the recombination will increase.[197] A faster electron transport property in the semiconductor is one of the solutions to reduce the recombination since the electrons injected to the conduction band of the semiconductor can be transported quickly to the external circuit before the recombination takes place. The results obtained in this section indicate that films with C343 as SDA can be a candidate for such a solution.

5.3.2. Characterization of re-ad (Eosin Y or C343) / ZnO (Eosin Y or C343 as SDA) films

In the last section, the electron transport properties of the ZnO films prepared in the presence of either EY or C343 as SDA were studied and a faster electron transport in the films with C343 as SDA was shown by the direct excitation of ZnO and hence the creation of electrons and holes. In dye- sensitized solar cells, however, there are no holes in the semiconductors since the excited electrons are created at the sensitizers and only those electrons are injected to the semiconductors. So the condition for the electron transport is different when the electrons are injected from sensitizers.

The photoelectrochemical characterizations were carried out here for the films which have different orientations and the sensitizer molecules adsorbed on the surface. EY and C343 were used as sensitizer. The films were investigated by measurements such as absorption spectrum, photocurrent transient, IMPS and IMVS. Electron transit times and lifetimes were estimated for such films. And moreover the diffusion coefficients of the electron and the diffusion lengths were obtained from IMPS results and electron lifetimes measured in IMVS.

5.3.2.1. Absorption spectrum

The absorption spectrum of the films was measured for the films investigated in this section. The spectra are shown in Fig. 5.44. A SnO_2 conductive substrate was used as reference.

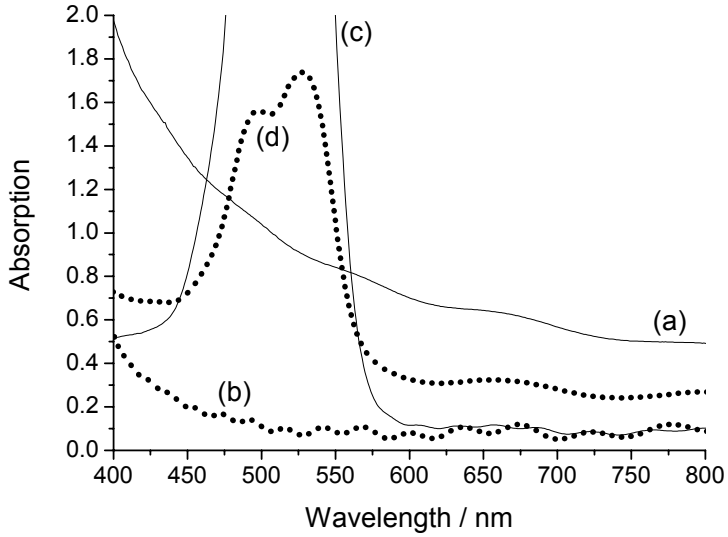

Fig. 5.44; Absorption spectra of the films; (a) re-ad C343 / ZnO (EY as SDA), (b) re-ad C343 / ZnO (C343 as SDA), (c) re-ad EY / ZnO (EY as SDA), (d) re-ad EY / ZnO (C343 as SDA). Reference: SnO_2 electrode.

The absorption was seen in the wavelengths attributed to the dye absorption in the solution. From the films which EY was adsorbed, the absorption from EY could be observed clearly, whereas the absorption was rather obscure in the films which C343 was adsorbed. The films with C343 as SDA were generally more transparent than the films with EY as SDA. The transparency of the film generally depends on the crystallinity and the size of particles. From the results of XRD and SEM, a significant difference was not observed for such factors. The reason of the different transparency is obscure so far. As one of the information, the one-step electrodeposited EY / ZnO films peel off sometimes by rinsing with water or by blowing air, whereas such a phenomenon does not appear for one-step electrodeposited C343 / ZnO films.[209] Such phenomenon must be related with the particles which were precipitated directly on the substrate at the initial stage of the deposition. Further investigations for such initial part of the precipitation are required. And it indicates the importance of the surface treatment for the substrate before the deposition. Since films with C343 as SDA have those characteristics such as high transparency and adherer property, it suggests the flexibility and easiness of films with C343 as SDA to use for the applications.

Table 6: Dye content, average film thickness, and dye concentration of the investigated films

	Dye content / 10^{-8} mol cm^{-2}	Film thickness / μm	Dye concentration / 10^{-4} mol cm^{-3}
re-ad C343 / ZnO (EY as SDA)	2.74	2.20	1.25
re-ad C343 / ZnO (C343 as SDA)	1.58	2.00	0.79
re-ad EY / ZnO (EY as SDA)	6.10	2.95	2.07
re-ad EY / ZnO (C343 as SDA)	2.50	1.90	1.32

The information about the films such as dye content, film thickness and dye concentration in the films is shown in Table 6. Since the films thickness of the films is adjusted to the similar range, the difference of the dye content reflects directly to the dye concentration in the film. The dye concentration of the films with EY as SDA is higher than the one of the films with C343 as SDA. At first sight, it seems that the adsorption of the sensitizers to the films with EY as SDA is preferred. The sensitizers might adsorb more efficiently to the surface of the 100 or the 101 plain of ZnO than the 002 plain. On the other hand, it is found by BET measurements that a film with EY as SDA has bigger surface area of 121 cm^2 / cm^2 than a film with C343 as SDA (26 cm^2 / cm^2).[173] Then a smaller amount of the dye content for the films with C343 as SDA is understandable due to its small surface area. From such point of view, the dye content can be normalized by the surface area and then it was found that the sensitizers existed in an even more condensed condition in the films with C343 as SDA. By this result, the outcome of this data is that the sensitizers have a preferable adsorption characteristic to the 002 plain of ZnO. But still the dye content for re-ad EY / ZnO (EY as SDA) is significantly higher than the others as it could be expected from the absorption spectrum of the film. It implies the preferable combination for the ZnO and the sensitizer. Since the ZnO (EY as SDA) was prepared in

the presence of EY, the surface state of ZnO might be specified for EY to adsorb.
The dye concentration in the films is one of the important factors for the photoelectrochemical performance. When the dye concentration is too high, the probability of the dye aggregation becomes higher. And when the dye concentration is too low, the probability of the recombination between the redox electrolyte and the bare semiconductor becomes higher. The optimization of such factor is necessary for electrodeposited films. Since the surface area of the semiconductor is one of the most important factors in dye-sensitized solar cells, the smaller surface area of the films with C343 as SDA is undesirable for the application. However, if the sensitizers have a preferable adsorption to the 002 plain of ZnO and if such adsorption improves the photoelectrochemical performance, such small surface area should be increased. The comparison of the films with the adjusted surface areas and dye contents would give the more critical answer for these questions.

5.3.2.2. Photocurrent transient

To see the different photoelectrochemical characteristics, photocurrent transients were measured for re-ad C343 / ZnO films and re-ad EY / ZnO films prepared in the presence of different SDAs, either EY or C343. The results are shown in Fig. 5.45 and Fig. 5.46. For the photoelectrochemical analysis, the measurements were carried out by the illumination from the substrate side. The electrolyte was 0.5 M TBAI and 0.05 M I_2 in a mixed solvent of ethylene carbonate / acetonitrile (4:1 by volume) in general. The size of the electrodes was 0.096 cm^2. A potential of -0.2 V vs.Ag/Ag^+ was applied to the electrode during the measurements. Pt wire was used as counter electrode. A blue LED for C343 and a green LED for EY were used as light source.

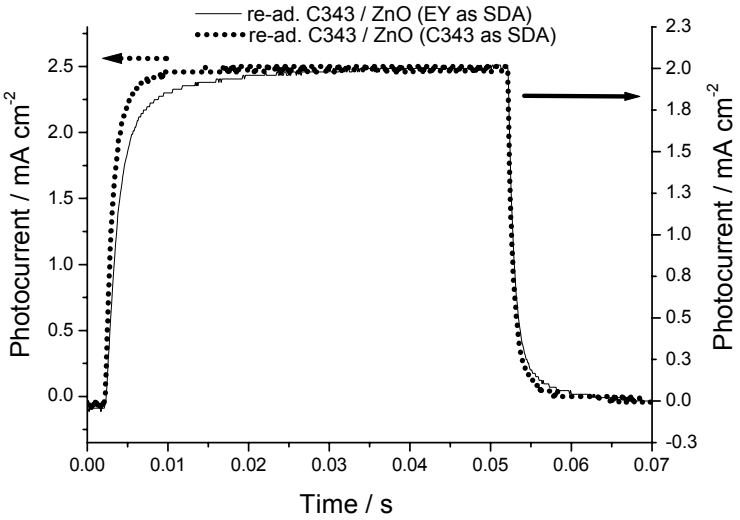

Fig. 5.45; Time-resolved photocurrents measured by using a blue LED for re-ad C343 / ZnO (EY as SDA) (solid line) and re-ad C343 / ZnO (C343 as SDA) (dashed line).

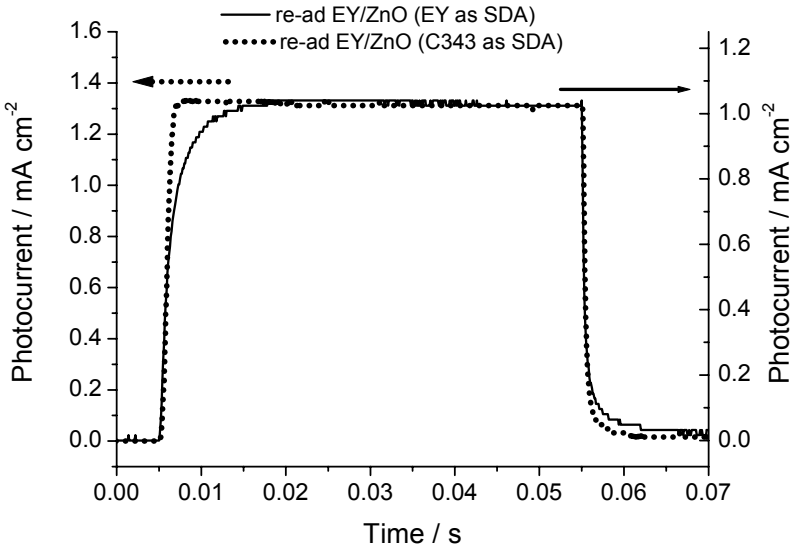

Fig. 5.46; Time-resolved photocurrent measured by using a green LED for re-ad EY / ZnO (EY as SDA) (solid line) and re-ad EY / ZnO (C343 as SDA) (dashed line). Note, for only these samples, the electrolyte of 0.5 M TBAI in the mix solvent of ethylene carbonate / acetonitrile (4:1 by volume) was used.

From Fig. 5.45, rather high photocurrents and quick responses for the illumination were observed. The light intensity of the LED is approximately 15 mW cm^{-2}. Considering the light intensity, the photocurrent is rather high. It might be related with relatively small size of the electrodes. Moreover, it should be mentioned that the measurements were carried out without using a mask. Then, the higher photocurrents might be obtained by underestimating the surface area since it was technically difficult to control the size of the contact part between the redox electrolyte and the electrode. And there is a possibility that the parts of the electrode which were out of the o-ring but had a contact with the electrolyte might have contributed some photocurrents.

For both sensitizers, the films with C343 as SDA showed a faster increase and decrease of the photocurrents with switching the illumination on and off. From these results, it suggests the faster electron transport property and/or smaller number of traps in the films with C343 as SDA also in these experiments, as it was observed for direct excitation of pure ZnO (chapter 5.3.1).
Since a significantly higher amount of EY is in the re-ad EY / ZnO (EY as SDA), such high concentration of the sensitizer effects to the absorption profile of the photons in the film and hence the profile of the photogenerated electrons. Then such an influence appeared also as a faster increase of the photocurrent. For the films of the identical absorption profiles, the improved transportation in ZnO with C343 as SDA would therefore even be more significant.

In all cases, photocurrents of approximately 1 - 2 mA cm^{-2} were observed. No overshoots

were found in any case. It indicates that the excited electrons are collected efficiently at the external circuit without problems of dye regeneration. The oxidized sensitizers following the injection of the excited electron can be recovered by the supply of an electron from the redox electrolyte. However, the photoelectrochemical efficiencies of these films have not appeared as 100 % of IPCE, as it was seen in Fig. 5.55. Since an efficient electron transport and collection can be expected from the shape of the time- resolved photocurrents and since a rather high light harvesting efficiency can also be expected by the calculation of the absorbance with the assumption that the extinction coefficients do not change from the one in the solution, the investigations so far suggest that the reason to decrease the photoelectrochemical performance is due to the electron injection efficiency from the LUMO of the sensitizer to the conduction band of the semiconductor. A more detailed investigation for such factors was carried out from the results of intensity modulated measurements. The electron transport properties of these films were compared by estimating electron diffusion coefficients and diffusion lengths.

5.3.2.3. IMPS, IMVS

IMPS and IMVS measurements were carried out to further study the photoelectrochemical properties of these films. To see the photoelectrochemical properties of different oriented films, the diffusion coefficient D_n can be obtained by using τ_n and by using the analytical solutions to fit the intensity modulated photocurrent responses. And moreover the diffusion length $L_n = (D_n\tau_n)^{1/2}$ can be obtained from the value of the diffusion coefficient and the electron lifetime. (See section 2.7) By investigating such constant, the influence of the different orientations of the ZnO is discussed.

For IMPS measurements, a potential was applied to the electrode by using the Ag/Ag^+ reference electrode. IMVS measurements were carried out in a two electrode setup. Pt wire was used as counter electrode. The electrodes were illuminated by a halogen lamp as bias illumination at the visible light intensity of 100 mW cm^{-2} and the modulation of the incident photon flux was carried out by using a blue LED for C343 and a green LED for EY respectively. From the IMPS and IMVS measurements shown here, the new setting for the light modulation (see Appendix 9) and the bias illumination were introduced. Introducing the bias illumination at a level similar to operating conditions of a prospective photovoltaic cell, beyond the monochromatic light of the LED, gives more practical situation for the analysis of the electron movement in the electrode because it gives both the electron transit time and the lifetime under working conditions and such parameters are effected by the electron concentration in the conduction band of the semiconductor. Especially for IMVS measurements, the recombination reaction with the redox electrolyte is dominated by the reaction via the conductive substrate with lower light intensity whereas it becomes minor and the recombination reaction is dominated by the reaction via the surface of the semiconductor in higher light intensity.[78,207,208]

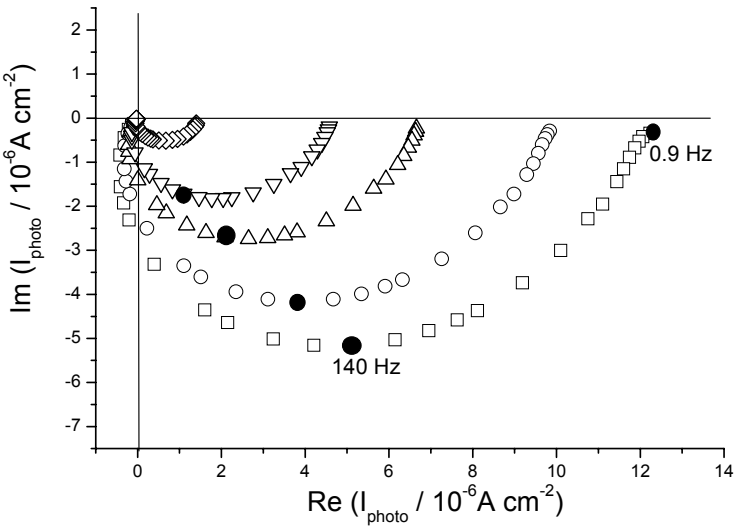

Fig. 5.47; Complex plane plot of IMPS response of re-ad C343 / ZnO (EY as SDA), measured with a blue LED and the bias white illumination. The modulated photon flux for the measurement is 0.59 x 10^{15} (□), 0.46 x 10^{15} (○), 0.29 x 10^{15} (△), 0.20 x 10^{15} (▽), 0.06 x 10^{15} (◇).

Fig. 5.47 shows typical IMPS responses measured for re-ad C343 / ZnO (EY as SDA) with several photon fluxes. The lag of the photocurrent behind the illumination with increasing the modulation frequency can be seen. Although the flattened shape of IMPS response is typical for nanocrystalline thin film electrodes,[151] rather semicircle shape of the IMPS responses were obtained for any light intensities. The obtained shape implies the fast electron transport in the ZnO matrix since flattened shape of IMPS response is characteristic for a distribution of delay times which is strongly related with the position of the electron generation.[156] It should be mentioned that the flattened shape reported by other researchers is observed from approximately 6 μm thick films and the film thickness of the measured film here is 2 μm. But the film thickness does not change the feature of the IMPS response anyway when the electrode has slow electron transport property. Efficient electron transport properties and no recombination processes are expected from these responses, because there are no responses at (+, +) quadrant in the plot and the responses tend to appear on or close to the x- axis at low frequencies. Such an outcome corresponds to the one observed in photocurrent transient measurements. Although the shape of the IMPS response was not changed by the difference of the light intensity, the values of f_{min} decreased with decreasing the light intensity. It means that the electrons take a longer time to reach to the external circuit. The responses in (-, -) quadrant are caused by either the effect of RC attenuation or the inhomogeneous distribution of the sensitizers when the electrode is illuminated from the substrate side. Consequently, the responses at (-, -) quadrant is caused by RC attenuation and the reason will be shown and discussed later in the fitting to obtain the electron diffusion coefficient.

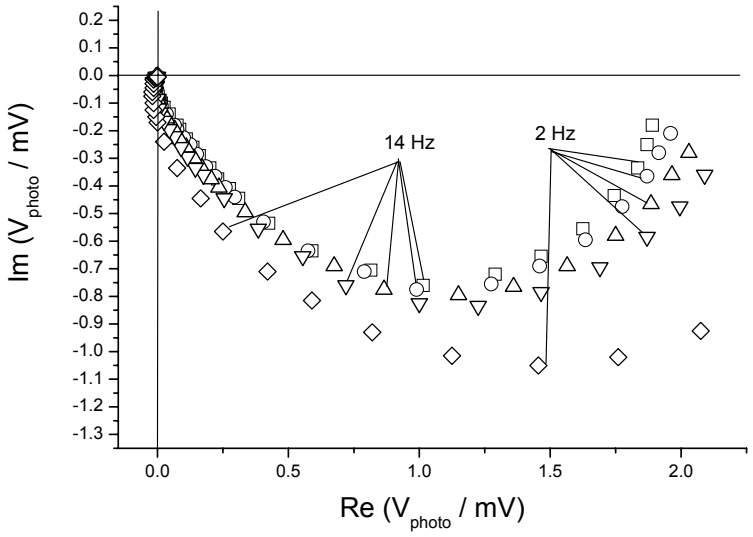

Fig. 5.48; IMVS plots of the re-ad C343 / ZnO (EY as SDA), measured with a blue LED and the bias white illumination. Photon flux for the measurement is 0.59 x 10^{15} (□), 0.46 x 10^{15} (○), 0.29 x 10^{15} (△), 0.20 x 10^{15} (▽), 0.06 x 10^{15} (◇).

IMVS was measured for re-ad C343 / ZnO (EY as SDA) at the same photon fluxes used in IMPS measurements. Using the same photon fluxes was obligatory to obtain the electron diffusion coefficient by fitting the IMPS response with the value of the electron lifetime obtained in IMVS. The photovoltage lags behind the illumination as the frequency becomes faster and it can be seen from the plot that the photovoltage lags even at 2 Hz and it becomes significant at 14 Hz. Since the change of the photovoltage mainly reflects the back reaction of the electrons with the redox electrolyte and the injected electrons from the sensitizer, such lag even in lower frequencies indicates the slow reaction of electrons with the redox electrolyte due to the longer lifetime of the electrons. It can be seen in the plot that the magnitude of the photovoltage decreases as the light intensity becomes higher. This is consistent with the finding at nanocrystalline TiO_2 electrodes that the photovoltage increases rather steeply with the light intensity in the range of lower light intensities, while the light intensity dependence becomes relatively weaker in higher light intensities.[79] The values of f_{min} decrease as the light intensity increased. It means that the back reaction of the electrons with the redox electrolyte becomes faster. It was reported by Cameron et al. that the back reactions with the redox electrolyte via the substrate are expected to occur predominately at lower light intensities.[208] To prevent such back reaction, they introduced a blocking layer under the nanocrystalline TiO_2 thin film.[208] In the case of electrodeposited ZnO films, Oekermann et al. have reported recently that the ZnO films electrodeposited in the presence of EY are rather bulky in the initial time of the deposition, approximately 4-5 minutes (approximately 0.6 μm of film thickness) and then the film becomes porous after the initial time.[160] It can be assumed that such bulky part of electrodeposited ZnO films works as blocking layer for the back reaction via the substrate.

The results of IMPS and IMVS for re-ad C343 / ZnO (EY as SDA) were shown in Fig. 5.47 and Fig. 5.48 and characteristics were discussed. Although the extents of each values such as magnitude of photocurrent, photovoltage and value of f_{min}, are not same, similar characteristics were principally observed for other films; re-ad C343 / ZnO (C343 as SDA), re-ad EY / ZnO (EY as SDA) and re-ad EY / ZnO (C343 as SDA). The results of IMPS and IMVS for all films are summarized as the electron transit times and the electron lifetimes in Fig. 5.49 and Fig. 5.50. (Further details are listed in Appendix 10)

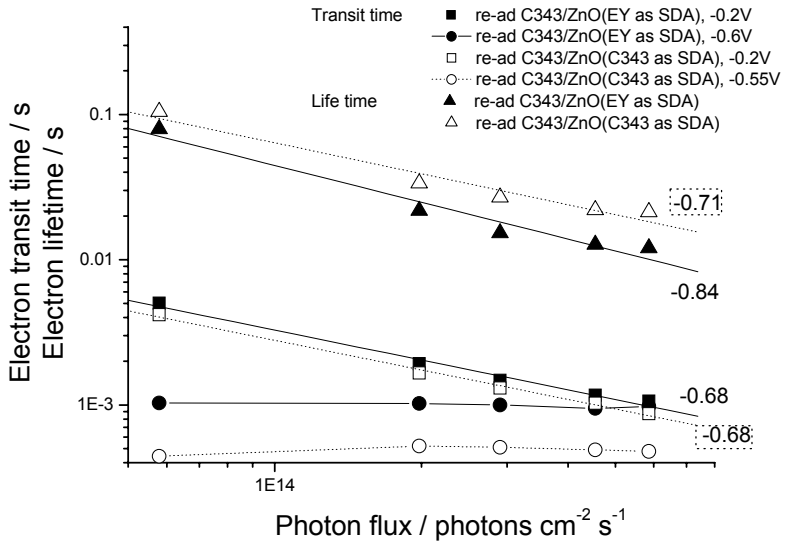

Fig. 5.49; Electron transit times τ_D and lifetimes τ_n for re-ad C343 / ZnO (EY as SDA) (τ_D = ■ at -0.2 V and ● at -0.6 V vs Ag/Ag^+, τ_n = ▲) and re-ad C343 / ZnO (C343 as SDA) (τ_D = □ at -0.2 V and ○ at -0.55 V vs Ag/Ag^+, τ_n = △) at different light intensities. The numbers described on the figure are the slope of the line.

The electron transit times obtained at -0.2 V vs. Ag/Ag^+ of the applied potential and at the potential where the dc photocurrent is close to zero, and the electron lifetimes for re-ad C343 / ZnO (EY as SDA) and re-ad C343 / ZnO (C343 as SDA) are shown in Fig. 5.49. It can be seen that both the transit time at -0.2 V vs. Ag/Ag^+ and the electron lifetime decrease as the light intensity increases. The decrease of the transit time at the higher intensities is caused by a higher trap occupancy, which leads to a higher effective diffusion coefficient because only shallow traps are able to retard electrons. And the light intensity dependence of the electron lifetime is caused by the variation of the electron transfer rate with energy level of trapped electrons.[80,162] From the plots, shorter electron transit time in re-ad C343 / ZnO (C343 as SDA) than the one of re-ad C343 / ZnO (EY as SDA) is indicated. And surprisingly, the electron lifetime of the film with C343 as SDA is longer than the one of the film with EY as SDA. Since these films are adjusted to the same range of the film thickness, the obtained results show the faster electron transport property in the film with C343 as SDA. The longer electron lifetime in the film with C343 as SDA than the film with EY as SDA is unreasonable since it can be expected that the electron has

higher possibility at an open circuit condition to react with the redox electrolyte when they can move faster in the ZnO matrix and actually these obtained values are relatively shorter compared to the values for dye- modified TiO_2 films prepared by sol-gel methods.[79,80,82,156,158,210] The most of open circuit photovoltages for the films with C343 as SDA films were slightly smaller than the films with EY as SDA. (see Fig. 5.53 or Appendix 10) Therefore smaller electron density, which can be expected from the smaller photovoltage, in the conduction band of the film with C343 as SDA than the other might effect to the electron lifetime. Or C343 might be a suitable sensitizer for the films with C343 as SDA to let the injected electrons stay longer in ZnO matrix. For both the SDA films, the difference of the electron transit time and the lifetime are almost one order. Then it can be assumed that there is enough time to collect the electrons efficiently before they recombine with the redox electrolyte. The electron transit times obtained at the potential where the dc photocurrent is close to zero do not show the dependence for the light intensity. Such tendency can be expected if IMPS responses reflect the RC time constant of the electrode.[151,160]

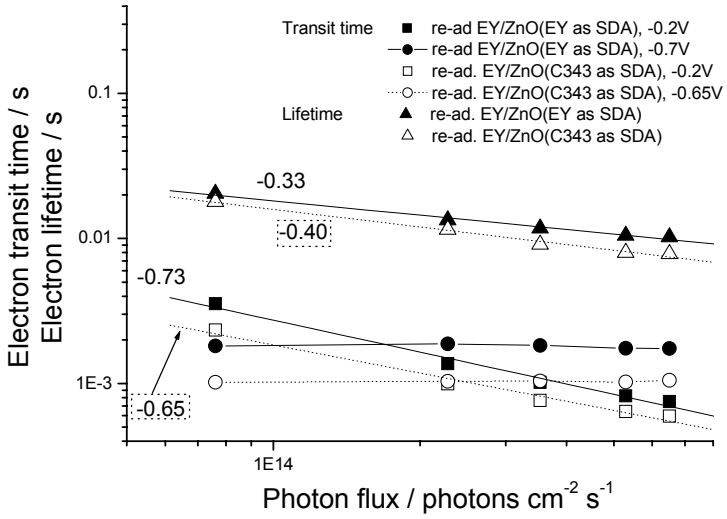

Fig. 5.50; Electron transit times τ_D and lifetimes τ_n for re-ad EY / ZnO (EY as SDA) (τ_D = ■ at -0.2 V and ● at -0.7 V vs Ag/Ag^+, τ_n = ▲) and re-ad EY / ZnO (C343 as SDA) (τ_D = □ at -0.2 V and ○ at -0.7 V vs Ag/Ag^+, τ_n = △) at the different light intensities. The numbers described on the figure are the slope of the line.

Similar results were also obtained for re-ad EY / ZnO (EY as SDA) and re-ad EY / ZnO (C343 as SDA). (Fig. 5.50) A difference is that the electron lifetimes for those films are rather shorter than the observed in Fig. 5.49. Since the electron lifetime is strongly related with the surface condition of electrodes, such different electron lifetimes indicate that the sensitizers modify the surface condition of ZnO. And it does not seem to depend on which plain of the ZnO the sensitizer adsorbs, as it could be seen in the photovoltage which showed a dependency by sensitizer. (see Fig. 5.53 or Appendix 10)
For these films, the electron lifetime for the film with C343 as SDA is shorter than the film

with EY as SDA. There seems no yield advantage if both the electron transit time and the electron lifetime become shorter. But, since the electron injection from the sensitizer is much faster than the transit time in the semiconductor, the shorter electron transit time is anyway good to reduce the kinetic redundancy in the electrode.
A similar slope for the transit time depending on the photon flux was obtained compared to the one obtained from the films with C343 as sensitizer. The obtained values are in the similar range with the values reported by other researchers.[79,82,148] On the other hand, rather large different slopes were observed for the electron lifetime. When C343 was adsorbed to the film as sensitizer, the electron lifetime becomes rather rapidly shorter as the light intensity increased, whereas the slope is much easier when EY was adsorbed to the film as sensitizer. It might imply the different or optional recombination routes when the photogenerated electrons react with the redox electrolyte. As one of the suggestions, the injected electrons might react with the redox electrolyte via the sensitizer when C343 is the sensitizer, and it does not happen when EY is the sensitizer.

To compare the electron transport properties of these different oriented ZnO films qualitatively, obtaining the effective diffusion coefficient, D_n, of these films with considering their film thickness and the dye content will leads their photoelectrochemical properties to a detailed comparison. The electron diffusion coefficients were obtained by fitting the experimental IMPS response in the product of eq (2.19) and (2.22). The examples of the fitting for re-ad C343 / ZnO (EY as SDA) and re-ad C343 / ZnO (C343 as SDA) are shown in Fig. 5.51 and Fig. 5.52 respectively.

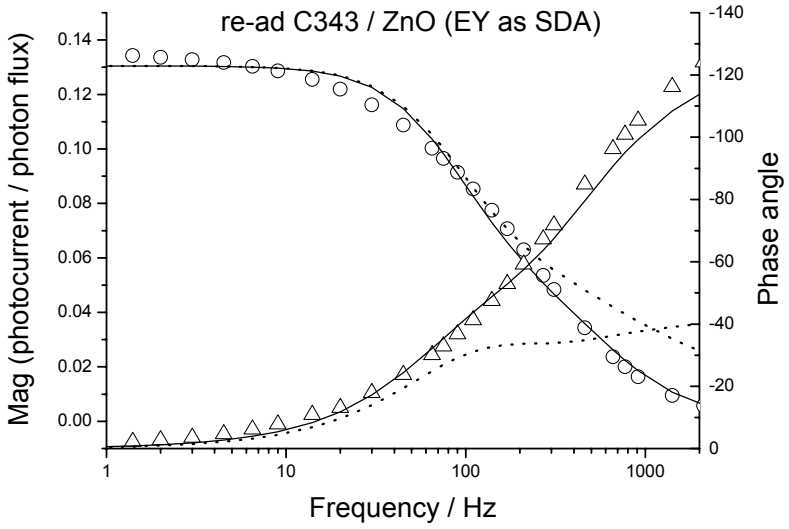

Fig. 5.51; Experimental value of IPCE (○) and phase angles (△) in IMPS for re-ad C343 / ZnO (EY as SDA). Experimental data was fitted by least-squares fits (solid line) and the dotted line is the plot in the absence of RC attenuation. The dc photocurrent was 0.15 mA / cm^{-2} during IMPS. Fitting parameter is following; photon flux $I_0 = 4.55 \times 10^{14}$ photons cm^{-2} s^{-1}, diffusion coefficient $D_n = 7.86 \times 10^{-6}$ cm^2 s^{-1}, lifetime $\tau_n = 0.01275$ s, absorption coefficient $\alpha = 5700$ cm^{-1}, film thickness d = 2.2 μm, resistance R = 10 Ω, capacitance C = 35.1 μF, injection efficiency $\Phi_{inj} = 0.206$.

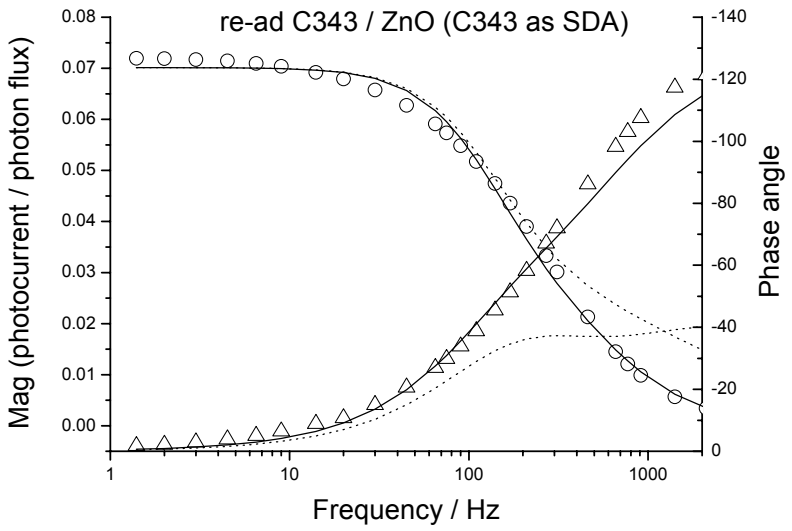

Fig. 5.52; Experimental value of IPCE (○) and phase angles (△) in IMPS for re-ad C343 / ZnO (C343 as SDA). Experimental data was fitted by least-squares fits (solid line) and the dotted line is the plot in the absence of RC attenuation. The dc photocurrent was 0.11 mA / cm^{-2} in the measurement. Fitting parameter is following; I_0 = 4.55 x 10^{14} photons cm^{-2} s^{-1}, D_n = 1.14 x 10^{-5} cm^2 s^{-1}, τ_n = 0.02202 s, α = 3600 cm^{-1}, d = 2.0 μm, R = 10 Ω, C = 30.6 μF, Φ_{inj} = 0.143.

In the equation (2.19), there are several parameters such as film thickness, absorption coefficient, electron lifetime, diffusion coefficient and injection efficiency. The film thickness and the electron lifetime were obtained by the stylus method and IMVS measurements. The absorption coefficient has a difficulty to estimate since the absorption profile of the sensitizer molecules in the film may vary by the reflection and the light scattering which depend on the crystallinity and the different size of the particles. Therefore, the values of the absorption coefficient were determined by using eq (2.8) routinely and the dye concentration in the film was calculated from the dye content in the film and the film thickness. The diffusion coefficient and the electron injection efficiency were determined by least-squares fits. In the fitting for the dye- modified TiO_2 and ZnO films prepared in colloidal method, the injection efficiency was assumed as unity and still such an assumption gives nice fits with experimental IMPS response. For electrodeposited ZnO films, however, the injection efficiency had to be set lower than unity, otherwise a nice fitting with experimental IMPS response could not be obtained, especially with the intercept. If RC attenuation was not taken into account for the fitting, good fits could not be obtained. RC attenuation was considered by multiplying eq. (2.19) to eq. (2.22). It has been found earlier that resistance and capacitance are caused by the interfaces between SnO_2 / TiO_2 and SnO_2 / electrolyte and their typical values are 10 to 20 Ω and 30 μF cm^{-2}. [155,159] In the fits carried out here, the resistance was fixed at 10 Ω. The experimental IMPS response was split into its real and imaginary component as a function of the frequency. The experimental results were fitted simultaneously for D_n, Φ_{inj}, and C by using fitting routines for least-squares fits written for the functions. In the figures, the case

when the RC attenuation is absent is also shown by inserting 0 for both R and C. Both Fig. 5.51 and Fig. 5.52 show that rather nice fits were obtained for the whole frequency when RC attenuation was involved. When the RC attenuation was absent in the fitting, on the other hand, significant deviations appear in the higher frequencies of over 300 Hz. From these results, it clearly indicates that the phenomena observed in the experiment that the phase angle exceeds -90 ° at the higher frequencies is caused by the effect of the RC attenuation. The electron diffusion coefficients of 7.86 x 10^{-6} and 1.14 x 10^{-5} cm^2 s^{-1} were obtained at the photon flux of 4.55 x 10^{14} photons cm^{-2} s^{-1} for re-ad C343 / ZnO (EY as SDA) and re-ad C343 / ZnO (C343 as SDA) respectively. From this result, it is indicated that the diffusion coefficient of the film with C343 as SDA is larger than the film with EY as SDA and therefore it can be said that the electron transport property is more efficient in the film with C343 as SDA than the film with EY as SDA. One reason of this better property is that the different orientation of ZnO and hence the different electron path way in the ZnO affects to the electron transport kinetics. Another reason is that the trap density in the film with C343 as SDA is smaller than the film with EY as SDA. The value of magnitude (Mag) for re-ad C343 / ZnO (C343 as SDA) is, however, smaller than the one of re-ad C343 / ZnO (EY as SDA). Such result is attributed to the difference of the light harvesting efficiency and the injection efficiency from the excited state of C343 to the conduction band of the ZnO. Since the light harvesting efficiencies of these films which were calculated from the absorption coefficients are 68 and 48 % for re-ad C343 / ZnO (EY as SDA) and re-ad C343 / ZnO (C343 as SDA) respectively, it can not fulfill the reason of the different magnitudes. The injection efficiency for re-ad C343 / ZnO (EY as SDA) was found by the fitting as 20.6 %, whereas 14.3 % for re-ad C343 / ZnO (C343 as SDA). Taking the light harvest efficiency and the injection efficiency into account, it was found that almost all injected electrons are collected at external circuit. The reason of the low injection efficiencies is unclear. A relatively large amount of C343 in the film compared to the surface area might form the aggregation of the sensitizer molecules or cause no binding between the sensitizer and the ZnO, and hence lower injection efficiency. The lower electron injection efficiency for re-ad C343 / ZnO (C343 as SDA) implies that there is a preferable plain for sensitizers to adsorb and to perform a better electron injection. The obtained results by fitting suggest that improving the electron injection efficiency by optimizing the adsorption condition for C343 will enhance the whole efficiency of the electrode dynamically since all injected electrons are collected at external circuit.

In Fig. 5.53, the diffusion coefficients obtained by fitting the IMPS response measured in the several photon fluxes for re-ad C343 / ZnO (C343 as SDA), re-ad C343 / ZnO (EY as SDA), re-ad EY / ZnO (C343 as SDA) and re-ad EY / ZnO (EY as SDA) are summarized as the function of the dc photocurrent and the photovoltage which were measured by the bias illumination from the halogen lamp.

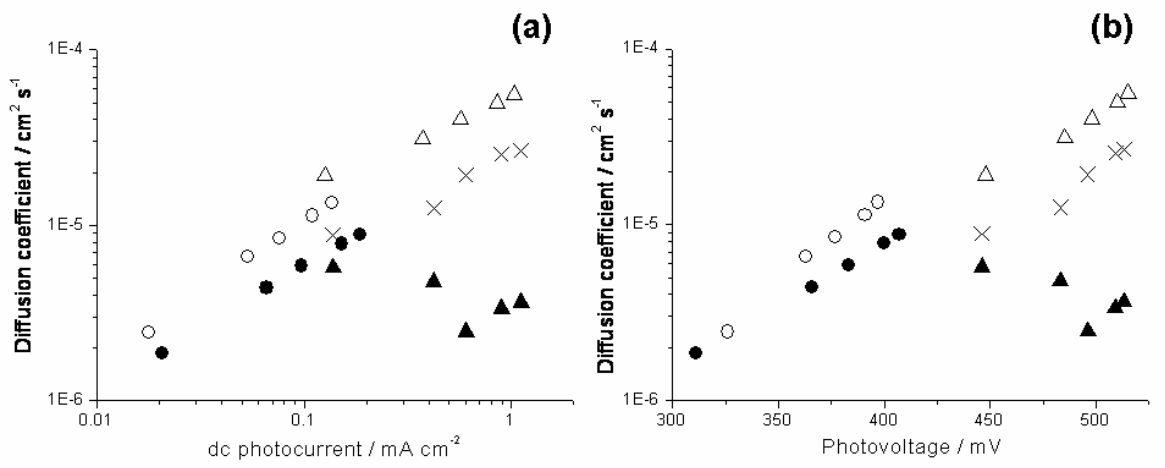

Fig. 5.53; Effective electron diffusion coefficients D_n as the function of the dc photocurrent (a) and the photovoltage (b) for re-ad C343 / ZnO (EY as SDA) (●), re-ad C343 / ZnO (C343 as SDA) (○) re-ad EY / ZnO (EY as SDA) (▲), and re-ad EY / ZnO (C343 as SDA) (△) obtained by fitting the IMPS response. The symbol (×) is the diffusion coefficient obtained when the absorption coefficient is set at 20000 for re-ad EY / ZnO (EY SDA). The parameters used for the fitting and the values obtained by fitting are indicated in Appendix 10.

Showing the obtained electron diffusion coefficients against the dc photocurrents instead of the photon flux gives a better comparison since the dc photocurrents are one of the measures for the concentration of the excess electrons in the conduction band of the ZnO and the electron diffusion coefficient is strongly related to the concentration of electrons as it can be seen from Fig. 5.53 (A). Larger electron diffusion coefficients for the films with C343 as SDA than the films with EY as SDA are clearly indicated. Although the electron diffusion coefficients are correlated to the dc photocurrents and hence the light intensity, unreasonable (nonlinear) results were obtained for re-ad EY / ZnO (EY as SDA) (▲ in Fig. 5.53). To obtain the tendency which is a linear for the dc photocurrents, the value of the absorption coefficient was modified from 43456 to 20000. Then a rather good linearity for the light intensity was obtained. (× in Fig. 5.53) It was caused by the overestimation of the adsorption coefficient. It happened also for re-ad TSPcZn / ZnO (C343 as SDA).(discussed later) As a tendency, it seems that the overestimation of the absorption coefficient happened when the film is rather transparent, although it did not happen for re-ad C343 / ZnO (C343 as SDA) which is also rather transparent. One of the reasons is that the absorption profile of the sensitizer molecules in the film might be modified by the light reflection and the scattering, while it does not happen for transparent films. Even after the modification of the absorption coefficient, the results still indicate the larger diffusion coefficients of the films with C343 as SDA. The diffusion coefficients were also plotted as function of the photovoltages. (Fig. 5.53 (b)) The photovoltage might give a better comparison of the diffusion coefficients with the function of the electron concentration in the conduction band of the ZnO than the dc photocurrent since the photocurrent would not only depend on the electron concentration, but also on other factors such as electron transport. The photovoltage is the difference between the Fermi

level in the semiconductor under illumination and the potential of the redox electrolyte. And the position of Fermi level is determined by the concentration of the electrons in the conduction band of the semiconductor. Therefore, since same redox electrolyte was used in the measurements, the magnitude of the photovoltage correlates to the position of the Fermi level of the ZnO. For this correlation, however, it must be assumed either that there is no band bending in the ZnO by the adsorption of the sensitizers or that the sensitizers cause the same band bending.[211] Interestingly, it can be seen from the plot that photovoltage is in the similar range even for differently oriented ZnO films when same sensitizer was adsorbed to the film. It indicates that the position of the Fermi level is effected by the sensitizers and hence the sensitizer plays a role to determine the position of the Fermi level in the ZnO and hence the photovoltage.[212] Considering an enhancement of the photoelectrochemical performance in dye-sensitized solar cells, finding the suitable sensitizer which has an efficient charge separation efficiency and shifts up the position of the Fermi level is the key issue. Generally, since the photocurrent in a short circuit condition has been reached almost maximum, the improvement of the open circuit photovoltage is a main subject for dye- sensitized solar cells at the moment. Therefore, the optimization of the sensitizers will be one of the solutions to improve the photoelectrochemical performance.[212] Especially, it is important for the electrodeposited ZnO films to find an optimized sensitizer since the efficient sensitizers, for example N3, N719 and so on, are optimized for TiO_2, not even for colloidal ZnO. Or the position shift of the Fermi level in the ZnO by sensitizers can be utilized to control the capacitance of the electrode. By optimizing the sensitizer for such direction, the electrodeposited ZnO film can be applied to the capacitor application.[212]

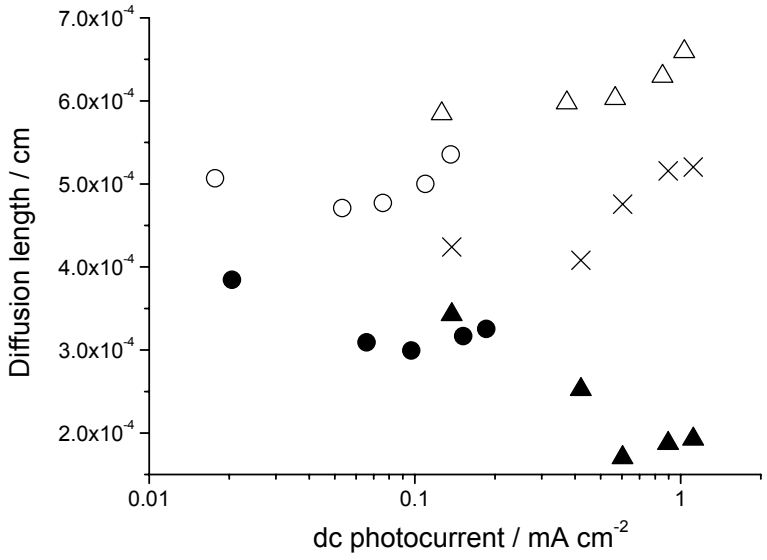

Fig. 5.54; Calculated diffusion lengths L as the function of the dc photocurrents obtained from D_n and τ_n for re-ad C343 / ZnO (EY as SDA) (●), re-ad C343 / ZnO (C343 as SDA) (○), re-ad EY / ZnO (EY as SDA) (▲) and re-ad EY / ZnO (C343 as SDA) (△). The symbol (×) is the diffusion length obtained when the absorption coefficient is set at 20000 for re-ad EY / ZnO (EY SDA).

The collection of the photogenerated electrons depends on the competition between the diffusion to the external circuit and the recombination (back reaction) with the redox electrolyte. This competition can be expressed by an electron diffusion length, $L_n = (D_n\tau_n)^{1/2}$. For the electrode which has a high photoelectrochemical performance, it should fulfill the conditions, $d > 1/\alpha$ and $d < L_n$ simultaneously. The diffusion lengths for the films studied here are calculated by using D_n and τ_n obtained by fitting the IMPS response and the f_{min} in IMVS respectively and shown in Fig. 5.54 as function of the dc photocurrents. Except for re-ad EY / ZnO (EY as SDA) (▲ in Fig. 5.54) with the absorption coefficient obtained routinely, all diffusion lengths are clearly larger than the film thickness, as needed. It means that all photogenerated and injected electrons are collected at the external circuit efficiently. A linear dependence of the diffusion lengths for the dc photocurrent and hence the light intensity was not clearly observed. Since the electron lifetime and the diffusion coefficient changes in opposite sense for the change of the light intensity, the electron diffusion length is only weakly dependent for the light intensity. Larger diffusion coefficients were obtained for the films with C343 as SDA than the films with EY as SDA. Since the difference of the electron lifetime for these differently oriented films were not significant, the relatively larger difference of the electron diffusion coefficients reflects to the diffusion length. By the investigations so far, it was indicated that the films with C343 as SDA have larger electron diffusion coefficients and diffusion lengths and hence better electron transport properties in the ZnO matrix than the films with EY as SDA.

Photocurrent action spectra (Fig. 5.55) measured for films prepared in the corresponding way clearly prove the high efficiency of these films as photoelectrodes.[194]

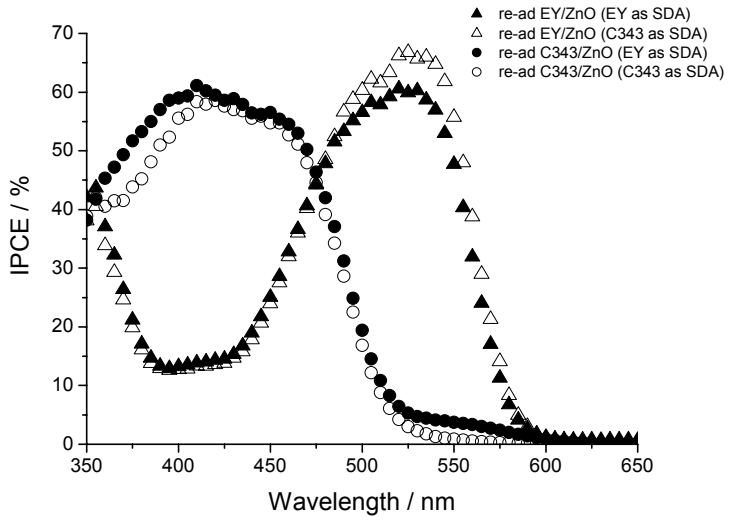

Fig. 5.55; Photocurrent action spectra measured for re-ad EY / ZnO (EY as SDA), (■), re-ad EY / ZnO (C343 as SDA), (□), re-ad C343 / ZnO (EY as SDA), (●), re-ad C343 / ZnO (C343 as SDA), (○). Note, data obtained by H. Hattori, Gifu University for the films prepared in parallel under the comparable conditions.

Although the film with C343 as SDA has an even improved electron transport property, however, such better characteristics do not directly lead to a further enhanced photoelectrochemical performance. It seems that the photoelectrochemical performance of the films with C343 as SDA is reduced by a relatively lower electron injection efficiency from the sensitizer to the semiconductor. The adsorption of the sensitizer to the 002 plain of ZnO might not be appropriate for the injection of the excited electrons. Or relatively higher amount of the sensitizer molecules compared to the surface area of the film with C343 as SDA found by BET measurements leads to the ineffective sensitizer molecules in the film and hence lower electron injection efficiencies. If the latter was the reason, increasing the surface area and optimizing the adsorption condition for sensitizers will improve the photoelectrochemical performance.

5.3.3. TSPcZn as sensitizer in transport-optimized films

In the last section, the films were prepared in the presence of either EY or C343 as SDA and such molecules were used later as sensitizers following the extraction of SDA. However, such molecules used for the surface modification (SDA) might create the preferable adsorption sites in the ZnO matrix when same molecules were adsorbed on the film as sensitizer. Other sensitizers can be used to allow an independent analysis of the differently oriented ZnO. TSPcZn was used as sensitizer in this section. As indicated above, it is also an interesting sensitizer by itself since it can efficiently utilize the red part of the visible spectrum and perform at high stability. As above, the deposition of the films and the extraction of SDA molecules have been carried out by collaboration partners in Gifu University, and the adsorption of TSPcZn was carried out in University of Giessen.

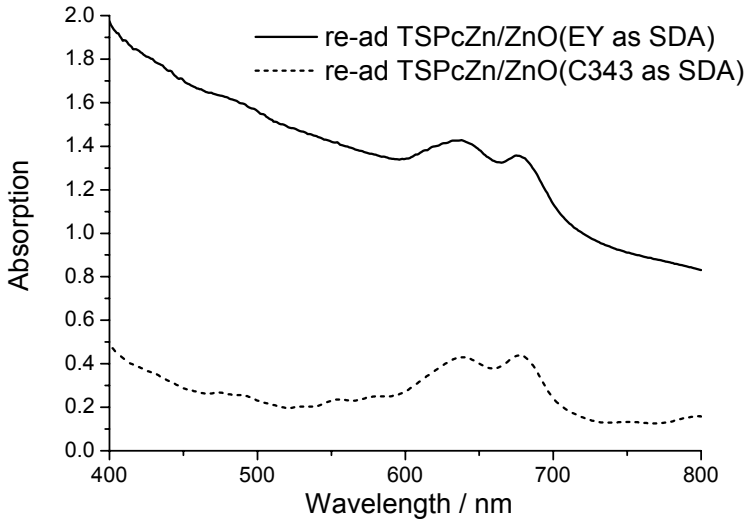

Fig. 5.56; Absorption spectra for re-ad TSPcZn / ZnO (EY as SDA), (solid line), and re-ad TSPcZn / ZnO (C343 as SDA), (dashed line). A SnO2 glass was used as reference.

The absorption spectra of the films are shown in Fig. 5.56. The absorption peaks which are corresponding to the Q- band of TSPcZn can be seen from the spectra. A rather strong light scattering was seen for re-ad TSPcZn / ZnO (EY as SDA), whereas re-ad TSPcZn / ZnO (C343 as SDA) was rather transparent. The amount of dye loaded in the film and the film thickness are almost identical for both films and hence is the dye concentration in the films. (Table 7) However, the surface area of the bare ZnO (C343 as SDA) was found smaller than the one of the films with EY as SDA[173] It implies more concentrated TSPcZn molecules on the inner surfaces of the film with C343 as SDA fortunately not leading, however, to increased aggregation as clearly seen by quite constant Uv-Vis spectra.

Table 7: Dye content, average film thickness, and dye concentration of the investigated films

	Dye content / 10^{-9} mol cm^{-2}	Film thickness / µm	Dye concentration / 10^{-5} mol cm^{-3}
re-ad TSPcZn / ZnO (EY as SDA)	4.46	2.46	1.81
re-ad TSPcZn / ZnO (C343 as SDA)	4.51	2.60	1.74

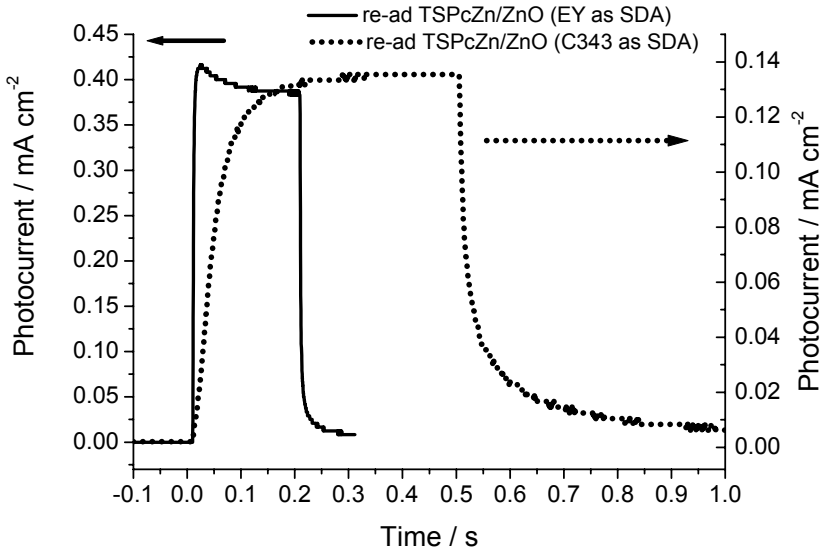

Fig. 5.57; Time-resolved photocurrents measured by using a red LED for re-ad TSPcZn / ZnO (EY as SDA) (solid line) and re-ad TSPcZn / ZnO (C343 as SDA) (dashed line).

The time- resolved photocurrents measured for re-ad TSPcZn / ZnO (EY as SDA) and re-ad TSPcZn / ZnO (C343 as SDA) are shown in Fig. 5.57. The re-ad TSPcZn / ZnO (EY as SDA) showed a rapid increase of the photocurrent as the illumination started and an overshoot was observed. Indicating the recombination reactions which are caused by slow hole transfer to the redox electrolyte. Such phenomenon can be seen when the electron collection in the electrode is so rapid.[185] For re-ad TSPcZn / ZnO (C343 as SDA), it took a rather long time of about 300 ms to reach the steady- state photocurrent speaking for a

large number of traps in the film. An active role of the sensitizer in the different ZnO matrices as already suggested in the last section is thereby shown and the complexity of the optimization of such electrodes is seen.

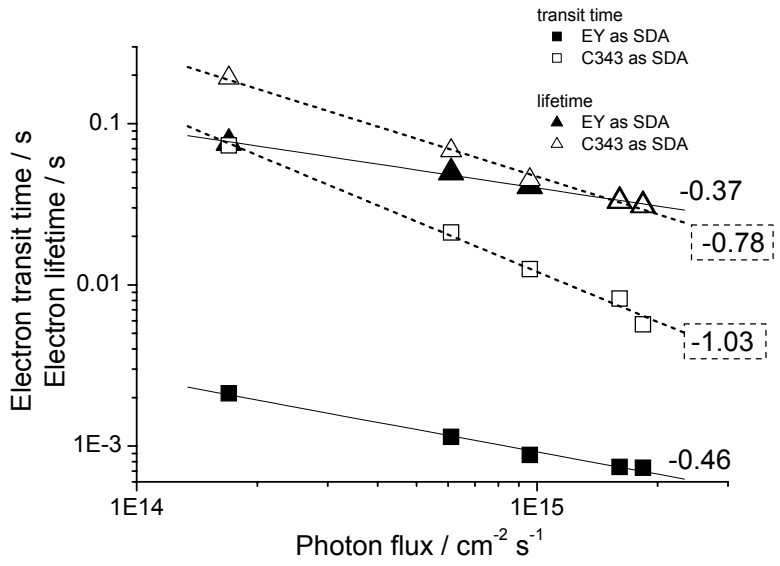

Fig. 5.58; Electron transit times τ_D and lifetimes τ_n for re-ad TSPcZn / ZnO (EY as SDA) (τ_D = ■ at -0.2 V vs. Ag/Ag^+, τ_n = ▲) and re-ad TSPcZn / ZnO (C343 as SDA) (τ_D = □ at -0.2 V vs. Ag/Ag^+, τ_n = △) at the different light intensities. The numbers described on the figure are the slope of the line.

The electron transit times and the electron lifetimes for these films were also obtained by IMPS and IMVS measurements and the time constants are shown in Fig. 5.58. As it was observed for other films, the electron transit time becomes shorter with increasing light intensity, which is caused by the higher electron density in the conduction band of the ZnO to fill the deep traps. Similarly the electron lifetime becomes shorter as the light intensity becomes higher. Higher electron density in the conduction band of ZnO leads to the higher possibility for the photogenerated electrons to recombine with the redox electrolyte. Significantly shorter electron transit time, the difference of approximately one order, for re-ad TSPcZn / ZnO (EY as SDA) compared to re-ad TSPcZn / ZnO (C343 as SDA) was found, whereas the electron lifetime was in similar time range for both films. The electron transit time of re-ad TSPcZn / ZnO (EY as SDA) is more than one order shorter than the electron lifetime in the film. So, efficient collection efficiency could be expected. However, it was observed clearly in the time- resolved photocurrent that there is an evidence of the recombination; a peak and a relaxation following the illumination starts. And the sign of the recombination was also seen in IMPS (not shown) as the responses in (+, +) quadrant. A relatively small difference of the electron transit time and the electron lifetime was found for re-ad TSPcZn / ZnO (C343 as SDA). Significantly steep slope implies the high density of traps in the ZnO matrix. These obtained results for both films again indicate the active role of the dye / ZnO interplay. One of the reasons is that the

photoelectrochemical properties of TSPcZn / ZnO strongly depend on the plain of ZnO where TSPcZn molecules adsorb or the role that it plays in suppressing the back reactions or compensating the trap levels. However, since a typical shape of the time- resolve photocurrent for re-ad TSPcZn / ZnO (EY as SDA) is shown in Fig. 5.16, the shape of the time- resolved photocurrent shown here is untypical.

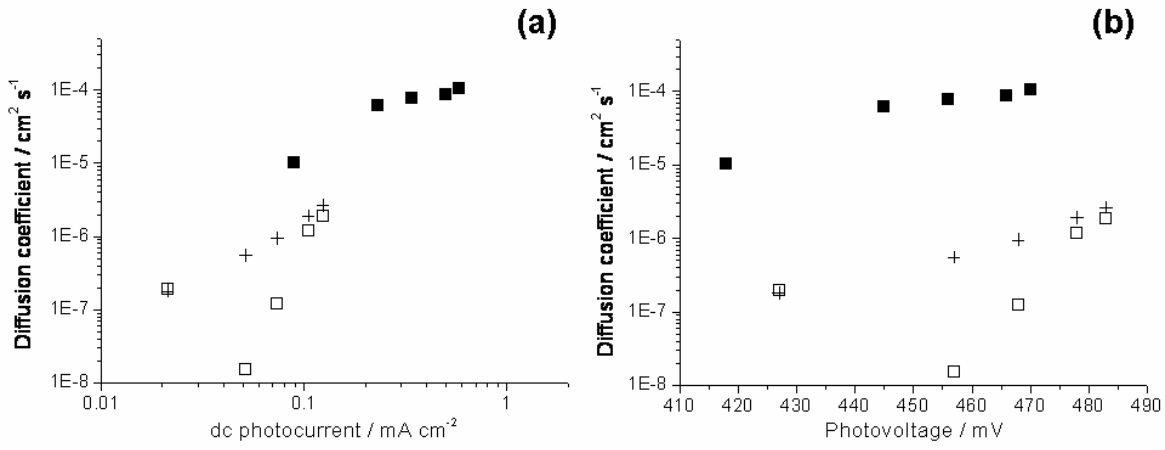

Fig. 5.59; Effective electron diffusion coefficients D_n as the function of the dc photocurrents (a) and the photovoltages (b) for re-ad TSPcZn / ZnO (EY as SDA) (■) and re-ad TSPcZn / ZnO (C343 as SDA) (□) obtained by fitting the IMPS response. The symbol (+) is the diffusion coefficient obtained when the absorption coefficient is set at 1000 for re-ad TSPcZn / ZnO (C343 SDA). The parameters used for the fitting and the values obtained by fitting are indicated in Appendix 10.

The electron diffusion coefficients were obtained for these films. (Fig. 5.59) Since these films have a similar dye content, film thickness and electron lifetime, the difference of the electron transit time reflects the differences in their electron diffusion coefficients. Again, the effective absorption coefficient had to be modified in order to obtain reasonable plots. (+ in Fig. 5.59) First of all, the calculation of the absorption coefficient from the dye concentration in the film will lead to an unavoidable deviation since TSPcZn molecules form the aggregation. And moreover, since the parameters like the dye content and the film thickness are almost same for these films (Table 7), the routine calculation for determination of the absorption coefficient gives almost similar values. However it is obvious from their absorption spectra (Fig. 5.56) that the absorption profile for those films is completely different by the light scattering. Nevertheless, larger diffusion coefficients were found for re-ad TSPcZn / ZnO (EY as SDA) than for re-ad TSPcZn / ZnO (C343 as SDA). This result stays opposite to the results in the last section and indicates the complicated role of the sensitizer both in the back reactions and the trap compensation, caused, for example, by adsorption of the same TSPcZn sensitizer on different plains of the two ZnO matrices. It should be noted, however, these films were prepared and SDA molecules were removed in Gifu University and only the adsorption of TSPcZn was carried out in Giessen. There were some weeks between the extraction of SDA molecules and the adsorption of the sensitizer. Normally, these procedures were carried within just two days. Then, such unusual interval could change their surface condition.

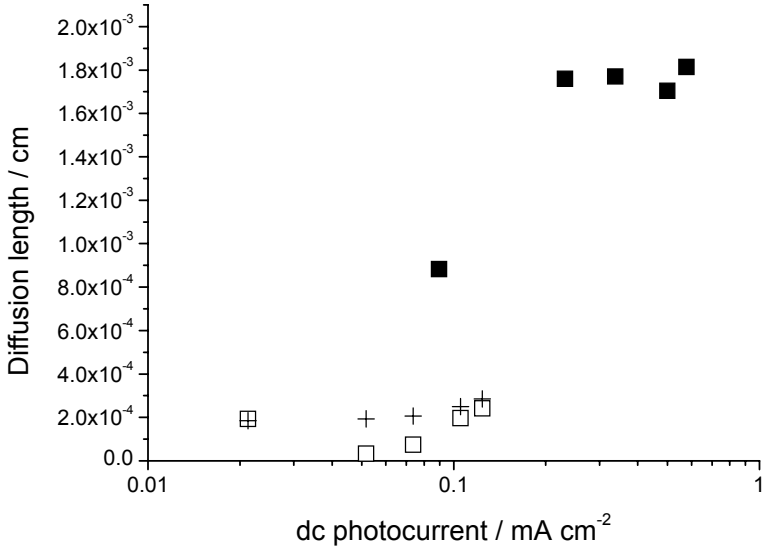

Fig. 5.60; Calculated diffusion lengths L as the function of the dc photocurrents for re-ad TSPcZn / ZnO (EY as SDA) (■) and re-ad TSPcZn / ZnO (C343 as SDA) (□) obtained from D_n and τ_n. The symbol (+) is the diffusion length obtained when the absorption coefficient is set at 1000 for re-ad TSPcZn / ZnO (C343 SDA).

The diffusion lengths were also calculated for these films. (Fig. 5.60) It was also shown here that the diffusion length is weakly dependent on the light intensity due to the compensation between the diffusion coefficient and the electron lifetime which changes in opposite sense to the light intensity. The relatively large diffusion coefficients of re-ad TSPcZn / ZnO (EY as SDA) reflect also to the diffusion length, obtained values exceeded significantly its films thickness, whereas the diffusion lengths for re-ad TSPcZn / ZnO (C343 as SDA) exceeded its film thickness only when the light intensity is strong, otherwise they are smaller than the film thickness, already indicating an inefficient collection.

Consequently, better photoelectrochemical properties were found for the film with EY as SDA when TSPcZn was used as sensitizer. It indicates that TSPcZn might have a preferable plain to adsorb and the difference of the adsorbed plain might significantly influence the electron transport property of the ZnO matrix. To compare the different oriented ZnO films further, other sensitizers should be tested.

5.3.4. Summary

The electron transport properties of the electrodeposited ZnO films which have different orientations have been compared by the photoelectrochemical analysis in this section. The orientation of the ZnO film was controlled by the choice of SDA for the electrochemical

deposition; either Eosin Y (EY) or Coumarin 343 (C343). It could be expected that the different electron path way due to the different orientations influences electron transport and that the photoelectrochemical performance of the electrode gets an influence by using another kind of SDA for the deposition. Since the kinetic difference between the fast electron injection and the relatively slow electron transport in the semiconductor matrix increases the electron density in the conduction band of the semiconductor and hence the probability of the recombination with the redox electrolyte, a faster electron transport property in the semiconductor matrix is attractive to minimize the kinetic redundancy and increase the collection efficiency. The photoelectrochemical characterization for these films with either EY or C343 as SDA was carried out for the ZnO films without sensitizer and with EY, C343 or TSPcZn as sensitizer.

The results of photocurrent transients and IMPS for the ZnO films without sensitizer showed that the films with C343 as SDA have faster electron transport properties. The faster increase and decrease of the photocurrent in the photocurrent transient measurements were observed for ZnO with C343 as SDA as the illumination started and cut off, and also the shorter transit time was found for the ZnO (C343 as SDA) in IMPS. The same was also concluded in the analysis with either EY or C343 as sensitizer. By considering the film thickness, the absorption profile and the electron lifetime, the electron diffusion coefficients were estimated for those films and the larger diffusion coefficients of $2 \times 10^{-6} - 5 \times 10^{-5}$ cm^2 s^{-1} for 0.02 – 1 mA cm^{-2} of the dc photocurrents were obtained from the films with C343 as SDA. By using C343 as SDA for the preparation of ZnO, electrodes with a faster electron transport can be obtained and this can be utilized to minimize the kinetic redundancy. However, the higher photoelectrochemical efficiency did not appear in the films with C343 as SDA than in the films with EY as SDA. It is due to the relatively smaller surface area and the lower electron injection efficiency. And moreover, although the discussion is not finished completely yet, it was found that there seems a preferable plain to adsorb for TSPcZn in the investigation with TSPcZn as sensitizer and it effects the photoelectrochemical performance. Since the films with C343 as SDA generally showed faster electron transport, by optimizing some parameters such as the surface area and the adsorption condition for the sensitizer, the photoelectrochemical efficiencies of electrodeposited ZnO films can be improved further.

5.4. Conclusion for this chapter

Photoelectrochemical properties of dye / ZnO films have been studied in this chapter for the application of dye- sensitized solar cells. The electrochemical deposition of ZnO in the presence of structure directing agents (SDA) such as Eosin Y (EY), sodium dodecyl sulfate (SDS) or Coumarin 343 (C343) gives the ZnO films which have a characteristic morphology, structure, orientation and high porosity. By extracting SDA molecules from the surface of the ZnO, the surface area of the film has been increased approximately from 1 – 2 cm^2 / cm^2 to typically 400 cm^2 / cm^2 and up to 1183 cm^2 / cm^2. Adsorbing the sensitizer to such porous ZnO films, the photoelectrochemical efficiency of the electrodeposited ZnO films (re-ad dye / ZnO) has been improved significantly, for example, 2.8 % of IPCE (Incident Photon to Current conversion Efficiency) at 525 nm in the one-step electrodeposited EY / ZnO has improved to 48 % of IPCE in re-ad EY / ZnO (EY as SDA). The results obtained in the study with EY as SDA indicate the importance of the surface area and the extraction of SDA molecules for obtaining the good photoelectrochemical performance. By the study with TSPcZn as sensitizer which was aimed to enhance the photoelectrochemical efficiency in the red part of the visible light, the highest IPCE of 31 % was obtained at 680 nm. It is a relatively high efficiency in such wavelength when considering the advantage of the fabrication procedure that it does not need any heat treatment.

The outcome that EY molecules are acting as SDA during the deposition to modify the ZnO structure opened the new concept to use a specific SDA molecule to increase the surface area and SDS was introduced as SDA for the deposition. By using SDS as SDA and following the extraction of SDS by using aqueous KOH or ethanol, the surface area was increased. But such large surface area did not increase the amount of the dye loaded in the film and hence the photoelectrochemical performance. It seems that SDS which stays in the film interacts with the sensitizer to depress the adsorption of sensitizers or the influence of SDS to the ZnO surface is not suitable for the adsorption. The influence of SDS to ZnO could be observed also in the photoelectrochemical analysis as a relatively slow electron transport property in the ZnO which indicates high density of traps. SDS was an attractive SDA to increase the surface area of the ZnO. However, the obtained results showed the unfavorable influences to the photoelectrochemical performance, caused by the SDS molecules stayed in the film. Quantitative analysis is necessary to know the influence of SDS to the ZnO and such analysis will support to improve their property for the photovoltaic application.

By utilizing the advantage of the electrochemical deposition, the orientation of the electrodeposited ZnO film can be changed. By using C343 as SDA instead of EY, the orientation of the electrodeposited ZnO film was turned 90 °. The influence of such differently oriented ZnO films to the photoelectrochemical properties showed the faster

increase of the photocurrents with the start of the illumination and the shorter electron transit times from the films with C343 as SDA than the films with EY as SDA. The electron diffusion coefficients were obtained by fitting the IMPS (Intensity Modulated Photocurrent Spectroscopy) responses with considering the film thickness, the absorption coefficient and the electron lifetime. It was found that ZnO with C343 as SDA has larger diffusion coefficients. Such better electron transport properties, however, have not appeared as higher photoelectrochemical efficiencies than the films with EY as SDA. It is due to the smaller surface area and the lower electron injection efficiency than the one of the films with EY as SDA. From the results obtained here, it can be suggested that the films with C343 as SDA has a higher possibility to improve the photoelectrochemical efficiency of the electrodeposited ZnO films further.

6. Conclusion and Outlook

Photoelectrochemical characterizations of the dye / ZnO electrode prepared by electrochemical deposition were carried out to optimize the ZnO matrix and enhance the photoelectrochemical efficiencies in the red part of the visible light. The dye / ZnO hybrid thin films were prepared in one-step and in low temperature of 70 ° by the electrochemical deposition in the presence of dye molecules. Such simple and low temperature process is one of the suitable methods to prepare the electrode for dye- sensitized solar cells. However, the properties of the electrodeposited ZnO were significantly influenced by the dye which was present in the deposition bath and the influence of the dye to the deposition of ZnO differed by each dyes. And moreover, the surface area of such dye / ZnO films was found close to 1 – 2 cm^2 / cm^2 since there was a tendency that the excess amount of dye molecules adsorbs to ZnO and such molecules filled the fine pores in the film. Such phenomena resulted in poor photoelectrochemical efficiencies.

Utilizing Eosin Y (EY) as structure directing agent (SDA) was a wise solution to obtain a highly porous and single crystalline ZnO. Extracting EY and adsorbing a sensitizer to ZnO (re-ad dye / ZnO) gave almost ideal structures for dye- sensitized solar cells. And the photoelectrochemical performance, especially under a short circuit condition, has been improved significantly.

Further subject for the application is the enhancement of the photovoltage. The photovoltage of the electrode seemed to be determined by the sensitizer. Therefore, the efficiency of the electrode is strongly correlated to the choice of the sensitizer. Further improvement of the photoelectrochemical efficiency depends on the finding or developing the ideal sensitizer which adsorbs the photons in the wide range of the visible light, injects the excited electrons efficiently to the conduction band of ZnO and keeps the Fermi- level of ZnO at higher position for the higher photovoltage.

Acknowledgment

This work was performed in the Institute for Pure and Applied Chemistry of Carl-vol-Ossietzky-University Oldenburg (4.2002 – 3.2004) and in the Institute of Applied Physics of the Justus-Liebig-University (4.2004 – 3.2006). And some experiments like photocurrent action spectrum measurement and I-V measurement were performed during research stays at Environmental and Renewable Energy Systems, graduate school of engineering in Gifu University (Japan).

First of all, I thank Prof. Dr. Derck Schlettwein for the kind offer to do PhD work in Germany and for supporting my whole PhD work.

Equally, I thank the members of a join research project on "Nanoparticulate dye-semiconductor hybrid materials formed by electrochemical self-assembly as electrodes in photoelectrochemical cells." supported by the Volkswagen Foundation, Dr. Esther Michaelis, Prof. Dr. Dieter Wöhrle, Prof. Dr. Nils Jaeger (University of Bremen), Dipl. Chem. Peter Kunze, Dipl. Phys. Jens Reemts, Dr. Achim Kittel, Prof. Dr. Katharina Al-Shamery, Prof. Dr. Jürgen Parisi (University of Oldenburg), Dr. Torsten Oekermann, Dr. Michael Wark (University of Hannover), Prof. Dr. Hideki Minoura and Prof. Dr. Tsukasa Yoshida (Gifu University) for continued fruitful discussions and numerous helpful suggestions.

I thank to

- All colleagues in AG Schlettwein, specially Dipl. Chem. Christian Kelting and Dipl. Chem. Thomas Loewenstein for the help and discussion to progress my work, and many supports and a lot of fun for the life in Germany.
- Dr. Esther Michaelis for the sample preparation and discussion.
- Dr. Torsten Oekermann for the many helps and the advices to understand photoelectrochemical measurements (Photocurrent transients, IMPS, IMVS)
- Dr. Jiri Rathousky (J. Heyrovsky Institute, Czech Republic) for BET measurement.
- Dr. Yan Shen, Dr. Chuan Zhao and Prof. Dr. Gunther Wittstock for the collaboration work
- Dr. Thierry Pauporte and Prof. Dr. Daniel Lincot (CNRS, France) for the collaboration and discussion.
- Dr. rer. Nat. habil. Andreas G. Neudeck (Chemical and Physical Research Thuringia-Vogtland Textile Research Institute) for the supply of conductive textile electrodes.
- Dipl. Phys. Thorsten Wagner for the help in mathematics to fit the IMPS plot.
- MS. Sc. Seiichi Sawatani for the discussion and the support when I did measurements in Gifu University.
- Prof. Hideki Minoura, Prof. Tsukasa Yoshida, MS. Sc. Daisuke Komatsu, Mr. Keigo

Ichinose and Mr. Shinya Hattori for the discussion, the sample preparation, the supply of data and the helpful advices.

- All people in the tennis club, “Polizeisportverein Oldenburg e. V.” for the nice time and a lot of fun in tennis.

I thank for the financial support from the Volkswagen foundation.

Finally I thank all my family, especially my parents for support and understanding to do my PhD study in Germany.

March 2006, Giessen
Kazuteru Nonomura

Appendix

Appendix 1 List of Symbols

A	absorbance
AM	air mass
C	capacitance
c	the concentration of absorbing species in the material
C343	Coumarin 343
CE	counter electrode
D_{cb}	diffusion coefficient of electrons in the conduction band
D_n	electron diffusion coefficient
D_0	the electron diffusivity in the dark
d	film thickness
EY	Eosin Y
f	modulation frequency
FF	fill factor
HOMO	highest occupied molecular orbital
I_0	the intensity of the incident light
I_1	the intensity after passing through the material
I_{sc}	Short circuit photocurrent
IMPS	intensity modulated photocurrent spectroscopy
IMVS	intensity modulated photovoltage spectroscopy
IPCE	incident photon to current conversion efficiency
j_{photo}	photocurrent
j_{ss}	steady states photocurrent
LUMO	lowest unoccupied molecular orbital
k	Boltzman constant
k_{ext}	rate constant for electron extraction at the substrate
k_t	first-order rate constant for trapping
k_d	first-order rate constant for detrapping
L_n	diffusion length
l	path length
LHE	light harvesting efficiency
n	the electron density under illumination
n_0	the equilibrium electron concentration in the dark
N3	[Ru(dcbpyH2)2(NCS)2] (dcbpyH = 2,2'-bipyridyl-4,4'-dicarboxylic acid)
N719	$(Bu_4N)_2[Ru(dcbpyH)_2(NCS)_2]$
q	the elementary charge
R	resistance
RDE	rotating disk electrode
RE	reference electrode

SDA structure-directing agent
SDS sodium dodecyl sulfate
T transmittance
TCTPPPd 5, 10, 15, 20-Tetrakis-(4-carboxyphenyl)-porphyrin-Pd (II)
TCTPPPt 5, 10, 15, 20-Tetrakis-(4-carboxyphenyl)-porphyrin-Pt (II)
TSPcZn 2,9,16,23-tetrasulfophthalocyaninatozinc
TSTPPZn 5,10,15,20-tetrakis-(4-sulfonatophenyl)porphyrinatozinc
V_{oc} Open circuit photovoltage
WE working electrode

α absorption coefficient
ε molar absorption coefficient
Φ_{inj} quantum yield for charge injection
η conversion efficiency
η_c charge collection efficiency
λ wavelength
τ_d transit time
τ_n electron lifetime

Appendix 2 Information for sensitizers

Table 8; Information of sensitizers, molecular weight, lambda maximum and molar absorption coefficient.

	Molecular weight / g mol^{-1}	Lambda max / nm	solvent	Molar absorption coefficient / M^{-1} cm^{-1}
Eosin Y[213]	691.9	514	water	91600
Coumarin 343[214]	285.3	409	ethanol	19900
TSTPPZn*	998.0	420	7N NH_3aq	178633
TSPcZn[66]	986.1	680	water	155800

* obtained by collaboration partner in University of Bremen, and used in this work. (Note, the value is different from which found in ref. 65)

Appendix 3 The spectrum of the filters used in Photocurrent transient measurement

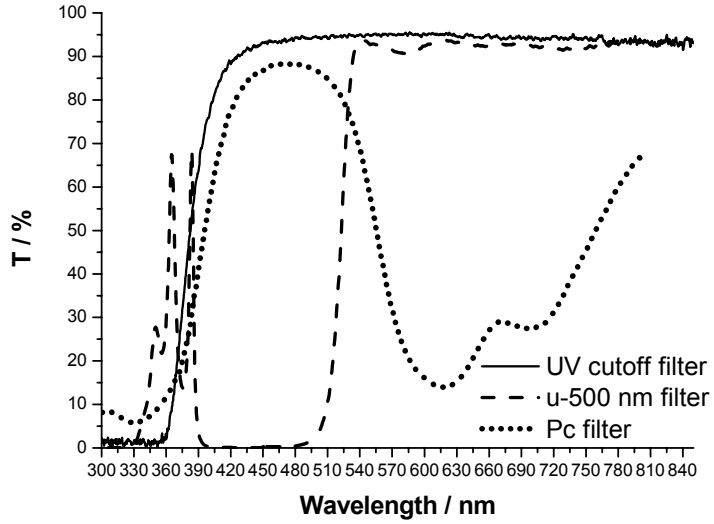

Fig.0.1; The transmission spectrum of UV cutoff filter, under 500 nm cutoff filter, and Pc filter. Those filters were used in photocurrent transient measurement.

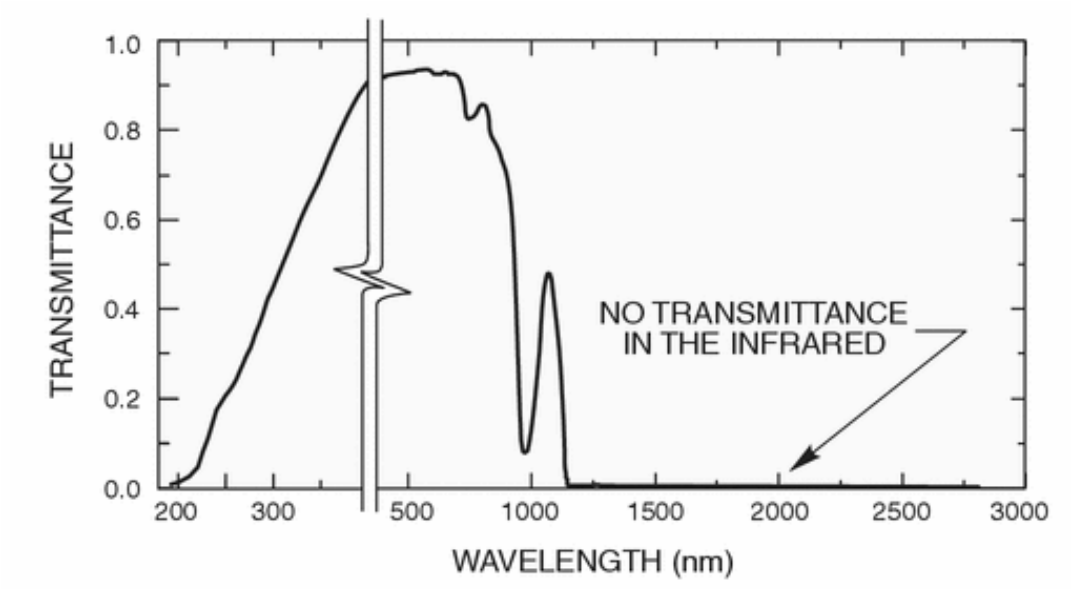

Fig. 0.2; Transmittance of liquid filter with distilled water. (taken from reference; ２１５)

Appendix 4 Spectrum of the LEDs used for photocurrent transient, IMPS and IMVS

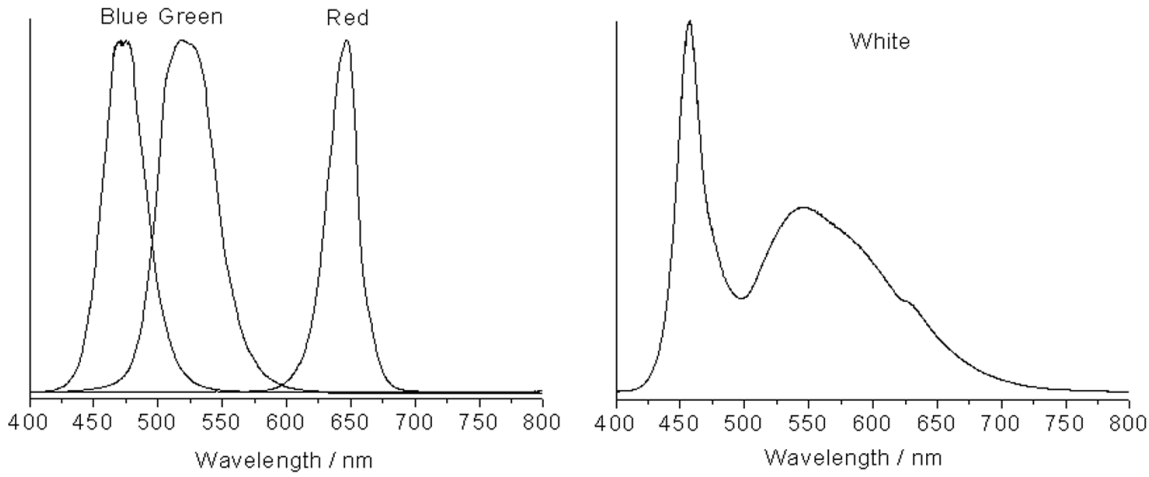

Fig. 0.3; The spectra of LEDs used in photocurrent transient measurements, IMPS and IMVS.

Appendix 5 The response time of the mechanical shutter and the LED used in photocurrent transient measurements

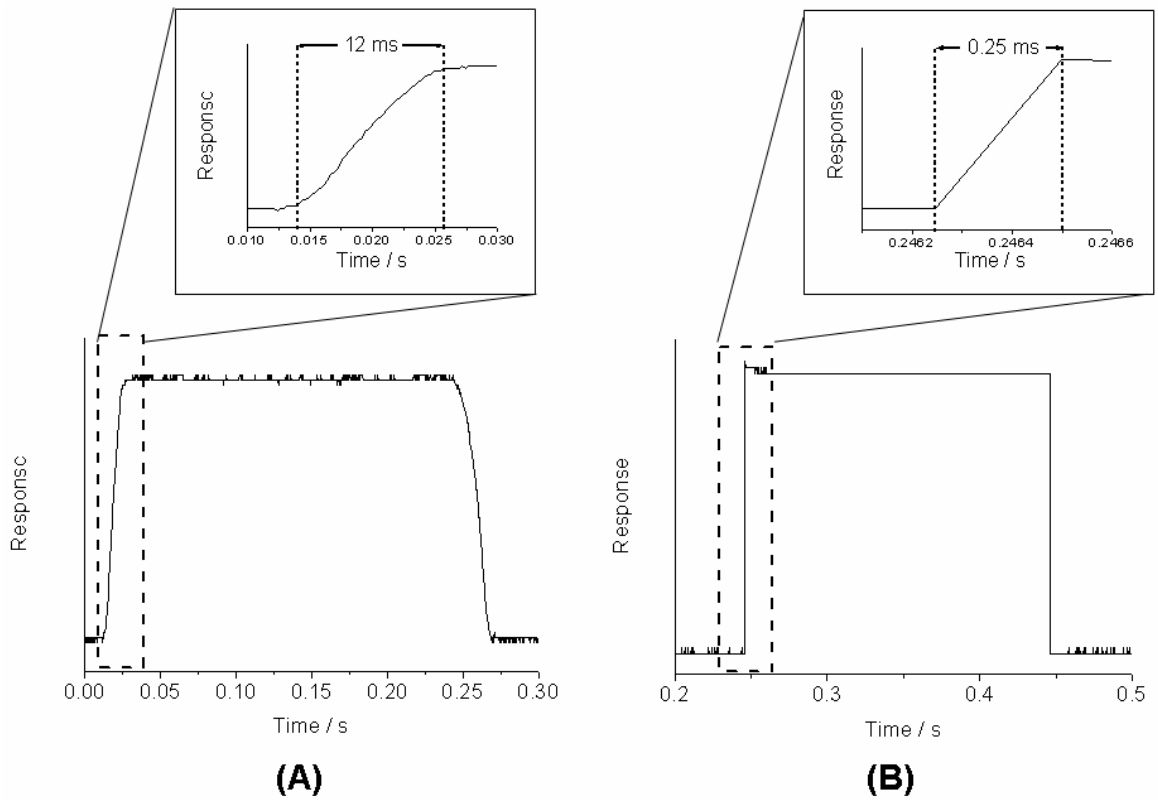

Fig. 0.4; The illumination profile in photocurrent transient measurements; (A) the mechanical shutter or (B) the LED was used to give the chopped illumination. The response was detected at photodiode.

Appendix 6 Information of the photodiode to calculate the photon number

Table 0.9: The data sheet for calculating the number of photon at specific wavelength

Wavelength / nm	Photocurrent correspond to 10^{15} photons cm^{-2} s^{-1} / 10^{-6} A
400	0.62
420	0.75
440	0.90
460	0.96
480	1.05
500	1.22
520	1.31
540	1.45
560	1.54
580	1.53
600	1.53
620	1.55
640	1.57
660	1.60
680	1.65
700	1.70
720	1.74
740	1.73
760	1.71
780	1.70
800	1.73
820	1.69
840	1.67
860	1.73
880	1.70
900	1.67

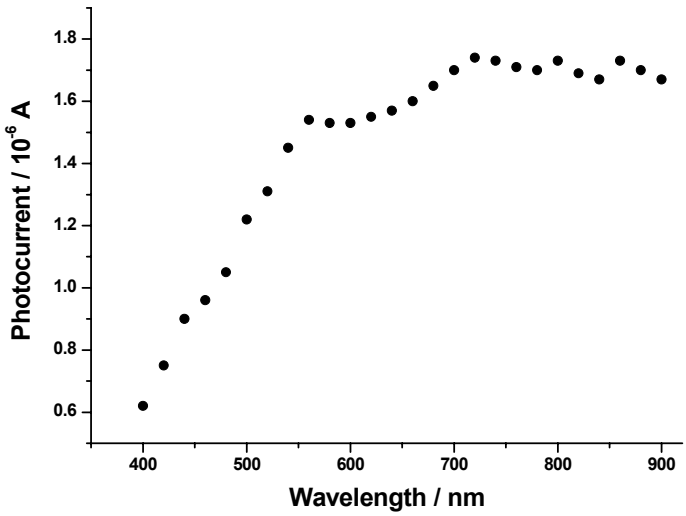

Fig.0.5: The sensitivity of the photodiode as the function of wavelength

Appendix 7 The setting of Lock-in amplifier for IMPS and IMVS

1. Input setup;
   input mode : A Volt, Input : Gnd/DC, Device : FET

2. Reference setup Menu;
   Ref. Source : internal, Harmonic : 1st, Demodulator Monitor control : off

3. Output setup Menu;
   expand : off, CH1 outputs CH2 : X%, Y%

4. Control Options Menu;
   Linefilt : off, AC Gain : automatic, TC's : ASYNC

5. Miscellaneous Option menu (*I do not know what this is for.)
   Trigger : 200Hz, Lights : on, Contrast : 0

6. RS232 Setup1 Menu
   BaudRate : 9600bps, Format : 7D + 1P, Parity : EVEN

7. RS232 Setup2 Menu
   Prompt : on, Echo : on, Delimiter : (044)

8. RS232 Setup3 Menu
   Address : 1,

9. GPIB Setup1 Menu
   Address : 1, Terminator : CR

10. GPIB Setup2 Menu
    SRQ Mask : 4, Test echo : disabled

11. Digital Outputs Setup Menu
    Decimal : 0,(*I do not know what it is. There are many numbers at the right-side display)

12. Control Setup Menu
    Default setting, Sample rate : 0,

Appendix 8 The setting of the modulation for LED in IMPS, IMVS

Table 0.10: The setting of the modulation for LED in IMPS and IMVS

Frequency / Hz	Time constant / s	Coupling	Waiting time / s
0.20	100	DC	500
0.30	100	DC	500
0.45	100	DC	500
0.65	50	DC	250
0.90	50	DC	250
1.4	20	DC	100
2.0	10	DC	50
3.0	10	DC	50
4.5	10	DC	50
6.5	5	DC	25
9	5	DC	25
14	2	AC	10
20	1	AC	10
30	1	AC	10
45	1	AC	10
65	1	AC	10
90	1	AC	10
140	1	AC	10
200	1	AC	10
300	1	AC	10
450	1	AC	10
650	1	AC	10
900	1	AC	10
1400	1	AC	10
2000	1	AC	10
3000	1	AC	10
4500	1	AC	10
6500	1	AC	10
9000	1	AC	10
14000	1	AC	10
20000	1	AC	10
30000	1	AC	10
45000	1	AC	10
65000	1	AC	10
90000	1	AC	10

Total time for the measurement is 2540 s = 42 min 20 s

Appendix 9 The past technical problem of the equipment in intensity modulated measurements.

It was found during the study that the equipment, which superimposes the dc voltage and the modulation signal from the lock-in amplifier, to give the modulated light to the electrode did not follow the reference signal from the lock-in amplifier. The reference signal was moved to forward in the lower frequency of less than 10 Hz. IMPS was measured by using a photodiode. It can be expected that photodiode is fast enough to follow the reference signal from the lock-in amplifier and then one value on x-axis is expected to appear in IMPS plot. However, the responses were appeared in (+,+) quadrant. (Fig. 0.6 (A)) It was not reasonable since photodiode was used for this measurement. The reason of this phenomenon was unclear. Nevertheless, to solve this problem, the potentiostat (IMP 83, Jaissle) was used instead of self- built controller box.

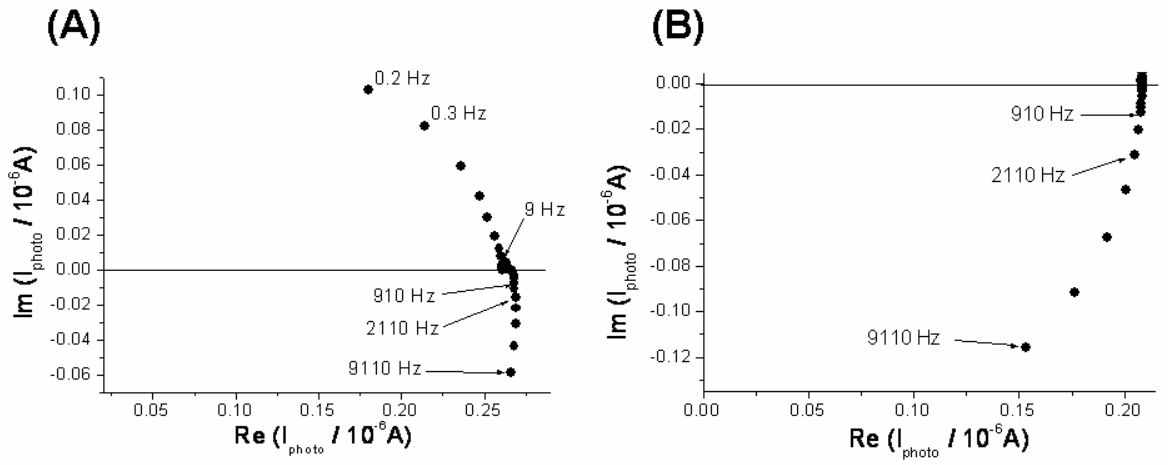

Fig. 0.6; IMPS plot measured by a photodiode. The bias voltage and the modulation signal were superimposed (A) at the previous equipment[167] and (B) at the potentiostat (IMP 83, Jaissle).

The IMPS plot is shown in Fig. 0.6 (A) in the case when the potentiostat was used to superimpose the signal. The most responses appeared on the x-axis. It indicates that the modulation of the generated current at the photodiode follows the reference signal from the lock-in amplifier. The response in (+,-) quadrant, which appeared over 1000 Hz, indicate that the modulation of the current has a delay against the reference signal. It is supposed that such delay is caused by the response limit of the potentiostat. Such delay in high frequency can be ignored for this study.

The results with the previous equipment were shown in chapter 5.2 and the results with new setting were shown in chapter 5.3.

Appendix 10 Parameters and the obtained values in the fitting of IMPS

re-ad C343/ZnO (EY as SDA) α[1]: 5700, d[2]: 2.2 x 10^{-4} cm, R[3]: 10Ω

obtained values by the measurement					obtained by fitting		
photon flux / 10^{15} cm^{-2} s^{-1}	dc current[4] / mA cm^{-2}	Photovoltage[4] / mV	Lifetime / s		diffusion coefficient / 10^{-6} cm^2 s^{-1}	capacitance / μF	injection efficiency
0.586	0.185	407	0.0120		8.810	32.8	0.196
0.455	0.152	400	0.0128		7.860	35.1	0.206
0.290	0.097	383	0.0153		5.880	41.1	0.222
0.198	0.066	366	0.0218		4.394	47.2	0.222
0.058	0.021	311	0.0796		1.858	79.0	0.223

re-ad C343/ZnO (C343 as SDA) α: 3600, d: 2.0 x 10^{-4} cm, R: 10Ω

0.586	0.136	397	0.0214		13.440	27.2	0.153
0.455	0.109	391	0.0220		11.350	30.6	0.143
0.290	0.076	377	0.0269		8.462	37.0	0.149
0.198	0.053	363	0.0336		6.600	49.4	0.153
0.058	0.018	326	0.1048		2.452	74.9	0.168

re-ad EY/ZnO (EY as SDA)1 α: 43456, d: 2.95 x 10^{-4} cm, R: 10Ω

0.651	1.115	513	0.0102		3.630	50.0	0.984
0.529	0.896	509	0.0105		3.354	60.0	1.000
0.353	0.604	496	0.0118		2.467	80.0	1.000
0.228	0.421	483	0.0134		4.772	110.0	1.000
0.076	0.138	446	0.0204		5.752	290.0	1.000

re-ad EY/ZnO (EY as SDA)2 α: 20000, d: 2.95 x 10^{-4} cm, R: 10Ω

0.651	1.115	513	0.0102		26.250	54.4	0.918
0.529	0.896	509	0.0105		25.400	59.8	0.933
0.353	0.604	496	0.0118		19.240	76.1	0.931
0.228	0.421	483	0.0134		12.470	96.3	0.999
0.076	0.138	446	0.0204		8.821	236.0	1.000

re-ad EY/ZnO (C343 as SDA) α: 28201, d: 1.9 x 10^{-4} cm, R: 10Ω

0.651	1.031	515	0.0078		55.670	63.2	0.469
0.529	0.854	510	0.0080		49.700	65.8	0.481
0.353	0.567	498	0.0091		39.930	80.1	0.527
0.228	0.373	485	0.0115		31.086	100.9	0.555
0.076	0.126	448	0.0179		19.088	232.0	0.599

re-ad TSPcZn/ZnO (EY as SDA) α: 6500, d: 2.46 x 10^{-4} cm, R: 10Ω

1.840	0.578	470	0.0312		105.300	79.9	0.111
1.610	0.500	466	0.0332		87.570	70.3	0.179
0.960	0.338	456	0.0408		76.720	87.1	0.159
0.610	0.231	445	0.0498		62.220	112.2	0.182
0.170	0.090	418	0.0758		10.280	113.7	0.232

re-ad TSPcZn/ZnO (C343 as SDA)1 α: 6223, d: 2.6 x 10^{-4} cm, R: 10Ω

1.840	0.124	483	0.0308		1.890	180.0	0.084
1.610	0.105	478	0.0329		1.170	200.0	0.083
0.960	0.074	468	0.0450		0.122	220.0	0.180
0.610	0.052	457	0.0681		0.016	330.0	0.415
0.170	0.021	427	0.1919		0.194	1470.0	0.123

re-ad TSPcZn/ZnO (C343 as SDA)2 α: 1000, d: 2.6 x 10^{-4} cm, R: 10Ω

1.840	0.124	483	0.0308		2.636	120.0	0.287
1.610	0.105	478	0.0329		1.897	130.0	0.276
0.960	0.074	468	0.0450		0.941	180.0	0.352
0.610	0.052	457	0.0681		0.547	250.0	0.394
0.170	0.021	427	0.1919		0.179	760.0	0.516

1; absorption coefficient, 2; film thickness, 3; resistance

4; measured with halogen lamp under the light intensity of 100 mW cm^{-2} (385 nm – 900 nm) and the light intensity was varied by using neutral density filter.

Appendix 11 Part of this work as presented in conference

- International Workshop on Nanostructured Semiconductor Electrodes, **Schloss Rauischholzhausen** near Giessen (Germany), 19–21, October, **2005**,
  "Comparison of the Photoelectrochemical Properties of Electrodeposited ZnO / Dye Hybrid Thin Films Which Have Different Orientation" (Poster)

- 2nd International Symposium on Complex Materials, Telekom Tagungszentrum, **Stuttgart** (Germany), 2-3, June, **2005**,
  "Dye-sensitized electrodeposited ZnO as active electrodes in photoelectrochemical cells" (Poster)

- 104. Hauptversammlung der Deutschen Bunsen-Gesellschaft für Physikalische Chemie e.V., **Frankfurt** (Germany) 5-7, Mai, **2005**,
  "Photoelectrochemical characterization of dye modified ZnO hybride thin films" (Poster)

- The 72th Spring Meeting of the Electrochemical Society of Japan, **Kumamoto** (Japan), 1–3, April, **2005**,
  "The difference of the photoelectrochemical properties between the dye modified ZnO hybrid thin films which have different orientation." (Oral)

- 15th International Conference on Photochemical Conversion and Storage of Solar Energy (IPS-15), **Paris** (France) , 4-9, July, **2004**,
  "Photoelectrochemical Characterization of Electrodeposited ZnO / Phthalocyanine Hybrid Films" (Oral)

- 103. Hauptversammlung der Deutschen Bunsen-Gesellschaft fÜr Physikalische Chemie e.V. **Dresden** (Germany), 20-22, Mai, **2004**,
  "Photoelectrochemical characterization of porphyrin- modified ZnO thin film" (Poster)

- The 7th Meeting on Electrode Reaction Mechanism and Interfacial Structure, **Koenigstein** (Germany), 3-6, April, **2003**,
  "Photoelectrochemical Properties of Dye-modified ZnO Thin Films Prepared by One-step Electrochemical Deposition" (Oral)

- 203rd Meeting of The Electrochemical Society, Palais des Congres de Paris, **Paris** (France), 28, April – 2, May, **2003**
  "Spectral Sensitization of ZnO by Phthalocyanine and/or Porphyrin Molecules Attached by Electrochemical Self- Assembly" (Poster)

- 1st International Symposium on Complex Materials, Universum Science Center, **Bremen** (Germany), 15-16, December, **2003**
  "Photoelectrochemical characterization of dye modified ZnO hybrid thin film prepared by electrochemical deposition" (Poster)

- 14th International Conference on Photochemical Conversion and Storage of Solar Energy (IPS-14), **Sapporo** (Japan), 4-9, August, **2002**
  "One-Step Electrochemical Synthesis of ZnO / $Ru(dcbpy)_2(NCS)_2$ Hybrid Thin Films and Their Photoelectrochemical Properties" (Poster)

- 53rd Annual Meeting of the International Society of Electrochemistry - Electrochemistry in Microscopic and Molecular Dimensions, Heinrich Heine Universitaet Duesseldorf, **Duesseldorf** (Germany), 15-20, September, **2002**,
  ”One-step electrochemical synthesis of ZnO / $Ru(dcbpy)_2(NCS)_2$ hybrid thin films and their photoelectrochemical properties" (Poster)

- The "Cormorant" Workshop on Nanomaterials for Photo Energy Conversion (Official Satellite Meeting of the 14th International Conference on Photochemical Conversion and Storage of Solar Energy (IPS-14), **Gifu** (Japan), 2-3, August, **2002**,
  "One-step electrochemical synthesis of ZnO / $Ru(dcbpy)_2(NCS)_2$ hybrid thin films and their photoelectrochemical properties" (Poster)

Appendix 12 Part of this work was published

Publication

- K. Nonomura, T. Loewenstein, E. Michaelis, D. Wöhrle, T. Yoshida, H. Minoura and D. Schlettwien, "Photoelectrochemical characterization and optimization of electrodeposited ZnO thin films sensitized by porphyrins and phathalocyanines", Physicalchemistry. *Phys. Chem. Chem. Phys.*, in submit.

- Y. Shen, K. Nonomura, D. Schlettwein, C. Zhao, G. Wittstock, "photoelectrochemical kinetics of Eosin Y-sensitized zinc oxide films investigated by scanning electrochemical microscopy", *Chemistry - A European Journal*, in press.

- T. Loewenstein, K. Nonomura, T. Yoshida, E. Michaelis, D. Wöhrle, J. Rathousky, M. Wark, D. Schlettwein, "Efficient sensitization of mesoporous electrodeposited zinc oxide by *cis*-bis(isothiocyanato)bis(2,2'-bipyridyl-4,4'-dicarboxylato)-ruthenium(II)", *J. Electrochemical Society*, **2006**, 153 (4), A699-A704

- T. Yoshida, M. Iwaya, H. Ando, T. Oekermann, K. Nonomura, D. Schlettwein, D. Wöhrle and H. Minoura, "Improved Photoelectrochemical Performance of Electrodeposited ZnO / Eosin Y Hybrid Thin Films by Dye Re-Adsorption", *Chem. Commun.*, **2004**, 400

- E. Michaelis, K. Nonomura, D. Schlettwein, T. Yoshida, H. Minoura and D. Wöhrle, "Hybrid Thin Films of ZnO with Porphyrins and Phthalocyanines Prepared by One-Step Electrodeposition", *J. Porphyrins and Phthalocyanin.*, **2004**, 8, 1336

Proceeding

- J. Rathousky, T. Loewenstein, K. Nonomura, T. Yoshida, M. Wark, D. Schlettwein, "Electrochemically self-assembled mesoporous dye-modified zinc oxide thin films", *Nanoporous materials IV studies in surface science and catalysis*, **2005**, 156, 315

References

1 H. Gerischer, H. Tributsch, *Ber. Bunsen-Ges. Phys. Chem.,* **1968**, 72, 437

2 M. P. Dare-Edwards, J. B. Goodenough, A. Hamnet, K. R. Seddon, R. D. Wright, *Faraday Discuss. Chem. Soc.* **1980**, 70,285

3 H. Tsubomura, M. Matsumura, Y. Noyamura, T. Amamiya, *Nature*, **1976**, 261, 402

4 D. Duonghong, N. Serpone, M. Greatzel, *Helv. Chim. Acta*, **1984**, 67, 1012

5 J. Desilvestro, M. Greatzel, L. Kavan, J. E. Moser, J. Augustynski, *J. Am. Chem. Soc*, **1985**, 107, 2988

6 N. Vlachopoulos, P. Liska, J. Augustynski, M. Greatzel, *J. Am. Chem. Soc*, **1988**, 110, 1216

7 B. O'Regan, M. Greatzel, *Nature*, **1991**, 335, 737

8 M. K. Nazeeruddin, A. Kay, L. Rodicio, R. Humphry-Baker, E. Muller, P. Liska, N. Vlachopoulos, and M. Grätzel, *J. Am. Chem. Soc.*, **1993**, 115, 6382

9 K. Keis, J. Lindgre, S.-E. Lindquist, and A. Hagfeldt, *Langmuir*, **2000**, 16, 4688

1 0 U. Björkstén, J. Moser, and M. Grätzel, *Chem. Mater.*, **1994**, 6, 858

1 1 S. Ferrere, A. Zaban, and B. A. Gregg, *J. Phys. Chem. B*, **1997**, 101, 4490

1 2 A. Turković, and Z. Crnjak Orel, *Sol. Energy Mater. Sol. Cells*, **1997**, 45, 275

1 3 K. Sayama, H. Sugihara, and H. Arakawa, Chem. Mater., 1998, 10, 3825

1 4 K. Hara, T. Horiguchi, T. kinoshita, K. Sayama, H. Sugihara, and H. Arakawa, *Sol. Energy Mater. Sol. Cells*, **2000**, 64, 115

1 5 K. Tennakone, G. K. R. Senadeera, V. P. S. Perera, I. R. M. Kottegoda, and L. A. A. De Silva, *Chem. Mater.*, **1999**, 11, 2474

1 6 A. Zaban, S. G. Chen, S. Chappel, and B. A. Gregg, *Chem. Commun.*, **2000**, 2231

1 7 K. Tennakone, J. Bandara, P. K. M. Bandaranayake, G. R. A. Kumara, and A. Konno, *Jpn. J. Appl. Phys., Part 2*, **2001**, 40, L 732

1 8 H. Matsumoto, T. Matsuda, T. Tsuda, R. Hagiwara, Y. Ito, and Y. Miyazaki, *Chem. Lett.*, **2001**, 26

1 9 F. Cao, G. Oskam, and P. C. Searson, *J. Phys. Chem.*, **1995**, 99, 17071

2 0 W. Kubo, K. Murakoshi, T. Kitamura, Y. Wada, K. Hanabusa, H. Shirai, and S. Yanagida, *Chem. Lett.*, **1998**, 1241

2 1 K. Murakoshi, R. Kogure, Y. Wada, and S. Yanagida, *Chem. Lett.*, **1997**, 471

2 2 K. Tennakone, G. R. R. A. Kumara, I. R. M. Kottegoda, and K. G. U. Wijayantha, *Semicond. Sci. Technol.*, **1997**, 12, 128

2 3 P. Péchy, F. P. Rotzinger, M. K. Nazeeruddin, O. Kohle, S. M. Zekeeruddin, R. Humphry-Baker, and M. Grätzel, *J. Chem. Soc., Chem. Commun.*, **1995**, 65

2 4 M. Yanagida, L. P. Singh, K. Sayama, K. Hara, A. Katoh, A. Islam, H. Sugihara, H. Arakawa, M. K. Nazeeruddin, and M. Grätzel, *J. Chem. Soc., Dalton Trans.*, **2000**, 2817

2 5 O. Enea, j. Moser, and M. Grätzel, *J. Electroanal. Chem.*, **1989**, 259, 59

2 6 K. Hara, K. Sayama, Y. Ohga, A. Shinpo, S. Suga, and H. Arakawa, *Chem. Commun.*, **2001**, 569

2 7 Y. Shen, L. Wang. Z. Lu, Y. Wei, Q. Zhou, H. Mao, and H. Xu, *Thin Solid Films*, **1995**, 257, 144

2 8 M. K. Nazeeruddin, R. Humphry-Baker, m. Grätzel, D. Wöhrle, G. Schnurpfeil, G. Schneider, A. Hirth, and N. Trombach, *J. Porph. Phtalocyanines*, **1999**, 3, 230

2 9 G. K. Boschloo, and A. Goossens, *J. Phys. Chem.*, **1996**, 100, 19489

3 0 A. Ehret, L. Stuhl, And M. T. Spitler, *Electrochim. Acta*, **2000**, 45, 4553

3 1 D. Zhang, W. Wang, Y. Liu, X. Xiao, W. Zhao, B. Zhang, and Y. Cao, *J. photochem. Photobiol. A: Chem.*, **2000**, 135, 235

3 2 K. Tennakone, G. R. R. A. kumara, I. R. m. Kottegoda, V. P. S. Perera, and P. S. R. S. Weerasundara, *J. Photochem. Photobiol. A: Chem.*, **1998**, 117, 137

33 Q. Dai, and J. Rabani, *Chem. Commun.*, **2001**, 2142
34 K. Hara, T. Sato, R. Katoh, A. Furube, Y. Ohga, A. Shinpo, S. Suga, K. Sayama, H. sugihara, and H. Arakawa, *J. Phys. Chem. B*, **2003**, 107, 597
35 K. Hara, Z. S. Wang, T. Sato, A. Furube, R. Katoh, H. Sugiraha, Y. Dan-oh, C. Kasada, A. Shinpo. S. Suga, *J. Phys. Chem. B*, **2005**, 109, 15476
36 B. O'Regan, and D. T. Schwartz, *J. Appl. Phys.*, **1996**, 80, 4749
37 T. N. Rao, L. Bahadur, *J. Electrochem. Soc.*, **1997**, 144, 179
38 L. Schmidt-Mende, U. Bach, R. Humphry-Baker, T. Horiuchi, H. Miura, S. Ito, S. Uchida, M. Grätzel, *Adv. Mater.*, **2005**, 17, 813
39 K. Hara, M. Kurashige, S. Ito, A. Shinpo, S. Suga, K. Sayama, H. Arakawa, *Chem. Commun.*, **2003**, 252
40 F. Gao, A. J. Bard, L. D. Kispert, *J. Photochem. Photobiol., A*, **2000**, 10, 49
41 N. Cherepy, G. P. Smestad, M. Grätzel, J. Z. Zhang, *J. Phys. Chem. B*, **1997**, 101, 9342
42 K. Tennakone, A. R. Kumarasinghe, G. R. R. A. Kumara, K. G. U. Wijayantha, P. M. Sirimanne, *J. Photochem. Photobiol. A*, **1997**, 108, 193
43 Q. Dai, J. Rabani, *New J. Chem.*, **2002**, 26, 421
44 G. Redmond, D. Fitzmaurice, and M. Grätzel, *Chem. Mater.*, **1994**, 6, 686
45 K. Tennakone, G. R. R. A. Kumara, A. R. Kumarasinghe, K. G. U. Wijayantha, P. M. Sirimanne, *Semicond. Sci. Technol.*, **1995**, 10, 1689
46 U. Bach. D. Lupo, P. Comte, J. E. Moser, F. Weissörtel, J. Salbeck, H. Spreitzer, and M. Grätzel, *Nature*, **1998**, 395, 583
47 Q. B. Meng, K. Takahashi, X. T. Zhang I. Sutanto, T. N. Rao, O. Sato, A. Fujishima, H. Watanabe, T. Nakamori, M. Uragami, *Langmuir*, **2003**, 19, 3572
48 M. K. Nazeeruddin, F. De Angelis, S. Fantacci, A. Selloni, G. Viscardi, P. Liska. S. Ito, T. Bessho and M. Greatzel, *J. Am. Chem. Soc*, **2005**, 127, 16835
49 M. Grätzel, *J. photochem. Photobiol. C: Photochem. Rev.*, **2003**, 4, 145
50 M. Izaki, T. Omi, *J. Electrochem. Soc.*, **1996**, 3, 143
51 M. Izaki, T. Omi, *J. Elctrochem. Soc.*, **1997**, 1, 144
52 S. Peulon, D. Lincot, *Adv. Mater.*, **1996**, 8, 166
53 S. Peulon, D. Lincot, *J. Electrochem. Soc.*, **1998**, 145, 864
54 T. Pauporté, D. Lincot, *Appl. Phys. Lett.*, **1999**, 75, 24
55 T. Yoshida, H. Minoura, *Adv. Mater.*, **2000**, 12, 1219
56 T. Yoshida, T. Pauporté, D. Lincot, T. Oekermann, and H. Minoura, J. Electrochem. Soc., 2003, 150, C608
57 T. Yoshida, K. Miyamoto, N. Hibi, T. Sugiura, H. Minoura. D. Schlettwein, T. Oekermann, G. Schneider, D. Wöhrle, *Chem. Lett.*, **1988**, 599
58 T. Yoshida, M. Tochimoto, D. Schlettwein, D. Wöhrle, T. Sugiura, H. Minoura, *Chem. Mater.*, **1999**, 11, 2657
59 T. Yoshida, K. Terada, D. Schlettwein, T. Oekermann, T. Sugiura, H. Minoura, *Adv. Mater.*, **2000**, 12, 1214
60 T. Yoshida, T. Oekermann, K. Okabe, D. Schlettwein, K. Funabiki, h. Minoura, *Electrochemistry*, **2002**, 70, 470
61 T. Yoshida, J. Yoshimura, M. Matsui, T. Sugiura, H. Minoura, *Trans. Mater. Res. Soc. Jpn.*, **1999**, 24, 497
62 S. Karuppchamy, T. Yoshida, T. Sugiura, H. Minoura, *Thin Solid Films*, **2001**, 397, 63
63 S. Karuppuchamy, K. Nonomura, T. Yoshida, T. Sugiura, H. Minoura, *Solid State Ionics*, **2002**, 151, 19
64 K. Nonomura, T. Yoshida, D. Schlettwein, H. Minoura, *Electrochim. Acta*. **2003**, 48, 3071
65 R. Purrello, E. Bellacchio, S. Gurrieri, R. Lauceri, A. Raudino, L. M. Scolaro, and A. M. Santoro, *J. phys. Chem. B*, **1998**, 102, 8852
66 G. Schneider, Dissertation, University Bremen, **1995**

6 7 H. Deng, H. Mao, H. Zhang, Z. Lu and H. Xu, *J. Porphyrins Phthalocyanin.*, **1998**, 2, 171

6 8 D. Wöhrle and A.D. Pomogailo, *Metal Complexes and Metals in Macromolecules*, Wiley-VCH, Weinhein, **2003**

6 9 T. Yoshida, M. Iwaya, H. Ando, T. Oekermann, K. Nonomura, D. Schlettwein, D. Wöhrle, and H. Minoura, *Chem.Commum.*, **2004**, 400

7 0 E. Michaelis, D. Wöhrle, J. Rathousky, M. Wark, *Thin Solid films*, **2006**, 497, 163

7 1 A. Hafeldt, M. Grätzel, *Acc. Chem. Res.*, **2000**, 33, 269

7 2 Y. Tachibana, J. E. Moser, M. Grätzel, D. R. Klug, J. R. Durrant, *J. Phys. Chem.*, **1996**, 100, 20056

7 3 J. B. Asbury, R. J. Ellingson, H. N. Ghosh, S. Ferrere, A. J. Nozik, T. Lian, *J. Phys. Chem. B*, **1999**, 103, 3110

7 4 S. Pelet, J. E. Moser, M. Grätzel, *J. Phys. Chem. B*, **2000**, 104, 1791

7 5 G. Benkö, B. Skarman, R. Wallenberg, A. Hagfeldt, V. Sundstrom, A. P. Yartsev, *J. Phys. Chem. B*, **2003**, 107, 1370

7 6 C. A. Kelly, F. Farzad, D. W. Thompson, J. M. Stipkala, G. J. Meyer, *Langmuir*, **1999**, 15, 7074

7 7 S. A. Haque, Y. Tachibana, R. L. Willis, J. E. Moser, M. Grätzel, R. D. Klug, J. R. Durrant,
J. Phys. Chem. B, **2000**, 104, 538

7 8 P. J. Cameron, and L. M. Peter, *J. Phys. Chem. B*, **2005**, 109, 7392

7 9 A. C. Fisher, L. M. Peter, E. A. Ponomarev, A. B. Walker, K. G. U. Wijayantha, *J. Phys. Chem. B*, **2000**, 104, 949

8 0 G. Schlichthörl, S. Y. Huang, J. Sprague, A J. Frank, *J. Phys. Chem. B*, **1997**, 101, 8141

8 1 J. Nelson, S. A. Haque, R. D. Klug, J. R. Durrant, *Phys. Rev. B*, **2001**, 63, 205321

8 2 T. Oekermann, T. Yoshida, H. Minoura, K. G. U. Wijayantha, and L. M. Peter, *J. Phys. Chem. B*, **2004**, 108, 8364

8 3 T. Oekermann, T. Yoshida, D. Schlettwein, T. Sugiura, and H. Minoura, *Phys. Chem. Chem. Phys.*, **2001**, 3, 3387

8 4 G. de la Torre, P. Vázquez, F. Agulló-López, and T. Torres, *J. Mater. Chem.*, **1998**, 8(8), 1671

8 5 Y. Haga, H. An, R. Yosomiya, *J. Mat. Sci.*, **1997**, 32, 3193

8 6 S. M. Tracey, S. N. B. Hodgson, A. K. Ray, *J. sol-gel, Sci, Tec*, **1998**, 13, 219

8 7 J. He, A. Hagfelde, S. E. Linquist, H. Grennberg, F. Korodi, L. Sun, B. Åkermark, *Langmuir*, **2001**, 17, 2743

8 8 Y. Amao, and T. Komori, *Langmuir*, **2003**, 19, 8872

8 9 H. Yanagi, S. Chem, P. A. Lee, K. W. Nebesny, N. R. Armstrong, A. Fujishima, *J. Phys. Chem.*, **1996**, 100, 5447

9 0 H. Deng, Z. Lu, H. Mao, H. Xu, *Chem. Phys.*, **1997**, 221, 323

9 1 J. He, G. Benkö, F. Korodi, T. Polivka, R. Lomoth, B. Åkermark, L. Sun, A. Hagfeldt, V. Sundström, *J. Am. Chem. Soc.*, **2002**, 124, 4922

9 2 A. S. Komolov, P. J. møller, J. Mortensen, S. A. Komolov, E. F. Lazneva, *Surface, Sci.*, **2005**, 586, 129

9 3 M. Calvete, G. Y. Yang, M. Hanack, *Synthe. Met.*, **2004**, 141, 231

9 4 D. Ino, K. Watanabe, N. Takagi, and Y. Matsumoto, *J. Phys. Chem. B*, **2005**, 109, 18018

9 5 C. L. Huisman, A. Goossens, And J. Schoonman, *J. Phys. Chem. B*, **2002**, 106, 10578

9 6 S. Taira, T. Miki, H. Yanagi, *App. Surf. Sci.*, **1999**, 143, 23

9 7 W. Liu, Y. Wang, L. Gui, and Y. Tang, *Langmuir*, **1999**, 15, 2130

9 8 M. Zabkowska-Waclawek, Z. Ziembik, *J. Mat. Sci.*, **2005**, 40, 1465

9 9 J. N. Clifford, E. Palomares, m. K. Nazeeruddin, M. Grätzel, J. Nelson, X. Li, N. J. Long, and J. R. Durrant, *J. Am. Chem. Soc.*, **2004**, 126, 5225

100 C. A. Bignozzi, R. Argazzi, C. Kleverlaan, *J. Chem. Soc. Rev.*, **2000**, 29, 87
101 S. Cherian and C. C. Wamser, *J. Phys. Chem. B*, **2000**, 104, 3624
102 K. Kalyanasundaram, N. Vlachopoulos, V. Krishanan, A. Monnier, and M. Grätzel, *J. Phys. Chem.*, **1987**, 91, 2342
103 W. M. Campbell, A. K. Burrell, D. L. Officer, K. W. Jolley, *Coord. Chem. Rev.* **2004**, 248, 1363
104 R. Dabestani, A. J. Bard, A. Campion, M. A. Fox, T. E. Mallouk, S. E. Webber, and J. M. White, *J. Phys. Chem.*, **1988**, 92, 1872
105 R. B. M. Koehorst, G. K. Boschloo, T. J. Savenije, A. Goossens, and T. J. Schaafsma, *J. Phys. Chem. B*, **2000**, 104, 2371
106 M. E. Milanesio, m. Gervaldo, L. A. Otero, L. Sereno, J. J. Silber, and E. N. Durantini, *J. Phys. Org. Chem.*, **2002**, 15, 844
107 F. Odobel, E. Blart, M. Lauree, M. Villeras, H. Boujtita, N. El Mur, S. Caramori, and C. A. Bignozzi, *J. Mater. Chem.*, **2003**, 13, 502
108 M. O. Liu, A. T. Hu, *J. Organomet. Chem.*.**2004**, 689, 2450
109 H. Ding, X. Zhang, M. K. Ram, C. Nicolini, *J. Colloid Interface Sci.*, **2005**, 290, 166
110 H. Deng, H. Mao, B. Liang, Y. Shen, Z. Lu, H. Xu, *J. Photochem. Photobio. A: Chemistry*, **1996**, 99, 71
111 H. Deng, H. Mao, Z. Lu, J. Li, H. Xu, *J. Photochem. Photobio. A: Chemistry*, **1997**, 110, 47
112 T. Pauporte, D. Lincot, *J. Electrochem. Soc.*, **2001**, 148(4), C310
113 J. A. Switzer, *Am. Ceram. Bull.*, **1987**, 66, 1521
114 T. A. Sorenson, S. A. Morton, G. D. Waddill, and J. A. Switzer, *J. Am. Chem. Soc.*, **2002**,124, 7604
115 L. Gal-Or, I. Siberman, and R. Chaim, *ibid.*, **1991**, 138, 1939
116 J. K. Barton, A. A. Vertegel, E. W. Bohannan, and J. A. Switzer, *Chem. Mater.*, **2001**, 13, 952
117 J. A. Switzer, M. G. Shumsky and E. W. Bohanan, *Science*, **1999**, 284, 293
118 C. Natarajan and G. Nogami, *ibid.*, **1996**, 143, 1547
119 M. Isaki, and T. Omi, *Appl. Phys. Lett.*, **1996**, 68, 2439
120 T. Pauporté, and D. Lincot, *Appl. Phys. Lett.*, **1999**, 75, 3817
121 R. Liu, A. A. Vertegel, E. W. Bohannan, T. A. Sorenson, and J. A. Switer, *Chem. Mater.*, **2001**, 13, 508
122 L. Stolt, J. Hedström, M. Rückh, J. Kessler, K. O. Velthaus, and H. W. Schock, *Appl. Phys. Lett.*, **1993**, 62, 597
123 T. Ikeda, J. Sato, Y. Wakayama, K. Adachi, and H. Nishiura, *Sol. Energy Mater. Sol. Cells*, **1994**, 34, 379
124 B. O'Regan, D. T. Schwartz, S. M. Zakeeruddin, M. Grätzel, *Adv. Mater*, **2000**, 12, 1263
125 K. Keis, E. Magnusson, H. Lindström, S. E. Lindquist, A. Hagfeldt, *Sol. Energy Mater. Sol. Cells*, **2002**, 73, 51
126 D. Gal, G. Hodes, D. Lincot, H. W. Schock, *Thin Solid Films*, **2000**, 361, 79
127 B. Canava, D. Lincot, *J. Appl. Electrochem.*, **2000**, 30, 711
128 T. Pauporté, D. Lincot, *Electrochim. Acta*, **2000**, 45, 3345
129 T. Yoshida, S. Ide, T. Sugiura, H. Minoura, *Trans. Mater. Res. Soc. Jpn.*, **2000**, 25, 1111
130 J. A. Dean, *Lange's Handbook of Chemistry, 14th ed*, McGraw-Hill, New York, **1992**, Sec. 6
131 T. Yoshida, D. Komatsu, N. Shimokawa, H. Minoura, *Thin Solid Films*, **2004**, 451-452, 166
132 M. Grätzel, *in Semiconductor Nanoclusters, Studies in Surface Science and Catalysis*, P. V. Kamat and D. Meisel (eds.), Elsevier Science B. V., **1996**, 103, 353
133 K. Schwarzburg and F. willing, J. Phys. Chem. B, 1997, 101, 2451
134 L.M. Peter, *Chem. Rev.*, **1990**, 90, 753

1 3 5 T. Oekermann, D. Schlettwein, and N. I. Jaeger, *J. Electroanal. Chem.*, **1999**, 462, 222

1 3 6 T. Oekermann, D. Schelttwein, N. I. Jaeger, and D. Wöhrle, *J. Porphyrins Phthalocyanin.*, **1999**, 3, 444

1 3 7 A. Solbrand, H. Lindstroem, H. Rensmo, A. Hagfeldt, S.-E. Lindquist, and S. Soedergren, *J. Phys. Chem. B*, **1997**, 101, 2514

1 3 8 M. J. Cass, F. L. Qtu, A. B. Walker, A. C. Fisher, and L. M. Peter, *J. Phys. Chem. B*, **2003**, 107, 113

1 3 9 D. Schlettwein, T. Oekermann, T. Yoshida, M. Tochimoto, and H. Minoura, *J. Electroanal. Chem.*, **2000**, 481, 42

1 4 0 A. Hagfeldt, M. Grätzel, *Chem. Rev.*, **1995**, 95, 49

1 4 1 N. S. Saricftci, L. Smilowitz, A. J. Heeger, F. Wudl, *Science*, **1992**, 258, (5087), 1474

1 4 2 T. Hannappel, B. Burfeindt, W. Storck, F. Willig, *J. Phys. Chem. B*, **1997**, 101, 6799

1 4 3 G. Benko, J. T. Kallioinen, P. Myllyperkio, F. Trif, J. R. I. Korppi-Tommola, A. P. Yartsev, V. Sundstrom, *J. Am. Chem. Soc.*, **2002**, 124, 3, 489

1 4 4 J. Schnadt, P. A. Bruhwiler, L. Patthey, J. N. O'Shea, S. Sodergren, M. Odelius, R. Ahuja, O. Karis, M. Bassler, P. Parsson, H. Siegbahn, S. Lunell, N. Martensson, *Nature*, **2002**, 418, 620

1 4 5 W. Stier, W. R. Duncan, O. V. Prezhdo, *Adv. Mater.*, **2004**, 16(3), 240

1 4 6 J Ashbury, E. Hao, Y. Wang, H. N. Ghosh, T. Lian, *J. Phys. Chem. B*, **2001**, 105, 4545

1 4 7 S. Södergren, A. Hagfeldt, J. Olsson, S. E. Lindquist, *J. Phys. Chem.*, **1994**, 98, 5552

1 4 8 F. Cao, G. Oskam. G. J. Meyer, P. C. Season, *J. Phys. Chem.*, **1996**, 100, 17021

1 4 9 P. E. de Jongh, and D. Vanmaekelbergh, *Phys. Rev. Lett.* **1996**, 77, 3427

1 5 0 D. Vanmaekelbergh, F. Iranzo Marin, and J. van de Lagemaat, *Ber. Bunsenges. Phys. Chem.* **1996**, 100, 616

1 5 1 L. M. Peter, and D. Vanmaekelbergh, *Advances in Electrochemical Science and Engeneering*, John Wiley and Sons, Weinheim, Germany, **1999**, 77

1 5 2 D. vanmaekelbergh, A. R. de Wit and F. Cardon, *J. Appl. Phys.* **1993**, 73, 5049

1 5 3 E. P. A. M. Bakkers, J. J. Kelly and D. Vanmaekelberg, *J. Electroanal. Chem.*, **2000**, 482, 48

1 5 4 E. P. A. M. Bakkers, A. L. Roest, A. W. Marsman, L. W. Jenneskens, L. I. De Jongh-van Steensel, J. J. Kelly and D. Vanmaekelberg, *J. Phys. Chem. B*, **2000**, 104, 7266

1 5 5 L. Dloczik, O. Ileperuma, I. Lauermann, L. M. Peter, E. A. Ponomarev, G. Redmond, N. J. Shaw, and I. Uhlendorf, *J. Phys. Chem. B*, **1997**, 101, 10281

1 5 6 L. M. Peter, K. G. U. Wihayantha, *Electrochem. Commun.*, **1999**, 1, 576

1 5 7 N. W. Duffy, L. M. Peter, R. M. G. Rajapakse, K. G. U. Wijayantha, *Electrochem. Commun.*, **2000**, 2, 658

1 5 8 L. M. Peter, K. G. U. Wijayantha, *Electrochem. Acta*, **2000**, 45, 4543

1 5 9 G. Franco, L. M. Peter, E. A. Ponomarev, *Electrochem. Commun.*, **1999**, 1, 61

1 6 0 T. Oekermann, T. Yoshida, C. Boeckler, J. Caro, and H. Minoura, *J. Phys. Chem. B*, **2005**, 109, 12560

1 6 1 L. Forro, O. Chauvet, D. Emin, L. Zuppirol, H. Berger, F. Lévy, *J. Appl. Phys.*, **1994**, 75, 633

1 6 2 G. Schlichthörl, N. G. Park, A. J. Frank, *J. Phys. Chem. B*, **1999**, 103, 782

1 6 3 E. Michaelis, Dissertation, University Bremen, **2005**

1 6 4 Personal communication with Prof. T. Yoshida

1 6 5 F. Rouquerol, J. Rouquerol and K. Sing, Adsorption by Powders and Porous Solids, Principles, Mthodology and Applications, *Academic Press*, London, **1999**

166 J. Rathousky, T. Lowenstein, K. Nonomura, T. Yoshida, M. Wark, and D. Schlettwein, *Nanoporous materials IV studies in surface science and catalysis*, **2005**, 156, 315
167 T. Oekermann, Dissertation, University Bremen, **2000**
168 M. Gouterman, in: D. Dolphin (Ed), *The Porphyrins, Academic Press*, New York, 1978
169 N. Kobayashi, H. Konami, in: C. C. Leznoff, A. B. P. Lever (Eds.), *Phthalocyanines: Properties and Applications*, VCH, New York, 1996
170 E. Michaelis, K. Nonomura, D. Schlettwein, T. Yoshida, H. Minoura, and D. Wöhrle, *J. Porphyrins and Phthalocyanin.*, **2004**, 8, 1366
171 T. Loewenstein, K. Nonomura, T. Yoshida, E. Michaelis, D. Wöhrle, J. Rathousky, M. Wark, D. Schlettwein, *J. Electrochem. Soc.,* **2006**, 153 (4), A699-A704
172 T. Loewenstein, Degree dissertation, University of Oldenburg, **2004**
173 J. Rathousky, unpublished data.
174 J. Zhang, D. Komatsu, T. Yoshida, H. Minoura, unpublished data
175 Y. Tachibana, S. Haque, I. Mercer, J. Durrant, and D. Klug, *J. Phys. Chem. B*, **2000**, 104, 1198
176 J. Clifford, G. Yahioglu, L. Milgrom, and J. Durrant, *Chem. Comm.*, **2002**, 1260
177 D. Schlettwein, E. Karmann, T. Oekermann, and H. Yanagi, *Electrochmica Acta*, **2000**, 45, 4697
178 Y. Tachibana, K. Hara, S. Takano, K. Sayama, H. Arakawa, *Chem. Phys. Let.*, **2002**, 364, 297
179 Y. Tachibana, S. A. Haque, I.P. Mercer, J. E. Moser, D. R. Klug, J. R. Durrant, J. Phys. Chem. B, 2001, 205, 7424
180 S. Y. Huang, G. Schlichthörl, A. J. Nozik, M. Grätzel, and A. J. Frank, *J. Phys. Chem. B*, **1997**, 101, 2576
181 Y. Liu, A. Hagfeldt, X. R. Xiao, S. E. Lindquist, Sol. Energy Mater. Sol. Cells, 1998, 5, 267
182 B. Enright, G. Redmond, D. Fitzmaurice, *J. Phys. Chem.*, **1994**, 98, 6195
183 K. Hara, T. Horiguchi, T. Kinoshita, K. Sayama, H. Arakawa, *Sol. Energy Mater. Sol. Cells*, **2001**, 70, 151
184 K. S. Choi, H. C. Lichtneegger, G. D. Stucky, *J. Am Chem. Soc.*, **2002**, 124, 12402
185 L. M. Peter, E. A. Ponomarev, G. Franco, N. J. Shaw, *Electrochm. Acta*, **1999**, 45, 549
186 Z. S. Wang. K. Hara, Y. Dan-oh, C. Kasada, A. Sinpo, S. Suga, H. Arakawa, H. Sugihara, *J. Phys. Chem. B*, **2005**, 109, 3907
187 K. Hara, Y. Tachibana, Y. Ohga, A. Shinpo, S. Suga, K. Sayama, H. Sugihara, H. Arakawa, *Sol. Energy Mater. Sol. Cells*, **2003**, 77, 89
188 J. M. Rehm. G. L. Mclendo, Y. Nagasawa, K. Yoshihara, J. Moser, M. Grätzel, *J. Phys. Chem.*, **1996**, 100, 9577
189 K. Murakoshi, S. Yanagida, M. Capel, E. W. Castner, *Jr. Interfacial Electron Transfer Dynamics of photosensitized Zinc Oxide Nanoclusters*; M. Moskovits, Ed; ACS: Washington, DC, **1997**, 221
190 J. E. Moser, M. Grätzel, *Chem. Phys.*, **1993**, 176, 493
191 H. N. Ghosh, *J. Phys. Chem., B*, **1999**, 103, 10382
192 G. Ramakrishna, H. N. Ghosh, *J. Phys. Chem. A*, **2002**, 106, 2545
193 K. Hara, K. Miyamoto, Y. Abe, M. Yanagida, *J. Phys. Chem. B*, **2005**, 109, 50, 23776
194 S. Hattori, T. Yoshida, H. Minoura, unpublished data, Gifu University
195 P. Wanger, R. Helbig, *J. Phys. Chem. Solids*, **1974**, 35, 327
196 A. R. Hutson, *J.Phys. Chem. Solids*, **1959**, 8, 467, 2
197 S. A. Haque, E. Palomares, B. M. Cho, A. N. M. Green, N. Hirata, D. R. Klug, and J. R. Durrant, *J. Am. Chem. Soc.*, **2005**, 127, 3456

198 Y. Tachibana, M. K. Nazeeruddin, M. Grätzel, D. R. Klug, J. R. Durrant, *Chem. Phys.*, **2002**, 285, 127
199 Y. Tachibana, I. V. Rubstov, I. Montanari, K. Yoshihara, D. R. Klug, J. R. Durrant, *J. Photochem. Photobiol., A*, **2001**, 142, 215
200 J. R. Durrant, *J. Photochem. Photobiol., A*, **2002**, 148, 5
201 J. Nelson, *Physical Review B-Condensed Matter*, **1999**, 59, 15374
202 J. Bisquert, A. Zaban, *Applied Physics a-Materials Science & Processing*, **2003**, 77, 507
203 J. Bisquert, *J. Phys. Chem. B*, **2004**, 108, 2323
204 J. Nelson, R. E. Chandler, *Coord. Chem. Rev.*, **2004**, 248, 1181
205 M. J. Cass, A. B. Walker, D. Martinez, L. M. Peter, *J. Phys. Chem. B*, **2005**, 109, 5100
206 N. W. Duffy, L. M. Peter, K. G. U. Wijayantha, *Electrochem. Commun.*, **2000**, 2, 262
207 P. J. Cameron, and L. M. Peter, *J. Phys. Chem. B*, **2003**, 107, 14394
208 P. J. Cameron, L. M. Peter, S. Hore, *J. Phys. Chem. B*, **2005**, 109, 930
209 D. Komatsu, personal communication
210 S. Nakade, T. Kanzaki, W. Kubo, T. Kitamura, Y. Wada, and S. Yanagida, *J. Phys. Chem. B*, **2005**, 109, 3480
211 T. Oekermann, L. M. Peter, personal communication
212 T. Oekermann, in preparation
213 F. J. Green, The sigma-aldrich handbook of stains dyes and indicators, *sigma-aldrich corporation,* **1991**
214 Home page of Acros Organics bvba (www.acros.be)
215 Home page of LOT Oriel (www.lot-oriel.com)